Department of Applied Physics

Quality Assurance Methods for Uncertainty Analysis in Reactor Physics with Applications

Risto Vanhanen

Aalto University

DOCTORAL DISSERTATIONS

Aalto University publication series
DOCTORAL DISSERTATIONS 58/2016

Quality Assurance Methods for Uncertainty Analysis in Reactor Physics with Applications

Risto Vanhanen

A doctoral dissertation completed for the degree of Doctor of Science (Technology) to be defended, with the permission of the Aalto University School of Science, at a public examination held at the lecture hall E of the school on 29 April 2016 at 13.

Aalto University
School of Science
Department of Applied Physics

Supervising professor
Prof. Filip Tuomisto, Aalto University, Finland

Thesis advisor
D.Sc. (Tech.) Jarmo Ala-Heikkilä, Aalto University, Finland

Preliminary examiners
Dr. Anu Kankainen, University of Jyväskylä, Finland
Dr. Gašper Žerovnik, Jožef Stefan Institute, Slovenia

Opponent
Prof. Guillem Cortés, Politechnical University of Catalonia (UPC), Spain

Aalto University publication series
DOCTORAL DISSERTATIONS 58/2016

ISBN 978-952-60-6729-2 (printed)
ISBN 978-952-60-6730-8 (pdf)
ISSN-L 1799-4934
ISSN 1799-4934 (printed)
ISSN 1799-4942 (pdf)
http://urn.fi/URN:ISBN:978-952-60-6730-8

Unigrafia Oy
Helsinki 2016

Finland

441 697
Printed matter

Aalto University

Abstract

Aalto University, P.O. Box 11000, FI-00076 Aalto www.aalto.fi

Author
Risto Vanhanen

Name of the doctoral dissertation
Quality Assurance Methods for Uncertainty Analysis in Reactor Physics with Applications

Publisher School of Science

Unit Department of Applied Physics

Series Aalto University publication series DOCTORAL DISSERTATIONS 58/2016

Field of research Engineering Physics

Manuscript submitted 17 November 2015 **Date of the defence** 29 April 2016

Permission to publish granted (date) 13 January 2016 **Language** English

☐ **Monograph** ☒ **Article dissertation** ☐ **Essay dissertation**

Abstract

The purpose of uncertainty analysis is to quantify the level of confidence one can have in calculated quantities of interest. In this respect, uncertainty is lack of confidence in the calculated values. In this Thesis uncertainty analysis is applied to reactor physics, which predicts the behavior of nuclear reactors based on radiation transport theories and nuclear data.

The motivation is mainly twofold. First, in order to assess reliability of the computed results all calculated quantities of interest should have representative uncertainty estimates. Second, in its recent Regulatory Guides on Nuclear Safety the Finnish Radiation and Nuclear Safety Authority allows, instead of conservative estimates, the usage of realistic, best-estimate values of safety parameters augmented by uncertainty estimates.

There are different sources of uncertainty and it is not always a priori obvious which of the components dominate the uncertainties in the quantities of interest. Therefore, an estimate for each component should be provided. It is usually presumed that uncertainty in nuclear data is the largest source of uncertainty. In this Thesis, this is verified in a few simple cases.

In the course of the work some of the present uncertainty estimates of nuclear data were found to be mathematically and physically improper. The noted improper qualities were non-positivity, that is, negative generalized variances, and inconsistency with respect to the sum rules of nuclear data. This is a problem in quality of the data and of prime importance since the results of calculations are at most as good as data used in them.

The problem in quality of the data was solved by developing and proposing quality assurance methods to detect improper covariances, and by developing and proposing methods to find nearby more proper energy-dependent covariances and methods to find the nearest proper covariances in multigroup form.

There are several nuclear data evaluation projects in the world. Their evaluated nuclear data have discrepancies. The best-estimate values might differ or the nuclear data community does not agree on how well a piece of nuclear data is known. This is another quality assurance issue, which is considered in this Thesis.

The most important practical implications of the work presented in this Thesis are introduction of quality assurance methods that can be and were implemented as computer routines and used to detect certain improper properties of covariances of nuclear data as a part of quality assurance programs. The other methods can be used to remove these improper components with minimal changes to the covariances of nuclear data. The methods have also other potential applications such as verifying that covariances of fission yields retain proper normalization.

Keywords quality assurance, uncertainty analysis, sensitivity analysis, nuclear data, covariance, positivity, consistency

ISBN (printed) 978-952-60-6729-2 **ISBN (pdf)** 978-952-60-6730-8

ISSN-L 1799-4934 **ISSN (printed)** 1799-4934 **ISSN (pdf)** 1799-4942

Location of publisher Helsinki **Location of printing** Helsinki **Year** 2016

Pages 149 **urn** http://urn.fi/URN:ISBN:978-952-60-6730-8

Tekijä
Risto Vanhanen

Väitöskirjan nimi
Laadunvarmistusmenetelmiä epävarmuusanalyysille reaktorifysiikassa sovelluksineen

Julkaisija Perustieteiden korkeakoulu

Yksikkö Teknillisen fysiikan laitos

Sarja Aalto University publication series DOCTORAL DISSERTATIONS 58/2016

Tutkimusala Teknillinen fysiikka

Käsikirjoituksen pvm 17.11.2015 **Väitöspäivä** 29.04.2016

Julkaisuluvan myöntämispäivä 13.01.2016 **Kieli** Englanti

☐ **Monografia** ☒ **Artikkeliväitöskirja** ☐ **Esseeväitöskirja**

Tiivistelmä

Epävarmuusanalyysin tarkoitus on määrittää, kuinka hyvin laskettuihin suureisiin voi luottaa. Tässä mielessä epävarmuus on luottamuksen puutetta laskettuja arvoja kohtaan. Tässä väitöksessä epävarmuusanalyysiä sovelletaan reaktorifysiikkaan. Reaktorifysiikassa ennustetaan ydinreaktoreiden toimintaa säteilyn kuljetusteorioiden ja ydinvakiotietojen pohjalta.

Työ on mielenkiintoinen lähinnä kahdesta syystä. Ensinnäkin, laskettujen arvojen luotettavuuden määrittämiseksi tulee arvioida laskettujen arvojen epävarmuutta. Toiseksi, säteilyturvakeskus sallii nykyisissä ydinturvallisuusohjeissaan turvallisuusanalyysien tekemisen käyttäen turvallisuusparametrien parhaita arvioita niin sanottujen konservatiivisten arvioiden sijasta, kunhan tulosten epävarmuudet arvioidaan.

Useat eri asiat aiheuttavat epävarmuutta, eikä ennalta ole aina selvää mikä epävarmuuden lähde hallitsee laskettujen suureiden epävarmuuksia. Tästä syystä jokaisen epävarmuuden lähteen suuruus täytyy arvioida. Usein oletetaan, että ydinvakiotietojen epävarmuus aiheuttaa eniten epävarmuutta. Tässä väitöksessä asia varmistetaan muutamassa yksinkertaisessa tapauksessa.

Työn aikana huomattiin, että jotkin nykyiset ydinvakioiden epävarmuusarviot olivat matemaattisesti ja fysikaalisesti epäsopivia. Havaitut puutteet olivat epäpositiivisuus, eli eräänlaisesti yleistettyjen varianssien negatiivisuus, ja sisäinen ristiitaisuus ydinvakioiden yhteenlaskusääntöjen suhteen. Kyseinen tiedon laatuun liittyvä ongelma on tärkeä, koska laskujen lopputulokset ovat korkeintaan niin hyviä kuin laskuissa käytetyt tiedot.

Tietojen laatuun liittyvä ongelma ratkaistiin kehittämällä ja ehdottamalla laadunvarmistusmenetelmiä, joilla voi huomata epäsopivat kovarianssit. Lisäksi kehitettiin ja ehdotettiin menetelmiä, joilla pystyy etsimään läheisiä laadukkaampia energiasta riippuvia kovariansseja sekä läheisimpiä vaaditut ominaisuudet täyttäviä moniryhmävakioiden kovariansseja.

Maailmassa on monia ydinvakiotietoja arvioivia ryhmiä. Heidän suosittelemissaan ydinvakioissa on eroavaisuuksia. Parhaat arviot voivat erota, tai näkemys siitä kuinka hyvin kyseinen ydinvakio on tunnettu voi erota. Työssä pohditaan myös tätä laadunvarmistuskysymystä.

Työn tärkeimmät käytännölliset seuraukset ovat mainittujen laadunvarmistusmenetelmien luominen ja käyttöön ottaminen. Menetelmät voidaan toteuttaa ja toteutettiin tietokoneohjelmina. Menetelmiä voidaan käyttää laadunhallinnan osana. Muita ehdotettuja menetelmiä voidaan käyttää epäsopivien ominaisuuksien poistamiseen siten, että muutokset kovariansseihin ovat mahdollisimman pieniä. Menetelmillä on myös muita mahdollisia sovelluskohteita kuten sen tarkistaminen, että fissiotuottojen kovarianssit säilyttävät näiden normalisaation.

Avainsanat laadunvarmistus, epävarmuusanalyysi, herkkyysanalyysi, ydinvakiotiedot, ydinvakiot, kovarianssi, positiivisuus, sisäinen ristiriidattomuus

ISBN (painettu) 978-952-60-6729-2 **ISBN (pdf)** 978-952-60-6730-8

ISSN-L 1799-4934 **ISSN (painettu)** 1799-4934 **ISSN (pdf)** 1799-4942

Julkaisupaikka Helsinki **Painopaikka** Helsinki **Vuosi** 2016

Sivumäärä 149 **urn** http://urn.fi/URN:ISBN:978-952-60-6730-8

Preface

The work presented in this Thesis was carried out in the Fission and Radiation Physics Group at the Department of Applied Physics in Aalto University. The topic for this Thesis did not emerge within the group: I am grateful to Anssu Ranta-aho from TVO, instructor of my Master's Thesis, for remarking that uncertainties in physical quantities can be taken into account even in complex calculations. In retrospect, without regrets, I should have known that.

This work would probably not have been possible without the long-term funding from the YTERA Doctoral Programme for Nuclear Engineering and Radiochemistry. I thank former group leader, professor emeritus Rainer Salomaa for providing this funding. I am also obliged to present group leader, professor Filip Tuomisto for his guidance towards the end of the dissertation process.

My instructor, Dr. Jarmo Ala-Heikkilä, deserves my gratitude for giving feedback on many manuscripts and teaching me English. I am indebted to Dr. Pertti Aarnio for his feedback on many manuscripts and both challenging and supporting my ideas. For many good moments and discussions, I thank also the rest of the research group: Aapo, Aarno, Eric, numerous summer students and other past members; Dr. Maria Pusa from VTT; and members of the Fusion group with whom we shared common premises for a long time.

Typing and otherwise working towards this Thesis would have been a different experience without many pieces of at least somehow free software. I appreciate the work of the people behind LaTeX, Octave, gcc, Valgrind, Linux, BLAS, LAPACK, OpenOffice, many smaller programs, and the programs shared via OECD/NEA Data Bank. I also appreciate the nuclear data evaluation projects that have made and kept their data publicly available – I hope my contribution will help to make the data even

better.

I am grateful to the preliminary examiners Dr. Gašper Žerovnik from Jožef Stefan Institute and Docent Anu Kankainen from University of Jyväskylä for their careful work and feedback on this manuscript. In advance, I thank professor Guillem Cortés from Politechnical University of Catalonia (UPC) for acting as my opponent in the[1] defense of this Thesis.

I thank my parents, Jaana and Pekka, and sister, Satu, for all their love and support so far. Finally, I thank my beloved better half Minna for everything else.

Espoo, January 15th, 2016,

Risto Vanhanen

[1] Hopefully successful.

Contents

List of Publications

This thesis consists of an overview and the following publications which are referred to in the text by their Roman numerals.

I R. Vanhanen. Computing positive semidefinite multigroup nuclear data covariances. *Nuclear Science and Engineering*, 179, *4*, 411–422, April 2015; http://dx.doi.org/10.13182/NSE14-75.

II R. Vanhanen. Computing more consistent multigroup nuclear data covariances. *Nuclear Science and Engineering*, 181, *1*, 60–71, September 2015; http://dx.doi.org/10.13182/NSE14-105.

III R. Vanhanen. Computing more proper covariances of energy dependent nuclear data. *Nuclear Engineering and Design*, 297, 148–157, February 2016; http://dx.doi.org/10.1016/j.nucengdes.2015.11.026.

IV R. Vanhanen and M. Pusa. Survey of prediction capabilities of three nuclear data libraries for a PWR application. *Annals of Nuclear Energy*, 83, 408–421, September 2015; http://dx.doi.org/10.1016/j.anucene.2015.03.044.

V R. Vanhanen. Uncertainty analysis of infinite homogeneous lead and sodium cooled fast reactors at beginning of life. *Nuclear Engineering and Design,* SI: NENE, 283, 168–174, March 2015; http://dx.doi.org/10.1016/j.nucengdes.2014.06.023.

Author's Contribution

The author is the sole author of the present Thesis and Publications I–III and V. The author's role in Publication IV is described below.

Publication IV: "Survey of prediction capabilities of three nuclear data libraries for a PWR application"

The author surveyed the status of the uncertainty estimates in nuclear data libraries, processed the necessary covariances of nuclear data to multigroup form, apportioned the propagated uncertainties to uncertainties of individual reactions and analyzed the results, wrote most of the article, and corresponded with the referees. The second author selected the test cases, computed sensitivity profiles and propagated the uncertainties using a code previously developed by her, and participated in writing the article.

1. Introduction

A prediction is a statement about future events. A useful prediction is only rarely certain, regardless of the scope and fidelity of the process that led to the prediction. Therefore, it is worthwhile to estimate how confident one is that the predicted events will occur. It is the purpose of uncertainty analysis to quantify this level of confidence [1]. The lack of confidence is referred to as uncertainty. The amount of uncertainty that can be tolerated in the predictions is application specific.

Uncertainty analysis can be applied to any field. Many fields are needed to predict behavior of nuclear reactors: reactor physics is essential for all reactors; thermal-hydraulics, heat transfer, and fields relevant to fuel behavior need to be considered for all but zero-power reactors. For safety analysis in accident situations even more fields, such as structural mechanics, might be relevant [2]. However, in this Thesis only applications to reactor physics are considered. In reactor physics the behavior of nuclear reactors is predicted based on radiation transport theories and nuclear data, which describe interaction of radiation with matter [3].

The results of calculations are at most as good as the data used in them and uncertainty analysis is not an exception. Uncertainties in nuclear data are a major source of uncertainty. Therefore, quality of the uncertainty estimates of nuclear data is of prime importance. Uncertainties in nuclear data are usually represented as covariances, which should have certain properties mandated by probability theory and physical constraints [4]. However, in practice the evaluated nuclear data files contain covariances that do not have these properties. If the covariances used in uncertainty analysis severely violate these properties, the results of uncertainty analysis are questionable, at the best. Proper quality assurance programs should detect improper data so that, for example, erroneous estimates of confidence in safety parameters are not trusted upon when assessing plant safety.

1.1 Background

Electricity generating nuclear power reactors are typically used to produce steam, which is used to drive conventional steam turbines. The turbines are coupled to a generator that produces electricity. The steam might be produced directly in a reactor like in, e.g., boiling water reactors and present graphite moderated water cooled reactors, or indirectly in heat exchangers like in, e.g., pressurized water reactors, gas cooled reactors and various fast neutron spectrum reactors. There are also reactors that are used for other peaceful purposes: ship propulsion, isotope production, medical irradiation, and research, for example [5]. Peaceful use of nuclear energy is typically regulated. In order to ensure that reactor operation is safe, it is necessary to demonstrate that the probability for a large radiation emission is very, very low and as low as practically possible. This is achieved through various safety analyses that are specific to plant-type, plant and operating cycle [2, 6, 7].

Until recently, the Finnish Radiation and Nuclear Safety Authority (STUK) required that safety analyses must be performed using conservative methods, in which the computational models and their parameter values are deliberately chosen to be those that yield the worst possible outcomes [6]. However, it is not always straightforward which parameter combinations yield the worst possible outcomes and, when several safety parameters are estimated simultaneously, conservative parameter values might not exist [2, 6, 7]. Therefore, the present safety standards of International Atomic Energy Agency (IAEA) recognize safety analysis based on realistic best-estimates of the safety parameters as an acceptable option as long as uncertainties in the predicted values of the safety parameters are estimated. This "best-estimate plus uncertainty" approach is also accepted in the 2013 version of the Regulatory Guides on Nuclear Safety (YVL) of the Finnish Radiation and Nuclear Safety Authority [8].

1.2 History

The procedures to generate uncertainty estimates for nuclear data were first widely discussed in the 1970s and 1980s [9]. A format to encode these in the evaluated nuclear data files, which were and are used to distribute estimates of nuclear data, was designed in 1973 prior to which the only method to include uncertainty estimates was through human-readable

documentation [10]. The first uncertainty estimates of nuclear data were released in 1975 for three materials and by 1985 there were uncertainty estimates for 24 materials [11]. The activity languished during the 1990s due to constrained resources and limited interest by users [12].

The interest of nuclear researchers, industry and regulators returned in this millennium with increasing demand for confidence bounds for model predictions [13]. Subsequently, there has been a proliferation of uncertainty estimates for nuclear data. The Japanese efforts for sodium cooled fast reactors resulted in uncertainty estimates for twenty relevant materials, which were released in 2002 [14]. The following release in 2011 contained uncertainty estimates for 95 materials [15]. The European collaboration resulted in 37 materials with uncertainty estimates in 2005 [16]. The work in the United States resulted in uncertainty estimates for 26 and 190 materials in 2006 and 2011, respectively [17, 18]. In addition, the American effort provided low-fidelity uncertainties for almost all of their 393 evaluated materials in 2008 [19]. These are intended to be replaced with high-fidelity uncertainty estimates in the future. The TALYS-based evaluated nuclear data library should also be mentioned for its paradigm in nuclear data evaluation [20]. It has resulted in even-quality uncertainty estimates for over 2000 materials above the energy region of resolved resonances.

1.3 Recent and related activity

The Nuclear Energy Agency of the Organisation for Economic Co-operation and Development (OECD/NEA) has a Nuclear Science Committee. The Nuclear Science Committee launched an expert group on Uncertainty Analysis in Modelling in 2005. In the following year, this resulted in a benchmark called “Uncertainty Analysis in Best-Estimate Modeling for Design, Operation and Safety Analysis of LWRs”, which focused on light water reactors – the most commonly employed power reactor type [13, 21, 22]. The benchmark covers fields relevant in neutronics calculations, thermal-hydraulics modeling and fuel behavior. Their combination provides additional challenges [23]. The example cases in Publication IV are exercises in this benchmark.

The Working Party on International Nuclear Data Evaluation Co-operation of the OECD/NEA Nuclear Science Committee established Subgroup 33 on “Methods and issues for the combined use of integral experiments

and covariance data" in 2009 [24]. Integral experiments provide indirect information about nuclear data, which must be assimilated to existing data in order to be useful. The procedure is generally called data adjustment and assimilation, and it can be used to calibrate models and, by the introduced new data, to improve their prediction capabilities [23]. However, the improvements are limited to systems that are similar to the system from which the integral data were measured.

IAEA's project "Global Assessment of Nuclear Data Requirements" aims to quantify the expected benefit of any nuclear data measurements in reducing the uncertainties of computed quantities of interest [25]. The ambitious work would result in useful guidance in determining which experimental data should be measured and which experimental techniques should be used. The project considers data from both differential experiments and integral experiments. However, the work requires the availability of a complete and consistent evaluation of nuclear data covariances. The covariance data in the present nuclear data libraries are really not adequate to serve as a uniform and consistent baseline for this kind of planning [25].

In addition, OECD/NEA has a programme called "Best Estimate Methods – Uncertainty and Sensitivity Evaluation" in the field of thermal-hydraulics [26]. Uncertainty analysis applied to thermal-hydraulics has also resulted in a few recent dissertations, e.g., Refs. [27, 28].

1.4 Terminology

The concept of uncertainty as a quantifiable attribute is historically relatively new although the concept of error and error analysis has long been understood [29]. The term "error" means difference between a value of a physical quantity and its true value although it is sometimes used to refer to a mistake or blunder [29, 30]. The term "uncertainty" means a measure of the lack of knowledge of the true value of a physical quantity [29]. Using "error" to refer to "uncertainty" causes confusion.

Positivity of variances and positive definiteness of covariance matrices and operators stem from the same physical argument. In cases where the data is at least partly redundant one talks about non-negativity of variances, positive semidefiniteness of covariance matrices and, confusingly, positivity of covariance operators. The distinction is made in Chapter 2 but, since only essentially finite dimensional operators are used in prac-

tice, subsequent chapters use mostly the terminology used with covariance matrices.

Uncertainty analysis can be performed using deterministic or statistical methods. A typical adjunct to uncertainty analysis is apportioning the uncertainty of a quantity of interest to uncertainties of parameters. In the context of statistical uncertainty analysis, this is referred to as "sensitivity analysis" [31]. However, in the context of deterministic uncertainty analysis "sensitivity analysis" means quantifying the effects of parameter variations on the quantities of interest [1]. It is hoped that the established dual use causes no confusion.

The methods presented in the Publications I–III are, in fact, algorithms since they terminate in a finite number of steps. While this is not an error, the inconvenient naming is solely the author's fault.

1.5 The main contributions of the Thesis

The main contributions of Publications I–III are quality assurance methods that can be used to verify whether evaluated covariances of nuclear data have certain properties or not. These can be used as a part of quality assurance programs. In addition, Publications I–III provide methods to compute nearby covariances that, depending on the details, either have the desired properties or at least violate the desired properties less.

The main contribution of Publication IV is the identification of several order-of-magnitude differences between different nuclear data libraries in uncertainty estimates of nuclear data that have a significant contribution to uncertainties of certain quantities of interest regarding pressurized water reactors. The used methods can be interpreted as an estimation of world view uncertainty.

The main contributions of Publication V are the consideration of different sources of uncertainty and inclusion of nuclide concentration uncertainty in parameter uncertainty. The estimates of their magnitudes verified that the uncertainty due to uncertainties in nuclear data dominated, as expected, in the considered cases.

1.6 Organization of the Thesis

The intention in this Thesis is to provide an introduction to uncertainty analysis in reactor physics although many of the presented methods are

general. Contributions of the Publications I–V are pointed out but not completely rewritten here. Interested readers are referred to the appendices.

The remainder of this Thesis is organized as follows. In Chapter 2 concepts for physical quantities that allow quantifying their uncertainties are introduced. It is important to note that the interesting quantities in different systems are also physical quantities in this sense, and interpretation of uncertainties of quantities of interest follows directly from the introduced concepts. The scope of Chapter 3 is nuclear data and models in reactor physics. It comments on present uncertainty estimates of nuclear data and presents two salient models. Chapter 4 presents uncertainty analysis in a general manner but discusses it from reactor physics point of view. A categorization for different sources of uncertainty is proposed. Summaries of the Publications are presented in Chapter 5 and finally concluding remarks are given in Chapter 6.

2. Physical quantities

Arguably the simplest physical quantities are quantities whose value[2] is a single real number in appropriate units [32]. However, the knowledge of the value is always imperfect: even in these simple cases the values of the physical quantities can not be known exactly [1,23]. A consequence of this simple statement is that the lack of knowledge of the values of physical quantities needs to be addressed.

The lack of knowledge of the values of physical quantities is also referred to as uncertainty in the physical quantities. There are many approaches that can be used to address uncertainty in the physical quantities [2]. One approach is to quantify the lack of knowledge. One way to quantify it is to assign subjective levels of confidence for statements that claim the value to be within a certain interval. The levels of confidence can be interpreted as probabilities [33, 34]. In the limit of suitable intervals non-contradicting probabilities form a probability distribution [35].

The interpretation of levels of confidence as probabilities can be categorized as a subjective probability interpretation, since the assigned probabilities can vary between persons with at least slightly different knowledge of the physical quantity in question [23]. Indeed, in this work objectivity is assumed in the sense that any rational person with the same information should assign the same probabilities [34].

In this work the knowledge of the value of a physical quantity is conceptually modeled as a subjective probability distribution, which describes how probably the value of a physical quantity is within any interval. Section 2.1 covers the case of a single physical quantity, and Section 2.2 generalizes the notion for finite numbers of physical quantities. The intelligible and intuitive interpretation of levels of confidence for each interval is

[2]Sometimes *the true value of a quantity* is used in lieu of *the value of a quantity*, and the term "value" is reserved for less specific meaning.

lost for more complex physical quantities, such as quantities that depend on a parameter [36]. Unfortunately, such quantities are encountered in practice. A model for these is presented in Section 2.3.

2.1 A physical quantity

The knowledge of the value of a physical quantity can be modeled as a probability distribution that allows calculating probabilities that the value of the physical quantity is within a given interval. In this work it is required that the probability distribution has a probability density function, which limits the probability distribution to be a continuous probability distribution [37]. The requirement can be relaxed, if necessary, at the expense of referring to a slightly more cumbersome cumulative distribution function rather than a probability density function.

To elaborate on probability density functions, consider a physical quantity α whose value is denoted by $\hat{\alpha}$. The probability that the value is within an interval $[\,a, b\,]$ is denoted by $\mathrm{P}[\,a \leq \hat{\alpha} \leq b\,]$. The probability density function is then defined as a non-negative function $p : \mathbb{R} \mapsto \mathbb{R}_0^+$ for which

$$\mathrm{P}[\,a \leq \hat{\alpha} \leq b\,] = \int_a^b p(\alpha)\, d\alpha. \tag{2.1}$$

Such a function exists as long as the assigned probabilities are not contradictory. It is conventional to assign 1 for $P[\,-\infty \leq \hat{\alpha} \leq \infty\,]$.

The first two moments of the distribution are commonly used in practice although their existence needs to be assumed. This restricts the possible probabilities that can be assigned. The first moment and the second central moment of the distribution are

$$\mathrm{mean}(\alpha) = \mathrm{E}[\,\alpha\,] \quad \text{and} \tag{2.2a}$$

$$\mathrm{var}(\alpha) = \mathrm{E}[\,(\alpha - \mathrm{E}[\alpha])^2\,], \tag{2.2b}$$

where the expectation operator, $\mathrm{E}[\,\cdot\,]$, maps functions to real numbers according to $\int_{-\infty}^{\infty} \cdot\; p(\alpha)\, d\alpha$ [38]. The first moment is also called mean, expected value, or best-estimate although the last name is susceptible to debate. The second central moment is positive, since the value of the physical quantity is not known. It is called variance and the positive square root of variance is standard deviation. The ratio of standard deviation to mean is called relative standard deviation.

Mean and standard deviation are indicators of the value of a physical quantity and its uncertainty, respectively. Sometimes these are the best

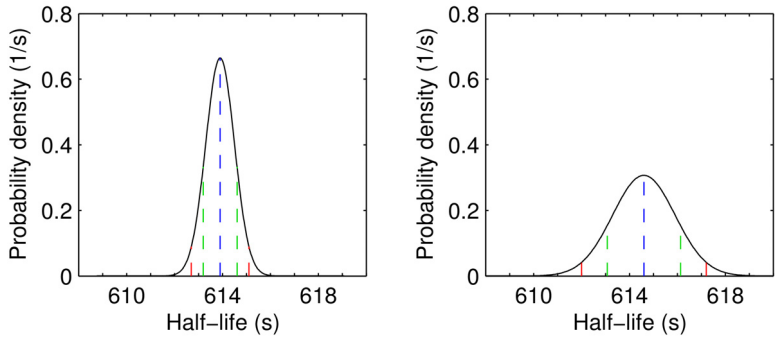

(a) `ENDF/B-VII.1` [18]. (b) `JEFF 3.1.1` [39].

Figure 2.1. Subjective distributions that describe the knowledge of the neutron half-life assuming that only the first two logarithmic moments and positivity to be known. The best-estimates differ slightly, and the knowledge in (a) is more certain than the knowledge in (b). The expected value is in shown in blue. There is about a $76.1\,\%$ ($95.4\,\%$) probability that the neutron half-life is between the green (red) bars.

indicators, particularly when the uncertainties are small [23]. The first two moments are illustrated in Fig. 2.1 for a physical quantity. Informally standard deviation may be referred to as uncertainty.

2.1.1 Characterizing the probability density function via experiments

In principle, the probability density function can be set arbitrarily, since the distribution is subjective. A more objective probability interpretation is required if it is required that, given the same information, any rational persons would assign the same probabilities. This requirement is highly encouraged. Information about physical quantities is obtained mostly from experiments [1].

In experiments a physical quantity, the measurand, is measured either directly or indirectly using a measuring instrument [1]. When the measurand is observed repeatedly, multiple measured values are obtained. In such a situation the frequentist probability interpretation, see e.g. Ref. [40], is straightforward [23]. In the interpretation, probability is seen as a relative frequency: the probability for the measured value to be within a given interval is determined, in principle, in the limit of infinite measurements [1]. In the frequentist view it is meaningless to assign a probability for the value of a physical quantity to be within an interval, since the unknown but fixed value of the physical quantity either is or is not in the given fixed interval. This is in contrast to the subjective

interpretation, where such a view is meaningful.

It is impossible to perform infinite measurements, and therefore even the probability distribution that describes the knowledge of the value of the measurand must be estimated. Type A estimation is based on statistical inference and Type B estimation on other, often subjective, means [29]. The decision on what properties to estimate is also subjective.

The most important features of measured values are the measures of location and dispersion [23]. The location is an indicator of the value of the measurand while the dispersion is an indicator of the non-reliability of the measurement [29]. The location of measured values is usually best described by mean, while their dispersion appears to be best described by standard deviation [23]. Therefore, the subjective choice is typically to estimate moments of the distribution although only the first few can be estimated. After estimating the first few moments there is considerable freedom in assigning the probabilities. This is a reason for modeling the knowledge of values of physical quantities as subjective rather than objective probability distributions. In fact, even if all moments of the distribution would be deduced, these would not fully specify it without further information [41].

Objectivity in decisions may be partially remedied by using the principle of maximum entropy [42, 43]. The maximum entropy principle states that after arbitrary properties of the distribution are specified, the distribution that contains least other information is the one with the largest entropy. Entropy has a direct relationship to information theory [44]. It should be noted that not specifying a known property of the distribution is a subjective decision to disregard the information that describes such a property.

2.1.2 Specific maximum entropy probability distributions

Consider a physical quantity α assuming that it has been measured and the mean μ and the standard deviation[3] σ of the observations have been inferred. Disregarding other information and applying the principle of maximum entropy results in a normal distribution [45]. Its probability density function is

$$p(\alpha) = \frac{1}{\sqrt{2\pi\sigma^2}} \exp\left(-\frac{(\alpha-\mu)^2}{2\sigma^2}\right). \tag{2.3}$$

[3]In reactor physics, the symbol σ is used to denote a physical quantity called microscopic cross section. It is hoped that this dual use causes no confusion.

In some cases, the values of physical quantities are inherently non-negative. If non-negativity, mean, $m = \mathrm{E}[\ln(\alpha)]$, and variance, $v^2 = \mathrm{E}[(\ln(\alpha) - m)^2]$, of the logarithms of the measured values are considered as all available information, the principle of maximum entropy results in a log-normal distribution [45]. Its probability density function is

$$p(\alpha) = \frac{1}{\sqrt{2\pi v^2 \alpha^2}} \exp\left(-\frac{(\ln(\alpha) - m)^2}{2v^2}\right), \quad \alpha > 0\,. \tag{2.4}$$

In terms of mean, μ, and variance, σ^2, of the measured values, the parameters m and v^2 are $\ln(\mu^2/\sqrt{\sigma^2 + \mu^2})$ and $\ln(\sigma^2/\mu^2 + 1)$, respectively [46].

These probability distributions are commonly used to describe the knowledge of values of physical quantities. The distributions are equivalent in the limit of diminishing relative uncertainty [30]. For example, the distributions in Fig. 2.1 are log-normal but equivalent normal distributions are indistinguishable for the eye.

It should be emphasized that usually some information has been disregarded before a specific probability density function is obtained. For inclusion of other information such as support on a bounded interval, or non-negativity and first two moments, see for example Ref. [45].

2.1.3 Probability distributions and random variables

Mathematically, each probability distribution describes a random variable [37]. Therefore, the approach in this work is to model the knowledge of the value of a physical quantity as a random variable. However, the concept of the random variable is unnecessary for the application. The natural language is misleading here, and it is emphasized that physical quantities are not inherently random, since physical quantities are characterized by a single unique value [29, 32].

However, the model of the knowledge of the values of physical quantities as probability distributions is not limited to physical quantities. The model is applicable to any variable, whose values vary with statistical regularity, that is, whose values can be measured and the measured values can be modeled as a probability distribution [1]. In such a case, the distribution describes both the knowledge of the variable and its statistical nature – the uncertainty is partly aleatory, which can not be removed since it is inherent in the variable [47]. In the case where the statistical nature of the variable dominates the distribution, the word “random variable” has its non-technical meaning.

2.2 Multiple physical quantities

The notion of the knowledge of the value of a physical quantity can be generalized for many but a finite number of physical quantities. Consider k physical quantities α_1 through α_k. It is useful to concatenate these into a vector $\alpha = (\alpha_1, \ldots, \alpha_k)^\mathsf{T}$. Their values are denoted by $\hat{\alpha} = (\hat{\alpha}_1, \ldots, \hat{\alpha}_k)^\mathsf{T} \in \mathbb{R}^k$. Given k intervals whose lower and upper bounds are $a = (a_1, \ldots, a_k)^\mathsf{T} \in \mathbb{R}^k$ and $b = (b_1, \ldots, b_k)^\mathsf{T} \in \mathbb{R}^k$, respectively, the joint probability that each value is simultaneously within their respective interval is denoted by $\mathrm{P}[\, a \leq \hat{\alpha} \leq b \,]$, where the comparison is to be made component-wise. The joint probability density function is then a function $p : \mathbb{R}^k \mapsto \mathbb{R}_0^+$ for which

$$\mathrm{P}[\, a \leq \hat{\alpha} \leq b \,] = \int_{a_1}^{b_1} \cdots \int_{a_k}^{b_k} p(\alpha_1, \ldots, \alpha_k)\, d\alpha_1 \cdots d\alpha_k. \tag{2.5}$$

The first moment and the second central moment of the distribution are, assuming their existence,

$$\mathrm{mean}(\alpha) = \mathrm{E}[\, \alpha \,] \in \mathbb{R}^k \quad \text{and} \tag{2.6a}$$

$$\mathrm{cov}(\alpha, \alpha) = \mathrm{E}[\, (\alpha - \mathrm{E}[\alpha])(\alpha - \mathrm{E}[\alpha])^\mathsf{T} \,] \in \mathbb{R}^{k \times k}, \tag{2.6b}$$

where the expectation operator, $\mathrm{E}[\ \cdot\ ]$, maps functions to real numbers according to $\int_{-\infty}^{\infty} \cdots \int_{-\infty}^{\infty} \ \cdot\ p(\alpha_1, \ldots, \alpha_k)\, d\alpha_1 \cdots d\alpha_k$ [38]. The names of the first moments follow the case of a single quantity but the second central moment is called covariance matrix or variance-covariance matrix since its diagonal contains the variances and off-diagonals pairwise covariances. The positivity of the variances is generalized by the requirement of positive definiteness of the covariance matrix. Assurance of this property is considered in Publication I. Correlation matrix is a scaled covariance matrix, that is,

$$\mathrm{corr}(\alpha, \alpha) = \mathrm{diag}(\mathrm{std}(\alpha))^{-1}\, \mathrm{cov}(\alpha, \alpha)\, \mathrm{diag}(\mathrm{std}(\alpha))^{-1}, \tag{2.7}$$

where $\mathrm{std}(\alpha)$ is the vector of standard deviations. The operator $\mathrm{diag}(\ \cdot\ )$ transforms a vector into a non-surprising diagonal matrix and, when applied to a matrix, the diagonal of the matrix into a non-surprising vector. The inverse exists since the standard deviations are strictly positive for imperfectly known physical quantities. The correlation matrix has a unit diagonal and contains correlation coefficients, or correlations, in off-diagonals [48].

The difference to the case of a single physical quantity is that the knowledge of the value of a physical quantity can depend on the knowledge of

the values of other physical quantities. Sets of physical quantities that are mutually independent can be treated as separate sets of physical quantities that have absolute nothing to do with each other. Sets of mutually independent variables imply that the covariance matrix can be ordered to be a block diagonal matrix where each matrix on the diagonal consists of a single block. This is exploited in the computational method presented in Publication I.

Typical causes of the dependency between different physical quantities are the use of the same measuring instrument at the same or different time, the use of the same calibration device or reference value, the use of the same measuring method, and even measurements that are performed by the same experimenters [23, 30]. Also measuring multiple materials in a single experiment, like in integral experiments, causes dependencies [49]. Estimation of the dependency is not always straightforward [30].

The difference is manifested in the correlations. The correlation coefficient is a measure of the degree of linear dependence between the knowledge of the values of the two physical quantities. These vanish if the knowledge is independent but the converse is not necessarily true: vanishing correlations do not imply that the knowledge is independent [23]. More importantly: non-vanishing correlation implies a dependency, linear or non-linear, between the knowledge of values of physical quantities.

For example, consider two physical quantities that are believed to be positively (negatively) correlated. If the value of the first quantity is slightly larger than the expected value, then it is believed that the value of the second quantity is also slightly larger (smaller) than its expected value.

As with the case of a single physical quantity, the experimenters need to make subjective decision on which properties of the distribution to estimate. It should be noted that correlation does not provide a complete description of the dependencies of all physical quantities. It is merely a part of the second central moment, and third and higher moments could be, at least in theory, estimated.

Consider the k physical quantities and assume that the means μ and the covariance matrix[4] Σ have been estimated. Disregarding other information and applying the principle of maximum entropy results in a mul-

[4]In reactor physics, the symbol Σ is usually used to denote a physical quantity called macroscopic cross section. It is hoped that this dual use causes no confusion.

tidimensional normal distribution [45]. Its probability density function is

$$p(\alpha) = \frac{1}{\sqrt{(2\pi)^k \det(\Sigma)}} \exp\left(-\frac{1}{2}(\alpha-\mu)^\intercal \Sigma^{-1}(\alpha-\mu)\right), \tag{2.8}$$

where $\det(\Sigma)$ is the determinant of the covariance matrix. If it is assumed that the physical quantities are inherently non-negative, and the means, $m = \mathrm{E}[\,\ln(\alpha)\,]$, and the covariance matrix, $V = \mathrm{E}[\,(\ln(\alpha)-m)(\ln(\alpha)-m)^\intercal\,]$, of the logarithms of the values have been estimated, the principle of maximum entropy results in a multidimensional log-normal distribution [45]. Its probability density function is

$$p(\alpha) = \frac{1}{\sqrt{(2\pi)^k \det(V) \prod_{i=1}^k \alpha_i^2}} \exp\left(-\frac{1}{2}(\ln(\alpha)-m)^\intercal V^{-1}(\ln(\alpha)-m)\right), \tag{2.9}$$

where $\alpha > 0$ component-wise. In terms of the means, μ, and covariance matrix, Σ, of the non-logarithmized values, the parameters m and V are $\ln(\mu^2/\sqrt{\mathrm{diag}(\Sigma)+\mu^2})$ and $\ln(\mathrm{diag}(\mu)^{-1}\Sigma\,\mathrm{diag}(\mu)^{-1}+1)$, respectively [46]. Here the logarithm, power, division and square root are applied component-wise and the "1" is a matrix of ones. The inverses exist since the average of measured values of imperfectly known inherently non-negative physical quantities are positive.

The author is not aware of transformation formulae for the case that inherently non-negative and unconstrained physical quantities are correlated. In such a case one can first take the logarithms of the measured values of the inherently non-negative physical quantities and then compute the means and covariance matrix.

2.3 Physical quantities that depend on a parameter

The notion of the knowledge of the value of a physical quantity is much less straightforward to generalize for a physical quantity that depends on a parameter[5] than for a finite number of physical quantities. The details depend on the cardinality of the parameter. Here it is assumed that the parameter has the cardinality of either a rational or a real number. These include parameters that depend on a finite number of rational or real numbers, respectively. Parameters with the cardinality of a finite set are equivalent to the case of multiple physical quantities and are not

[5] An intended application is, for example, a piecewise continuous cross section, whose parameter is energy. Such quantities are usually measured indirectly. The discussion is still kept at a general but practical level.

reconsidered here.

In this work the physical quantities that depend on a parameter are referred to as physical functions. In probability theory, the generalizations are called random functions [50–54]. A random function can be understood as a collection of random variables whose cardinality is the same as that of the parameter. For a fixed value of the parameter, the random function reduces to a random variable. When physical functions are smooth enough, e.g., continuous, they can be described by a countable number of random variables [51]. As with the finite dimensional cases, one usually assumes a finite variance for the random functions [51].

A problem with the theory is that the probability density function does not exist in general [36], and the definition via the system of all finite distribution functions is awkward. This makes the interpretation of a random function considerably harder than the interpretation of multiple of physical quantities. There is, however, no technical reason not to consider physical functions as random functions.

Usually, physical functions are not measured directly although there are direct methods for certain cases. Therefore, the usual procedure is to perform an indirect measurement: a finite number of physical surrogate quantities that describe the physical function are measured [29, 30]. Consider k surrogate quantities, which are concatenated into the vector $\beta = (\beta_1, \ldots, \beta_k)^\intercal$, and for which the interpretation described by Eq. (2.5) holds. Consider also l physical functions $\alpha = (\alpha_1(x;\beta), \ldots, \alpha_l(x;\beta))^\intercal$ that depend on the surrogate quantities and the parameter x through the measurement model. Naturally the measurement model depends on the physical function and the chosen surrogate quantities [1]. The measurement model might also bring theoretical information to the results. However, the measurement model is always an idealization and therefore introduces additional uncertainty, which must be accounted for. The probabilistic nature of these physical functions is completely determined by the surrogate quantities, and therefore they are effectively finite dimensional [55]. Interested readers are referred to Publication III and references therein.

The first two moments of the physical functions are

$$\operatorname{mean}(\alpha(x)) = \mathrm{E}[\,\alpha(x;\beta)\,] \quad \text{and} \tag{2.10a}$$

$$\operatorname{cov}(\alpha(x), \alpha(x')) = \mathrm{E}[\,\alpha(x;\beta)\alpha(x';\beta)^\intercal\,] - \mathrm{E}[\alpha(x;\beta)]\,\mathrm{E}[\alpha(x';\beta)^\intercal], \tag{2.10b}$$

where the expectation is taken over the surrogate quantities. The mean

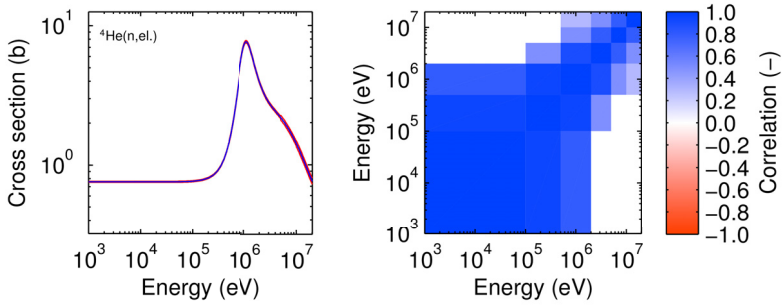

(a) Best-estimates. (b) Correlations.

Figure 2.2. Subjective distributions that describe the knowledge of the neutron elastic scattering cross section from $^4_2$He as a function of neutron incident energy and assuming that only the first two moments to be known. The cross section is well known. (a) The expected value is in shown in blue, and there is about a $99.4\,\%$ probability that the values of the cross section are between the red lines. (b) The correlations are mainly positive. Best-estimates from `ENDF/B-VII.0` [17] with the low-fidelity covariance data [19]. Figure adapted from Publication III.

is a function of the value of the parameter and belongs to a direct sum of l function spaces. A typical choice is direct sum of L^2-spaces. The covariance is a function of a pair of the values of the parameters and is a measure of the correlation between these values. The covariance belongs to a direct sum of $l \times l$ function spaces, which are, again, typically chosen to be L^2-spaces. The covariances form the kernel of a covariance operator. Since the operator effectively represents the surrogate quantities, it includes redundant data and should be positive rather than positive definite, i.e., the operator should have a non-negative spectrum. Again, correlations are scaled covariances, that is,

$$\operatorname{corr}(\alpha(x), \alpha(x')) = \operatorname{diag}(\operatorname{std}(\alpha(x)))^{-1} \operatorname{cov}(\alpha(x), \alpha(x')) \operatorname{diag}(\operatorname{std}(\alpha(x')))^{-1} \tag{2.11}$$

for all x and x'. Here $\operatorname{std}(\alpha(x))$ contains the standard deviations. The inverse exists since the standard deviations are strictly positive for imperfectly known physical quantities. The first two moments are illustrated in Fig. 2.2 for a single physical function for which the dependent parameter is energy.

The choice of surrogate quantities is naturally subjective and has an effect on the resulting physical function. The subjectivity of the choice is, however, common to all physical quantities that are measured indirectly. The author is not aware that the principle of maximum entropy would have been applied to random functions.

3. Nuclear data and models in reactor physics

Physical quantities that describe interactions between neutrons or gamma radiation and matter, and physical quantities that describe properties of radioactive nuclei and neutrons are referred to as nuclear data in reactor physics. In this work gamma radiation is not considered further. The main reason for this is the lack of uncertainty estimates for its interaction data in the general-purpose nuclear data libraries.

Nuclear data are most often measured in differential experiments, which are predominantly compiled in the Experimental Nuclear Reaction Data (EXFOR) database[6] [56]. Additionally, data from criticality experiments are compiled by the International Criticality Safety Benchmark Evaluation Project [57]. Even more data are available from various other integral experiments, which include operating reactors. Usually, the integral data are not utilized since their usage would inevitably lead to dependencies between physical quantities. However, the experimental data are not usable for reactor physics without an evaluation, which is a process of analyzing experimental data and theoretical predictions in order to form a, presumably subjective, distribution that describes the evaluators' knowledge of the nuclear data [11].

Evaluations that cover all relevant nuclear data for a material are called, simply and confusingly, evaluations. The materials are usually nuclides, i.e., individual species of nuclei, but might be, for example, certain isomer of a nuclide, natural element of several isotopes or, a nuclide bound in a chemical compound.

A nuclear data library contains a collection of evaluations. The collection is usually validated as a whole against selected integral experiments.

[6]The EXFOR database has for long had the possibility to include variances of experimental results [25]. However, the possibility to include correlations was implemented only recently [56]. Therefore, any correlations in the older data sets must be collected from possible documentation or crudely estimated if the former is not possible.

There are several evaluation projects in the world that maintain a nuclear data library. The projects are not completely independent since there are collaboration and data exchange between the projects. Sometimes individual evaluations are taken as-is from the other projects. It should be emphasized that in uncertainty analyses the used data defines the results. Therefore, the quality of the characterization of nuclear data is of prime importance in uncertainty analyses in reactor physics [23].

The canonical format in which evaluations are presented is the evaluated nuclear data file format, which is currently at its sixth version and abbreviated as ENDF-6 format [11]. Despite format changes, extensions and improvements, the format has certain historical design limitations, which restrict the subjective beliefs that the evaluators can express. Therefore the evaluated nuclear data files contain only approximations of the evaluators' knowledge of nuclear data. It has been proposed that the ENDF-6 format should be replaced by a new generalized nuclear data, GND, format [58, 59]. Although more flexible and extensible, the proposed format will not, at its present version, remove all design limitations.

It is important to note that, irrespective of the format, individual evaluations contain approximations of evaluators' subjective knowledge of nuclear data. Even though any rational persons with the same information would come to the same conclusions about the nuclear data, the evaluators do not possess the same information and conclusions may be biased due to evaluators' reasoning and personal choices. Therefore, if desired, it is usually possible to obtain another opinion by using an evaluation from another nuclear data library. Differing evaluations can be seen as differing world views. Sometimes the differences are in the best-estimate values, and sometimes the best-estimate values are surprisingly close to each other but the evaluations lack agreement on how well the physical quantities are known. In Publication IV several order-of-magnitude differences between world views of important pieces of nuclear data of a few nuclear data libraries were identified.

Three general-purpose nuclear data libraries contain a considerable number of evaluations with uncertainty estimates: the United States evaluated nuclear data file, ENDF/B [18], OECD/NEA Data Bank coordinated joint evaluated fission and fusion file, JEFF [60], and Japan evaluated nuclear data file, JENDL [15]. In addition, the low-fidelity covariance project [19] should be mentioned for its completeness in covariance data, and the TALYS-based evaluated nuclear data library, TENDL [20], for its complete-

ness and paradigm in evaluation of nuclear data above energy region of resolved resonances. Other present general-purpose nuclear data libraries contain mostly best-estimates only.

Reactor physics uses nuclear data from nuclear data libraries, design parameters and sometimes other parameters to predict the behavior of nuclear reactors. These are all physical quantities. The computational chain in reactor physics contains many phases from evaluated nuclear data files, design parameters and other data to the relatively few quantities that describe the safety and behavior of the modeled physical system. Nuclear data for reactor physics are described in Section 3.1. In addition, the detection and interpretation of improper covariances of nuclear covariance data are described. The definition of multigroup nuclear data covariances is clarified since there has been some confusion. In Section 3.2, the most common models in reactor physics are described.

3.1 Nuclear data in reactor physics

3.1.1 Nuclear reactions

A binary nuclear reaction occurs when two nuclear particles – two nuclei or a nucleus and a subatomic particle, e.g., a neutron – interact causing a change in at least one nucleus [5]. Interactions not involving a neutron and interactions involving more than two nuclear particles are not relevant to the present work. The standard definition does not regard elastic scattering as a nuclear reaction but due to its importance in reactor physics it will be referred to as such.

The nuclear reactions that are relevant in reactor physics involve a neutron and a nucleus.[7] The reactions can be considered to occur predominantly in three ways. *The first way* is the compound nucleus formation [62] where the interacting particles form an unstable compound nucleus, which decays by emitting one or more particles. The formation of the compound nucleus is much more probable if the energies of interacting particles correspond to an excited state of the compound nucleus. These energies are called resonance energies. For nucleus-neutron interactions resonance energies are typically within typical energies of neutrons in re-

[7] The following description is from reactor physics point of view and considerably simplified compared to nuclear physics. See, for example, Ref. [61], and references therein for a more complete description.

actors. *The second way* is direct reaction, which is more likely to occur when the wavelength of the neutron is smaller than the wavelength of the nucleus [49]. In such a case, the compound nucleus is not formed. This occurs for relatively high-energy neutrons in reactors. *The third way* is more likely to occur when the wavelength of the neutron is comparable to the interatomic spacing, and the neutron interacts with an aggregate of bound nuclei instead of a single nucleus [3]. If the bound nuclei have a regular structure, this gives rise to neutron diffraction. This occurs for relatively low-energy neutrons in reactors. Alternatively, the reactions can be classified by the number of intranuclear collisions [49, 61].

The most relevant nuclear reactions in reactor physics are the fission, radiative capture and elastic scattering reactions. *In a fission reaction* the nucleus splits into two or more smaller nuclei, called fission products, a number of prompt neutrons and gamma radiation. The fission products are unstable and decay usually by beta emission and subsequent gamma radiation. Sometimes a neutron is emitted in the beta decay chain. These are important for reactor control and are called delayed neutrons to differentiate them from the prompt neutrons. In fissions, energy is released and it is divided in a complex way between the emitted particles. Fissions may occur via compound nucleus formation or as direct reactions. *In a radiative capture reaction* a compound nucleus is formed. The compound nucleus decays by emitting gamma radiation. *An elastic scattering reaction* may undergo either by compound nucleus formation, which decays by neutron emission and leaves the target nucleus in its original state; by potential scattering, in which compound nucleus is not formed; or by neutron diffraction [3].

3.1.2 Resonance parameters and cross sections

A cross section is a measure of the interaction probability between an incident particle and a stationary target. Cross sections can be interpreted as the effective cross-sectional area of the target nucleus. For each material there are different cross sections for every reaction. Also, the interaction probabilities depend on the kinetic energy of the incident neutron. The cross section at energy E for reaction x of i'th material is denoted by $\sigma_{i,\mathrm{x}}(E)$. Therefore cross sections are physical quantities that depend on a parameter – the neutron energy.

In addition to cross sections that describe individual reactions, there are redundant cross sections that are linear combinations of their par-

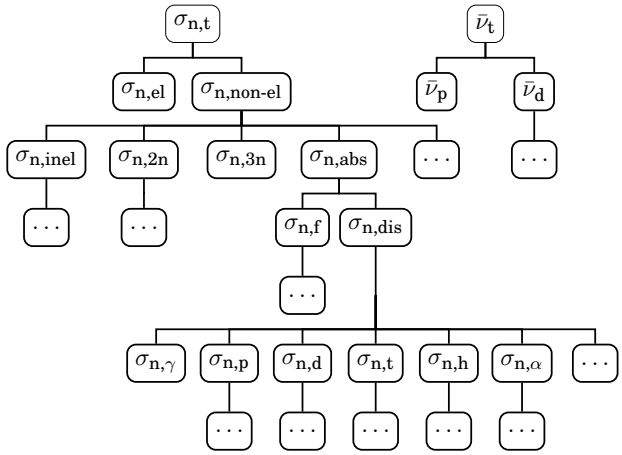

Figure 3.1. Part of the forest of redundancies of nuclear data according to the reaction model in ENDF-6. The trees for cross sections, σ, and average numbers of neutrons emitted from fissions, $\bar{\nu}$, are shown. The dots show where the trees are truncated. Parents are redundant nuclear data while children correspond to partial nuclear data. The sum coefficients are unity for all children. Figure adapted from Publication II.

tial cross sections. The linear combinations are often loosely referred to as sum rules. One such cross section is the total cross section that is a measure of probability that any interaction between the neutron and the nucleus will occur. These redundancies can be represented as a tree. The reactions defined in the ENDF-6 format are illustrated in Fig. 3.1. For covariances, this implies that covariances between the redundant cross section and its partials sum up to the self-covariance of the redundant cross section. This is illustrated in Fig. 3.2.

Resonance parameters are surrogate quantities of the cross sections in the low-medium energy region of the cross sections. These describe the resonance energy, and relative strengths of fission, radiative capture, elastic scattering, other reactions and other properties [12]. There is no predictive theory for neutron-induced reactions in the resonance energy range but resonance reactions can be well described by the R-matrix theory [63, 64]. In measurements some of the resonances can be resolved individually, some as averages over an energy interval and some remain completely unresolved. However, the resonance parameters themselves can not be measured directly, and are therefore already surrogate quantities of the actually measured physical quantities. Above the energy region described by resonance parameters the surrogate quantities can be average cross sections whose form is, perhaps, described by a nuclear model.

In the ENDF-6 format there is a possibility to encode the first two mo-

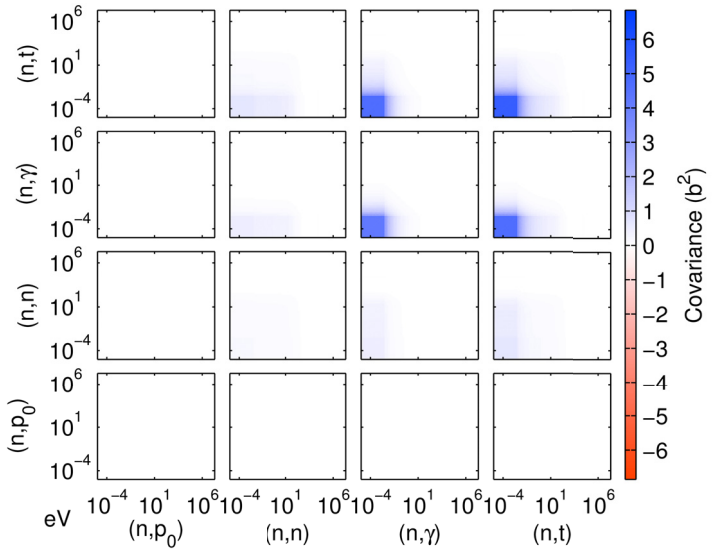

Figure 3.2. Multigroup averaged covariances of cross sections of $^{35}_{17}$Cl. The data are consistent in the sense that the sum of the first three columns give the fourth column. The corresponding sum rule is $\sigma_{\mathrm{n,t}} = \sigma_{\mathrm{n,p_0}} + \sigma_{\mathrm{n,n}} + \sigma_{\mathrm{n,\gamma}}$, since the covariances for other reactions are zero. These are absolute covariances and thus not scale free: depending on energy, the (n,$\mathrm{p_0}$) reaction is two or more orders-of-magnitude smaller than the total reaction, and hence its uncertainty is about two or more orders-of-magnitude smaller and barely visible at the best. Original data from `ENDF/B-VII.1` [18]. Figure adapted from Publication I.

ments of the evaluators' knowledge of the resonance parameters. However, the format does not allow resonance parameters of different materials to be correlated. For unresolved resonances this option is even more limited.

In reactor physical calculations the resonance parameters are only occasionally used directly, and usually the energy-dependent cross sections are constructed from the resonance parameters. In the `ENDF-6` format the first two moments of the evaluators' knowledge of the cross sections may be encoded with minor limitations. Any cross-reaction and cross-material correlations may be described. Any contributions from the resonance parameters to cross sections must be added to both the first moment and the second central moment. The present nuclear data libraries contain rather complete sets of uncertainty estimates for the most important materials and reactions.

3.1.3 Thermal neutron scattering laws

The chemical state does not considerably affect the high-energy cross sections of nuclei. However, at thermal energies bound nuclei behave differently from free nuclei. Therefore, the evaluations are prepared for individual nuclides and the low-energy portions of important nuclides in bound states are evaluated separately. However, only the first moment of the evaluators' knowledge of the latter quantities can be encoded in the ENDF-6 format, and no uncertainty estimates may be given in computer readable form.

3.1.4 Average number of emitted neutrons per fission

In a fission reaction zero or more neutrons are emitted. The average number of neutrons emitted from fission is an important parameter in reactor physics. It is a function of incident energy of the neutron that caused the fission, and hence a physical quantity that depends on a parameter. The average number of emitted neutrons per fission for i'th material is denoted by $\bar{\nu}_{i,\mathrm{x}}(E)$, where x stands for total, prompt, delayed or one of the delayed groups. The redundancies are illustrated in Fig. 3.1.

In ENDF-6 format their treatment is essentially identical to the treatment of cross sections. The first two moments of the evaluators' knowledge of the average number of neutrons emitted per fission can be described with minor limitations. Any cross-reaction and cross-material correlations may be described but cross-quantity correlations, e.g., correlation between a fission cross section and the average number of neutrons emitted from it, can not be described. This restriction is being lifted in the generalized nuclear data format [59]. The present nuclear data libraries contain rather complete sets of uncertainty estimates for the most important materials and reactions.

3.1.5 Angular distributions of emitted neutrons

Neutrons are emitted in many reactions, such as elastic and inelastic scattering, neutron duplication, and fission reactions. The neutrons might be emitted isotropically, i.e., equally probably to all directions, or some angles between the directions of motion of incident and emitted neutrons might be preferred. The angular distribution for neutrons emitted in reaction x that occurred at energy E in i'th material is denoted by $f_{i,\mathrm{x}}(\mu, E)\, d\mu$, which

is the probability that the emitted neutron will be emitted to interval $d\mu$ about an angle whose cosine is μ. This representation assumes azimuthal symmetry. Therefore the angular distribution is a physical quantity that depends on two parameters.

In theory, and some practical cases, the resonance parameters are surrogate quantities for angular distributions, i.e., the resonance parameters are used to calculate the angular distributions. In ENDF-6 format the evaluators can encode the first two moments with minor limitations although the description of the second central moment will be either long or approximative since essentially four-dimensional data are described. There is also a possibility to correlate cross sections and angular distributions. The present nuclear data libraries contain rather complete sets of uncertainty estimates for the most important materials and reactions. However, the general-purpose libraries contain no estimates for $^{1}_{1}$H, which is the most important moderator in light water reactions, and only one library contains an uncertainty estimate of $^{16}_{8}$O.

3.1.6 Energy distributions of emitted neutrons

Generally, the energy of the emitted neutrons is different from the energy of the incident neutron and may depend on the emission angle. The energy-angle distribution of the emitted neutrons in reaction x that occurred at energy E in i'th material is denoted by $p_{i,\mathrm{x}}(\mu, E \rightarrow E')\, d\mu dE'$, which is the probability that the emitted neutron will be emitted to interval $d\mu$ about an angle whose cosine is μ and within energy dE' about E'. Therefore the energy-angle distribution is a physical quantity that depends on three parameters.

In ENDF-6 format only the first moment of the evaluators' knowledge of the energy-angle distributions can be encoded. The second central moment can only be given to the angle-integrated version of the energy-angle distribution. The covariance must be encoded as piecewise constant in incident energies and there may be no correlation between different incident energy intervals.

Fortunately, in elastic and discrete inelastic scattering the angular distribution defines the energy distribution also, and for fission reaction the angular distribution is highly isotropic and insensitive to incident energies in the low-medium energies, so the use of the piecewise constant angle-integrated distribution is a good approximation. The present nuclear data libraries contain rather complete sets of uncertainty estimates for

neutrons emitted from the fission reactions of the most important materials but not for other reactions.

3.1.7 Other nuclear data

There are also other nuclear data that describe interactions between a neutron and matter and properties of radioactive nuclei.

The energy released in fission, and its division into fission products, prompt and delayed neutrons, gamma and beta radiation and neutrinos depend on the energy of the incident neutron that caused the fission. In ENDF-6 format their description, however, differs from the description of the cross sections. The first moment of the evaluators' knowledge of these quantities can be encoded rather freely but, essentially, the quantities are assumed to be independent. Implicitly, a correlation between the redundant full energy release and its components should be presumed. This interpretation is made if the heuristic characterization method from Publication II is used.

The yields[8] of fission products depend on the energy of the neutron that caused the fission. In ENDF-6 format the first moment of the evaluators' knowledge of the fission yields can be encoded with minor limitations: the quantities are assumed to be independent although it is known that on average very close to two fission products are yielded per fission. Inclusion of this knowledge makes the yields dependent and, conversely, for independent yields this knowledge is disregarded. As a result, a recent uncertainty analysis study did not include the normalization [65]. The method to find the nearest consistent covariance matrix, presented in Publication II, can be adapted to compute the nearest covariance matrix when this information is added. The method can use any of the norms presented in Publication III.

Radioactive decay data are physical quantities such as half-lives, branching ratios and decay energies for each decay branch. These are also used to describe spontaneous fission neutron yields, delayed neutrons and their emission spectra. In ENDF-6 format the first two moments of the evaluators' knowledge of these quantities may be encoded but, again, the quantities are assumed to be independent. The format proposes a correction that is a special case of methods presented in Publication II and III.

[8] Here the term "yield" refers to the independent yields and not to the cumulative yields, and the term "independent" is used in its statistical meaning.

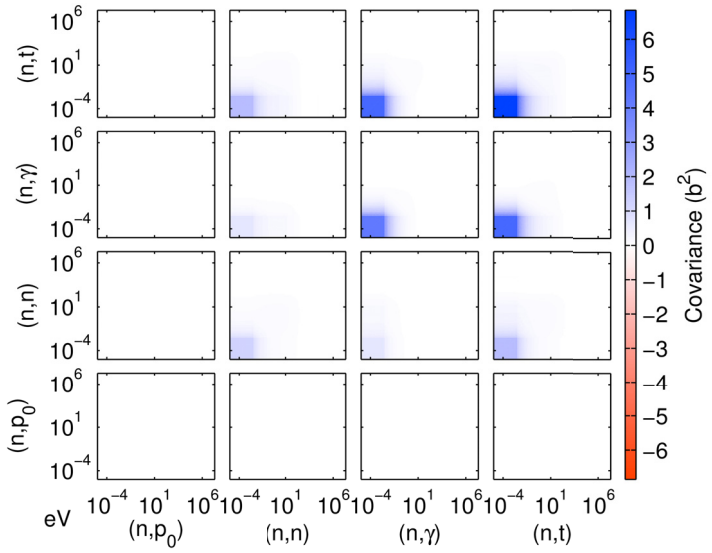

(a) The nearest positive semidefinite covariances.

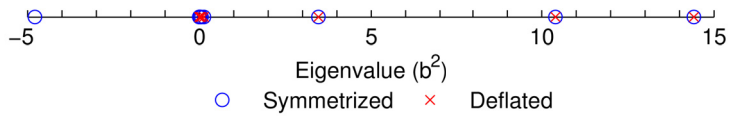

(b) Eigenvalues of the covariances before and after postprocessing.

Figure 3.3. (a) Multigroup averaged and postprocessed covariances of cross sections of $^{35}_{17}$Cl. (b) Eigenvalues of postprocessed ("deflated") and original ("symmetrized") covariances. The latter are presented in Fig. 3.2. Four negative eigenvalues were deflated, one of whose magnitude was large. Original data from `ENDF/B-VII.1` [18]. Figure adapted from Publication I.

3.1.8 Detecting and interpreting improper covariances of nuclear data

Probability theory requires the covariances to be a positive operator[9]. However, there are evaluations whose covariances have negative eigenvalues, which might manifest themselves as negative variances after uncertainty propagation. Publication I proposes a quality assurance method

[9]The redundancy of nuclear data is described by zero eigenvalues, so that the operator can not be positive. The remedy used in this work is to consider only a set of non-redundant reactions and interpret the redundant data as being derived from non-redundant data whenever necessary.

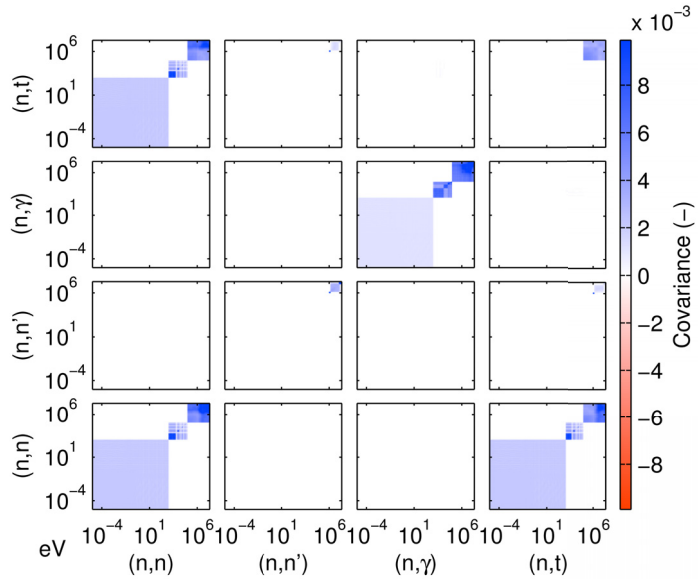

(a) Heuristically characterized covariances.

Figure 3.4. Multigroup averaged relative covariances of cross sections of $^{94}_{40}$Zr. The relative covariances are the absolute covariances scaled with inverses of best-estimates. Covariances with neutron duplication are omitted due to their small magnitude. Covariances whose absolute value is larger than 10^{-2} are shown with the extreme colors. The largest covariance is 0.4475. (a) The self-covariances, on the main block-diagonal, are the original data. The heurestic characterization method assigns the row sums as the cross-covariances with the total cross section. The end result is still inconsistent covariances. *(continues)*

that can be used to detect negative eigenvalues in covariances of multigroup averaged nuclear data. In Publication III a similar method is proposed for energy-dependent nuclear data in the ENDF-6 format. In addition, Publications I and III present a method to deflate the detected negative eigenvalues with minimal changes to the covariances. This is illustrated in Figs. 3.2 and 3.3.

The ENDF-6 format requires redundant nuclear data to be consistent with the sum rules of nuclear data. This implies, for example, that the total cross section must be the sum of elastic and non-elastic cross section or its partials if the non-elastic cross section is not present. Similarly, the self-covariances of total cross section should be the sum of cross-covariances between total and elastic reactions, and total and non-elastic covariances. Again, the covariance between total and non-elastic cross

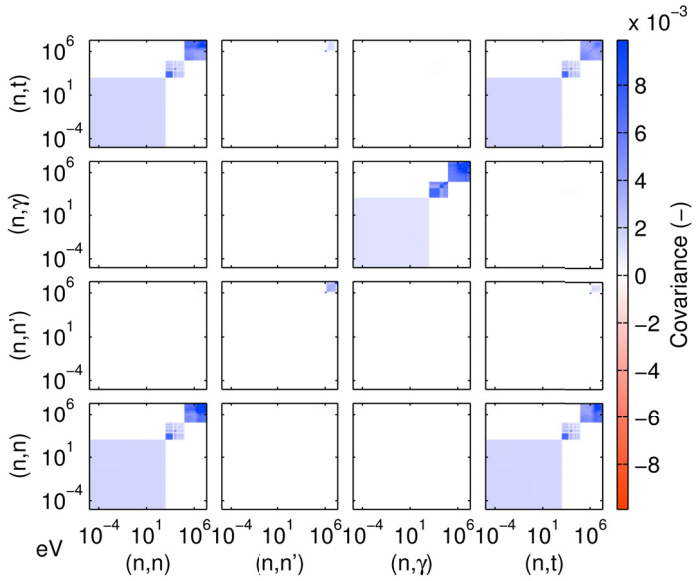

(b) The nearest more consistent covariances.

Figure 3.4. *(continued)* (b) The nearest more consistent covariances are consistent for about 14 digit arithmetic. Notably the low and medium energy regions of self-covariances of the total cross section have emerged. Original data from `ENDF/B-VII.1` [18]. Figure adapted from Publication II.

section may be replaced by its partials if the piece of covariance is not present. However, in practice there are evaluations whose covariances are not consistent. For these evaluations physically equivalent formulations of the problem will give different answers. Publication II proposes a quality assurance method that can be used to detect inconsistent covariances of multigroup averaged nuclear data. In Publication III a similar method is proposed for energy-dependent nuclear data in the `ENDF-6` format. In addition, Publications II and III present a method to find a nearby more proper covariances with minimal changes to the covariances. This is illustrated in Fig. 3.4.

The `ENDF-6` format allows the evaluators to specify an approximation of the first two moments of their knowledge of nuclear data. However, the `ENDF-6` format does not require evaluators to provide the second moments, i.e., covariances. According to the format, lack of covariances does not imply zero uncertainty. This causes a practical problem of selecting non-zero values that are not provided by the evaluator. The history section of

the ENDF-6 format manual states [11]:

> At the 1961 Vienna Conference on the Physics of Fast and Intermediate Reactors, Ken Parker [66] indicated some of the requirements for the neutron cross section libraries. They had to specify reaction processes available or else a zero value cross section would automatically be assumed.

Interestingly, the last sentence describes the present issue. This issue is considered in Publication II and illustrated in Fig. 3.4(a).

The three issues of non-positivity, inconsistency and lack of covariances can be approached in various ways. Publications I–III provide a solution to the issues as follows:

1. The non-zero components may be approximatively characterized by one of the characterization methods presented in Publication II. This step may be omitted if all covariances have been characterized by the evaluator.

2. The resulting covariances can be checked for negative eigenvalues and those may be deflated by the methods presented for (2a) multigroup nuclear data in Publication I or (2b) energy-dependent nuclear data in Publication III. Any of the weights described in Publication III may be used in deflating the negative eigenvalues.

3. The resulting covariances can be checked for consistency with respect to the sum rules of nuclear data by the method presented for (3a) multigroup nuclear data in Publication II or (3b) energy-dependent nuclear data in Publication III. For the case of inconsistent covariances, Publications II andIII present methods to find nearby more consistent covariances. Again, the weights described in Publication III may be used.

It is advisable to check the resulting covariances, compare them with the originals and decide whether the resulting covariances are suitable for the intended application. The resulting covariances can be considered to be low-fidelity covariances, which are better than no covariances and should be replaced by high-fidelity covariances in the future.

The methods described here will not check all necessary properties of nuclear data covariances. They should be used as a part of a quality assurance program. Other necessary or useful properties are described, for example, in Refs. [4, 67].

3.1.9 Covariances of multigroup nuclear data

There has been some confusion about the definition of covariances of multigroup nuclear data. In the following, it is remarked that both response-independent and response-specific covariances can be used but the sensitivities that should be used in the first-order uncertainty analysis differ.

Generally, a piece of multigroup nuclear data is defined by

$$\alpha_{i,g}(\beta) = \frac{\int_g w(E)\alpha_i(E;\beta)\,dE}{\int_g w(E)\,dE}, \tag{3.1}$$

where the integration is carried out over the energy interval of the g'th group, $w(E)$ is a suitable weight function, and β contains the surrogate quantities.

The response-independent multigroup nuclear data covariance between i'th and j'th pieces of multigrouped nuclear data in energy groups g and g', respectively, is straightforwardly

$$\begin{aligned} C_{ijgg'} &= \mathrm{E}[\,\alpha_{i,g}(\beta)\alpha_{j,g'}(\beta)\,] - \mathrm{E}[\,\alpha_{i,g}\,]\,\mathrm{E}[\,\alpha_{j,g'}\,] \\ &= \frac{\int_g w(E)\int_{g'} C_{ij}(E,E')w(E')\,dE'dE}{\int_g w(E)\,dE\int_{g'} w(E')\,dE'}, \end{aligned} \tag{3.2a}$$

where $C_{ij}(E,E')$ denotes the covariances between i'th and j'th energy dependent pieces of nuclear data. For example, `NJOY` [68] and `PUFF-IV` [69] compute this kind of multigroup covariances. However, the covariances contain no spectral fine-structure effects [70]. Therefore, the sensitivities must be equal to the integral of the energy-dependent sensitivity profile for the first-order uncertainty analysis.

The response-specific multigroup nuclear data covariances are sensitivity weighted covariances. That is, the multigroup nuclear data covariance between i'th and j'th pieces of multigrouped nuclear data in energy groups g and g', respectively, for responses f and h is formally

$$\tilde{C}_{ijgg'fh} = \frac{\int_g S_{f,i}(E)\int_{g'} C_{ij}(E,E')S_{h,j}(E')\,dE'dE}{\int_g S_{f,i}(E)\,dE\int_{g'} S_{h,j}(E')\,dE'}. \tag{3.2b}$$

Here the sensitivity profiles $S_{f,i}(E)$ and $S_{h,j}(E)$ corresponding to the responses f and h, respectively, are evaluated at the best-estimate values. Since the energy-dependent sensitivities are built into the covariances, the sensitivity analysis for the first-order uncertainty analysis must be applied to the multigroup nuclear data. Otherwise the spectral fine structure effects are counted twice.

3.2 Models in reactor physics

3.2.1 Neutron transport

Neutron transport is a process in which neutrons propagate in a physical system. A model of the system is defined by a geometry in which nuclide compositions and material temperatures are presumed to be known[10]. The geometry, temperature, initial compositions and certain composition changes are considered as design parameters since the designer can easily manipulate them.

The properties of the medium are described by effective cross sections, which are temperature dependent. In this work, the temperature dependency is not explicitly marked nor discussed further. For a recent account on the temperature effects see, for example, Ref. [71].

The macroscopic cross section for reaction $\mathtt{x}$ may be written as

$$\Sigma_{\mathtt{x}}(\bar{\boldsymbol{r}}, E, t) = \sum_i n_i(\bar{\boldsymbol{r}}, t)\sigma_{i,\mathtt{x}}(E), \tag{3.3}$$

where n_i denotes the nuclide concentrations and $\sigma_{i,\mathtt{x}}$ the effective microscopic cross section of the i'th material. The macroscopic cross section can be interpreted as an interaction probability per path length traversed by a neutron.

In certain reactions neutrons are emitted. The emitted neutrons can be described by the macroscopic double differential cross section

$$\begin{aligned} &m\Sigma_{\mathtt{x}}(\bar{\boldsymbol{r}}, \hat{\Omega} \to \hat{\Omega}', E \to E', t) \\ &\quad = \sum_i n_i(\bar{\boldsymbol{r}}, t) m_{i,\mathtt{x}}(E)\sigma_{i,\mathtt{x}}(E) p_{i,\mathtt{x}}(\hat{\Omega} \cdot \hat{\Omega}', E \to E'), \end{aligned} \tag{3.4}$$

where the "ligature" $m\Sigma_{\mathtt{x}}$ should be interpreted as a single symbol. Here $m_{i,\mathtt{x}}$ is the multiplicity of the reaction and other terms are explained in Section 3.1.

For fission reactions the multiplicity is customarily written as $\bar{\nu}$, and it is further customary to write

$$\bar{\nu}\Sigma_{\mathtt{f},\mathtt{p}}(\bar{\boldsymbol{r}}, E \to E', t) = \sum_i n_i(\bar{\boldsymbol{r}}, t)\chi_{i,\mathtt{p}}(E \to E')\bar{\nu}_{i,\mathtt{p}}(E)\sigma_{i,\mathtt{f}}(E), \tag{3.5a}$$

$$\bar{\nu}\Sigma_{i,j,\mathtt{f},\mathtt{d}}(\bar{\boldsymbol{r}}, E, t) = n_i(\bar{\boldsymbol{r}}, t)\bar{\nu}_{i,j,\mathtt{d}}(E)\sigma_{i,\mathtt{f}}(E), \tag{3.5b}$$

[10] It is possible to include heat transfer, thermal-hydraulics and other phenomena in the model. However, the resulting model is unnecessarily complex, and usually more approximative models are used when several fields are considered simultaneously.

for prompt neutrons and neutrons in the j'th delayed group, respectively. The energy spectra of neutrons emitted from fissions are denoted by χs. Note that Eq. (3.5) does not define double differential cross sections.

The neutron transport phenomenon is described by the neutron transport equation, which is a balance equation for the number of neutrons, $N(\bar{\boldsymbol{r}}, \hat{\Omega}, E, t)\, d\bar{\boldsymbol{r}} d\hat{\Omega} dE$, in a volume $d\bar{\boldsymbol{r}}$ about $\bar{\boldsymbol{r}}$, traveling with a solid angle $d\hat{\Omega}$ about $\hat{\Omega}$ within energy dE about E at time t, when neutron streaming, interactions and sources are considered. However, the formulation is usually made for the neutron angular flux that is defined as

$$\psi(\bar{\boldsymbol{r}}, \hat{\Omega}, E, t) = vN(\bar{\boldsymbol{r}}, \hat{\Omega}, E, t), \tag{3.6}$$

where speed of a neutron, v, is defined by its kinetic energy, E. Almost all quantities of interest in reactor physics can be derived from the scalar neutron flux, ϕ, and the neutron current, $\bar{\boldsymbol{J}}$. These are related to the angular neutron flux by

$$\phi(\bar{\boldsymbol{r}}, E, t) = \int_{4\pi} \psi(\bar{\boldsymbol{r}}, \hat{\Omega}, E, t)\, d\hat{\Omega} \quad \text{and} \tag{3.7a}$$

$$\bar{\boldsymbol{J}}(\bar{\boldsymbol{r}}, E, t) = \int_{4\pi} \hat{\Omega}\psi(\bar{\boldsymbol{r}}, \hat{\Omega}, E, t)\, d\hat{\Omega}. \tag{3.7b}$$

The neutron transport equation is

$$\begin{aligned} \frac{1}{v}\frac{\partial}{\partial t}\psi(\bar{\boldsymbol{r}}, \hat{\Omega}, E, t) + \hat{\Omega} \cdot \nabla\psi(\bar{\boldsymbol{r}}, \hat{\Omega}, E, t) + \Sigma_{\mathtt{t}}(\bar{\boldsymbol{r}}, E, t)\psi(\bar{\boldsymbol{r}}, \hat{\Omega}, E, t) \\ = S(\bar{\boldsymbol{r}}, \hat{\Omega}, E, t; \psi), \end{aligned} \tag{3.8}$$

where the sources are divided into neutron emitting reactions except fission, fission and application dependent external sources as

$$S(\bar{\boldsymbol{r}}, \hat{\Omega}, E, t; \psi) = S_{\mathtt{n}}(\bar{\boldsymbol{r}}, \hat{\Omega}, E, t; \psi) + S_{\mathtt{f}}(\bar{\boldsymbol{r}}, \hat{\Omega}, E, t; \psi) + S_{\mathtt{e}}(\bar{\boldsymbol{r}}, \hat{\Omega}, E, t). \tag{3.9}$$

With the exception of the external sources, these are explicitly

$$S_{\mathtt{n}} = \sum_{\mathtt{x} \neq \mathtt{f}} \int_{4\pi} \int_0^\infty m\Sigma_{\mathtt{x}}(\bar{\boldsymbol{r}}, \hat{\Omega}' \to \hat{\Omega}, E' \to E, t)\psi(\bar{\boldsymbol{r}}, \hat{\Omega}', E', t)\, dE' d\hat{\Omega}', \tag{3.10a}$$

$$\begin{aligned} S_{\mathtt{f}} = &\frac{1}{4\pi} \int_0^\infty \bar{\nu}\Sigma_{\mathtt{f,p}}(\bar{\boldsymbol{r}}, E' \to E, t)\phi(\bar{\boldsymbol{r}}, E', t)\, dE' \\ &+ \frac{1}{4\pi} \sum_{i,j} \chi_{i,j,\mathtt{d}}(E)\lambda_{i,j}C_{i,j}(\bar{\boldsymbol{r}}, t), \end{aligned} \tag{3.10b}$$

where the delayed neutron precursor concentrations for the j'th delayed neutron group of the i'th material are given by

$$\frac{\partial}{\partial t}C_{i,j}(\bar{\boldsymbol{r}}, t) = \int_0^\infty \bar{\nu}\Sigma_{i,j,\mathtt{f,d}}(\bar{\boldsymbol{r}}, E', t)\phi(\bar{\boldsymbol{r}}, E', t)\, dE' - \lambda_{i,j}C_{i,j}(\bar{\boldsymbol{r}}, t). \tag{3.11}$$

The above form of the neutron transport equation contains several minor assumptions. For example, decay of free neutrons and neutron-neutron

interactions are neglected, the delayed neutron precursors are assumed to be immobile and the fission neutrons are assumed to be emitted isotropically. The first two are considered good approximations in all reactors, the third one fails considerably only for fluid fueled reactors, and the last one might not hold for fissions caused by relatively high-energy neutrons.

At the reactor boundary one usually considers the boundary condition

$$\psi(\bar{\boldsymbol{r}}, \hat{\Omega}, E, t) = 0 \quad \text{for } \hat{\Omega} \cdot \bar{\boldsymbol{n}} < 0, \tag{3.12}$$

where $\bar{\boldsymbol{n}}$ is the outward normal vector at boundary point $\bar{\boldsymbol{r}}$. The boundary condition implies that neutrons that cross the boundary will not re-enter the reactor. Also an initial condition for the angular neutron flux must be given.

For most applications the time-dependent transport equation is unnecessarily complex and the criticality equation

$$\begin{aligned} &\hat{\Omega} \cdot \nabla\psi(\bar{\boldsymbol{r}}, \hat{\Omega}, E) + \Sigma_{\mathtt{t}}(\bar{\boldsymbol{r}}, E)\psi(\bar{\boldsymbol{r}}, \hat{\Omega}, E) \\ &= \sum_{\mathtt{x} \neq \mathtt{f}} \int_{4\pi} \int_0^\infty m\Sigma_{\mathtt{x}}(\bar{\boldsymbol{r}}, \hat{\Omega}' \to \hat{\Omega}, E' \to E)\psi(\bar{\boldsymbol{r}}, \hat{\Omega}', E')\, dE' \mathrm{d}\hat{\Omega}' \\ &\quad + \frac{1}{4\pi k} \int_0^\infty \bar{\nu}\Sigma_{\mathtt{f},\mathtt{t}}(\bar{\boldsymbol{r}}, E' \to E)\phi(\bar{\boldsymbol{r}}, E')\, dE' \end{aligned} \tag{3.13}$$

is solved instead. A multiplication factor k has been introduced, which ensures that a solution exists when the physical system is not in steady state. Physically, this can be seen as arbitrarily varying the number of neutrons emitted from fission.

For derivations, equivalent forms and further approximations, interested readers are referred to one of the text-books [3, 5, 72–75].

For reference to Chapter 4 it is useful to identify model parameters, phase space and state variables. The parameters of the model consist of the nuclide concentrations $n_i(\bar{\boldsymbol{r}}, t)$, the temperature field $T(\bar{\boldsymbol{r}}, t)$, the external sources $S_{\mathtt{e}}(\bar{\boldsymbol{r}}, \hat{\Omega}, E, t)$, the microscopic cross sections $\sigma_{i,\mathtt{x}}(E)$, the energy-angle distributions $p_{i,\mathtt{x}}(\hat{\Omega} \cdot \hat{\Omega}', E \to E')$, including fission spectra, the multiplicities $m_{i,\mathtt{x}}(E)$, including the average numbers of neutrons emitted from fission, and the decay constants $\lambda_{i,j}$. These are required for all materials and reactions. It should be noted that parameters with dependence on the position vector define the geometry of the model. The phase space of the model is $(\bar{\boldsymbol{r}}, \hat{\Omega}, E, t)$. The state variables of the model are the angular neutron flux $\psi(\bar{\boldsymbol{r}}, \hat{\Omega}, E, t)$ and the delayed neutron precursor concentrations $C_{i,j}(\bar{\boldsymbol{r}}, t)$ for the transport equation or the multiplication factor k for the criticality equation. The inhomogeneous sources are the external sources.

3.2.2 Transmutation of nuclides

Transmutation of nuclides is a process in which nuclides transform into other nuclides through radioactive decay, and nuclear reactions, including fission. A model of the system is defined by the scalar neutron flux and material temperatures. With effective, temperature adjusted, cross sections these define reaction rates. It is customary to consider only a single spatial position, so that the position vector can be dropped.

The reaction rate densities for reaction x in the i'th material are defined as

$$r_{i,\mathrm{x}}(t) = \bar{\sigma}_{i,\mathrm{x}}(t)\bar{\phi}(t)n_i(t), \tag{3.14}$$

where the effective 1-group flux, $\bar{\phi}(t)$, is defined by $\int_0^\infty \phi(E,t)\,dE$ and the effective 1-group cross section, $\bar{\sigma}_{i,\mathrm{x}}(t)$, by $\int_0^\infty \sigma_{i,\mathrm{x}}(E)\phi(E,t)\,dE/\bar{\phi}(t)$.

Considering all nuclear reactions, the production of the i'th material through them is $\sum_j \bar{\sigma}_{j\to i}(t)\bar{\phi}(t)n_j(t)$ and, conversely, the destruction of the material is $\sum_j \bar{\sigma}_{i\to j}(t)\bar{\phi}(t)n_i(t)$. It should be noted that the effective transmutation cross section, $\bar{\sigma}_{j\to i}(t)$, includes fission yields and other reactions in which transmutations occur.

The decay rate of the i'th material is $\lambda_i n_i(t)$ and the production rate from decay of other materials is $\sum_j b_{j\to i}\lambda_j n_j(t)$, where $b_{j\to i}$ is the branching ratio.

In total these give the transmutation equation

$$\begin{aligned}\frac{\partial}{\partial t}n_i(t) = &\sum_j \bar{\sigma}_{j\to i}(t)\bar{\phi}(t)n_j(t) - \sum_j \bar{\sigma}_{i\to j}(t)\bar{\phi}(t)n_i(t)\\ &+ \sum_j b_{j\to i}\lambda_j n_j(t) - \lambda_i n_i(t).\end{aligned} \tag{3.15}$$

The equation is also called burnup equation, depletion equation, and decay and transmutation equation. For a recent accurate and efficient solution method for time-independent 1-group constants, see Ref. [76], and for using these to approximate time-dependent solutions, see Ref. [77]. Since this is a differential equation in time, initial conditions must be provided for the nuclide concentrations.

It is again useful to identify model parameters, phase space and state variables. The parameters of the model consist of the temperature field $T(t)$, the transmutation cross sections $\sigma_{i\to j,\mathrm{x}}(E)$, including fission yields, the scalar flux with power normalization $\phi(E,t)$, the decay constants λ_i and the branching ratios $b_{j\to i}$. These are required for all materials. The phase space of the model is time and the state variables of the model are the nuclide concentrations $n_i(t)$.

4. Uncertainty analysis in reactor physics

Some physical systems have interesting properties that can be described by quantities of interest. Quantities of interest can be predicted by physical models that map model parameters to quantities of interest. The quantities of interest are sometimes referred to as responses, physical models as models, and model parameters as parameters. Both parameters and responses are presumed to be either physical quantities or at least quantities that can be described as probability distributions that describe the knowledge of the quantity.

The purpose of uncertainty analysis is to quantify the level of confidence one can have in calculated quantities of interest, that is, to quantify the knowledge of the values of the quantities of interest. There are many sources of uncertainty in the calculations [23]. Typically a major source of uncertainty is the parameter uncertainty, i.e., the lack of knowledge of the values of the quantities of interest. This is sometimes the only considered source of uncertainty [1]. If all sources of uncertainty are accounted for, the inverses of the standard deviations of the quantities of interest are a measure of the prediction capability of the model [1]. A categorization of sources of uncertainty for the quantities of interest in physical models is presented in Section 4.1.

Uncertainty analysis quantifies uncertainties of responses. The quantified uncertainty can, for example, be used to calculate probabilities that a quantity of interest is within a given, possibly unbounded, interval. The probability is only rarely, if ever in practical applications, a certainty. That is, usually uncertainty analysis can only provide evidence for a conclusion but not a solid proof of it. Therefore deductive reasoning can not be used and one must settle for inductive reasoning [78].

A typical adjunct to uncertainty analysis is apportioning the uncertainties in the responses to the uncertainties in the parameters [31]. This

results in a parameter importance ranking table [23]. The table can be used, for example, to prioritize efforts to reduce uncertainty.

For the present work the physical model is specified as follows. The model parameters are denoted by $\alpha(x) = (\alpha_1(x), \ldots, \alpha_k(x))^\intercal \in \mathcal{E}_\alpha$, where $\mathcal{E}_\alpha$ is a normed linear space. The model parameters may depend on the n-dimensional phase space, which is denoted by $x = (x_1, \ldots, x_n)^\intercal \in \Omega \subset \mathbb{R}^n$. The state variables, $u(x) = (u_1(x), \ldots, u_m(x))^\intercal \in \mathcal{H}_u$, belong to a Hilbert space with the inner product $\langle \cdot\,, \cdot \rangle_u$ and describe the internal state of the model around each point of phase space and depend on the parameters via

$$N(u(x), \alpha(x)) = Q(\alpha(x)), \quad x \in \Omega, \tag{4.1a}$$

where the operator $Q(\alpha(x)) = (Q_1(\alpha(x)), \ldots, Q_m(\alpha(x)))^\intercal$ contains the inhomogeneous source terms that operate on the parameters and belongs to a normed linear space $\mathcal{E}_Q$, and the operator $N(u(x), \alpha(x)) = (N(u(x), \alpha(x)), \ldots, N(u(x), \alpha(x)))^\intercal$ belongs to a normed linear space $\mathcal{E}_N$ and describes other than inhomogeneous terms [1]. The domains of both operators may be restricted when necessary. When Q is zero, the equation can be an eigenvalue problem, for which the operator N is singular [79]. If Eq. (4.1a) contains differential operators, then suitable boundary conditions must be provided as

$$B(u(x), \alpha(x)) = A(\alpha(x)), \quad x \in \partial\Omega, \tag{4.1b}$$

where $\partial\Omega$ is the boundary of Ω and A and B are non-linear operators [1]. The boundary is presumed to be sufficiently smooth. It is assumed that the model has a unique model solution, i.e., unique $u(x)$ for given model parameters. Therefore, the state variables can alternatively be seen to depend on the model parameters, i.e., $u(\alpha(x)) = (u_1(\alpha(x)), \ldots, u_m(\alpha(x)))^\intercal$, since the parameters and Eq. (4.1) are enough to define them.

The model responses, $R = (R_1, \ldots, R_l)^\intercal$ are usually formulated as linear or non-linear functions or operators of the state variables and parameters, i.e., $R : \mathcal{D}_R \subset \mathcal{H}_u \times \mathcal{E}_\alpha \to \mathcal{E}_R$, where $\mathcal{E}_R$ is a normed linear space [1]. In this work, the responses are assumed to be functionals, that is, the space $\mathcal{E}_R$ is assumed to be the space of real numbers. More general responses can be considered [1]. Formally, the responses can be seen to depend only on the parameters, partially implicitly, since the state variables depend on the parameters.

A rather broad class of physical models can be described in this form. For example, the energy-dependent criticality equation, transmutation equation and their various approximations can be described in the form

of Eq. (4.1). The considered responses might be chosen to be, for example, relevant reaction rates, ratios of reaction rates or nuclide concentrations [79].

Requirements for uncertainty analysis in reactor physics are usually characterized by a large number of model parameters, models that are computationally relatively expensive to evaluate, and a small number of model responses. The methods of uncertainty analysis can be divided into two categories: deterministic and statistical. The latter are also referred to as probabilistic or stochastic methods. Although neither category excels at all purposes, both can be and have been used in practical uncertainty analysis in reactor physics [80]. Sections 4.2 and 4.3 provide an overview of the most common and simplest deterministic and statistical methods in uncertainty analysis, respectively. There are several variations to each method and hence only salient features are presented. Interested readers are referred to the bibliography for further details.

4.1 Sources of uncertainty

The sources of uncertainty can be categorized in a variety of ways. A categorization is presented in Table 4.1, which is not fully compatible with the categorizations in Refs. [1,7,11,13,23,28,47,49,80,81]. The actual categorization is less important than consideration of all sources of uncertainty, for which categorization is a conceptual aid.

Ideally, the physical model contains only system uncertainty, model uncertainty and parameter uncertainty. The physical model is presumably discretized into a computational model that can be used to compute the quantities of interest using a digital computer. The discretization causes discretization uncertainty. However, sometimes the ideal is not achieved and physical approximations need to be applied to a partially discretized system. In such a case, the categorization is not as important as estimating the uncertainty and including it in a category. The relative magnitudes of most sources of uncertainty were quantified in Publication V for two cases.

System uncertainty is inherent to the physical system or its boundary and is aleatory in nature [47]. System uncertainty does not include uncertainty from totally unpredictable phenomena but only uncertainty due to phenomena that have statistical regularity [1]. All systems do not have inherent uncertainty. System uncertainty can not be reduced, since it is

Table 4.1. Sources of uncertainty in modeling of physical systems.

Category	Cause of uncertainty
System uncertainty	The physical system
Model uncertainty	Idealized description of the system
Parameter uncertainty	Imperfect knowledge of the values of the model parameters
Discretization uncertainty	Replacement of continuous parts of the model and continuous parameters by discrete approximations

inherent to the system being modeled – the model should reflect the fact and either produce statistically varying results or present the responses as distributions. In typical applications of reactor physics system uncertainty is not a large component of uncertainty.

Model uncertainty is caused by lack of knowledge of physical laws or a choice to exclude known physics from the model, perhaps due to their complexity. Irrespective of the complexity of the model, it is always an idealization of the system and can not be exact [82]. Uncertainty caused by model uncertainty can be estimated if a more accurate model is available by comparing results of the two models. The uncertainty can also be reduced by using the more accurate model. If the model is already the most faithful to known physics, model validation is necessary to estimate uncertainty in the model [23]. In such a case model uncertainty can be reduced only by improvements in known physics. In reactor physics model uncertainties include ignoring neutron-neutron interaction, handling of unresolved resonances and many approximations in the deterministic codes. In typical applications of reactor physics model uncertainty is comparable to parameter uncertainty in deterministic models but much smaller than parameter uncertainty in stochastic models [22, 83].

Parameter uncertainty is caused by lack of knowledge of the values of the model parameters. It can only be reduced by increasing the knowledge of the values by, for example, performing new measurements using measurement instruments of a new kind, by incorporating new theoretical information or sometimes by a more refined analysis of existing data [11]. For nuclear data, these actions are usually more expensive than reduction of other sources of uncertainty, and hence it should be the dominating source of uncertainty. In typical models in reactor physics parameters

include geometry, composition and nuclear data. Estimating the uncertainty caused by parameter uncertainty is the subject of the upcoming sections.

World view uncertainty is a part of parameter uncertainty. It is caused by incomplete information exchange, due to which parameter uncertainties are estimated without complete information. It can be crudely measured by comparing results gained by using different world views. In Publication IV the main differences in world views of three nuclear data libraries for a pressurized water reactor application were identified.

Discretization uncertainty is caused by replacing continuous parts of the model by their discrete counterparts. For example, differential equations might be replaced by finite difference equations. Consistent and stable discretizations converge to the non-discretized solution in the limit of vanishing discretization [75]. For such discretizations, the uncertainty can be practically estimated using engineering convergence tests. Similarly, such discretization uncertainty can be reduced to be considerably smaller than the dominating source of uncertainty by adjusting the discretization parameters. Examples in reactor physics include time discretization of transmutation equations and linearization of interpolation of nuclear data. Alas, in reactor physics there are deterministic models that are not consistent. For these other ways to estimate and reduce uncertainty are needed. Examples are certain implementations of nodal diffusion methods in hexagonal geometries [84].

Statistical uncertainty is a part of discretization uncertainty. It is present in stochastic models and is caused by finite sample size. Its estimation using statistical inference and reduction by increasing sample size is straightforward. Therefore it is not a major source of uncertainty even in reactor physics applications.

Numerical uncertainty is a part of discretization uncertainty. It occurs because of replacement of real numbers by a finite dimensional approximation, typically by floating point numbers. Its magnitude can be estimated by rounding error analysis[11], running error analysis or replacing real numbers with arbitrary precision numbers [85, 86]. The last method can also be used to reduce the uncertainty. In typical applications of reactor physics numerical uncertainty is not a major source of uncertainty.

Sometimes user effect is considered as a source of uncertainty, for ex-

[11] In this paragraph "error" is part of customary names of techniques, and does not mean a blunder.

ample in Ref. [7]. User effect occurs, e.g., because different users make different assumptions about phenomena to model or choose different submodels. Hence the user effect arises because different models are used without estimating model uncertainty. In this work, any user effect is considered an error rather than a source of uncertainty.

4.2 Deterministic uncertainty analysis

In deterministic uncertainty analysis, the first few moments of the distribution that describes the knowledge of the values of the model responses are estimated. The distribution is not fully characterized since the process does not provide enough information to define a distribution. Remedies require subjective decisions.

The standard approach is to disregard all other information except the first few moments that are estimated. Subsequently, the distribution is characterized using the principle of maximum entropy. Alternatively, if the first two moments exist, have been estimated, and one is interested in finding out upper bounds of probabilities that the responses are in certain intervals, one can use the inequality,

$$\begin{aligned} \mathrm{P}[\,|R_i - \mathrm{mean}(R_i)| \geq k\,\mathrm{std}(\,R_i\,)\,] \leq \frac{1}{k^2} \\ \text{for } k > 0 \text{ and } i = 1, \ldots, l, \end{aligned} \tag{4.2}$$

which gives upper bounds for probabilities that the values of the responses are far from the mean values [87]. The estimate is much more conservative than assuming a normal distribution [38]. However, the estimate might be too conservative for practical applications. The inequality has several extensions, see e.g. Refs. [53, 88–91], some of which are sharper but require further assumptions and some of whose formulation might be more useful in specific applications.

In principle, the first two moments, assuming their existence, can be calculated from

$$\mathrm{mean}(R) = \mathrm{E}[\,R(\alpha(x))\,] \in \mathbb{R}^l \quad \text{and} \tag{4.3a}$$

$$\begin{aligned} \mathrm{cov}(R,R) = {} & \mathrm{E}[\,R(\alpha(x))R(\alpha(x'))^\intercal\,] \\ & - \mathrm{E}[\,R(\alpha(x))\,]\,\mathrm{E}[\,R(\alpha(x'))^\intercal\,] \in \mathbb{R}^{l\times l}, \end{aligned} \tag{4.3b}$$

where the implicit form of the responses is used and the expectations are calculated over the knowledge of the values of the parameters. However, in practice these can be evaluated only approximatively by using the first-order uncertainty analysis, in which the responses are linearized with

respect to the parameters. The use of higher-order uncertainty analysis has not proven to be feasible, as discussed later in this section.

The main deficiency of the first-order uncertainty analysis is its inability to account for non-linearities [30, 49]. Whether non-linearities are important or not depends on the details of the model. As a rule of thumb, small uncertainties in the parameters, $\mathrm{std}(\alpha(x)) \ll \mathrm{mean}(\alpha(x))$, might be well enough described by linearization, but if this is not true the results are likely to be unacceptably biased [30]. Hence caution must be exercised.

However, the first-order uncertainty analysis can be applied to models with a large number of parameters [23]. It is transparent in propagation of uncertainties to the responses [30]. A consequence of this is that apportioning the uncertainties in the responses to the uncertainties in the parameters, i.e., the construction of a parameter importance ranking table, is straightforward [23, 92]. The method is also quite fast if the sensitivities can be computed efficiently [23].

4.2.1 The first-order uncertainty analysis

In the first-order uncertainty analysis the implicit form of the responses is linearized with respect to the model parameters at the best-estimate values of the parameters. For this, it is convenient to restrict the space of parameters, $\mathcal{E}_\alpha$, to be a Hilbert space, which will be denoted by $\mathcal{H}_\alpha$. Its inner product will be denoted by $\langle \cdot\,,\, \cdot \rangle_\alpha$.

The linearized responses are then

$$\begin{aligned} R(\alpha(x)) = R(\mathrm{E}[\,\alpha(x)\,]) + \langle\, S(\mathrm{E}[\,\alpha(x)\,])\,,\, \alpha(x) - \mathrm{E}[\,\alpha(x)\,] \,\rangle_\alpha \\ + \mathcal{O}(\|\alpha(x) - \mathrm{E}[\,\alpha(x)\,]\|_\alpha^2), \end{aligned} \tag{4.4}$$

where the inner products are taken response-wise, and the sensitivities $S(\mathrm{E}[\,\alpha(x)\,])$ contain concatenated sensitivities for each response, that is, $S(\mathrm{E}[\,\alpha(x)\,]) = (S_1(\mathrm{E}[\,\alpha(x)\,]), \ldots, S_l(\mathrm{E}[\,\alpha(x)\,]))^\intercal$. The response specific sensitivities $S_i(\mathrm{E}[\,\alpha(x)\,]) \in \mathcal{H}_\alpha$, contain partial functional derivatives of the responses with respect to parameter variations and are evaluated at the best-estimate values of the parameters [23]. The sensitivities contain both direct effects, which occur directly due to parameter variations, and indirect effects, which occur indirectly due to variations in the state variables due to variations in the parameters. The linearization is accurate up to the second-order in parameters [1]. When the linearization is applied to the fully discretized model, $\mathcal{H}_\alpha$ is $\mathbb{R}^k$ and the sensitivities reduce to a Jacobian, which contains the response specific sensitivities.

Using the linearized responses the first two moments of the knowledge of the values of the responses are estimated as

$$\mathrm{mean}(R) = R(\mathrm{E}[\,\alpha(x)\,]) + \mathcal{O}(\|\alpha(x) - \mathrm{E}[\,\alpha(x)\,]\|_\alpha^2) \quad \text{and} \tag{4.5a}$$

$$\begin{aligned}\mathrm{cov}(R,R) = \langle\, S(\mathrm{E}[\,\alpha(x)\,])\,,\ \langle\, \mathrm{cov}(\alpha(x),\alpha(x'))\,,\ S(\mathrm{E}[\,\alpha(x)\,])^\intercal \,\rangle'_\alpha\ \rangle_\alpha \\ + \mathcal{O}(\|\alpha(x) - \mathrm{E}[\,\alpha(x)\,]\|_\alpha^3),\end{aligned} \tag{4.5b}$$

where the primed inner product refers to the primed phase space. With the exception of sensitivities, the equations are readily evaluable at relatively low computational cost.

The interpretation of Eq. (4.5a) is often overlooked: the best-estimate of the responses is only approximatively the model evaluated at the best-estimate parameters, unless the model is linear. The best-estimate of the responses should be corrected by second-order sensitivities applied to the covariances. Had the linearization not been performed at the best-estimate values, the equation for the mean would have been accurate only up to the first-order and a linear correction would have been needed for the present accuracy. Similarly, a third-order correction should be applied to the covariances.

4.2.2 The first-order sensitivity analysis

The objective of local sensitivity analysis[12] is to quantify the effects of parameter variations on the responses [1]. The first-order sensitivity analysis, or linear perturbation theory, aims to compute the first-order sensitivities accurately and efficiently [1]. In reactor physics various forms of it are known as classical perturbation theory and generalized perturbation theory [93, 94]. Local sensitivities, or sensitivities, can be computed exactly only by deterministic methods [80]. These methods involve some kind of differentiation.

In general, the differentiation and discretization of the model do not commute, i.e., their order of application matters [23]. It is possible to compute the sensitivities to certain discretization parameters, if the system is first discretized and the system is differentiated regarding the discretization parameters as model parameters [1]. These can be useful in estimating the discretization uncertainty. However, the two sets of equations are not consistent if they are not identical in the limit of vanishing

[12] It should be mentioned that in statistical uncertainty analysis the word "sensitivity analysis" is used to mean apportioning the uncertainty in the individual responses to the uncertainty in the individual parameters [31].

discretization parameters. In these cases it is advisable to first perform the differentiation and then discretize the resulting equations [1].

The model recalculation method is perhaps the most straightforward method to estimate the sensitivities but can only be applied to the computational models [23]. In the method, the model is first evaluated once at the best-estimate values of the parameters. Subsequently, a model parameter is varied by a smallish fraction of its standard deviation and the model is re-evaluated. Suitable fractions are typically between $0.1\,\%$ and $10\,\%$ but need to be determined case-by-case. The varied parameter is then returned to its best-estimate value and procedure is repeated for every model parameter. The sensitivities are then estimated by using a finite difference approximation.

The estimated sensitivities contain both direct and indirect effects since the model is re-evaluated after each variation. The method is conceptually simple, but it is not completely accurate due to the use of finite differences, and may fail if the parameter variations are selected to be too small, due to finite numerical precision, or too large, due to non-linearities. The number of required model evaluations required grows linearly with the number of parameters.

The adjoint-based sensitivity analysis methods are efficient but reasonably complicated methods to evaluate sensitivities [1, 79]. The methods can be applied to the physical model or to the computational model. The methods are based in a variation $h_\alpha(x)$ in the parameters that causes a variation $h_u(x)$ in the state variables, both of which cause variations in the responses. Dropping the phase-space argument for convenience and using the explicit form of the responses, the variation at the best-estimate values is

$$\delta R(\mathrm{E}[\,u\,], \mathrm{E}[\,\alpha\,]; h_u, h_\alpha) = R'_\alpha(\mathrm{E}[\,u\,], \mathrm{E}[\,\alpha\,])h_\alpha + R'_u(\mathrm{E}[\,u\,], \mathrm{E}[\,\alpha\,])h_u, \qquad (4.6)$$

where the best-estimate state variables are computed by solving Eq. (4.1) for the best-estimate parameter values, and R'_α and R'_u denote the partial functional derivatives with respect to α and u, respectively [1]. Assuming that the responses are suitably smooth the variation in the responses will be linear in both the variations in the parameters and the state variables [1].

To construct the linear term in Eq. (4.4) a mapping between variations in the state variables and parameters is needed. For this, the methods need an adjoint model in addition to the usual (forward) model. Assuming that $\mathcal{E}_Q$ is a Hilbert space with the inner product $\langle\ \cdot\ ,\ \cdot\ \rangle_Q$, the adjoint

model for the i'th response is formally

$$N^\dagger(u_i^\dagger, \mathrm{E}[\,\alpha\,]) = \nabla_u R_i(\mathrm{E}[\,u\,], \mathrm{E}[\,\alpha\,]), \quad x \in \Omega, \tag{4.7a}$$

$$B^\dagger(u_i^\dagger, \mathrm{E}[\,\alpha\,]) = A^\dagger(\mathrm{E}[\,\alpha\,]), \quad x \in \partial\Omega, \tag{4.7b}$$

where $R'_u h_u = \langle\, \nabla_u R_i, h_u \,\rangle_u$, $u_i^\dagger(x)$ is the adjoint state of the i'th response, and the dagger indicates adjoint operators for which the boundary conditions must be chosen suitably [1]. Interestingly, certain adjoint equations can be derived purely from physical considerations [95]. The adjoint model needs to be solved once for each response at the best-estimate values, after which the linear term in Eq. (4.4) can be formed from

$$\begin{aligned} \langle\, S(\mathrm{E}[\,\alpha(x)\,]), h_\alpha \,\rangle_\alpha = {} & R'_\alpha(\mathrm{E}[\,u\,], \mathrm{E}[\,\alpha\,]) h_\alpha \\ & + \langle\, u_i^\dagger(x)\,,\, Q'(\mathrm{E}[\,\alpha\,]) h_\alpha - N'_\alpha(\mathrm{E}[\,u\,], \mathrm{E}[\,\alpha\,]) h_\alpha \,\rangle_Q \\ & - P(h_\alpha, u_i^\dagger(x), \mathrm{E}[\,\alpha\,]) \end{aligned} \tag{4.8}$$

where Q' is the functional derivative of the inhomogeneous sources, N'_α is the partial functional derivative of N with respect to model parameters, and P contains certain boundary terms [1]. All the terms are linear in h_α so that the sensitivities can be computed [1].

The computational cost of the solution of the adjoint model is comparable to the cost of solution of the original model. Therefore the adjoint-based approach is advantageous when there are more parameters than responses [92]. However, its implementation to existing computational models might require considerable development work [1]. For details, see e.g. Refs. [1, 79, 80, 95]. In reactor physics, most sensitivities are computed with respect to nuclear data, but also the composition of the reactor has been considered in the criticality equation, see e.g. Refs. [70, 96], and Publication V, and in the transmutation equation, see e.g. Ref. [97]. In addition, sensitivities with respect to the geometry of the reactor have been considered [96, 98].

It should be mentioned that local first-order sensitivities have other uses than sensitivity analysis [23]. For example, the sensitivities can be used to determine effects of parameter variations on responses, which allows optimization of the system by changing the design parameters. The sensitivities can lead to greater understanding of the system by highlighting important data, and to reduced parameter models by allowing elimination of less important data. The sensitivities can also be used to prioritize the introduction of parameter uncertainties, if some parameters have no uncertainty estimates.

4.2.3 Higher-order uncertainty analysis

There are no theoretical reasons not to include second and higher-order terms in the series expansion of responses with respect to parameters in Eq. (4.4). However, in general there are practical reasons for not doing so in reactor physics.

The resulting equations for second- and higher-order deterministic uncertainty analysis require knowledge of the third and higher-order moments of the distribution that describes the knowledge of the values of the parameters. These are generally not available for two reasons. *Firstly*, the storage requirements of subsequent moments grow, literally, exponentially. Therefore only a few more moments could, in theory, be stored. *Secondly*, the form of the distribution is not set in the ENDF-6 format [11]. Otherwise higher-order moments could, in some situations, be constructed from the second-order data. However, it has been proposed that the form of the distribution should be set as either normal or log-normal, after which the higher-order moments would be known [46, 99].

The resulting equations for second- and higher-order deterministic uncertainty analysis require computation of the second and higher-order sensitivities. Even the adjoint-based sensitivity analysis does not help here, since the computation of second-order sensitivities requires as many adjoint model evaluations as there are parameters [1]. For few-parameter models this might be a feasible approach, but not in transmutation and lattice calculations in reactor physics.

Therefore, deterministic methods are not suitable for characterization of the full distribution that describes the knowledge of the values of the responses. Their strength is in order-of-magnitude estimates of uncertainty especially for computing resource intensive models with a large number of parameters or relevant responses, and in situations where the parameters are well known or the responses have mostly linear dependence for the least known parameters.

4.3 Statistical uncertainty analysis

In statistical uncertainty analysis the distribution of the knowledge of the values of the model responses is estimated by repeatedly evaluating the model with varied model parameters, and computing responses using their explicit forms. Even in this way the distribution will not be

fully characterized, since only a finite number of re-evaluations can be performed. However, with large enough computational resources the distribution can be characterized as precisely as necessary.

In the following it is assumed that statistical uncertainty analysis is applied to the computational model. The parameters will then belong to $\mathbb{R}^k$, where k will be large in reactor physics applications. This might cause problems apportioning uncertainty in the responses to the uncertainty in the parameters. The number of parameters can be reduced if their contribution to uncertainty is ignored.

All statistical uncertainty analysis methods generate a sample from the distributions that describe the knowledge of the model parameters. A single set of values for the model parameters is called a realization. A sample of s realizations is

$$\alpha^i = (\alpha_1^i), \ldots, \alpha_k^i)^\intercal \in \mathbb{R}^k, \quad i = 1, \ldots, s, \tag{4.9}$$

where the superscript i refers to the index of the realization. For sample size selection see, for example, Ref. [100]. There are several sampling techniques that can be used to obtain a sample. The model is evaluated using the values of each realization, so that the corresponding set of state variables $\{u^i\}_{i=1}^s$ is obtained. This is usually the most computationally expensive phase – especially in reactor physics. The responses $\{R(u^i, \alpha^i)\}_{i=1}^s$ are computed after model evaluations. The method can account for all non-linearities, since the method is re-evaluated for all realizations [23].

Assuming that the sampling technique is not biased, uncertainty analysis can be readily performed using the set of computed responses: for each response these form a piecewise constant estimate of the cumulative distribution function – this provides an estimate of the complete information of the marginal probability distributions [31]. Similarly, the computed responses form an estimate of the multidimensional cumulative distribution function [31]. Customary indicators of the marginal distribution are sample means and variances, which should only be reported if the distribution is well described by its first two moments [23]. Alternatively, if one is interested in finding upper bounds of probabilities that the responses are in certain intervals, one can use inequalities similar to Eq. (4.2), as long as the chosen sampling technique allows [101, 102].

The main deficiency of the statistical uncertainty analysis is the inability to handle very large numbers of parameters and requirement of extensive computational resources for models that are computationally expensive to evaluate [30]. The computational requirements are even larger if

near zero or near one probabilities need to be estimated. However, special sampling techniques are available for these cases [31]. In addition, the statistical nature of the method implies lack of unique results and, for example, exact sensitivities [1, 30].

However, statistical uncertainty analyses are impervious to non-linear effects and can, in principle, be applied to all models [30]. The method is conceptually straightforward and requires relatively little development work [1, 31]. In reactor physics applications statistical uncertainty analysis methods have been especially applied to the transmutation equation, e.g. Ref. [103] but also to the criticality equation, e.g. Ref. [27].

4.3.1 Realizations of parameters

Realizations of single parameters are straightforward to obtain as long as a supply of random numbers or pseudorandom numbers from the uniform distribution on the unit interval is available.

Let α denote a parameter whose cumulative distribution function is $F(b)$. This is equal to the probability that the value of the parameter is less than b, i.e., $F(b) = \mathrm{P}[-\infty \leq \hat{\alpha} \leq b] = \int_{-\infty}^{b} p(\alpha)\, d\alpha$, and hence the range of the cumulative distribution function is the unit interval. In inverse transform sampling a random number γ from the uniform distribution on the unit interval is realized. The realization is mapped through the inverse of cumulative distribution function, so that $F^{-1}(\gamma)$ becomes the realization of the parameter. In the cases when the inversion can not be performed analytically, other means such as the rejection sampling method can be used [104]. There are specialized methods for the certain common distributions, see, for example, Ref. [105].

The procedure can be generalized for finite numbers of independent parameters by applying it separately to each parameter. Obtaining realizations of dependent parameters is less straightforward.

Diagonalization can be used to obtain realizations of dependent parameters if the multidimensional distribution is a normal distribution. For other distributions the method is approximative. The multidimensional normal distribution of the parameters $\alpha = (\alpha_1, \ldots, \alpha_k)^\intercal$ is fully characterized by its mean $\mathrm{mean}(\alpha) \in \mathbb{R}^k$ and covariance $\mathrm{cov}(\alpha, \alpha) \in \mathbb{R}^{k \times k}$. The covariance matrix can be diagonalized as

$$\mathrm{cov}(\alpha, \alpha) = Q\, \mathrm{cov}(\beta, \beta) Q^\intercal, \tag{4.10}$$

where Q is an orthogonal matrix and $\mathrm{cov}(\beta, \beta)$ is a diagonal covariance

matrix for a new set of parameters $\beta = (\beta_1, \ldots, \beta_k)$. The new parameters are linear combinations of the original variables, i.e., $\beta = Q^\intercal \alpha$ and vice-versa, i.e,

$$\alpha = Q\beta. \tag{4.11}$$

Since the new parameters are jointly normal and uncorrelated, they are independent [106]. Therefore, the new parameters can be sampled one-by-one using the inverse transform sampling, and their realizations can be transformed into the realizations of the original parameters by using Eq. (4.11). The procedure can be applied to any distribution but for non-normal distributions it preserves only the first two moments of the distribution [49].

Other approaches to obtain realizations from dependent parameters include the Metropolis-Hastings algorithm [107, 108]. The algorithm requires some development work and is not capable of handling many dependent parameters in reasonable computation times [49]. An interesting recent method is correlated sampling, which can be used to sample correlated parameters whose distributions are, in principle, arbitrary, and, in practice, normal or log-normal [109].

4.3.2 Sampling techniques

Arguably the simplest sampling technique is the simple random sampling, in which each realization is generated without considering the other realizations in the sample [27, 31]. Since the realizations are independently chosen, the realizations can be generated at will and sample size does not have to be set a priori. The technique produces unbiased estimates from which uncertainty analysis can be readily performed [31]. Any method can be used to obtain the realizations of dependent parameters, if necessary. However, the realizations are not guaranteed to cover the space of parameters to any extent: subsets with low probability and extreme values of the responses are likely to be missed [31].

A popular sampling technique is the Latin hypercube sampling [110, 111]. The technique can only be applied to independent parameters, which restricts the available methods to handle dependent parameters. The technique generates a predetermined number of realizations, which form the sample. That is, the sample size must be decided before the sample generation. To generate a sample of s realizations, as in Eq. (4.9), the distributions of each of the k parameters are divided into s disjoint intervals

of equal probability. For each parameter and interval a value is selected. Hence, there is a pool of s values for each parameter. A realization is then constructed by drawing a value from the pools for each parameter. The value is not returned to the pool. Additional realizations are constructed so that s realizations are constructed, at which point the pools are empty. The technique guarantees that extreme values of each parameter are included in the realizations although combinations that produce extreme values for the responses might still be missed. Amazingly, the technique provides unbiased estimates for the cumulative distribution function [31]. The technique might be usable for correlated parameters at the expense of somewhat biased results [112].

For comparison of the described sampling techniques in reactor physics see, for example, Ref. [27]. There are also other sampling techniques, such as stratified random sampling, which is useful if very high or very low quantiles of the distribution that describes the knowledge of the responses need to be estimated but it requires, sometimes significant, extra development work [23]. For more sampling techniques, see, for example, Ref. [31].

4.3.3 Sensitivity analysis

The objective of the sensitivity analysis[13] is to study how the uncertainty in the individual responses can be apportioned to uncertainties in the individual parameters [31]. This is not straightforward for non-linear models. In the following a large enough sample size is assumed.

A simple way to perform sensitivity analysis is to make scatter plots of the pairs $(\alpha_n^i, R_m(\alpha^i))$, where the implicit form of the responses is used for convenience [23]. However, if the model consists of more than a modest number of parameters and responses, the number of plots becomes impractical.

Another method is linear regression analysis, in which a linear relationship between the parameters and the responses is fitted. However, the fitting requires a larger sample size than the number of parameters, and if the parameters are strongly correlated the fit might produce unstable regression coefficients – diagonalization is advised to transform the strongly correlated parameters into independent ones [23]. If the linear

[13] It should be mentioned that in deterministic uncertainty analysis the word "sensitivity analysis" is used to mean quantifying the effects of parameter variations on the responses [1].

model does not adequately describe the results, a more general regression model can be used although its interpretation might not be straightforward.

Variance decomposition methods apportion the variance of the response to the variances of the parameters and their second and higher-order interactions [113]. The method requires independent parameters, and contributions of the interactions are computationally demanding to evaluate especially for a large number of parameters [31]. However, the method accounts for the non-linear effects [31]. The second-order interactions have been evaluated, e.g., for a fuel performance simulation with a modest number of parameters [114].

The strengths of statistical uncertainty and sensitivity analysis lie in complex models with non-linear uncertainty contributions and relatively fast-to-evaluate models. Sensitivity analysis is the most practical for quite a small number of parameters. For description of further sensitivity analysis methods, see, for example, Refs. [23, 31, 80].

5. Summaries of the publications

This chapter summarizes the Publications of this Thesis and discusses their theoretical and practical implications.

5.1 Publication I: Computing Positive Semidefinite Multigroup Nuclear Data Covariances

In Publication I a novel application of a method to compute the nearest positive semidefinite matrices is proposed: the method should be applied to all covariance matrices of multigroup nuclear data. This ensures, under exact arithmetic, that the covariance matrices will be positive semidefinite, that is, positive definite except for the description of redundancies. Under exact arithmetic the method has several good properties: It does not modify positive semidefinite matrices, and can, therefore, be applied to proper covariance matrices. It preserves eigenvectors whose eigenvalues are not negative, and consequently it preserves the sum rules that describe redundancies in the nuclear data. The method will never decrease variances and therefore, conservatively, never reduce propagated uncertainties.

Under finite precision arithmetic the method is nearly as good as in exact arithmetic: positive semidefinite matrices are not modified. The negative eigenvalues are deflated, except for tiny negative eigenvalues that arise in extreme situations due to round-off errors. The sum rules are preserved in typical cases for spectral yields but not certainly for other types of nuclear data such as cross sections. Surprisingly, the variances are never decreased even with finite precision arithmetic. These results are both theoretical and seen in the practical examples. The excellent numerical properties are largely due to the excellent stability of eigenvalues of symmetric matrices. The method is illustrated in Figs. 3.2 and 3.3.

The covariance matrices of nuclear data are block matrices, whose sub-matrices are self-covariance matrices of individual quantities or cross-covariance matrices of two such quantities. For example, Fig. 3.4 illustrates these blocks. The sub-matrices are typically loosely connected, which can be exploited in computations by finding connected components of the partitioned covariance matrix. However, the method can be applied to any matrix, and perhaps more importantly, to any covariance matrix – whatever quantities it describes.

Only the Frobenius norm is considered in Publication I but it is suggested that other norms could be used. In Publication III, the class of weighted Frobenius norms is considered.

The method, when used as a post-processing tool in nuclear data processing codes, can be used as a quality assurance method. To facilitate this, a practical implementation is described in detail. However, large negative eigenvalues, compared to the largest positive eigenvalue, should not be deflated silently since they indicate errors in the original evaluation or the processing codes.

5.2 Publication II: Computing More Consistent Multigroup Nuclear Data Covariances

In Publication II, a novel method to find the nearest covariance matrices with given null vectors is proposed. It is also proposed that the method should be applied to find the nearest consistent covariance matrices of multigroup nuclear data with respect to their sum rules. This ensures, under exact arithmetic, that the covariance matrices satisfy the sum rules of nuclear data. Even under exact arithmetic the method is not completely satisfactory: it modifies eigenvectors that are not consistent with the sum rules, and therefore can reduce the variances and propagated uncertainties. In fact, the method will never increase variances. The method is illustrated in Fig. 3.4.

Under finite precision arithmetic the method modifies consistent covariance matrices, and therefore should not be applied to them. Therefore, Publication II presents a method to detect inconsistent covariance matrices. The given consistency criterion is strict enough for practical purposes but can be made even stricter. However, the method is numerically normwise backwards stable, which implies that large components are computed correctly but can not guarantee that small components would be

computed to high relative precision. This is also seen in the practical examples. Hence the title claims “more consistent” and not “consistent”.

In Publication II, the interpretation of partially specified inconsistent covariances of nuclear data is discussed. Two characterization methods to interpret inconsistent covariance matrices are considered. A third characterization method is described. None of them is adequate in every situation, which means that the choice of interpretation should not be built into processing codes but left to the user. The heuristic characterization method is illustrated in Fig. 3.4.

The method can be applied to any symmetric matrix with given null vectors. For most of the sum rules of nuclear data there is a special band structure in the null vectors, which could be exploited. In Publication II this is left as future work.

Only the Frobenius norm is considered in Publication II but it is suggested that other norms could be used. In Publication III the class of weighted Frobenius norms is considered.

The methods to detect inconsistent covariance matrices and find the nearest consistent covariance matrices can be used as a part of a quality assurance program. To facilitate this, a practical implementation is described in detail. However, large inconsistencies should not be corrected silently, since they indicate errors in the original evaluation or the processing codes.

5.3 Publication III: Computing More Proper Covariances of Energy Dependent Nuclear Data

Publication III is a generalization of Publications I and II for covariances of energy-dependent nuclear data, for which conditions for positivity and consistency with respect to the sum rules of nuclear data are presented. Sufficient and necessary conditions for positivity and consistency with respect to the sum rules of nuclear data are presented for covariances in the ENDF-6 format. The ENDF-6 format covariances are of finite rank, and the methods to detect improper covariance matrices in anterior Publications can be used with reinterpretation.

The nearest positive covariances can be found in certain typical situations by reinterpreting the method in Publication I. However, in typical situations the nearest consistent covariances can not be represented in the ENDF-6 format, so that reinterpreting the method in Publication II

yields only nearby covariances. The issues with precision of the method to find the nearest consistent covariances still stand. Therefore, Publication III settles for offering nearby more proper covariances and not the nearest proper covariances.

In Publication III the class of weighted Frobenius norms is considered and several different practical weights are considered. Examples demonstrate that norms that are scale-free in at least one sense have good properties for larger changes but not as good numerical properties as unweighted norms. The user of these methods should judge which norm, if any, to use case-by-case.

The methods to detect improper covariances can be used by the evaluators to detect blunders. The methods to remove improper parts can be used by the users of evaluations, if re-evaluations are not feasible. Necessary modifications to the earlier methods are described.

5.4 Publication IV: Survey of prediction capabilities of three nuclear data libraries for a PWR application

Publication IV is an application of uncertainty analysis to pressurized water reactors (PWRs). The emphasis is in determining world view uncertainty for three nuclear data libraries `ENDF/B-VII.1`, `JEFF-3.2`, and `JENDL-4.0u` for the application of generating two-group homogenized assembly constants for a steady state diffusion model for PWRs. Fresh uranium and mixed oxide assemblies are taken to represent PWRs.

The first-order sensitivity and uncertainty analysis is applied since its linearity allows straightforward apportioning the uncertainty of the responses to uncertainties of the nuclear data. However, the method is indirect and approximative. Significant contributors to the variances of the responses are identified, and the contributions are compared between the nuclear data libraries to identify large differences in contributions. Looking at the uncertainty estimates of nuclear data, there are evident differences in a few significant cases.

Between `ENDF/B-VII.1` and `JENDL-4.0u` order-of-magnitude differences in variances are found above about 1 MeV for the effective scattering cross section[14] of ^{238}U, on all relevant energies for radiative capture of ^{240}Pu

[14]The effective scattering cross section is specific to `CASMO` and defined as the sum of elastic, inelastic and neutron duplication cross sections. However, the neutron duplication cross sections are added only to certain nuclide specific energy regions.

and below $1\,\mathrm{eV}$ for radiative capture of ^{241}Pu. If the evaluations are not in error, nuclear data community does not agree on how well the nuclear data are known in these cases.

Another contribution is the enumeration of the status of uncertainty quantification in the libraries. The uncertainty estimates in `ENDF/B-VII.1` and `JENDL-4.0u` contain uncertainty estimates for all fuel nuclides, while `JEFF-3.2` only for three out of eight. However, `JEFF-3.2` contains the largest number of structural materials with uncertainty estimates.

5.5 Publication V: Uncertainty analysis of infinite homogeneous lead and sodium cooled fast reactors at beginning of life

Publication V is an application of first-order uncertainty analysis to lead and sodium cooled fast reactors. Fast reactors are of interest because they use uranium resources more efficiently than thermal reactors, and thereby allow a longer use of uranium and production of less minor actinides. Fast reactors also suffer from higher radiation damage, which are mainly due to fast neutrons, and nuclear data are less well known in the relevant energy range of fast reactors. In addition, the magnitudes of different sources of uncertainty are estimated.

In Publication V, the ratio of generated fuel to spent fuel, i.e., breeding ratio, the ratio of damage energy deposition to heat deposition and the ratio of ^{241}Am transmutation to heat deposition are estimated using the first-order sensitivity and uncertainty analysis. A reactor that can produce more fuel than it consumes, i.e., the breeding ratio is more than one, is a breeder. The results show that it is unknown whether either of the reactors would be breeders or not, since their breeding ratios are 1.06 ± 0.07 and 0.98 ± 0.08, for lead and sodium cooled reactors, respectively. For the other quantities of interest, 3–10 % uncertainties are predicted. The uncertainties are not exact since the linearity assumption might be violated. Therefore the results should be understood as order-of-magnitude estimates, rather than exact values.

In Publication V, parameter uncertainty, modeling uncertainty, and numerical uncertainty are estimated. For these cases, they are on the order of $10\,\%$, $1\,\%$ and $10^{-4}\,\%$, respectively. The latter two could be reduced by improving the model or computational methods but there is no need to do that as long as parameter uncertainty is the dominant source of uncertainty.

6. Concluding remarks

Uncertainty analysis in reactor physics is a mature field. The main contributions of this Thesis are the proposed quality assurance methods, the methods to find nearby more proper covariances, the identification of order-of-magnitude differences in uncertainty estimates of nuclear data libraries, the remarks on other sources of uncertainty than the parameter uncertainty and verification, in a few cases, that uncertainty due to nuclear data is the largest source of uncertainty. These contributions enable higher quality and more complete estimates of levels of confidence in the calculated quantities of interest.

The quality assurance methods can be used by users of evaluations of nuclear data and evaluators of nuclear data as a part of quality assurance programs. Quality of the uncertainty estimates of nuclear data is of prime importance since the results are directly defined by the data. Practical implementations are needed by both groups, and for this purpose an implementation for each method has been described in detail in Publications I–III.

For the users of evaluations, the methods should be incorporated to nuclear data processing software as a part of its quality assurance routines. It is hoped that the methods soon become obsolete in the sense that no evaluated covariances will be improper and no nuclear data processing software contains errors that make the processed covariances improper. Nevertheless, the quality assurance routines provide an additional check, which can detect blunders.

The evaluators benefit mostly from the energy-dependent versions of the methods. The methods to find nearby more proper covariances adds to the evaluation process: It can be used either to finalize an evaluation, which is almost, but not completely, proper, or to find the energy region and pieces of nuclear data which are not proper for further analysis. The

methods can be incorporated in to existing quality assurance programs.

The order-of-magnitude differences in uncertainty estimates of nuclear data identified in Publication IV should be further checked by the nuclear data community. Small differences are permissible and expected, since the evaluation process includes expert judgment, which the evaluators use slightly differently, and available experimental data and theoretical information change in time. However, the larger differences in the apportioned uncertainties signal that an evaluator has not included all significant information in the uncertainty estimates. The significant information might be missing from the evaluation with the larger or smaller uncertainties since new information might increase or decrease the uncertainties. There is also a possibility that an evaluation is simply erroneous. In both cases the comparison works as an ad hoc quality assurance method.

The uncertainty caused by uncertainty in nuclear data was the largest source of uncertainty in the cases considered in Publication V. However, the analyzed cases were simple and can not be directly generalized for more complex situations. Especially in deterministic codes uncertainty caused by various approximations in the model might cause significant modeling uncertainty.

6.1 Future prospects

The estimation of model uncertainty in deterministic codes should be performed. This can be done by comparing several results to a model with a more faithful representation of physics, for example, a model in a Monte Carlo code.

The origin of inconsistent covariances for $^{232}_{90}$Th was not resolved in Publication II. The origin might have been the processing of resonance parameters in `NJOY` or the issue might also be with the evaluation itself. The issue should be resolved.

The method to find nearby consistent covariance matrices is not described for cross-material covariances in Publications II and III. The necessary steps have been derived and the method implemented, but the implementation has not been documented in the Publications.

Further applications for the quality assurance methods and the methods to find nearby proper covariances are proposed in Section 3.1. These include application of the methods to uncertainties of fission yields, so that

their normalization could be included in the distribution that describes the evaluators' knowledge of the fission yields: presumably the evaluator does, indeed, know about the normalization. The impact of the added knowledge should be tested. Possible alternative approaches include the use of Bayesian inference and different filtering techniques.

In the present work, the TALYS-based evaluated nuclear data library has been left relatively untouched due to data processing issues. The proposed quality assurance methods should be applied to it.

Determining the correlations in older entries of the EXFOR database is a completion problem that is in parts similar to the one considered in Section 3.1.8. If the documentation in these entries is not sufficient, the methods can, perhaps, be adapted to the specific situation.

There is a need for high-fidelity uncertainty estimates for most parameters. In reactor physics, an obvious need is for uncertainty estimates for interaction of gamma radiation with matter to be included in the general-purpose nuclear data libraries. This needs new formats as well as evaluations of the data.

The practical deterministic uncertainty analysis methods lack the possibility to account for non-linearities, and the statistical methods are inadequate for large numbers of parameters especially when apportioning the uncertainties of the responses to the uncertainties of the parameters is required. Hence there is no known general method that could handle non-linearities for a large number of parameters efficiently. For complex large-scale systems there is a need for such an uncertainty analysis method.

Any project that requires more proper nuclear data covariances will benefit from the application of the proposed quality assurance methods. For example, the related fields of data adjustment and assimilation benefit from more proper prior data if the quality assurance methods are applied to all covariances of nuclear data before its publication. In addition, verification of the resulting covariances provides assurance for the quality of the intermediate calculations.

Bibliography

[1] D. G. Cacuci, *Sensitivity and Uncertainty Analysis: Theory*. Chapman & Hall/CRC, 2003.

[2] "Deterministic safety analysis for nuclear power plants specific safety guide," IAEA Safety Standards Series SSG-2, International Atomic Energy Agency, Vienna, Austria, 2009.

[3] W. M. Stacey, *Nuclear Reactor Physics*. John Wiley & Sons, 2007.

[4] D. L. Smith, "Evaluated nuclear data covariances: The journey from ENDF/B-VII.0 to ENDF/B-VII.1," *Nuclear Data Sheets*, vol. 112, no. 12, pp. 3037–3053, 2011. Special Issue on ENDF/B-VII.1 Library.

[5] J. R. Lamarsh and A. J. Baratta, *Introduction to nuclear engineering*. Addison-Wesley Publishing Company, 3rd ed., 2001.

[6] "Safety assessment and verification for nuclear power plants," IAEA Safety Standards Series NS-G-1.2, International Atomic Energy Agency, Vienna, Austria, 2009.

[7] "Best estimate safety analysis for nuclear power plants: Uncertainty evaluation," IAEA Safety Report Series No. 52, International Atomic Energy Agency, Vienna, Austria, 2008.

[8] Finnish Radiation and Nuclear Safety Authority (STUK), "Regulatory guides on nuclear safety (YVL)." `http://plus.edilex.fi/stuklex/en/lainsaadanto/luettelo/ydinvoimalaitosohjeet/`, cited 1.10.2015.

[9] D. L. Smith, *Probability, statistics, and data uncertainties in nuclear science and technology*. American Nuclear Society, LaGrange Park, 1991.

[10] G. Perey, "Expectations for ENDF/B-V Co-variance Files: Coverage, Strength and Limitations," in *A Review of the Theory and Application of Sensitivity and Uncertainty Analysis: Proceedings of a Seminar-Workshop* (C. R. Weisbin, R. W. Roussin, H. R. Hendrickson, and E. W. Bryant, eds.), (Oak Ridge, Tennessee, 22-24 August 1978), pp. 311–318, February 1979.

[11] A. Trkov, M. Herman, and D. A. Brown, eds., *ENDF-6 Formats Manual*. Brookhaven National Laboratory, 2011. Report BNL-90365-2009 Rev.2.

[12] R. C. Block, Y. Danon, F. Gunsing, and R. C. Haight, "Neutron cross section measurements," in *Handbook of Nuclear Engineering* (D. G. Cacuci, ed.), pp. 3–81, Springer US, 2010.

[13] K. Ivanov, M. Avramova, S. Kamerow, *et al.*, "Benchmarks for uncertainty analysis in modelling (UAM) for the design, operation and safety analysis of LWRs," NEA/NSC/DOC(2013)7, OECD Nuclear Energy Agency, November 2013. Version 2.1.

[14] K. Shibata, T. Kawano, T. Nakagawa, *et al.*, "Japanese Evaluated Nuclear Data Library Version 3 Revision-3: JENDL-3.3," *Journal of Nuclear Science and Technology*, vol. 39, no. 11, pp. 1125–1136, 2002.

[15] K. Shibata, O. Iwamoto, T. Nakagawa, *et al.*, "JENDL-4.0: A new library for nuclear science and engineering," *Journal of Nuclear Science and Technology*, vol. 48, no. 1, pp. 1–30, 2011.

[16] A. Koning, R. Forrest, M. Kellett, R. Mills, H. Henriksson, and Y. Rugama, eds., *The JEFF-3.1 Nuclear Data Library*. OECD/NEA Data Bank, 2006. JEFF Report 21.

[17] M. B. Chadwick, P. Obložinský, M. Herman, *et al.*, "ENDF/B-VII.0: Next generation evaluated nuclear data library for nuclear science and technology," *Nuclear Data Sheets*, vol. 107, pp. 2931–3118, December 2006.

[18] M. B. Chadwick, M. Herman, P. Obložinský, *et al.*, "ENDF/B-VII.1 nuclear data for science and technology: Cross sections, covariances, fission product yields and decay data," *Nuclear Data Sheets*, vol. 112, no. 12, pp. 2887 – 2996, 2011. Special Issue on ENDF/B-VII.1 Library.

[19] R. C. Little, T. Kawano, G. D. Hale, *et al.*, "Low-fidelity covariance project," *Nuclear Data Sheets*, vol. 109, no. 12, pp. 2828–2833, 2008.

[20] A. J. Koning and D. Rochman, "Modern nuclear data evaluation with the TALYS code system," *Nuclear Data Sheets*, vol. 113, p. 2841, 2012.

[21] "Technology relevance of the uncertainty analysis in modelling project for nuclear reactor safety," NEA/NSC/DOC(2007)15, OECD Nuclear Energy Agency, 2007.

[22] R. N. Bratton, M. Avramova, and K. Ivanov, "OECD/NEA Benchmark for uncertainty analysis in modeling (UAM) for LWRs – summary and discussion of neutronics cases (phase I)," *Nuclear Engineering and Technology*, vol. 46, no. 3, pp. 313 – 342, 2014.

[23] D. G. Cacuci and M. Ionescu-Bujor, "Sensitivity and uncertainty analysis, data assimilation, and predictive best-estimate model calibration," in *Handbook of Nuclear Engineering* (D. G. Cacuci, ed.), pp. 1913–2051, Springer US, 2010.

[24] M. Salvatores, G. Palmiotti, G. Aliberti, *et al.*, "Methods and issues for the combined use of integral experiments and covariance data: Results of a NEA international collaborative study," *Nuclear Data Sheets*, vol. 118, pp. 38 – 71, 2014.

[25] D. W. Muir, "Global assessment of nuclear data requirements (GANDR project)," IAEA report (7 volumes), International Atomic Energy Agency, Vienna, Austria, 2011.

[26] "Best-estimate methods (including uncertainty methods and evaluation) qualification and application. First meeting of the programme committee." NEA/SEN/SIN/AMA(2003)8, 2003.

[27] A. Hernández-Solís, *Uncertainty and sensitivity analysis applied to LWR neutronic and thermal-hydraulic calculations*. PhD thesis, Chalmers University of Technology, 2012.

[28] J. Vihavainen, *VVER-440 Thermal Hydraulics as a Computer Code Validation Challenge*. PhD thesis, Lappeenranta University of Technology, 2014.

[29] Joint Committee for Guides in Metrology, *Evaluation of measurement data – Guide to the expression of uncertainty in measurement*, 2008.

[30] D. L. Smith and N. Otuka, "Experimental nuclear reaction data uncertainties: Basic concepts and documentation," *Nuclear Data Sheets*, vol. 113, no. 12, pp. 3006 – 3053, 2012. Special Issue on Nuclear Reaction Data.

[31] J. C. Helton and F. J. Davis, "Latin hypercube sampling and the propagation of uncertainty in analyses of complex systems," *Reliability Engineering & System Safety*, vol. 81, no. 1, pp. 23 – 69, 2003.

[32] Joint Committee for Guides in Metrology, *International vocabulary of metrology – Basic and general concepts and associated terms (VIM)*, 2012.

[33] P. S. de Laplace, *Théorie analytique des probabilités*. Mme Ve Courcier, 1812. In English: *A philosophical essay on probabilities*, New York, J. Wiley; London, Chapman & Hall, 1902.

[34] E. T. Jaynes, *Probability Theory: The Logic of Science*. Cambridge University Press, 2003.

[35] A. N. Kolmogorov, *Grundbegriffe der Wahrscheinlichkeitrechnung, Ergebnisse Der Mathematik*. Springer-Verlag, Berlin, 1933. In English: *Foundations of Probability*, Chelsea Publishing Company, New York, 1950.

[36] A. Delaigle and P. Hall, "Defining probability density for a distribution of random functions," *The Annals of Statistics*, vol. 38, pp. 1171–1193, April 2010.

[37] O. Knill, *Probability Theory and Stochastic Processes with Applications*. Overseas Press, 2009.

[38] D. G. Cacuci and M. Ionescu-Bujor, "Mathematics for nuclear engineering," in *Handbook of Nuclear Engineering* (D. G. Cacuci, ed.), pp. 643–749, Springer US, 2010.

[39] M. A. Kellett, O. Bersillon, and R. W. Mills, eds., *The JEFF-3.1/-3.1.1 radioactive decay data and fission yields sub-libraries*. OECD/NEA Data Bank, 2009. JEFF Report 20.

[40] J. Venn, *The Logic of Chance: An Essay on the Foundations and Province of the Theory of Probability, with Especial Reference to Its Logical Bearings and Its Application to Moral and Social Science*. Macmillan, 1866.

[41] N. I. Akhiezer, *The classical moment problem and some related questions in analysis*. Oliver & Boyd Ltd, 1965. First English Edition.

[42] E. T. Jaynes, "Information theory and statistical mechanics," *Physical Review Series II*, vol. 106, pp. 620–630, May 1957.

[43] E. T. Jaynes, "Information theory and statistical mechanics. II," *Physical Review Series II*, vol. 108, pp. 171–190, October 1957.

[44] C. E. Shannon, "A mathematical theory of communication," *The Bell System Technical Journal*, vol. 27, pp. 379–423 and 623–656, 1948.

[45] J. N. Kapur, *Maximum-entropy Models in Science and Engineering*. Wiley, 1989.

[46] G. Žerovnik, A. Trkov, D. L. Smith, and R. Capote, "Transformation of correlation coefficients between normal and lognormal distribution and implications for nuclear applications," *Nuclear Instruments and Methods in Physics Research Section A: Accelerators, Spectrometers, Detectors and Associated Equipment*, vol. 727, pp. 33 – 39, 2013.

[47] A. D. Kiureghian and O. Ditlevsen, "Aleatory or epistemic? Does it matter?," *Structural Safety*, vol. 31, no. 2, pp. 105 – 112, 2009. Risk Acceptance and Risk Communication.

[48] K. Pearson, "Notes on regression and inheritance in the case of two parents," *Proceedings of the Royal Society of London*, vol. 58, pp. 240–242, 1895.

[49] G. Žerovnik, *Use of covariance matrices for estimating uncertainties in reactor calculations*. PhD thesis, University of Ljubljana, 2012.

[50] J. L. Doob, "Stochastic processes depending on a continuous parameter," *Trans. Am. Math. Soc.*, vol. 42, pp. 107 – 140, 1937.

[51] K. Karhunen, *Über lineare Methoden in der Wahrscheinlichkeitsrechnung*. PhD thesis, University of Helsinki, 1947. Ann. Acad. Sci. Fennicae. Ser. A. I. Math.-Phys. In English: *On Linear Methods of Probability Theory*, US Air Force, 1960.

[52] J. L. Doob, *Stochastic processes*. New York, Wiley, 1953.

[53] A. Blanc-Lapierre and R. Fortet, *Théorie des fonctions aléatoires: applications a divers phénomènes de fluctuation*. Masson, Paris, 1st ed., 1953. In English: *Theory of Random Functions*, vols. 1 and 2, Gordon and Breach Science Publishers Ltd., New York, 2nd ed., 1967 and 1968.

[54] N. S. Pugachev, *Theory of Random Functions and its Application to Control Problems*. International Series of Monographs on Automation and Automatic Control, Pergamon Press, 1965.

[55] M. Hazewinkel, ed., *Encyclopedia of Mathematics*, vol. 9. Kluwer Academic Publishers, 1993.

[56] N. Otuka, E. Dupont, V. Semkova, *et al.*, "Towards a more complete and accurate experimental nuclear reaction data library (EXFOR): International collaboration between nuclear reaction data centres (NRDC)," *Nuclear Data Sheets*, vol. 120, pp. 272 – 276, 2014.

[57] *International Handbook of Evaluated Criticality Safety Benchmark Experiments*. Nuclear Energy Agency, Paris. September 2014 edition.

[58] C. M. Mattoon, B. R. Beck, N. R. Patel, N. C. Summers, G. W. Hedstrom, and D. A. Brown, "Generalized nuclear data: A new structure (with supporting infrastructure) for handling nuclear data," *Nuclear Data Sheets*, vol. 113, no. 12, pp. 3145 – 3171, 2012. Special Issue on Nuclear Reaction Data.

[59] C. M. Mattoon, "Covariances in the generalized nuclear data (GND) structure," *Nuclear Data Sheets*, vol. 123, pp. 36 – 40, 2015. Special Issue on International Workshop on Nuclear Data Covariances April 28 - May 1, 2014, Santa Fe, New Mexico, USA.

[60] OECD/NEA Data Bank, "JEFF-3.2." `http://www.oecd-nea.org/dbdata/jeff/`, September 2015.

[61] A. Koning, S. Hilaire, and S. Goriely, "TALYS-1.6, a nuclear reaction program," user manual, 2013.

[62] N. Bohr, "Neutron capture and nuclear constitution," *Nature*, vol. 137, pp. 344 – 348, 1936.

[63] E. P. Wigner and L. Eisenbud, "Higher angular momenta and long range interaction in resonance reactions," *Phys. Rev.*, vol. 72, pp. 29–41, Jul 1947.

[64] F. Fröhner, "Evaluation and analysis of nuclear resonance data," Tech. Rep. JEFF Report 18, OECD/NEA, 2000.

[65] J. S. Martinez, W. Zwermann, L. Gallner, *et al.*, "Propagation of neutron cross section, fission yield, and decay data uncertainties in depletion calculations," *Nuclear Data Sheets*, vol. 118, pp. 480 – 483, 2014.

[66] K. Parker, "Physics of fast and intermediate reactors." IAEA, Vienna, 3-11 August 1961 (1962).

[67] C. M. Mattoon and P. Obložinský, "Issues in neutron cross section covariances," *Journal of the Korean Physical Society*, vol. 59, no. 23, pp. 1242–1247, 2011.

[68] A. C. Kahler, R. E. MacFarlane, D. W. Muir, and R. M. Boicourt, *The NJOY Nuclear Data Processing System, Version 2012*. Los Alamos National Laboratory, December 2012.

[69] D. Wiarda, G. Arbanas, L. Leal, and M. E. Dunn, "Recent advances with the AMPX covariance processing capabilities in PUFF-IV," *Nuclear Data Sheets*, vol. 109, no. 12, pp. 2791–2795, 2008.

[70] E. Greenspan, "Sensitivity functions for uncertainty analysis," in *Advances in Nuclear Science and Technology: Sensitivity and Uncertainty Analysis of Reactor Performance Parameters* (J. Lewins and M. Becker, eds.), vol. 14, pp. 193–246, Plenum Press, New York, 1982.

[71] T. Viitanen, *Development of a stochastic temperature treatment technique for Monte Carlo neutron tracking*. PhD thesis, Aalto University, 2015.

[72] G. I. Bell and S. Glasstone, *Nuclear Reactor Theory*. Van Nostrand Reinhold Inc.,U.S., 1970.

[73] J. J. Duderstadt and L. J. Hamilton, *Nuclear Reactor Analysis*. John Wiley & Sons, Inc, 1976.

[74] R. J. J. Stamm'Ler and M. J. Abbate, *Methods of steady-state reactor physics in nuclear design*. Academic Press, London, United Kingdom, 1983.

[75] C. Demaziére, "Modelling of nuclear reactors." Lecture Notes, Chalmers University of Technology, Gothenburg, Sweden, 2015.

[76] M. Pusa, *Numerical methods for nuclear fuel burnup calculations*. PhD thesis, Aalto University, 2013.

[77] A. Isotalo, *Computational Methods for Burnup Calculations with Monte Carlo Neutronics*. PhD thesis, Aalto University, 2013.

[78] I. M. Copi, C. Cohen, and D. E. Flage, *Essentials of Logic*. Pearson Prentice Hall, 2007.

[79] M. L. Williams, "Perturbation theory for nuclear reactor analysis," in *CRC Handbook of Nuclear Reactors Calculations* (Y. Ronen, ed.), vol. III, pp. 64–188, CRC Press Inc., 1986.

[80] D. G. Cacuci, M. Ionescu-Bujor, and I. M. Navon, *Sensitivity and Uncertainty Analysis: Applications to Large-Scale Systems*. Taylor & Francis, 2005.

[81] M. C. Kennedy and A. O'Hagan, "Bayesian calibration of computer models," *Journal of the Royal Statistical Society: Series B (Statistical Methodology)*, vol. 63, no. 3, pp. 425–464, 2001.

[82] R. Bellman and R. Corporation, *Dynamic Programming*. Rand Corporation research study, Princeton University Press, 1957.

[83] A. Taavitsainen, "Coupled FINIX-DRAGON calculation chain for an LWR pin cell case," 2015. Special Assignment, Aalto University.

[84] Y. A. Chao and Y. A. Shatilla, "Conformal mapping and hexagonal nodal method – II: Implementation in the ANC-H code," *Nuclear Science and Engineering*, vol. 121, pp. 210 – 225, 1995.

[85] B. N. Parlett, *The Symmetric Eigenvalue Problem*. Society for Industrial and Applied Mathematics, 1998.

[86] N. J. Higham, *Accuracy and Stability of Numerical Algorithms*. Society for Industrial and Applied Mathematics, second ed., 2002.

[87] P. Chebyshev, "Des valeurs moyennes," *Journal de mathématiques pures et appliquées*, vol. 12, pp. 177–184, 1867.

[88] Z. W. Birnbaum, J. Raymond, and H. S. Zuckerman, "A generalization of Tshebyshev's inequality to two dimensions," *The Annals of Mathematical Statistics*, vol. 18, pp. 70–79, March 1947.

[89] I. Olkin and J. W. Pratt, "A multivariate Tchebycheff inequality," *The Annals of Mathematical Statistics*, vol. 29, pp. 226–234, March 1958.

[90] I. R. Savage, "Probability inequalities of the Tchebycheff type," *Journal of Research of the National Bureau of Standards-B. Mathematics and Mathematical Physics B*, vol. 65, pp. 211–222, 1961.

[91] D. F. Vysochanskij and Y. I. Petunin, "Justification of the 3σ rule for unimodal distributions," *Theory of Probability and Mathematical Statistics*, vol. 21, pp. 25–36, 1980.

[92] G. Chiba, M. Tsuji, and T. Narabayashi, "Uncertainty quantification of neutronic parameters of light water reactor fuel cells with JENDL-4.0 covariance data," *Journal of Nuclear Science and Technology*, vol. 50, no. 7, pp. 751–760, 2013.

[93] E. P. Wigner, "Effect of small perturbations on pile period," Tech. Rep. CP-3048, 1945.

[94] L. N. Usachev, "Perturbation theory for the breeding ratio and for other number ratios pertaining to various reactor processes," *J. Nucl. Energy A/B*, vol. 18, p. 571, 1964.

[95] J. Lewins, *Importance: the Adjoint Function*. Pergamon Press, Oxford, 1965.

[96] E. Greenspan, "Developments in perturbation theory," in *Advances in Nuclear Science and Technology* (E. Henley and J. Lewins, eds.), vol. 9, pp. 181–268, Plenum Press, New York/London, 1976.

[97] E. Greenspan, "New developments in sensitivity theory," in *Advances in Nuclear Science and Technology: Sensitivity and Uncertainty Analysis of Reactor Performance Parameters* (J. Lewins and M. Becker, eds.), vol. 14, pp. 313–361, Plenum Press, New York, 1982.

[98] A. A. Abagyan, E. E. Petrov, and V. Y. Pupko, "On optimizing the shape of the medium in the presence of radiation," *Soviet Atomic Energy*, vol. 27, no. 3, pp. 935–939, 1969.

[99] A. Trkov and G. Žerovnik, "Proposed changes to the ENDF-6 format," 2013. `http://ndclx4.bnl.gov/gf/download/trackeritem/900/3035/Trkov_Zerovnik_ENDF-6_CSWEG_2013_v31.pdf`, referenced 30.8.2015.

[100] A. Guba, M. Makai, and L. Pál, "Statistical aspects of best estimate method–I," *Reliability Engineering & System Safety*, vol. 80, no. 3, pp. 217 – 232, 2003.

[101] J. G. Saw, M. C. K. Yang, and T. C. Mo, "Chebyshev inequality with estimated mean and variance," *The American Statistician*, vol. 38, no. 2, pp. 130–132, 1984.

[102] A. Kabán, "Non-parametric detection of meaningless distances in high dimensional data," *Statistics and Computing*, vol. 22, no. 2, pp. 375–385, 2012.

[103] C. J. Díez, O. Buss, A. Hoefer, D. Porsch, and O. Cabellos, "Comparison of nuclear data uncertainty propagation methodologies for PWR burn-up simulations," *Annals of Nuclear Energy*, vol. 77, pp. 101 – 114, 2015.

[104] J. von Neumann, "Various techniques used in connection with random digits. Monte Carlo methods," *Nat. Bureau Standards*, vol. 12, pp. 36–38, 1951.

[105] G. E. P. Box and M. E. Muller, "A note on the generation of random normal deviates," *Ann. Math. Statist.*, vol. 29, pp. 610–611, June 1958.

[106] L. Bain and M. Engelhardt, *Introduction to probability and mathematical statistics*. Duxbury Press, 1987.

[107] N. Metropolis, A. W. Rosenbluth, M. N. Rosenbluth, A. H. Teller, and E. Teller, "Equation of state calculations by fast computing machines," *The Journal of Chemical Physics*, vol. 21, no. 6, pp. 1087–1092, 1953.

[108] W. K. Hastings, "Monte Carlo sampling methods using Markov chains and their applications," *Biometrika*, vol. 57, no. 1, pp. 97–109, 1970.

[109] G. Žerovnik, A. Trkov, and I. A. Kodeli, "Correlated random sampling for multivariate normal and log-normal distributions," *Nuclear Instruments and Methods in Physics Research Section A: Accelerators, Spectrometers, Detectors and Associated Equipment*, vol. 690, pp. 75 – 78, 2012.

[110] M. D. McKay, R. J. Beckman, and W. J. Conover, "A comparison of three methods for selecting values of input variables in the analysis of output from a computer code," *Technometrics*, vol. 21, no. 2, pp. 239–245, 1979.

[111] R. L. Iman, J. C. Helton, and J. E. Campbell, "An approach to sensitivity analysis of computer models, part 1. Introduction, input variable selection and preliminary variable assessment," *Journal of Quality Technology*, vol. 13, no. 3, pp. 174–183, 1981.

[112] R. L. Iman and W. J. Conover, "A distribution-free approach to inducing rank correlation among input variables," *Communications in Statistics - Simulation and Computation*, vol. 11, no. 3, pp. 311–334, 1982.

[113] I. M. Sobol', "Sensitivity estimates for nonlinear mathematical models," *Mathematical Modeling & Computational Experiment*, vol. 1, no. 4, pp. 407–414, 1993. Original in Russian: *Matematicheskoe Modelirovanie*, vol. 2, pp. 112-118., 1990.

[114] T. Ikonen and V. Tulkki, "The importance of input interactions in the uncertainty and sensitivity analysis of nuclear fuel behavior," *Nuclear Engineering and Design*, vol. 275, pp. 229 – 241, 2014.

Errata

Unfortunately, the final versions of the Publications contain a few errors and the author apologizes for any inconvenience these may have caused. The following errors have been identified.

Publication I

- It is not mentioned that the gap, as estimated in Eq. (20), can not be negative.
- In discussion (Section VI.) it is advised to use the absolute (relative) version of the method when absolute (relative) covariances are going to be used. It is not mentioned clearly enough that the advice stems from numerical considerations.

Publication V

- A transposition is missing in Eq. (6b). The correct form of the equation is
$$\mathrm{cov}(\alpha, \alpha) = \langle (\alpha - E(\alpha))(\alpha - E(\alpha))^{\mathrm{T}} \rangle .$$
- Below Eq. (6b), the inline equation $\langle \cdot \rangle = \int \cdot \int p(\alpha) d\alpha$ has an extra integral sign. The correct form is $\langle \cdot \rangle = \int \cdot p(\alpha) d\alpha$.

Publication I

R. Vanhanen. Computing positive semidefinite multigroup nuclear data covariances. *Nuclear Science and Engineering*, 179, *4*, 411–422, April 2015; `http://dx.doi.org/10.13182/NSE14-75`.

NUCLEAR SCIENCE AND ENGINEERING: **179**, 411–422 (2015)

Computing Positive Semidefinite Multigroup Nuclear Data Covariances

Risto Vanhanen*

Aalto University School of Science, Department of Applied Physics
P.O. Box 14100, FI-00076 Aalto, Finland

Received May 7, 2014
Accepted June 17, 2014
http://dx.doi.org/10.13182/NSE14-75

Abstract—*We propose a novel application of a method to compute the nearest positive semidefinite matrix. When applied to covariance matrices of multigroup nuclear data, the method removes unphysical components of the covariances while preserving the physical components of the original covariance matrix. The result is a mathematically proper covariance matrix.*

We show that the method preserves the so-called zero sum rule of covariances of distributions in exact arithmetic. The results also hold for typical cases of finite precision arithmetic. We identify conditions that might damage the zero sum rule.

Rounding can distort the eigenvalues of a symmetric matrix. We give a known bound on how large distortions can occur due to round-off. Consequently, there is a known upper bound on how large negative eigenvalues can be attributed to round-off error. Current evaluations and processing codes do produce larger negative eigenvalues.

Three practical examples are processed and analyzed. We demonstrate that satisfactory results can be achieved.

We discuss briefly the relevance of the method, its properties, and alternative approaches. The method can be used as a part of a quality assurance program and would be a valuable addition to nuclear data processing codes.

I. INTRODUCTION

Modern nuclear data files are evaluations that contain best estimates and uncertainty estimates of nuclear data. When the latter are used in deterministic codes, the data are usually processed into approximative multigroup form with codes such as NJOY (Ref. 1) or PUFF-IV (Ref. 2). The generated multigroup covariance matrices are typically slightly asymmetric, and even if they are symmetric, they are typically not positive semidefinite. Strictly speaking, the generated covariance matrices are typically improper. If the covariance matrices contain large negative eigenvalues, the results of subsequent calculations are questionable at best.

Lately, the issue has been raised by Kodeli,[3] who provided a program to check for symmetry and eigenvalues of the generated intrareaction covariance matrices, and the Low-fidelity Covariance Project,[4] in which it was noted that small negative eigenvalues might be caused by round-off error. More recently, Mattoon and Obložinský[5] gave a more comprehensive list of desirable properties of covariance matrices in the context of quality assurance programs and provided a program to check for these properties for the generated intrareaction covariance matrices.

Earlier, Peelle[6] had proposed a method to modify a covariance matrix to ensure its positive definiteness. Alas, the method is applicable only to a covariance matrix whose smallest nonnegative eigenvalue is much greater than the absolute value of the most negative eigenvalue. This is not a typical situation.

In this paper we propose a novel application of a method to compute a nearest positive semidefinite covariance matrix from any generated covariance matrix.

*E-mail: risto.vanhanen@aalto.fi

The method was originally published by Higham,[7] but it seems that it has not been previously applied for covariances of nuclear data. The method can be applied to any generated covariance matrix since it will not modify positive semidefinite matrices.

If the Frobenius norm is used to measure the nearness, then the nearest symmetric positive covariance matrix is unique.[7] Using the Frobenius norm also seems to give the lowest, and acceptable, computational cost.

It should be noted that the proposed method does not produce strictly positive definite matrices. At least, data assimilation and best-estimate adjustment[6,8] require positive definite covariance matrices. However, covariances of spectral yields and covariances of cross sections of redundant reactions mandate zero eigenvalues to physically sound covariance matrices. These zero eigenvalues signal only that the system includes redundant information.

Rounding can distort the eigenvalues of a symmetric matrix. We give a known bound on how large distortions can occur due to round-off (see, e.g., Ref. 9). Consequently there is a known upper bound on how large negative eigenvalues can be attributed to round-off error.

The paper is organized as follows. Theoretical background is briefly presented in Sec. II. Details about a practical implementation are given in Sec. III. Three test cases are described in Sec. IV, and their results analyzed in Sec. V. We include cross-reaction covariance matrices but exclude cross-material covariance matrices, although the methodology is also readily applicable to cross-material covariance matrices. The method and results are discussed in Sec. VI. Finally, in Sec. VII the conclusions are given.

II. THEORY

For the terminology and practical implementation, we need the following results.

II.A. The Frobenius and Spectral Norms

For $A \in \mathbb{R}^{n\times n}$ the Frobenius norm is defined by

$$\|A\|_F^2 = \sum_{i,j} a_{ij}^2 \,, \tag{1}$$

and the spectral norm is defined by

$$\|A\|_2^2 = \lambda_{\max}\left(A^T A\right) \,. \tag{2}$$

It is also known as the 2-norm.

II.B. A Nearest Symmetric Matrix

Fan and Hoffman[10] solved the matrix nearness to symmetry problem for the unitarily invariant norms. The following is a special case of the result.

Let $A \in \mathbb{R}^{n\times n}$. The unique nearest symmetric matrix A_s in the Frobenius norm is

$$A_s = \frac{1}{2}\left(A + A^T\right) \,, \tag{3}$$

i.e., the symmetric part of A.

By the nearest symmetric matrix, we mean the nearest symmetric matrix as measured by the Frobenius norm.

II.C. A Nearest Symmetric Positive Semidefinite Matrix

Higham[7] proves the following result.

Let $A \in \mathbb{R}^{n\times n}$ and set $A_s = (A + A^T)/2$ to be the nearest symmetric matrix of A. The unique nearest symmetric positive semidefinite matrix A_{psd} in the Frobenius norm to A is

$$A_{psd} = X \max(\Lambda, 0) X^T \,, \tag{4}$$

where $A_s = X\Lambda X^T$ is the eigendecomposition of the nearest symmetric matrix and $\max(\Lambda, 0)$ contains the nonnegative eigenvalues with negative eigenvalues replaced by zeros.

By the nearest (symmetric) positive semidefinite matrix, we mean the nearest symmetric positive semidefinite matrix as measured by the Frobenius norm.

II.D. Deflation Preserves the Scaled Zero Sum Property

Let $A \in \mathbb{R}^{n\times n}$ be a symmetric matrix with the scaled zero sum property

$$\sum_i s_i a_{ij} s_j = 0 \tag{5}$$

and $A = X\Lambda X^T$ be its eigendecomposition. Then, the deflated matrix $B = A - \lambda x x^T$, with any eigenpair (λ, x), has the scaled zero sum property

$$\sum_i s_i b_{ij} s_j = 0 \,; \tag{6}$$

i.e., deflation preserves the scaled zero sum property in exact arithmetic.

Proof: For eigenpair $(0, x)$ or scale $s_j = 0$, there is nothing to prove. For eigenpair $(\lambda, x) \neq (0, x)$ and scale $s_j \neq 0$, we have

$$Ax = \lambda x \Leftrightarrow \sum_j a_{ij} x_j = \lambda x_i \tag{7}$$

so that

$$\sum_i s_i x_i = \sum_i s_i \sum_j a_{ij} \frac{x_j}{\lambda} = \sum_j \frac{x_j}{\lambda} \sum_i s_i a_{ij} = 0 \tag{8}$$

due to the original scaled zero sum property. Now, for $B = A - \lambda x x^T$,

$$\sum_i s_i b_{ij} s_j = \sum_i s_i (a_{ij} - \lambda x_i x_j) s_j$$
$$= \sum_i s_i a_{ij} s_j - s_j \lambda x_j \sum_i s_i x_i = 0 \qquad (9)$$

due to the original scaled zero sum property and the intermediate result.

Note that the nearest positive semidefinite matrix can be expressed as

$$A_{psd} = A - \sum_k \lambda_k x_k x_k^T , \qquad (10)$$

where the summation runs over negative eigenvalues of A. Therefore, application of the proposed method preserves the scaled zero sum property in exact arithmetic.

Note that absolute covariances of spectral yields of emitted neutrons have the zero sum property with unit scales. Relative covariances of spectral yields of emitted neutrons have the zero sum property with spectral yields as scales. In both cases the original zero sum property is preserved under deflation in exact arithmetic.

II.E. Eigenvalues of the Sum of Two Symmetric Matrices

Wilkinson (Ref. 9, Chap. 2, Sec. 44) proves the following useful result.

Let A, B, and C be $\in \mathbb{R}^{n \times n}$ symmetric matrices and

$$A + B = C . \qquad (11)$$

Denote their eigenvalues by α_i, β_i, and γ_i, respectively, where all three sets are arranged in nonincreasing order. The s'th eigenvalue of C is bound by

$$\alpha_s + \beta_n \le \gamma_s \le \alpha_s + \beta_1 . \qquad (12)$$

III. IMPLEMENTATION

III.A. Block Structure of a Covariance Matrix

A generated covariance matrix A can be represented in $\mathbb{R}^{n \times n}$, where $n = pg$, g is the number of groups, and p is the number of (material, reaction) pairs whose covariances are described. That is, the generated full covariance matrix is partitioned into a $p \times p$ matrix of $g \times g$ covariance matrices as illustrated in Fig. 1. The partitioned matrix is usually sparse due to the low number of cross-reaction and cross-material covariances.

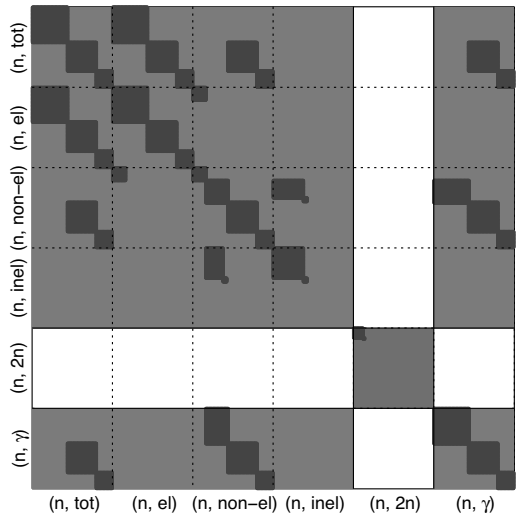

Fig. 1. The $n \times n$ generated covariance matrix of $^{207}_{82}$Pb of ENDF/B-VII.1 (Ref. 16). The locations of nonzero elements of each $g \times g$ block are emphasized. The smaller connected component of the partitioned $p \times p$ matrix consists of only the $(n, 2n)$ reaction and the larger of the other reactions. In principle, this is part of a larger covariance matrix of all (material, reaction) pairs but is not connected to any of them since $^{207}_{82}$Pb lacks cross-material covariances.

In principle we could apply the proposed method to the full matrix directly, but it is possible to take advantage of the sparseness. This saves considerable amounts of processing time, reduces the memory requirements, and makes the results somewhat more accurate since we need to work with smaller matrices.

The idea is to find connected components of the $p \times p$ matrix of $g \times g$ covariance matrices. Then, the $p \times p$ matrix can be, in principle, permuted into block diagonal form, with connected components on the diagonal. In practice, we assemble the connected components after we have identified them.

We identify the connected components by forming an adjacency matrix, where the (material, reaction) pair is connected to the (material1, reaction1) pair if the covariance matrix between them is nonzero. We run a depth first search to identify connected components. This is fast since the number of (material, reaction) pairs is usually small.

III.B. Application of the Proposed Method

We apply the proposed method to every connected component separately.

III.B.1. Eigendecomposition

We use the expert driver DSYEVR (Ref. 11) of LAPACK (Refs. 11 and 12) to compute the eigendecomposition:

$$A = \sum_{i=1}^{n} \lambda_i x_i x_i^T \ . \tag{13}$$

Here, finite precision plays a role. Instead of true eigenvalues λ_i and true eigenvectors x_i, we get computed eigenvalues $\hat{\lambda}_i$ and computed eigenvectors $\hat{x}_i$.

In general, the eigenvalues are solved rather well. Given the Rayleigh quotient $\hat{\rho}_i = \hat{x}_i^T A \hat{x}_i / \hat{x}_i^T \hat{x}_i$, we have

$$|\hat{\lambda}_i - \lambda_i| \le |\hat{\lambda}_i - \hat{\rho}_i| + |\hat{\rho}_i - \lambda_i| \ , \tag{14}$$

from which we can compute the first term and use one of the following upper bounds for the latter term (Ref. 13, Theorem 4.5.1):

$$|\hat{\rho}_i - \lambda_i| \le \|r(\hat{x}_i)\|_2 \ , \tag{15}$$

where the residual $r(\hat{x}_i)$ is $A\hat{x}_i - \hat{\rho}\hat{x}_i$. If the gap between the Rayleigh quotient and the nearest eigenvalue that the Rayleigh quotient is not approximating, i.e., $g_i = \min_{\lambda_j \neq \lambda_i} |\hat{\rho}_i - \lambda_j|$, is large enough, we have tighter bounds (Ref. 13, Theorem 11.7.1):

$$|\hat{\rho}_i - \lambda_i| \le \|r(\hat{x}_i)\|_2^2 / g_i \ . \tag{16}$$

The eigenvectors are solved less accurately. The computed eigenvector $\hat{x}_i$ can be expressed as[13]

$$\hat{x}_i = x_i \cos\theta_i + w_i \sin\theta_i \ , \tag{17}$$

where w_i is a unit vector orthogonal to x_i in the plane spanned by x_i and $\hat{x}_i$, and θ_i is the angle between x_i and $\hat{x}_i$. There is no general guarantee about the quality of the eigenvectors, except the orthogonality property[11]:

$$\hat{x}_i^T \hat{x}_j = \mathcal{O}(\epsilon_m) \quad \text{for } i \neq j \ , \tag{18}$$

where ϵ_m is the machine epsilon, and except the acute angle between the computed and true eigenvector (Ref. 13, Theorem 11.7.1):

$$|\sin\theta_i| \le \|r(\hat{x}_i)\|_2 / g_i \ . \tag{19}$$

There is a tendency for the blocks to contain near-zero eigenvalues for which the absolute gap is very small. Eigenvectors for these are badly determined. The analysis does not cover eigenvalues with nonunity multiplicity, but we have not encountered a need to work with such things.

In practice, we compute the norm of the residual directly and estimate the gap by

$$g_i \approx \min_{j=i\pm1} (|\hat{\rho}_i - \hat{\rho}_j| - \|r(\hat{x}_i)\|_2) \ . \tag{20}$$

Then, the bounds for the Rayleigh quotients are estimated as the smaller of Eqs. (15) and (16). The bounds for the eigenvalues are estimated using Eq. (14), but we acknowledge that we cannot expect better than $|\hat{\lambda}_i - \lambda_i| \le \epsilon_m |\hat{\lambda}_i|/2$. The bounds for the acute angles of the eigenvectors are estimated directly using Eq. (19), but we acknowledge that we cannot have worse than $|\sin\theta| \le 1$.

III.B.2. Deflation

We deflate all eigenpairs whose eigenvalue is negative, given the estimated bound b_i, by subtraction. This gives us the computed nearest positive semidefinite matrix $\hat{A}_{psd}$. We use LAPACK's symmetric rank 1 update function DSYR (Ref. 11) for each eigenpair:

$$\hat{A}_{psd} = A - \sum_{\hat{\lambda}_i < -b_i} \hat{\lambda}_i \hat{x}_i \hat{x}_i^T + H \ , \tag{21}$$

where H describes the induced rounding error due to summation. Parlett[13] has shown that because of the orthogonality property of the computed eigenvectors, the changes in the nondeflated eigenvalues and eigenvectors are dominated by this rounding error.

III.B.2.a. Zero Sum Property with Finite Precision Deflation

When applied to absolute covariance matrices, the deflation preserves the zero sum property in finite precision arithmetic for well-separated eigenvalues and for relatively well-separated eigenvalues. When applied to relative covariance matrices, the zero sum property is preserved in a relative sense for the same cases. These are shown in the following, but the analysis does not cover eigenvalues with nonunity multiplicity.

Consider an absolute covariance matrix A with the zero sum property. For the computed matrix $\hat{B} = A - \hat{\lambda}\hat{x}\hat{x}^T + H$, where H represents the round-off error, the absolute value of the row sum is bound by

$$|\sum_i \hat{b}_{ij}| \le |\sum_i a_{ij}| + |\sum_i \hat{\lambda}\hat{x}_i\hat{x}_j| + |\sum_i h_{ij}| \ , \tag{22}$$

where $|h_{ij}|$ is at most $3\epsilon_m |a_{ij}|$ and

$$|\sum_i h_{ij}| \le f(n)\epsilon_m \|A\|_2 \ , \tag{23}$$

where $f(n)$ is typically a small constant, but in the worst case $f(n)=3n$. Now,

$$\begin{aligned}|\sum_i \hat{\lambda}\hat{x}_i\hat{x}_j| &\le |\hat{x}_j||\hat{\lambda}||\sum_i (x_i\cos\theta + w_i\sin\theta)| \\ &= |\hat{x}_j||\hat{\lambda}||\sum_i w_i\sin\theta| \\ &\le |\hat{x}_j||\hat{\lambda}|\|r(\hat{x})\|/g \qquad (24)\end{aligned}$$

$$\le |\hat{x}_j|\|r(\hat{x})|/\gamma\,, \qquad (25)$$

where $\gamma = g/|\hat{\lambda}|$ is the relative gap.[a] Equations (24) and (25) show the cases for well-separated eigenvalues and relatively well-separated eigenvalues, respectively.

Consider a relative covariance matrix C, calculated from A so that $s_i c_{ij} s_j = a_{ij}$. For the computed matrix $\hat{D} = C - \hat{\mu}\hat{z}\hat{z}^T + H$, the scaled row sum is bound by

$$\begin{aligned}|\sum_i s_i\hat{d}_{ij}s_j| &\le |\sum_i s_i c_{ij}s_j| + |\sum_i s_i\hat{\mu}\hat{z}_i\hat{z}_j s_j| + |\sum_i s_i h_{ij}s_j| \\ &\le |s_j|\|s\|_\infty|\hat{z}_j||\hat{\mu}||\sin\theta| + |s_j|\|s\|_\infty f(n)\epsilon_m\|C\|_2 \\ &= |s_j|\|s\|_\infty\left(|\hat{z}_j||\hat{\mu}||\sin\theta| + f(n)\epsilon_m\|C\|_2\right)\,, \qquad (26)\end{aligned}$$

where the details are essentially the same as with the absolute case. However, any induced error is amplified by the factor $|s_j|\|s\|_\infty$.

In practice, we monitor the magnitude of the term in Eq. (24) with $|\hat{x}_j| \le 1$ and compare it with the magnitude of the round-off term with $f(n)=100$. We also monitor $\|s\|_\infty^2$ so that any large amplifiers can be detected. However, for properly normalized spectral yields $\|s\|_\infty \le 1$.

The above bounds are even better if the zero sum property is originally only approximately met—that is, if

$$|\sum_i \hat{a}_{ij}| = |\sum_i s_i\hat{c}_{ij}s_j| \le \epsilon_s|s_j|\|s\|_\infty\,, \qquad (27)$$

where $\epsilon_s \ge \epsilon_m$ gives the tolerance for the initial row sum.[b] However, the spectral decomposition of $\hat{A}$ only approximates the spectral decomposition of A.

III.C. Distortion of Eigenvalues due to Round-Off Error

Consider a symmetric matrix $A \in \mathbb{R}^{n\times n}$. The rounded matrix is equal to $A+B$, where $B \in \mathbb{R}^{n\times n}$ contains the round-off errors. The magnitude of the round-off error is bounded so that $|b_{ij}| \le \epsilon_r|a_{ij}|$, where ϵ_r is the rounding precision. For example, we have $\epsilon_r = 5\times 10^{-n}$ for rounding to n decimals. This implies that $\|B\|_2 \le \epsilon_r n \max_{ij}|a_{ij}|$ (Ref. 9, Chap. 2, Secs. 44 and 45).

As a direct consequence of Sec. II.E, the round-off error can distort eigenvalues of A by at most $\|B\|_2$. The bound of $\epsilon_r n \max_{ij}|a_{ij}|$ gives an upper limit for what can be attributed to round-off error. Any negative eigenvalue whose magnitude is larger than the bound results from something other than round-off error.

IV. CALCULATIONS

We use a slightly modified NJOY 2012.8 (Ref. 1) to process the ENDF-6 format[15] nuclear data from the ENDF/B-VII.1 (Ref. 16) evaluation into multigroup covariances. We present three cases where we apply the method to covariance matrices with negative eigenvalues. The cases were selected to cover a variety of data types and group structures. In all cases the magnitudes of the negative eigenvalues are larger than what the round-off error would give in the worst case and larger than typical in the first two cases.

All the cases use a relative reconstruction tolerance of 10^{-5} and temperature of 300 K, and Maxwell + 1/E + fission spectrum weight is used with a 0.1-eV thermal break, 820.3-keV fission break, and 1.4-MeV fission temperature. The module PURR is run with 40 bins and 80 ladders. We extract the covariances from ERRORR in their processing (double) precision, but note that the original data are roughly in single precision only.

The first case is absolute covariances of cross sections of $^{35}_{17}$Cl. The evaluation contains covariances for elastic scattering, radiative capture, and proton emission that are connected through cross-reaction covariances and therefore form a single connected component. We use the XMAS 172-group structure[17] with the lowest boundary set to 10^{-5} eV and a 20-MeV boundary added.

The second case is relative covariances of average cosine of the scattering angle in the laboratory system for elastic scattering of neutrons of $^{232}_{90}$Th—that is, relative covariances of $\bar{\mu}$ of $^{232}_{90}$Th. We use the group structure of the evaluation, which contains 25groups.

The third case is relative covariances of spectral yields of neutrons emitted from $^{252}_{98}$Cf fission for incident neutron energies between 10^{-5} eV and 5 MeV—that is, relative covariances of χ of $^{252}_{98}$Cf. We use the VITAMIN-J 175-group structure[17] augmented with a 20-MeV boundary.

V. RESULTS

V.A. Absolute Covariances of Cross Sections of $^{35}_{17}$Cl

The absolute difference between the original and deflated absolute covariances of cross sections of $^{35}_{17}$Cl is shown in Fig. 2. The variances do not decrease when the

[a]The definition here is somewhat different from, for example, in Refs. 11 and 14.

[b]The ENDF-6 format[15] specifies $\epsilon_s = 10^{-5}1/\text{eV}/\|s\|_\infty$ for covariances of spectral yields.

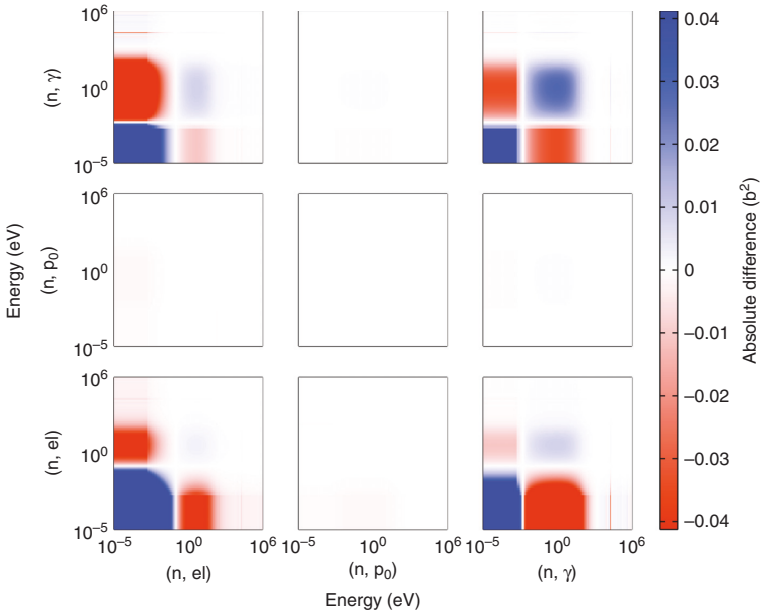

Fig. 2. Absolute difference between the original and the deflated absolute covariances of cross sections of $^{35}_{17}$Cl.

covariance matrix is deflated. The asymmetry of the original covariances is so slight that it is not visible. The largest changes occur in the thermal-epithermal regions of the cross sections of elastic scattering and neutron capture. Their cross-reaction covariances are also affected by the deflation. The absolute changes in the (n, p_0) reaction are small although small differences in the cross-reaction covariances with elastic scattering are somewhat visible.

The largest absolute deviation from symmetry in the original covariance matrix is 5.77×10^{-15} b^2 and occurs between groups in the thermal region of the (n, γ) reaction. The largest relative deviation from symmetry is found between groups in the thermal and epithermal regions of covariances of (n, p_0) and is on the order 10^{-8}%. The absolute asymmetry is typical, but the relative asymmetry is larger than typical, although still small.

The eigenvalues of the symmetrized and deflated covariance matrices are shown in Fig. 3. The bottom figure shows that the large positive eigenvalues are well preserved while the large negative eigenvalues are shifted toward zero. Two of the eigenvalues of the symmetrized covariance matrix are certainly not induced by round-off error.

The near-origin magnification shows the cluster of near-zero eigenvalues with few well-separated eigenvalues nearby. Most of the smaller negative eigenvalues are shifted to zero, while the visible positive eigenvalues are preserved. The symmetrized covariance matrix has 24 negative eigenvalues and 388 eigenvalues that might be zero, given

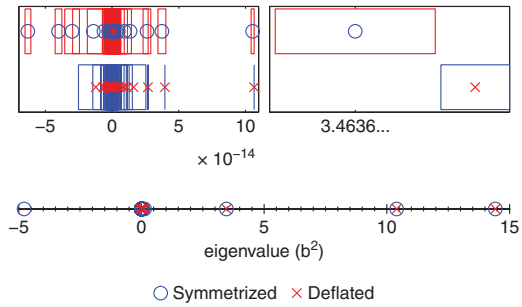

Fig. 3. Eigenvalues of absolute covariances of cross sections of $^{35}_{17}$Cl before and after deflation. The box around each eigenvalue presents the estimated bounds due to finite precision computation [box colors inverted (color online)]. Number line: All eigenvalues. The boxes are hardly visible. Top left: Magnification of a region near the origin. Top right: Magnification of the largest absolute distortion to an eigenvalue. The width of the axis is 42 ulps $\approx 2 \times 10^{-14}$b^2.

their estimated bounds. After the deflation, two negative, but tiny, eigenvalues are left: $(-5.30 \pm 2.79) \times 10^{-15}$b^2 and $(-2.89 \pm 2.73) \times 10^{-15}$b^2, where the bounds are estimated as described in Sec. III.B.1. However, five of the near-zero eigenvalues become positive, but tiny. The distortions occur due to the accumulated round-off errors during deflation.

The top-right figure in Fig. 3 shows the largest absolute distortion in an eigenvalue. The distortion is 9.33×10^{-15} b^2 and occurs due to rounding errors.

The standard deviations from the symmetrized and deflated covariance matrices are shown in Fig. 4. For the elastic scattering the standard deviation is roughly doubled in the lowest-energy energy group. This occurs because of deflation of the largest negative eigenvalue. The large contribution is shown in Fig. 5. Here, the contribution means the square root of the effect to variance [see Eq. (21)]. In the epithermal and high-energy regions, the changes to the standard deviations of elastic scattering due to deflation are mostly small, $<2\%$, except in one group, where it is 8%.

The relative standard deviations in the (n, p_0) reaction change the most: For the 10^3- to 10^6-eV region, the relative standard deviations change from at most 354% to at most 7330% (out of scale in Fig. 4) in a few groups. For the (n, γ) reaction the same occurs, but the final standard deviations are at most 601%. However, the changes in absolute covariances are small. For the (n, p_0) reaction the change in the relative standard deviation does not come from the first few eigenpairs but predominantly from the fourth and subsequent eigenpairs. The increase in standard deviations of (n, γ) is mostly due to the largest eigenpair.

The large changes in relative standard deviations occur because the cross sections, and therefore absolute

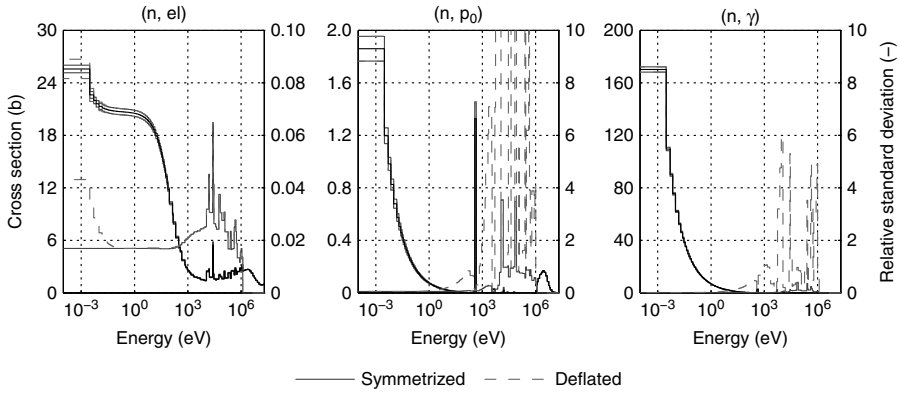

Fig. 4. Standard deviations of the cross sections of $^{35}_{17}$Cl before and after deflation (the nearest absolute positive semidefinite covariance matrix). Left axes: absolute standard deviations. Right axes: relative standard deviations.

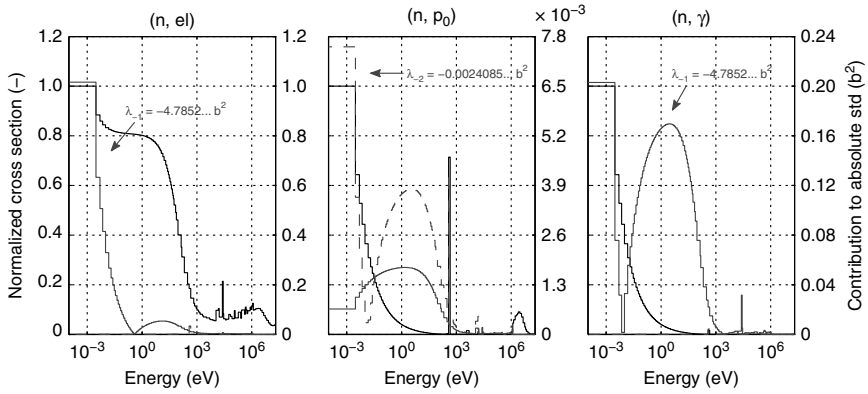

Fig. 5. Selected contributions of deflated eigenpairs to changes in absolute standard deviations of the (n, n), (n, p_0), and (n, γ) cross sections of $^{35}_{17}$Cl.

covariances, vary by orders of magnitude. A smallish absolute change in the covariances of small cross sections is a large relative change. The distance between the absolute symmetrized and the absolute nearest positive semidefinite matrix is measured in absolute units. That is, the measure is for absolute changes, not relative changes, and therefore, the nearest positive semidefinite matrix in the absolute sense is sought.

Finding the nearest relative covariance matrix would yield different results. In this case there was a larger change in the thermal region of the covariances of elastic scattering, including a few sharp peaks, but almost no change in the epithermal to high-energy region of the (n, p_0) and (n, γ) reactions. This is illustrated in Fig. 6.

Application of the method took <1s, and NJOY ran for ~ 10 min.

V.B. Relative Covariances of $\bar{\mu}$ of $^{232}_{90}Th$

The absolute difference between the original and deflated relative covariances of $\bar{\mu}$ of $^{232}_{90}$Th is shown in Fig. 7. The variances do not decrease when the covariance matrix is deflated. The asymmetry of the original covariances is so slight that it is not visible. The largest changes occur near the 1-MeV region. The intrareaction covariances that have either component in the 1-MeV region are also affected by the deflation.

The largest absolute deviation from symmetry in the original covariance matrix is 4.34×10^{-19} and occurs between groups near 200 keV. The largest relative deviation from symmetry is found in the covariances between groups near 3 and 20 MeV and is on the order 10^{-14}%. These slight asymmetries are typical.

The eigenvalues of the symmetrized and deflated covariance matrices are shown in Fig. 8. The bottom figure shows that the large positive eigenvalues are well preserved while the large negative eigenvalues are shifted toward zero. Note that the largest eigenvalue is only 1.87×10^{-2}. All four of the negative eigenvalues of the symmetrized covariance matrix are certainly not induced by round-off error.

The near-origin magnification shows that all eigenvalues are well separated from each other. The smaller negative eigenvalues are shifted to zero, while most of the visible positive eigenvalues are preserved. The symmetrized covariance matrix has four negative eigenvalues and only one eigenvalue that might be zero, given their estimated bounds. All the negative eigenvalues are deflated. However, one of the near-zero eigenvalues becomes positive, but tiny. This occurs due to the accumulated round-off errors during deflation.

The top-right figure of Fig. 8 shows the largest absolute distortion in an eigenvalue. The distortion is 4.16×10^{-17} and occurs due to the rounding errors.

The standard deviations from the symmetrized and deflated covariance matrices are shown in Fig. 9. The original standard deviations are imaginary in four groups, as indicated in Fig. 9. After the deflation the standard devations in these groups are positive.

The cluster of three energy groups with imaginary standard deviations near 1 MeV is explained by the three most negative eigenpairs. This is partly illustrated in Fig. 10. The fourth energy group with the imaginary standard deviation near 5 MeV is mostly due to the fourth and first negative eigenpairs.

Application of the method took <1 s, and NJOY ran for ~ 40 min.

V.C Relative Covariances of Spectral Yields of $^{252}_{98}Cf$

The absolute difference between the original and deflated relative covariances of spectral yields of $^{252}_{98}$Cf is

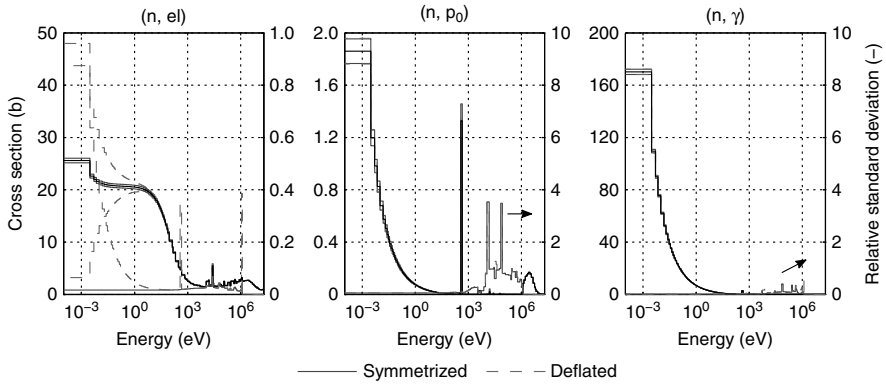

Fig. 6. Standard deviations of the cross sections of $^{35}_{17}$Cl before and after deflation (the nearest relative positive semidefinite covariance matrix). Left axes: absolute standard deviations. Right axes: relative standard deviations.

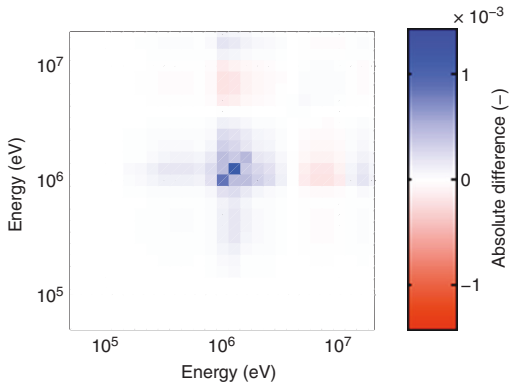

Fig. 7. Absolute differences between the original and the deflated relative covariances of $\bar{\mu}$ of $^{232}_{90}$Th.

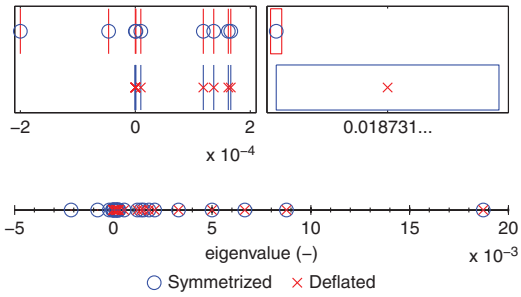

Fig. 8. Eigenvalues of relative covariances of $\bar{\mu}$ of $^{232}_{90}$Th before and after deflation. The box around each eigenvalue presents the estimated bounds due to finite precision computation (box colors inverted). Number line: All eigenvalues. The boxes are hardly visible. Top left: Magnification of a region near the origin. Top right: Magnification of the largest absolute distortion to an eigenvalue. The width of the axis is $26\,\text{ulps} \approx 9 \times 10^{-17}$.

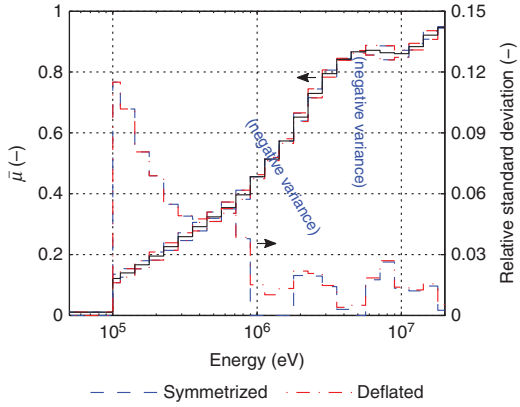

Fig. 9. Standard deviations of $\bar{\mu}$ of $^{232}_{90}$Th before and after deflation. The original variance is negative in four indicated groups. Left axis: absolute standard deviations. Right axis: relative standard deviations.

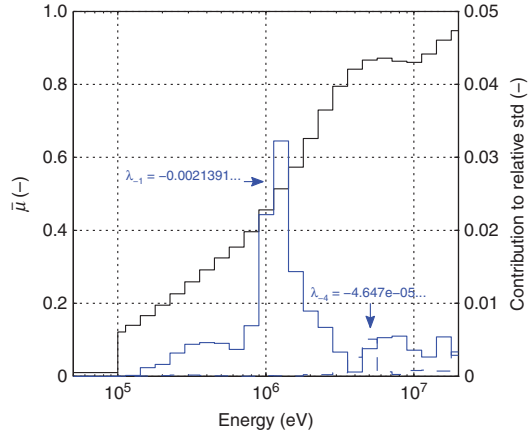

Fig. 10. Selected contributions of deflated eigenpairs to changes in relative standard deviations of $\bar{\mu}$ of $^{232}_{90}$Th.

shown in Fig. 11. The variances do not decrease when the covariance matrix is deflated. The asymmetry of the original covariances is so slight that it is not visible. The largest changes occur in the thermal region. The intrareaction covariances that have either component in the thermal region are also affected by the deflation.

The largest absolute deviation from symmetry in the original covariance matrix is 1.33×10^{-15} and occurs between groups in the high-energy region. The largest relative deviation from symmetry is also found between groups in the high-energy region and is on the order 10^{-13}%. These slight asymmetries are typical.

The eigenvalues of the symmetrized and deflated covariance matrices are shown in Fig. 12. The bottom figure shows that the large positive eigenvalue is well preserved. Twenty-one of the eigenvalues of the symmetrized covariance matrix are certainly not induced by round-off error.

The near-origin magnification shows the cluster of near-zero eigenvalues. Here, all eigenvalues might be zero, given their estimated bounds. The symmetrized covariance matrix has 30 negative eigenvalues and 105 eigenvalues that might be zero, given their estimated bounds. After the deflation there are 135 eigenvalues that might be zero given their estimated bounds. That is, the 30 negative eigenvalues are deflated within working

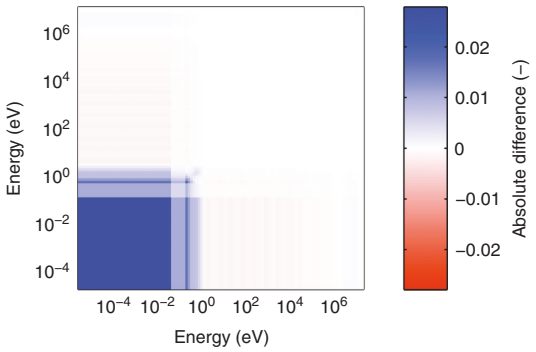

Fig. 11. Absolute differences of the original and the deflated relative covariances of spectral yields of $^{252}_{98}$Cf.

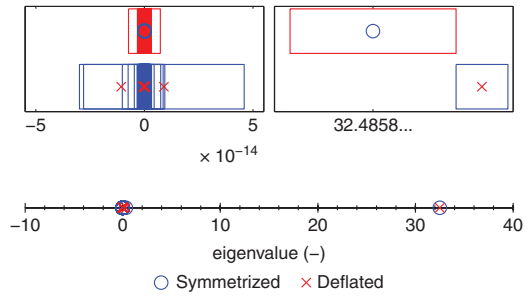

Fig. 12. Eigenvalues of relative covariances of spectral yields of $^{252}_{98}$Cf before and after deflation. The box around each eigenvalue presents the estimated bounds due to finite precision computation (box colors inverted). Number line: All eigenvalues. The boxes are hardly visible. Top left: Magnification of a region near the origin. Top right: Magnification of the largest absolute distortion to an eigenvalue. The width of the axis is 43 ulps $\approx 3 \times 10^{-13}$.

precision. Note that there should be at least one zero eigenvalue due to the scaled zero sum property.

The top-right figure of Fig. 12 shows the largest absolute distortion in an eigenvalue. The distortion is 1.49×10^{-13} and occurs due the rounding errors.

The standard deviations from the symmetrized and deflated covariance matrices are shown in Fig. 13. In the high-energy region the relative standard deviations go up to 1.72 but change $<0.1\%$ during deflation. The standard deviation is increased by an order of magnitude in the lowest-energy energy group. This occurs because of deflation of the two largest negative eigenvalues. Their contributions are shown in Fig. 14. The contributions are large in the lowest-energy energy group. In other energy regions the changes to standard deviations due to deflation are small.

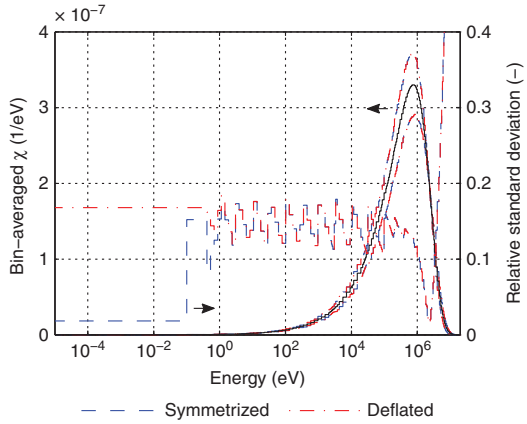

Fig. 13. Standard deviations of spectral yields of neutrons emitted from $^{252}_{98}$Cf fission before and after deflation. Left axis: absolute standard deviations. Right axis: relative standard deviations.

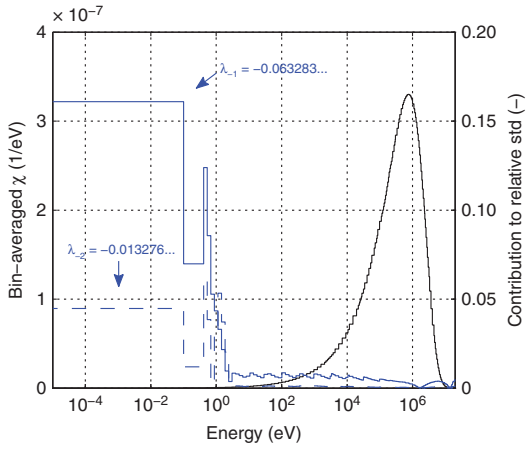

Fig. 14. Selected contributions of deflated eigenpairs to changes in relative standard deviations of the spectral yields of neutrons emitted from $^{252}_{98}$Cf fission.

The zero sum property is well preserved during deflation. Before the deflation the maximum absolute value of the row sum per spectral yield was 1.833×10^{-6} 1/eV, and the average value was 2.812×10^{-7} 1/eV. After the deflation these had changed to 1.840×10^{-6} 1/eV and 2.807×10^{-7} 1/eV, respectively, giving an increase of 0.4022% and decrease of 0.1956%, respectively. These are small changes.

Application of the method took <1 s, and NJOY ran for ~ 5 min.

VI. DISCUSSION

The negative eigenvalues are a result of unphysical data, errors in the processing code, or round-off error. The first two should be corrected rather than ignored by computing a nearby mathematically valid covariance matrix. The magnitude of the third one can be controlled by the bound given in Sec. III.C. In any case the proposed method can be used as part of a quality assurance program to detect these problems.

However, the data might be mostly correct and negative eigenvalues small in magnitude. In such case the use of a nearby positive semidefinite covariance matrix might be justified. Any covariance matrix with large negative eigenvalues can be rejected and smaller negative eigenpairs deflated. If the results are to be rounded, the maximum error induced by rounding gives a practical measure on how small eigenpairs should be deflated.

The method, in exact arithmetic, has some good qualities that should be mentioned. It is conservative for propagation of uncertainty in the sense that variances for any response will not decrease due to application of the method, and the method preserves eigenvalues and eigenvectors, which implies that the sum rules of redundant (derived) cross sections are preserved.

The example of chlorine shows that some negative eigenvalues may remain after deflation. These are due to the accumulated rounding errors during deflation and as such are tiny. The method could be reapplied, but this requires further analysis on deflation of near-zero gap eigenvalues. Alternatively, a better method of deflation like deflation by similarity transformations might help here.

There are other possible approaches when computing a nearby positive semidefinite covariance matrix. For example, one could use a different norm than the Frobenius norm as a measure[7] or compute a nearest correlation matrix[18] and scale it back to a covariance matrix. In their current forms these methods seem to be iterative and computationally more expensive than the proposed method. Computing a nearest correlation matrix would have the advantage of preserving variances. However, such a method could not handle the example of thorium with negative variances.

The method can be applied to absolute or relative covariance matrices. The example of chlorine shows that the results can be quite different, at least when large negative eigenvalues are present. Therefore, it is advisable to apply the method to the covariance matrix that is going to be used. One should, however, consider finding and correcting the underlaying problem rather than making large corrections. After all, the method has no physical interpretation but merely removes unphysical information with the fewest changes to the data in the sense of the Frobenius norm.

In principle, the eigenvalues can be mapped back to physical parameters from which the covariances were derived, if such data trail exists. Mapping the negative eigenvalues can yield insight into which physical parameters have unphysical values. The near-zero eigenvalues give insight to irrelevant parameters.

It would suffice to compute only negative eigenvalues instead of the full spectrum. However, we did not find a suitable standard linear algebra method to compute them with the described properties. The error analysis should be reworked in those cases.

Alternatively, one could compute only the positive eigenvalues. The eigenpairs with positive eigenvalues contain all the information that is needed in subsequent applications. This also solves the issue of zero eigenvalues, since the eigenpairs with positive eigenvalues describe the relevant physical parameters.

VII. CONCLUSIONS

The proposed method to find the nearest symmetric positive semidefinite matrix has been applied to covariance matrices of multigroup nuclear data. It has been demonstrated that the method can, in typical cases, provide positive semidefinite covariance matrices and, in extreme cases, provide symmetric matrices with only tiny negative eigenvalues.

Application of the method, alternative approaches, and possible enhancements for the extreme cases were discussed briefly. A known upper bound for the magnitude of negative eigenvalues induced by round-off error is given.

The method has some good qualities. It is computationally affordable, and it preserves the sum rules of derived cross sections and the zero sum rules. It is conservative in the sense that it does not reduce variances of the data. However, it lacks physical interpretation.

The method can be applied to cross-material, cross-reaction, and intrareaction covariances. It can be used as a part of a quality assurance program to detect large problems and correct small ones. Use of the method would be a valuable addition to programs that generate multigroup covariance matrices.

ACKNOWLEDGMENTS

The author thanks P. A. Aarnio, M. Pusa, and L. Rintala for their valuable comments and interest in this work and acknowledges the financial support of the YTERA Doctoral Programme for Nuclear Engineering and Radiochemistry.

REFERENCES

1. A. C. KAHLER et al., "The NJOY Nuclear Data Processing System, Version 2012," Los Alamos National Laboratory (Dec. 2012); http://t2.lanl.gov/nis/codes/NJOY12/NJOY2012.8.pdf (accessed Feb. 19, 2014).

2. D. WIARDA et al., "Recent Advances with the AMPX Covariance Processing Capabilities in PUFF-IV," *Nucl. Data Sheets*, **109**, *12*, 2791 (2008); http://dx.doi.org/10.1016/j.nds.2008.11.011.

3. I.-A. KODELI, "VITAMIN-J/COVA/EFF-3 Cross-Section Covariance Matrix Library and Its Use to Analyse Benchmark Experiments In Sinbad Database," *Fusion Eng. Des.*, **75–79**, 1021 (2005); http://dx.doi.org/10.1016/j.fusengdes.2005.06.034.

4. R. LITTLE et al., "Low-Fidelity Covariance Project," *Nucl. Data Sheets*, **109**, *12*, 2828 (2008); http://dx.doi.org/10.1016/j.nds.2008.11.018.

5. C. MATTOON and P. OBLOŽINSKÝ, "Issues in Neutron Cross Section Covariances," *J. Korean Phys. Soc.*, **59**, *23*, 1242 (2011); http://dx.doi.org/10.3938/jkps.59.1242.

6. R. W. PEELLE, "Uncertainty in the Nuclear Data Used for Reactor Calculations," *Advances in Nuclear Science and Techonology*, Vol. 14, "Sensitivity and Uncertainty Analysis of Reactor Performance Parameters," p. 11, J. LEWINS and M. BECKER, Eds., Plenum Press, New York (1982).

7. N. HIGHAM, "Computing a Nearest Symmetric Positive Semidefinite Matrix," *Linear Algebra Appl.*, **103**, 103 (1988); http://dx.doi.org/10.1016/0024-3795(88)90223-6.

8. D. G. CACUCI and M. IONESCU-BUJOR, "Sensitivity and Uncertainty Analysis, Data Assimilation, and Predictive Best-Estimate Model Calibration," *Handbook of Nuclear Engineering*, p. 1913, D. G. CACUCI, Ed., Springer (2010).

9. J. H. WILKINSON, *The Algebraic Eigenvalue Problem*, Clarendon Press, Oxford, United Kingdom (1965).

10. K. FAN and A. J. HOFFMAN, "Some Metric Inequalities in the Space of Matrices," *Proc. Amer. Math. Soc.*, **6**, 111 (1955); http://dx.doi.org/10.1090/S0002-9939-1955-0067841-7.

11. E. ANDERSON et al., *LAPACK Users' Guide*, 3rd ed., Society for Industrial and Applied Mathematics (1999).

12. "AMD Core Math Library (ACML), Version 5.3.0," Advanced Micro Devices; http://developer.amd.com/acml (accessed Feb. 20, 2014).

13. B. N. PARLETT, *The Symmetric Eigenvalue Problem*, Classics in Applied Mathematics, Society for Industrial and Applied Mathematics (1998).

14. J. BARLOW and J. DEMMEL, "Computing Accurate Eigensystems of Scaled Diagonally Dominant Matrices," *SIAM J. Numer. Anal.*, **27**, *3*, 762 (1990); http://dx.doi.org/10.1137/0727045.

15. A. TRKOV, M. HERMAN, and D. A. BROWN, "ENDF-6 Formats Manual," Brookhaven National Laboratory (2012); http://www.nndc.bnl.gov/csewg/docs/endf-manual.pdf (accessed Feb. 20, 2014).

16. M. CHADWICK et al., "ENDF/B-VII.1 Nuclear Data for Science and Technology: Cross Sections, Covariances, Fission Product Yields and Decay Data," *Nucl. Data Sheets*, **112**, *12*, 2887 (2011); http://dx.doi.org/10.1016/j.nds.2011.11.002.

17. E. SARTORI, "Standard Energy Group Structures of Cross Section Libraries for Reactor Shielding, Reactor Cell and Fusion Neutronics Applications: VITAMIN-J, ECCO-33, ECCO-2000 and XMAS," JEF/DOC-315, Rev. 3, Draft, Organisation for Economic Co-operation and Development/Nuclear Energy Agency Data Bank (Dec. 1990).

18. R. BORSDORF and N. HIGHAM, "A Preconditioned Newton Algorithm for the Nearest Correlation Matrix," *IMA J. Numer. Anal.*, **30**, *1*, 94 (2010); http://dx.doi.org/10.1093/imanum/drn085.

Publication II

R. Vanhanen. Computing more consistent multigroup nuclear data covariances. *Nuclear Science and Engineering*, 181, *1*, 60–71, September 2015; http://dx.doi.org/10.13182/NSE14-105.

NUCLEAR SCIENCE AND ENGINEERING: **181**, 60–71 (2015)

Computing More Consistent Multigroup Nuclear Data Covariances

Risto Vanhanen

Aalto University School of Science, Department of Applied Physics
P.O. Box 14100, FI-00076 Aalto, Finland

Received September 30, 2014
Accepted December 14, 2014
http://dx.doi.org/10.13182/NSE14-105

Abstract—*It is not uncommon that the covariances of multigroup nuclear data do not obey the sum rules of nuclear data. We present a matrix nearness problem of finding a nearest symmetric matrix with given null vectors and solve it when the distance is measured in the Frobenius norm. The problem appears to be new. We propose that the method should be used to find nearest consistent multigroup covariance matrices with respect to the sum rules of redundant nuclear data.*

If the multigroup covariances cannot be easily interpreted in a consistent manner, there is some ambiguity in choosing values for the covariances that are not explicitly mentioned. We present and compare a simple and a heuristic characterization method.

Three practical examples are processed and analyzed: relative covariances of cross sections of $^{94}_{40}Zr$ and absolute covariances of cross sections of $^{50}_{24}Cr$ and $^{232}_{90}Th$. We demonstrate that satisfactory results can be achieved.

We discuss the properties of the proposed method and the characterization methods and suggest possible improvements. The methods can be used as a part of a quality assurance program and might be valuable additions to nuclear data processing codes.

I. INTRODUCTION

Evaluated nuclear data files contain information that describe physical quantities referred to as nuclear data. In modern nuclear data files, the information consists of best estimates and uncertainty estimates of the nuclear data. These can be interpreted as an approximative representation of a distribution, which describes the evaluator's knowledge of the nuclear data. The covariances of the nuclear data are the second central moment of this distribution. When the covariances are used in deterministic codes, the data are usually processed into a more approximative multigroup form with codes such as NJOY (Ref. 1) or PUFF-IV (Ref. 2). It is not uncommon for the generated multigroup covariance matrices to be inconsistent in the sense that they violate the so-called sum rules of redundant nuclear data. If the covariance matrices are far from consistent, the results of subsequent calculations are questionable at best.

The requirement of consistency has been identified at least in a quality assurance procedure as reported by Smith.[3] However, the quality assurance procedure does not require that the evaluations should be consistent: it only notes that covariance matrices may contain zero eigenvalues due to the consistency. Overall the issue has received little attention.

It is possible to generate consistent covariances by ignoring the covariances of redundant nuclear data and using the propagation-of-errors formula to generate the redundant information when needed. We refer to this method as the standard method. Alas, this ignores that usually the redundant nuclear data are known the best. The ENDF-6 Formats Manual,[4] for example, states: "The total is often the best-known cross section," "The elastic scattering cross section is generally not known to the same accuracy as the total cross section," and "The nonelastic cross section, or any part thereof, is not generally measured with the same energy resolution as the total cross section." Therefore, when the redundant data are ignored, the uncertainties are unnecessarily overestimated.

*E-mail: risto.vanhanen@aalto.fi

In this paper we introduce a novel method to find a nearest symmetric matrix with specified null vectors in the sense that the required modifications are the smallest in a norm. We solve the problem for the Frobenius norm and note that the solution is unique. We show that the solution can be applied to find the nearest consistent multigroup covariance matrix.

The proposed method does not ignore any covariances; i.e., it uses all available information. However, under finite-precision computation the method modifies consistent covariance matrices, and therefore should not be applied to them. We give a practical criterion to identify consistent covariance matrices to avoid damaging consistent covariance matrices.

Before any use, the covariances need to be characterized, i.e., given some values. Usually the evaluator has characterized many, but not all, covariances, and the processing code faithfully generates only those multigroup covariance matrices that the evaluator has characterized. When the evaluation can be easily interpreted in a consistent manner, the missing covariances are easily characterized consistently. When the interpretation is not possible, there is some ambiguity in characterizing the covariances. We compare a simple and a heuristic characterization method, which can be used to complete the characterization by using the covariances characterized by the evaluator. Neither characterization method is clearly superior to the other.

The paper is organized as follows. The theoretical background is presented in Sec. II. Details of a practical implementation are given in Sec. III. Three examples are described in Sec. IV and their results analyzed in Sec. V. The method and results are discussed in Sec. VI, and finally in Sec. VII the conclusions are given.

II. THEORY

We need the following results for the terminology, theoretical background, and a practical implementation.

II.A. The Frobenius and Spectral Norms, and an Inequality

For $A \in \mathbb{R}^{m\times n}$, the Frobenius norm is defined by

$$\|A\|_F^2 = \sum_{i,j} a_{ij}^2 \ , \tag{1}$$

and the spectral norm (2-norm) is defined by

$$\|A\|_2^2 = \lambda_{\max}(A^{\mathsf{T}}A) \ , \tag{2}$$

where $\lambda_{\max}(A^{\mathsf{T}}A)$ is the largest eigenvalue of $A^{\mathsf{T}}A$.

It follows from Horn's note[5] that for $A \in \mathbb{R}^{m\times n}$, $B \in \mathbb{R}^{n\times k}$, and $C \in \mathbb{R}^{k\times p}$, the inequality

$$\|ABC\|_U \leq \|A\|_2 \|B\|_U \|C\|_2 \tag{3}$$

holds for any unitarily invariant norm $\|\cdot\|_U$. The Frobenius and spectral norms are unitarily invariant.

II.B. Generalized Inverses

Penrose[6] proves the following:

Let $A \in \mathbb{R}^{m\times n}$ and $G \in \mathbb{R}^{n\times m}$. For any A, the four equations

$$AGA = A \ , \tag{4}$$

$$GAG = G \ , \tag{5}$$

$$(AG)^{\mathsf{T}} = AG \ , \tag{6}$$

and

$$(GA)^{\mathsf{T}} = GA \tag{7}$$

have a unique solution for G. The solution is called the generalized inverse of A and is denoted by A^{+}.

We also refer to minimum-norm reflexive generalized inverses, which satisfy Eqs. (4), (5), and (7), are not unique, and are denoted by $A^{\tilde{}}$. However, $A^{\tilde{}}A$ is unique (Ref. 7, Theorems 2.12 and 2.13). See, for example, Refs. 7 and 8 for further details.

II.C. Symmetric Solution of a Linear Matrix Equation

Don[9] proves the following:

Let $A \in \mathbb{R}^{m\times n}$ and $B \in \mathbb{R}^{m\times n}$ be general matrices and $X \in \mathbb{R}^{n\times n}$ a symmetric matrix. The system $AX = B$ is consistent if and only if $AA^{\tilde{}}B = B$ and $AB^{\mathsf{T}} = BA^{\mathsf{T}}$. In that case it has the general solution

$$X = A^{\tilde{}}B + (I - A^{\tilde{}}A)(A^{\tilde{}}B)^{\mathsf{T}} + (I - A^{\tilde{}}A)Z(I - A^{\tilde{}}A) \ , \tag{8}$$

with $Z \in \mathbb{R}^{n\times n}$ an arbitrary symmetric matrix. The minimum norm solution results for $Z = 0$. The consistency for any $A^{\tilde{}}$ implies consistency for all minimum-norm reflexive generalized inverses.

Note. The minimum norm solution refers to the minimum of the Frobenius norm, although the restriction of the norm is not explicitly stated by Don.

II.D. Finding a Nearest Symmetric Matrix with Specified Null Vectors

The problem of finding a nearest symmetric matrix with specified null vectors can be formulated as the

following matrix nearness problem: For given $U \in \mathbb{R}^{m\times n}$ containing the specified null vectors in columns and symmetric $C \in \mathbb{R}^{m\times m}$, find the minimum distance

$$d(C) = \min\{\|X\| : (C+X)U = 0; \\ C, X \in \mathbb{R}^{m\times m}, \text{sym.}; U \in \mathbb{R}^{m\times n}\} , \tag{9}$$

and a symmetric $X \in \mathbb{R}^{m\times n}$ achieving the minimum.

For the Frobenius norm, the solution is the following: the unique minimum is achieved by $X = PCP - C$, where $P = I - (U^{\mathsf{T}})^{\sim}U^{\mathsf{T}}$.

Similar problems for nonsymmetric matrices have been considered before, but we have not found a prior formulation for this matrix nearness problem.

Proof. The equation $(C+X)U = 0$ can be expressed as $U^{\mathsf{T}}X = -U^{\mathsf{T}}C$. Don's result can be applied with $A = U^{\mathsf{T}}$ and $B = -U^{\mathsf{T}}C$. It is easy to confirm that the system is consistent and therefore has a solution. The minimum solution is the claimed one. Uniqueness follows from the uniqueness of $(U^{\mathsf{T}})^{\sim}U^{\mathsf{T}}$.

Note. Since $(U^{\mathsf{T}})^{\sim}U^{\mathsf{T}}$ is unique, one may use the identity $(U^{\mathsf{T}})^{+} = (U^{+})^{\mathsf{T}}$ to replace $(U^{\mathsf{T}})^{\sim}$s. This gives $P = I - UU^{+}$.

Note. It is straightforward to verify that P is an orthogonal projection matrix; i.e., $P^2 = P$ and $P = P^{\mathsf{T}}$, and therefore $\|P\|_2 \leq 1$. Now, using Eq. (3), $\|C+X\|_U = \|PCP\|_U \leq \|C\|_U$ for both the Frobenius and spectral norms. This shows that the nearest symmetric matrix with specified null vectors does not grow and might be reduced in the norms compared to the original symmetric matrix.

Note. If C is positive semidefinite, i.e., $x^{\mathsf{T}}Cx \geq 0$ for all $x \in \mathbb{R}^m$, then $x^{\mathsf{T}}(C+X)x = x^{\mathsf{T}}PCPx = y^{\mathsf{T}}Cy \geq 0$, which shows that $C+X$ is also positive semidefinite. Naturally the same does not apply for strict positive definiteness since zero eigenvalues are introduced for the null vectors.

II.E. Multigroup Nuclear Data and Their Covariances

The multigroup form of a piece of nuclear data, e.g., cross sections of reactions or average number of neutrons emitted in a fission, can be represented as

$$x_k = (x_{k,1}, \ldots, x_{k,g}) \in \mathbb{R}^g , \tag{10}$$

where g is the number of energy groups. The multigroup nuclear data of a single material can be represented as

$$x = (x_1, x_2, \ldots, x_n) \in \mathbb{R}^m , \tag{11}$$

where n is the number of pieces of nuclear data and $m = ng$. Their covariances can be represented as an $n \times n$ matrix of $g \times g$ covariance matrices, which form the symmetric partitioned matrix:

$$C = \begin{bmatrix} \text{cov}(x_1,x_1) & \text{cov}(x_1,x_2) & \cdots & \text{cov}(x_1,x_n) \\ \text{cov}(x_2,x_1) & \text{cov}(x_2,x_2) & \cdots & \text{cov}(x_2,x_n) \\ \vdots & \vdots & \ddots & \vdots \\ \text{cov}(x_n,x_1) & \text{cov}(x_n,x_2) & \cdots & \text{cov}(x_n,x_n) \end{bmatrix} \\ \in \mathbb{R}^{m\times m} . \tag{12}$$

The covariances can be either relative or absolute. Properties of the covariances are given, for example, in Chapter 10 of Ref. 1.

II.F. Propagation of Errors

Some of the nuclear data can be expressed as linear combinations of other nuclear data. These are sometimes called redundant or summation nuclear data. The linear combination can be expressed with a set of coefficients a_i, for which it holds

$$x_I = \sum_{i\neq I} a_i x_i . \tag{13}$$

Using the linearity of the covariances, these give the propagation-of-errors formula

$$s_I \,\text{cov}(x_I,x_j) s_j = \sum_{i\neq I} a_i s_i \,\text{cov}(x_i,x_j) s_j , \tag{14}$$

where a scale s_k is $\text{diag}(x_k)$ for relative covariances and $I_g - \text{diag}(\delta(x_k))$ for absolute covariances, where δ is the Kronecker delta, applied componentwise.[a] The left side of Eq. (14) is the absolute covariance between the I'th and j'th reactions. We use $s_{k,i}$ when referring to the i'th diagonal element of s_k. The transpose is implied in Eq. (14).

II.G. Finding a Nearest Consistent Covariance Matrix

The consistency of covariances with respect to linearly redundant nuclear data can be expressed with null vectors, i.e., eigenvectors with zero eigenvalue, of the covariance matrix. Equation (13) can be written as

$$\sum_{i=1}^{n} a_i x_i = 0 , \tag{15}$$

when the coefficient a_I is defined to be -1. We refer to both sets of a_i, rather loosely, as a sum rule. The linearity of covariances implies

[a]Later on the delta accounts for the implied convention $x_{k,i} = 0 \Rightarrow \text{cov}(x_{k,i},x_{k',j}) = 0$. If such a convention is not applied, $s_k = I_g$ for absolute covariances will do.

$$\sum_{i=1}^{n} a_i s_i \operatorname{cov}(x_i,x_j) s_j = 0 \ . \qquad (16)$$

Since this must hold for all energy groups, the following must be eigenvectors of the covariance matrix with zero eigenvalue:

$$\upsilon_i^{\mathsf{T}} = [a_1 s_{1,i}, \ldots, a_n s_{n,i}] \otimes e_i^{\mathsf{T}} \ \text{ for } \ i = 1, \ldots, g \ , \qquad (17)$$

where e_i is the i'th Cartesian basis vector of g-dimensional real space and $\cdot\otimes\cdot$ is the Kronecker product.

It proves advantageous to collect the eigenvectors into columns of $V \in \mathbb{R}^{m\times g}$ so that

$$V = [\upsilon_1, \ldots, \upsilon_n] \quad \Rightarrow \quad V^{\mathsf{T}} = [a_1 s_1, \ldots, a_n s_n] \ . \qquad (18)$$

The nonzero eigenvectors are clearly linearly independent.

The nearest consistent covariance matrix in the Frobenius norm can be calculated by collecting l different sum rules as $U = [V_1, \ldots, V_l] \in \mathbb{R}^{m\times p}$, where $p = gl$ and finding the nearest symmetric matrix to the covariance matrix C, with null vectors specified by U. This gives a nearest consistent covariance matrix with respect to the l sum rules. By the nearest consistent multigroup covariance matrix, we mean the nearest consistent multigroup covariance matrix in the Frobenius norm. Note that sequentially finding the nearest symmetric matrix with null vectors specified by V_k, $k = 1, \ldots, l$, might not yield a consistent covariance matrix.

II.H. Applying Householder Transformations

Wilkinson (Ref. 10 and references therein) studied finite-precision effects of Householder transformations. The following is a weaker version of Higham's formulation (Ref. 11, Lemma 19.3):

Consider the sequence of transformations $A_{k+1} = H_k A_k$, $k = 1, \ldots, r$, where $A_1 = A \in \mathbb{R}^{m\times n}$ and $H_k = I - \upsilon_k \upsilon_k^{\mathsf{T}} \in \mathbb{R}^{m\times m}$ is a Householder matrix. Here $\tilde{\gamma}_m = cmu/(1 - cmu)$, where u is the unit roundoff and c a small integer constant. The number of transformations r is bounded by $r\tilde{\gamma}_m < 1/2$. Assume that the transformations are performed using computed Householder vectors $\hat{\upsilon}_k$ that satisfy $\hat{\upsilon}_k = \upsilon_k + \Delta\upsilon_k$, $|\Delta\upsilon_k| \le \tilde{\gamma}_m$, and $\|\upsilon_k\| = \sqrt{2}$. The computed matrix $\hat{A}_{r+1}$ satisfies

$$\hat{A}_{r+1} = Q^{\mathsf{T}}(A + \Delta A) \ , \qquad (19)$$

where $Q^{\mathsf{T}} = H_r H_{r-1} \cdots H_1$ and $\|\Delta A\|_F \le r\tilde{\gamma}_m \|A\|_F$.

Note. For the inverse sequence of transformations, i.e., $A_{k+1} = H_{r+1-k} A_k$, $k = 1, \ldots, r$, we have $\hat{A}_{r+1} = Q(A + \Delta A)$ with the above bound for ΔA. If $A \in \mathbb{R}^{n\times m}$ is postmultiplied by the transformations, we get $\hat{A}_{r+1} = (A + \Delta A)Q$ and $\hat{A}_{r+1} = (A + \Delta A)Q^{\mathsf{T}}$ with the same bound for ΔA.

III. IMPLEMENTATION

We apply the following to every material separately.

III.A. Constructing the Sum Rules

The redundancies of nuclear data can be expressed as a forest of disjoint trees. Two of the trees are illustrated in Fig. 1, where the cross-section tree follows the ENDF sum rules.[4] The partials of a redundant nuclear data piece are represented as their children. All shown partials have unit coefficients. These form an elementary set of sum rules. The elementary sum rules do not represent directly applicable sum rules, since in a practical case some of the redundant nuclear data do not have any covariances; i.e., the covariances for some of the redundant nuclear data are missing.

An obvious approach is to derive the missing redundant covariances by using the propagation-of-errors formula. Then the elementary sum rules represent the directly applicable sum rules.

An alternative approach is to deduce the sum rules for the present redundant nuclear data. In the sum rules, it suffices to replace recursively any partial that is also redundant and is not present by its partials. A simple tree-traversal with the replacing logic will create the sum rules, when the traversal is started from each redundant nuclear data piece that has at least some covariances present.

A specific issue to ENDF-6 Formats[4] is lumped covariances, which are covariances for evaluator-defined sums of nuclear data pieces. In both approaches any partial of a lumped covariance should be considered to be present, and the partials should be replaced by the lumped covariance after the sum rules have been deduced. However, the obvious approach will not work if an evaluation contains lumped covariances whose partials are not direct partials of a single redundant nuclear data piece. The alternative approach works for somewhat more

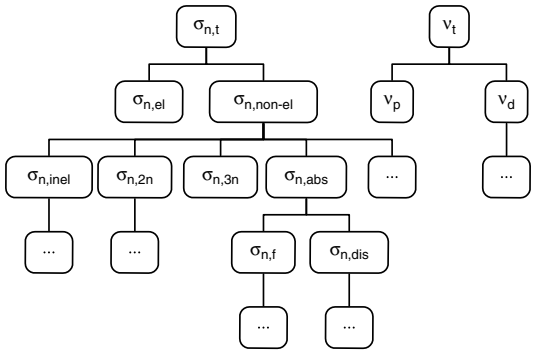

Fig. 1. Part of the forest of redundancies of nuclear data. The trees for σ and ν are shown. The dots show where the trees are truncated.

general lumped covariances. Neither approach can solve the general problem with lumped covariances, which is that the presence of lumped covariances might transform the trees into general graphs.

In favorable conditions, we get a set of sum rules with either approach, which can be used to assemble the null vectors of Eq. (17). We use the alternative approach.

III.B. Detecting Inconsistency

For each null vector v of Eq. (17), the sums $s = Cv$ should be zero for consistent covariance matrices. Assuming that values in C and v can be represented as finite-precision numbers, computing the sum using the finite-precision arithmetic gives the computed result $\hat{s}$. The computed result is bound by the following (Ref. 11, Sec. 3.5):

$$|s - \hat{s}| \leq \gamma_t |C||v| \ . \tag{20}$$

Here the absolute value $|\cdot|$ and comparison $\cdot \leq \cdot$ are to be interpreted elementwise, γ_t is $tu/(1-tu)$, u is the unit roundoff, and t is the number of nonzero elements in the null vector: at most the number of nuclear data pieces in the sum rule. If the evaluated values cannot be represented as the used finite-precision numbers, two should be added to t to account for the initial rounding.

Assuming that the covariances are consistent, we have $s = 0$. If the criterion in Eq. (20) is violated, then the assumption is wrong and the covariances are not consistent. The results can be interpreted in terms of the sum rule and group to gain insight into which sum rules are consistent and which are not in different energy regions. By consistent covariances, we mean that the covariances are consistent given the criterion in Eq. (20) with $s = 0$. A tighter criterion can be constructed by using extended-precision inner products.

Usually the covariance matrix, and in the relative case the null vectors, are approximations for which $\hat{C} = C(1+\delta)$ and $\hat{v} = v(1+\delta)$ for some $|\delta| \leq \breve{u}$ and $\breve{u} \gg u$. In this case we get the bound

$$|s - \hat{s}| \leq (\gamma_t + \breve{\gamma}_2)|C||v| \ , \tag{21}$$

where $\breve{\gamma}_t = t\breve{u}/(1 - t\breve{u})$. We refer to the covariances, which, with $s = 0$, fulfill the criterion in Eq. (21) but not the consistency criterion in Eq. (20), as covariances that are consistent up to the precision of the data.

In practice we compute the absolute sum $s = |Cv|$, the sum of absolutes $a = |C||v|$, and their fraction $\hat{s}/\hat{a}$. The fraction is compared to γ_t and $\gamma_t + \breve{\gamma}_2$ in terms of the sum rule and group. We also ignore any sum whose sum of absolutes is less than $um\max(|C||v|)$, where m is the length of vector v. This omits very small inconsistent components, which the implementation of the following section often produces due to rounding errors.

III.C. Computing the Nearest Consistent Covariance Matrix

We denote the rank of $U = [V_1, \ldots, V_l]$ of Sec. II.G by r. The rank of V_k is g minus the number of zero columns in V_k. It is quite clear that r is the sum of ranks of V_k, $k = 1, \ldots, l$, as long as each sum rule is included at most once. Hence, a full rank $U_r \in \mathbb{R}^{m \times r}$ is acquired by dropping the zero column vectors from U.

The essential part of the projector P of Sec. II.D can be calculated using the economy size QR decomposition of U_r and the identity

$$U_r U_r^+ = QR(R^\mathsf{T} Q^\mathsf{T} QR)^{-1} R^\mathsf{T} Q^\mathsf{T} = QQ^\mathsf{T} \ . \tag{22}$$

It is crucial that U_r and therefore R is of full rank. This ensures that R has an inverse. The nearest consistent covariance matrix $D = C + X$ can be formed using

$$D = C - QQ^\mathsf{T} C - CQQ^\mathsf{T} + QQ^\mathsf{T} CQQ^\mathsf{T} \ . \tag{23}$$

III.C.1. Error Analysis

We compute U_r and note that in the typical situation it is the exact U_r, since typically all $a_i = \pm 1$. In the general case we get $\hat{U}_r = U_r \circ (I + \Delta)$, where $\cdot\circ\cdot$ is the elementwise product, $|\Delta_{ij}| \leq u$, and u is the unit roundoff. We ignore the roundoff and continue by assuming that the computed U_r is exact.

We compute the economy size QR decomposition of $\hat{U}_r$ using LAPACK's (Refs. 12 and 13) DGEQRF. Actually we get a series of Householder matrices represented by computed Householder vectors. These can be applied to any matrix with the effect of pre- or postmultiplying with Q or Q^T. We use LAPACK's DORMQR to perform the multiplications.

We compute $C_1 = Q^\mathsf{T} C$, where C is the covariance matrix, but get $\hat{C}_1 = Q^\mathsf{T}(C + \Delta C)$, where $\|Q^\mathsf{T}\Delta C\|_F \leq \|\Delta C\|_F \leq r\tilde{\gamma}_m \|C\|_F$. The first inequality uses Eq. (3) and $\|Q\|_2 \leq 1$, and the second inequality is due to the error analysis in Sec. II.H. Then we compute $C_2 = Q\hat{C}_1$ and get

$$\hat{C}_2 = Q(\hat{C}_1 + \Delta\hat{C}_1) = QQ^\mathsf{T} C + \Delta\tilde{C}_2 \ , \tag{24}$$

where $\|\Delta\tilde{C}_2\|_F \leq r\tilde{\gamma}_m(2 + r\tilde{\gamma}_m)\|C\|_F$. Computing $C_3 = \hat{C}_2 Q$ and $C_4 = \hat{C}_3 Q^\mathsf{T}$ gives $\hat{C}_4 = QQ^\mathsf{T} CQQ^\mathsf{T} + \Delta\tilde{C}_4$, where $\|\Delta\tilde{C}_4\|_F \leq r\tilde{\gamma}_m(4 + 9r\tilde{\gamma}_m)\|C\|_F$.

We compute D by subtracting $\hat{C}_2$ and $\hat{C}_2^\mathsf{T}$ from C and then adding $\hat{C}_4$ to the result. By a longish algebraic manipulation we get

$$\hat{D} = D + \Delta\tilde{D} \ , \tag{25}$$

where

$$\|\Delta\tilde{D}\|_F \leq (r\tilde{\gamma}_m(8 + 11r\tilde{\gamma}_m) + u(21 + 40r\tilde{\gamma}_m))\|C\|_F \leq r\tilde{\gamma}'_m\|C\|_F$$

and the integer factor c in $\tilde{\gamma}'_m$ is larger than in

$\tilde{\gamma}_m$. It is likely that tighter a priori bounds could be achieved, but the result is enough to show normwise numerical stability. However, small components might not be computed to high relative accuracy.

III.D. Two Methods to Characterize Covariances

The proposed method cannot be applied if some of the covariances have not been characterized, i.e., given any values. This occurs when the evaluator has not been able to determine how well the data are known and, when using ENDF-6 Formats,[4] also when the covariances are evaluated as zeros and omitted. Prior to any use, including detecting whether the covariances are consistent, the required and missing covariances need to be characterized. We try two characterization methods: a simple one and a heuristic one.

In both characterization methods covariances for redundant pieces of nuclear data for which all covariances are missing are calculated using the standard method whenever their covariances are needed. For example, they are not needed when using the alternative approach to construct the sum rules.

In the simple characterization method, any other missing covariances are characterized as zeros.

In the heuristic characterization method, covariances for redundant pieces of nuclear data that have at least some characterized covariances are characterized using the propagation-of-errors formula, Eq. (14). Any other missing covariances are characterized as zeros.

The difference between the characterization methods is the treatment of covariances of redundant pieces of nuclear data that have some but not all covariances present. The heuristic characterization method gives consistent covariances for redundant pieces of nuclear data if their partials are properly characterized. The simple characterization method gives consistent covariances only if the covariances were omitted due to being zero.

IV. CALCULATIONS

We use a slightly modified NJOY 2012.8 (Ref. 1) to process nuclear data in ENDF-6 Formats[4] from the ENDF/B-VII.1 nuclear data library[14] into multigroup covariances. We apply the method to three examples where NJOY generates inconsistent multigroup covariance matrices, given the precision of the data. That is, the inconsistencies cannot be explained by roundoff. The examples were selected to cover a variety of sum rules, and to demonstrate a few properties of the two characterization methods, and the proposed method for finding the nearest consistent multigroup covariance matrix. We do not imply that applying the proposed method is necessarily the best way to handle the inconsistencies in the examples.

All NJOY computations use a relative reconstruction tolerance of 10^{-5} and a temperature of 300 K. A Maxwell $+1/E+$ fission spectrum weight is used with a 0.1 eV thermal break, 820.3 keV fission break, and 1.4 MeV fission temperature. The module PURR is run with 40 bins and 80 ladders, when applicable. The covariances of resonance parameters are processed in ERROR using NJOY's default 1% sensitivity method. The settings are listed for reproducibility and should be considered only as an example. We extract the covariances from ERROR in their processing (double) precision, but note that the original data are roughly in single precision only.

For each example, we run four cases: (A) using the simple characterization method, (B) using the simple characterization method and finding the nearest consistent covariance matrix, (C) using the heuristic characterization method, and (D) using the heuristic characterization method and finding the nearest consistent covariance matrix.

IV.A. The Relative Covariances of Cross Sections of $^{94}_{40}Zr$

The first example is relative covariances of cross sections of $^{94}_{40}Zr$. The evaluation contains covariances for total, elastic scattering, inelastic scattering, radiative capture, and neutron duplication cross sections. Therefore, after applying either of the characterization methods, the only sum rule for the covariances is

$$\sigma_{n,t} = \sigma_{n,el} + \sigma_{n,inel} + \sigma_{n,\gamma} + \sigma_{n,2n} \ . \tag{26}$$

The covariances are inconsistent with respect to the sum rule in the whole energy range. We use the ECCO 33 group structure[15] with the lowest boundary set to 10^{-5} eV and 20 MeV upper boundary added.

IV.B. The Absolute Covariances of Cross Sections of $^{50}_{24}Cr$

The second example is absolute covariances of cross sections of $^{50}_{24}Cr$. The evaluation contains covariances for 18 cross sections, 3 of which are redundant so that for the covariances,

$$\sigma_{n,t} = \sigma_{n,el} + \sigma_{n,non\text{-}el} \ , \tag{27a}$$

$$\sigma_{n,non\text{-}el} = \sigma_{n,inel} + \sigma_{n,2n} + \sigma_{n,\gamma} + \sigma_{n,p} + \sigma_{n,d} + \sigma_{n,\alpha} + \sigma_{n,np} + \sigma_{n,n\alpha} \ , \tag{27b}$$

and

$$\sigma_{n,inel} = \sum_{i=1}^{6} \sigma_{n,n'_i} + \sigma_{n,n_c} \ , \tag{27c}$$

after applying either of the characterization methods. We use the VITAMIN-J 175 group structure[15] augmented with a 20-MeV upper boundary.

The derivation rules in the evaluation mandate the processing code to derive the covariances of the total cross section using $\sigma_{n,t} = \sigma_{n,el}$ between 10^{-5} eV and 0.783 MeV, the covariances of the elastic cross section between 0.783 and 20 MeV using Eq. (27a), and the covariances of the inelastic cross section between, 0.79881 and 20 MeV using Eq. (27b). The energy 0.79881 MeV is the threshold for the inelastic reaction. These make the evaluation consistent with respect to the sum rule Eq. (27a) above 0.783 MeV, the sum rule Eq. (27b) above 0.79881 MeV, and the sum rule Eq. (27c) below 0.79881 MeV, but otherwise the covariances are inconsistent.

IV.C. The Absolute Covariances of Cross Sections of $^{232}_{90}$Th

The third example is absolute covariances of cross sections of $^{232}_{90}$Th. The evaluation contains covariances for 12 cross sections, 5 of which are lumped cross sections. After applying either of the characterization methods, the only sum rule for the covariances is

$$\sigma_{n,t} = \sigma_{n,n'_1} + \sigma_{n,el} + \sigma_{n,any} + \sigma_{n,3n} + \sigma_{n,f} + \sigma_{n,\gamma} + \sigma_1 + \sigma_2 + \sigma_3 + \sigma_4 + \sigma_5 \ , \quad (28)$$

where the lumped cross sections σ_l, $l = 1, \ldots, 5$, are defined as

$$\sigma_1 = \sigma_{n,2n} + \sigma_{n,2na} + \sigma_{n,2np} \ , \quad (29a)$$

$$\sigma_2 = \sum_{i=2}^{10} \sigma_{n,n'_i} \ , \quad (29b)$$

$$\sigma_3 = \sum_{i=11}^{20} \sigma_{n,n'_i} \ , \quad (29c)$$

$$\sigma_4 = \sum_{i=21}^{39} \sigma_{n,n'_i} + \sigma_{n,n'_c} + \sigma_{n,n\alpha} + \sigma_{n,np} \ , \quad (29d)$$

and

$$\sigma_5 = \sigma_{n,p_0} + \sigma_{n,p_c} + \sigma_{n,\alpha_0} + \sigma_{n,\alpha_c} \ . \quad (29e)$$

We use the evaluator's group structure between 10^{-5} eV and 20 MeV. The cases (A) and (C), and cases (B) and (D), are identical for this example, since all covariances are characterized by the evaluator.

The derivation rules in the evaluation mandate the processing code to derive the covariances of the total cross section in the whole energy interval using Eq. (28). This should make the covariances described in MF 33 consistent. However, the covariances are not consistent in the same energy interval as the covariances of the resonance parameters (MF 32) are defined, i.e., below 0.1 MeV. Therefore, it seems that the description of covariances of the resonance parameters or their processing cause the inconsistency.

V. RESULTS

V.A. Consistencies

We measure consistency by the fraction of absolute sums to the sum of absolutes (see Sec. III.B). The largest fractions for the example cases are tabulated in Table I. Neither characterization method, cases (A) and (C), creates consistent covariances. However, the computed nearest consistent covariances, cases (B) and (D), are consistent given the data, but not up to the full precision. This highlights that with the described implementation of finding the nearest consistent covariance matrix, there is no need for a tighter criterion of consistency.

Many small inconsistencies were ignored in Table I. For example in the $^{50}_{24}$Cr case (B), the ignored component with the largest sum of absolutes has

TABLE I

Largest Fractions of Absolute Sums to Sums of Absolutes for Each Example Case and Upper Limits of the Fraction for Consistencies*

	$^{94}_{40}$Zr	$^{50}_{24}$Cr			$^{232}_{90}$Th
Equation	(26)	(27a)	(27b)	(27c)	(28)
Case (A)	1	1	1	1	1
Case (B)	4.8×10^{-14}	1.4×10^{-10}[a]	2.3×10^{-13}[a]	5.7×10^{-14}[a]	6.0×10^{-8}[a]
Case (C)	1	1	1	1	1
Case (D)	1.8×10^{-14}	1.4×10^{-11}[a]	3.8×10^{-13}[a]	6.8×10^{-14}[a]	6.0×10^{-8}[a]
γ_t	5.6×10^{-16}	3.3×10^{-16}	1.0×10^{-15}	8.9×10^{-16}	1.3×10^{-15}
$\tilde{\gamma}_t$	3.0×10^{-7}	1.8×10^{-7}	5.4×10^{-7}	4.8×10^{-7}	7.2×10^{-7}

*All cases are inconsistent, but some cases are consistent given the precision of the data.
[a]Some small absolute sums were ignored.

$\hat{s} = \hat{a} = 1.85 \times 10^{-15}$ b^2, when the largest sum of absolutes of all components is 104 b^2. Therefore, the ignored component is clearly inconsistent, but unlikely to cause much trouble.

It is possible to compute the precision of the data for which it is consistent by the criterion in Eq. (20) with $s = 0$. The criterion would be fulfilled when the covariances are consistent up to 16.0-digit precision. The computed nearest consistent covariance matrices are consistent up to 14.0-digit precision for $^{94}_{40}$Zr, and up to 10.3-digit precision for $^{50}_{24}$Cr. The example of $^{232}_{90}$Th shows that with the described implementation, the roundoff error can accumulate so that consistency only up to 8.3-digit precision is achieved. The little better than single precision consistency is the worst result that we have observed. Note that results for $^{232}_{90}$Th are worse than for $^{94}_{40}$Zr, despite that the dimensions of its covariance matrix are smaller than those of $^{94}_{40}$Zr.

V.B. Differences in the Characterization Methods

Among the examples, the two characterization methods differ the most for $^{94}_{40}$Zr: the Frobenius norm for the difference of the cases (A) and (C) is 0.1243, while the Frobenius norms for the cases (A) and (C) are 0.8553 and 0.8643, respectively. The two characterization methods are much less different for $^{50}_{24}$Cr: the Frobenius norm of the difference is 0.5351 b^2, while the Frobenius norms for the cases (A) and (C), 182.8 b^2, have six common significant digits. For $^{232}_{90}$Th, the two characterization methods coincide, since the evaluator has characterized all covariances.

The differences in the characterization methods can be illustrated with Fig. 2. Figure 2 shows the covariances using the heuristic characterization method, for which the cross-reaction covariances with the redundant total cross section have been derived using the propagation-of-errors formula, since those were not characterized by the evaluator. Note that $\mathrm{cov}(\sigma_{n,t},\sigma_{n,\gamma})$ and $\mathrm{cov}(\sigma_{n,t},\sigma_{n,n'})$ are not zero but only small. Both characterization methods set the other cross-reaction covariances to zero. The simple characterization method sets the cross-reaction covariances with the total cross section to zero, but otherwise the covariances are identical.

The $^{94}_{40}$Zr case (D) is shown in Fig. 3. The case (B) is qualitatively similar, but the absolute values of covariances below about 10^5 keV are about half to two-thirds of case (D). Case (B) also has a strong negative correlation between elastic and inelastic scattering above the inelastic scattering threshold energy. This feature is not present in case (D).

Since the two characterization methods yield different covariance matrices, their nearest consistent covariance matrices are also different, and they modify the covariances characterized by the evaluator differently. We measure the change in the covariances characterized by the evaluator by restricting the Frobenius norm to the covariances that were characterized by the evaluator. These are tabulated in Table II. To give scales, the restricted Frobenius norms vary between 0.850 and 0.865 in all four cases for $^{94}_{40}$Zr. For $^{50}_{24}$Cr, the norm is 182.78 b^2 in cases (A) and (C) and 143 b^2 in cases (B) and (D), within the digits shown. For $^{232}_{90}$Th the norm is 3.64 b^2, within the digits shown, in all cases.

The heuristic characterization method seems to respect the evaluator's characterization more than the simple characterization method, as can be seen for the

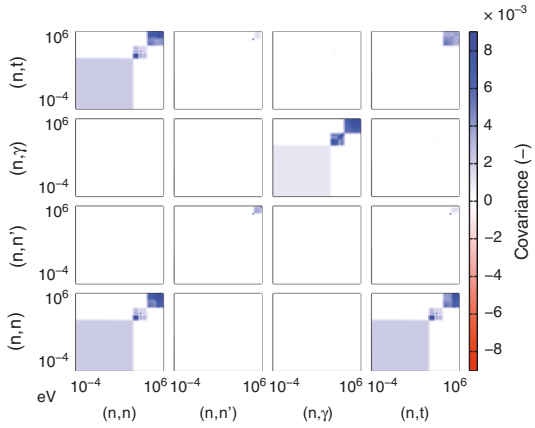

Fig. 2. Covariances of case (C) of $^{94}_{40}$Zr. Covariances with absolute value higher than 9.015×10^{-3} have the extreme colors (color online): the largest covariance is 0.4475. Covariances for $(n,2n)$ are not shown.

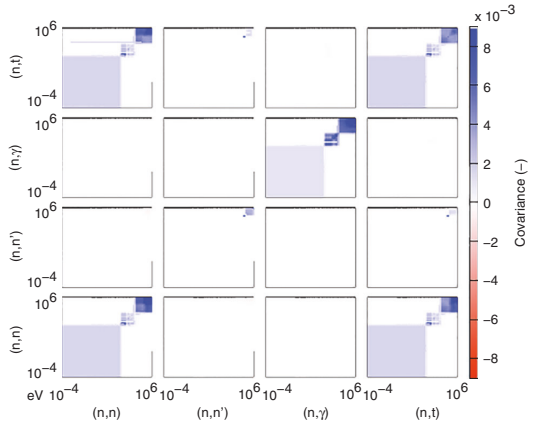

Fig. 3. Covariances of case (D) of $^{94}_{40}$Zr. Covariances with absolute value higher than 9.015×10^{-3} have the extreme colors (color online): the largest covariance is 0.4475. Covariances for $(n,2n)$ are not shown.

TABLE II

Restricted Frobenius Norms of Differences*

Difference Between	$^{94}_{40}$Zr	$^{50}_{24}$Cr (b^2)	$^{232}_{90}$Th (b^2)
Case (A) and (B)	6.114×10^{-2}	111.6	5.436×10^{-2}
Case (C) and (D)	3.911×10^{-2}	111.6[a]	5.436×10^{-2}

*See text for scales.
[a]Smaller only in the sixth decimal.

examples in Table II. The behavior seems stronger in evaluations that lack covariances between different pieces of nuclear data.

The heuristic characterization method seems to create covariance matrices with more and larger negative eigenvalues than the simple characterization method. For the examples, this can be seen in Table III. The behavior is understandable, since the heuristic characterization method does not make the block diagonal any larger but introduces nonzero values to off-diagonal parts, thereby reducing the diagonal dominance of the covariance matrices.

V.C. Changes by the Proposed Method

Finding the nearest consistent covariance matrix changes inconsistent parts of the covariances. Figures 2 and 3 show that the main changes of $^{94}_{40}$Zr from case (C) to (D) are the increase in intrareaction covariances of the total cross section below about 10^5 eV, a reduction of intrareaction covariances of the elastic scattering cross section in the same energies, and a reduction of the cross-reaction covariance between these reactions in the same energies. From case (A) to (B), the changes are qualitatively similar, except stronger in magnitude. Also the cross-reaction covariance between the total and elastic scattering cross sections increases instead of decreasing, since it was originally characterized as zero in case (A). Changes in $^{50}_{24}$Cr and $^{232}_{90}$Th are qualitatively similar, but more complicated due to a larger number of pieces of nuclear data with covariances.

Figure 4 shows the relative changes in variances of cross sections of $^{94}_{40}$Zr. The variances change little for the cross sections of inelastic scattering, neutron duplication, and radiative capture. The reduction of variances of elastic scattering from case (A) to (B) is over two-thirds, while it is less than one-third from case (C) to (D) below about 10^5 eV. In the same energy region, the variances of total cross section increase from zero in both changes, giving the 100% (capped) relative change. Above about 10^5 eV, the variances actually increase from case (C) to (D), but decrease from case (A) to (B).

Figure 5 shows the relative changes in selected variances of cross sections of $^{50}_{24}$Cr. The main changes are

TABLE III

Chosen Eigenvalues of the Covariance Matrices of the Examples

$^{94}_{40}$Zr	Smallest Eigenvalue	Negative Eigenvalues	Zero Eigenvalues[a]
Case (A)	-1.094×10^{-8}	5	112
Case (B)	-9.314×10^{-14}	1	123
Case (C)	-2.263×10^{-2}	21	101
Case (D)	-4.442×10^{-4}	14	116
$^{50}_{24}$Cr	Smallest Eigenvalue (b^2)	Negative Eigenvalues	Zero Eigenvalues[a]
Case (A)	-8.836×10^{-8}	2	2277
Case (B)	-7.781×10^{-8}	1	2395
Case (C)	-1.218×10^{-1}	139	2136
Case (D)	-7.335×10^{-2}	53	2393
$^{232}_{90}$Th		Negative Eigenvalues	Zero Eigenvalues[a]
Cases (A) and (C)		0	265
Cases (B) and (D)		0	280

[a]Indistinguishable from zero.[16]

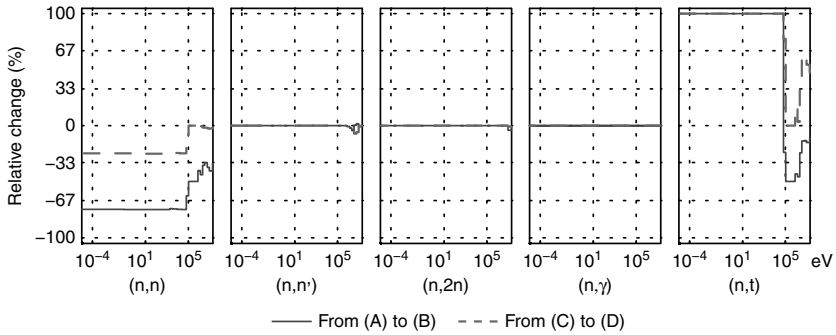

Fig. 4. Relative change in the variances of cross sections of $^{94}_{40}$Zr. Changes have been capped to ±100%.

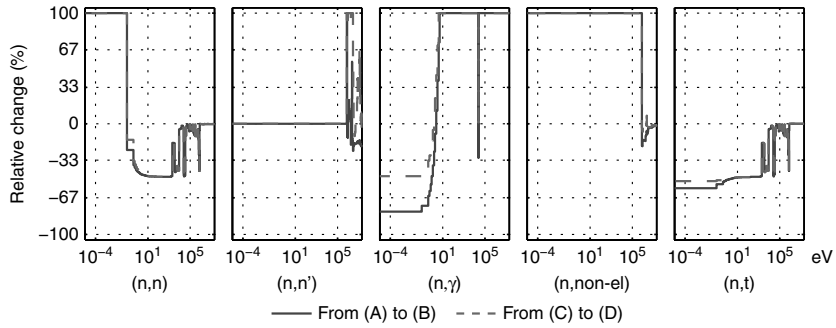

Fig. 5. Relative change in selected variances of cross sections of $^{50}_{24}$Cr. Changes have been capped to ±100%.

the two-thirds reduction in variances of total cross section below about 10^3 eV, the about one-third increase of variances of elastic scattering cross section between 10^{-1} and 10^5 eV, and an about 50% or 80% decrease in the variances of radiative capture cross section below about 1 eV, depending on the characterization method. Interestingly, in the energy group between 2.358×10^4 and 2.412×10^4 eV, the variance of the radiative capture changes much less than in the neighboring energy groups. The changes in the variances omitted from Fig. 5 occur only in the high energies, mostly above 5×10^5 eV.

Figure 6 shows the relative changes in selected variances of cross sections of $^{232}_{90}$Th. Since the covariance matrix is inconsistent only below 10^5 eV, there are no changes above 10^5 eV except those caused by rounding

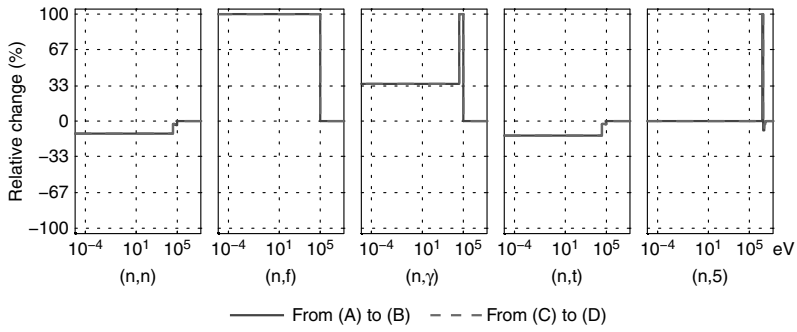

Fig. 6. Relative change in selected variances of cross sections of $^{232}_{90}$Th. Changes have been capped to ±100%.

errors. An example of those is in the energy group between 2.2536 and 1.7901 MeV for the lumped reaction number 5: the variance of the cross section increases from 7.188×10^{-7} to 3.933×10^{-6} b^2, or by 447%. Otherwise, the largest relative changes are in the variances of the fission reaction, for which the cross section was evaluated as exactly known below 10^5 eV, even though the fission cross section is nonzero in the region. Also the variances of radiative capture are increased, while variances of elastic scattering and total cross section are reduced by about 10%. The changes in the variances omitted from Fig. 6 are small.

The proposed method seems to shift some eigenvalues to zero. For the example cases, this can be seen in Table III. This is expected, since some of the zero eigenvalues contain information that the covariances are consistent. The shifted eigenvalues might originally have been either negative or positive.

The only originally positive semidefinite example is thorium, and for it the proposed method preserved positive semidefiniteness. However, rounding errors might damage positive semidefiniteness.

VI. DISCUSSION

Inconsistent covariance matrices are a result of either unphysical data, or errors in the processing codes, or rounding errors. The example of $^{94}_{40}$Zr contains unphysical covariances, whereas the inconsistencies in the examples of $^{50}_{24}$Cr and $^{232}_{90}$Th might originate from the evaluation or the processing code: some issues with covariances of resonance parameters of $^{232}_{90}$Th have been observed.[17] Generally both error types should be corrected, rather than finding a nearest consistent covariance matrix. However, when a small correction is enough to make the data consistent, the correction might be justified. In any case, the method to detect inconsistent nuclear data can be used as a part of a quality assurance procedure.

The proposed method is not conservative in the sense that it might reduce variances, and when used prior to uncertainty analysis it is likely to give smaller variances than using the standard method. However, use of the standard method unnecessarily overestimates the uncertainty.

The proposed method gives different results when applied to relative or absolute covariances, since the method minimizes the changes of the relative or absolute entries. In both cases, the same relative change for values farther from zero is larger in distance than for values closer to zero. Therefore, small (absolute) entries are likely to be changed more. Since absolute covariances are not scale free, covariances whose multigroup constant are small are likely to be changed more than those whose multigroup constants are not small.

The practical implementation of the proposed method has some room for improvement, although the used criterion for consistency is tight. There are at least two modifications that might give better numerical behavior: applying the sum rules groupwise, thereby reducing the dimensions of the sum rule matrix; and using Givens rotations instead of Householder transformations, thereby exploiting the special band structure of the null vectors. If needed, the null vectors can also be arranged so that they are lower trapezoidal. It should be noted that V^+ is easy to calculate analytically for single sum rules, but forming $U^{\sim}$ or U^+ from these is not trivial.

Applying the heuristic characterization method groupwise might improve its performance. This might give realistic estimates for the covariances that the evaluator has characterized only partially. For example, the low energy part of the covariance of the total cross section of the zirconium example and the low energy part of the covariance of the fission cross section of the thorium example might have been realistically characterized by applying the heuristic method groupwise.

The proposed method is intended for evaluations whose covariances have been characterized. If there are many uncharacterized covariances, a more natural approach is to use the remaining degrees of freedom so that the covariances are characterized in a consistent manner. We leave finding such method as future work. Finding the solution to the nearness problem in Sec. II.D using a more general norm might give such a method or an approximation of such a method. However, the approach will not work in cases where there are not enough degrees of freedom left to make the covariances consistent, in which case one must modify some of the covariances characterized by the evaluator.

The lumped cross sections in the example of thorium are an illustration of the cases for which the obvious approach in constructing sum rules will fail. The obvious approach requires propagating covariances for the inelastic cross section by summing its partials. The lumped covariances in Eqs. (29b), (29c), and (29d) contain the partials, but Eq. (29d) contains also covariances of $\sigma_{n,n\alpha}$ and $\sigma_{n,np}$. Since the covariances of $\sigma_{n,n\alpha}$ and $\sigma_{n,np}$ are not in the evaluation, their contributions cannot be separated. Therefore, the covariances for the inelastic cross section cannot be formed. While the alternative approach does not have any problems with the example of thorium, one should avoid lumping covariances for pieces of nuclear data that are not direct partials of the same piece of redundant nuclear data.

The proposed method can be applied to covariances of intramaterial multigroup quantities. Application to cross-material covariances can be constructed, with some effort, using the described null vectors and projectors as building blocks. With reinterpretation the proposed method can be used with MF 31 and 33 covariances, but it is not directly applicable to covariances of resonance parameters, i.e., MF 32.

The proposed method can also be applied to find the nearest normalized covariance matrix for a probability distribution, e.g., covariances for energy distributions of secondary particles. The null vectors are $v = [1, \ldots, 1]^T$ for absolute covariances and $v = [p_1, \ldots, p_g]^T$ for relative covariances, where the components of p are the probability distribution. These yield different formulas than the correction proposed in ENDF-6 Formats Manual (Ref. 4, Chapter 35.3) for covariances for energy distributions of secondary particles.

VII. CONCLUSIONS

An apparently new method to find a nearest symmetric matrix with given null vectors has been introduced and applied to find the nearest consistent multigroup covariance matrix with respect to the sum rules of redundant nuclear data. It has been demonstrated that a practical implementation is possible and that the practical implementation gives satisfactory, but improvable, results.

If the covariances cannot be easily interpreted so that they are consistent, there is some ambiguity in the covariances that are not characterized, i.e., given some values. Neither the simple nor the heuristic characterization method outperforms the other. The covariances given by the simple characterization method seems to have less and smaller negative eigenvalues, but they seem to be farther from consistency than the covariances given by the heuristic characterization method.

Merely using a method to detect inconsistent covariances would be a valuable addition to programs that generate multigroup covariance matrices. It could be used as a part of a quality assurance program. The programs might benefit from having an option to choose either of the two characterization methods, and from an option to use the proposed method to find the nearest consistent multigroup covariance matrix.

ACKNOWLEDGMENTS

The author thanks P. Aarnio, J. Ala-Heikkilä, and E. Dorval for their valuable comments and interest in the work and acknowledges the financial support of the YTERA Doctoral Programme for Nuclear Engineering and Radiochemistry.

REFERENCES

1. A. C. KAHLER et al., "The NJOY Nuclear Data Processing System, Version 2012," Los Alamos National Laboratory (Dec. 2012).

2. D. WIARDA et al., "Recent Advances with the AMPX Covariance Processing Capabilities in PUFF-IV," *Nucl. Data Sheets*, **109**, *12*, 2791 (2008); http://dx.doi.org/10.1016/j.nds.2008.11.011.

3. D. L. SMITH, "Evaluated Nuclear Data Covariances: The Journey From ENDF/B-VII.0 to ENDF/B-VII.1," *Nucl. Data Sheets*, **112**, *12*, 3037 (2011); http://dx.doi.org/10.1016/j.nds.2011.11.004.

4. A. TRKOV, M. HERMAN, and D. A. BROWN, "ENDF-6 Formats Manual," Brookhaven National Laboratory (2012).

5. R. HORN, *Topics in Matrix Analysis*, p. 211, Cambridge University Press (1994).

6. R. PENROSE, "A Generalized Inverse for Matrices," *Math. Proc. Cambridge Philos. Soc.*, **51**, 406 (1955); http://dx.doi.org/10.1017/S0305004100030401.

7. Z. NASHED, ed., "Generalized Inverses and Applications," *Proc. Advanced Seminar Sponsored by the Mathematics Research Center*, University of Wisconsin–Madison, October 8–10, 1973, Academic Press (1976).

8. R. PRINGLE and A. RAYNER, *Generalized Inverse Matrices with Applications to Statistics*, Griifin's Statistical Monographs & Courses, Griffin, London, United Kingdom (1971).

9. H. F. DON, "On the Symmetric Solutions of a Linear Matrix Equation," *Linear Algebra Appl.*, **93**, *C*, 1 (1987); http://dx.doi.org/10.1016/S0024-3795(87)90308-9.

10. J. H. WILKINSON, *The Algebraic Eigenvalue Problem*, Clarendon Press, Oxford, United Kingdom (1965).

11. N. HIGHAM, *Accuracy and Stability of Numerical Algorithms*, 2nd ed., Society for Industrial and Applied Mathematics (2002).

12. E. ANDERSON et al., *LAPACK Users' Guide*, 3rd ed., Society for Industrial and Applied Mathematics, Philadelphia, Pennsylvania (1999).

13. "AMD Core Math Library, Version 5.3.0," http://developer.amd.com/acml (current as of Feb. 20, 2014).

14. M. CHADWICK et al., "ENDF/B-VII.1 Nuclear Data for Science and Technology: Cross Sections, Covariances, Fission Product Yields and Decay Data," *Nucl. Data Sheets*, **112**, *12*, 2887 (2011); http://dx.doi.org/10.1016/j.nds.2011.11.002.

15. E. SARTORI, "Standard Energy Group Structures of Cross Section Libraries for Reactor Shielding, Reactor Cell and Fusion Neutronics Applications: VITAMIN-J, ECCO-33, ECCO-2000 and XMAS," JEF/DOC-315, Rev. 3 draft, Organisation for Economic Co-operation and Development/Nuclear Energy Agency Data Bank (Dec. 1990).

16. R. VANHANEN, "Computing Positive Semidefinite Multigroup Nuclear Data Covariances," *Nucl. Sci. Eng.*, **179**, 411 (2014); http://dx.doi.org/10.13182/NSE14-75.

17. G. ŽEROVNIK, A. TRKOV, and L. C. LEAL, "Challenges and Solutions for Random Sampling of Parameters with Extremely Large Uncertainties and Analysis of the ^{232}Th Resonance Covariances," *Nucl. Instrum. Methods Phys. Res., Sect. A*, **743**, 39 (2014); http://dx.doi.org/10.1016/j.nima.2014.01.012.

Publication III

R. Vanhanen. Computing more proper covariances of energy dependent nuclear data. *Nuclear Engineering and Design*, 297, 148–157, February 2016; http://dx.doi.org/10.1016/j.nucengdes.2015.11.026.

Nuclear Engineering and Design 297 (2016) 148–157

Contents lists available at ScienceDirect

Nuclear Engineering and Design

journal homepage: www.elsevier.com/locate/nucengdes

Computing more proper covariances of energy dependent nuclear data

R. Vanhanen*

Aalto University School of Science, P.O. Box 14100, FI-00076 Aalto, Finland

HIGHLIGHTS

- We present conditions for covariances of energy dependent nuclear data to be proper.
- We provide methods to detect non-positive and inconsistent covariances in ENDF-6 format.
- We propose methods to find nearby more proper covariances.
- The methods can be used as a part of a quality assurance program.

ARTICLE INFO

Article history:
Received 29 July 2015
Received in revised form 20 October 2015
Accepted 14 November 2015

ABSTRACT

We present conditions for covariances of energy dependent nuclear data to be proper in the sense that the covariances are positive, i.e., its eigenvalues are non-negative, and consistent with respect to the sum rules of nuclear data. For the ENDF-6 format covariances we present methods to detect non-positive and inconsistent covariances. These methods would be useful as a part of a quality assurance program.

We also propose methods that can be used to find nearby more proper energy dependent covariances. These methods can be used to remove unphysical components, while preserving most of the physical components. We consider several different senses in which the nearness can be measured. These methods could be useful if a re-evaluation of improper covariances is not feasible.

Two practical examples are processed and analyzed. These demonstrate some of the properties of the methods.

We also demonstrate that the ENDF-6 format covariances of linearly dependent nuclear data should usually be encoded with the derivation rules.

1. Introduction

The true values of physical quantities are never known (Cacuci and Ionescu-Bujor, 2010). Therefore, physical quantities need to be expressed as probability distributions that describe our knowledge of the physical quantities. In the practical application of evaluated nuclear data files, only the best-estimates and most of the covariances of the probability distributions are included. These are an approximation of the evaluator's knowledge of nuclear data. In some cases the covariances are improper in the sense that they are not positive, i.e., some of the eigenvalues are negative, or inconsistent with the sum rules of nuclear data. The conditions are equivalent to the best-estimates of physically positive quantities to be negative, or any quantity being inconsistent with the sum rules. The users of evaluated nuclear data files should, at the very least, be aware if the file contains improper data. This article addresses only the covariance data.

The issue of non-positive covariances has been raised by the low-fidelity covariance project (Little et al., 2008), and in the context of multigroup covariance matrices by Kodeli (2005), Mattoon and Obložinský (2011), and Vanhanen (2015b). Both Kodeli, and Mattoon and Obložinský provided a program to classify certain multigroup covariance matrices, and Vanhanen presented a method to verify positive semidefinity of arbitrary multigroup covariance matrices. For sufficiently improper multigroup covariance matrices, Vanhanen also proposed to use a method by Higham (1988) to find the nearest positive semidefinite multigroup covariance matrix in the Frobenius norm. In the context of covariance matrices of resonance parameters, Žerovnik et al. (2014) proposed to use a method by Higham (2002) to find the nearest correlation matrix of resonance parameters in the Frobenius norm.

* Tel.: +358 504331135.
E-mail address: risto.vanhanen@aalto.fi

http://dx.doi.org/10.1016/j.nucengdes.2015.11.026
0029-5493/

The issue of inconsistency with respect to the sum rules of nuclear data has received less attention. The zero eigenvalues due to consistency have been identified by Smith (2011) and Smith and Otuka (2012), and in the context of multigroup covariance matrices by Vanhanen (2015a). Vanhanen presented a method to verify consistency of intra-material multigroup covariance matrices, and provided a method to find the nearest consistent covariance matrix in the Frobenius norm.

In this paper we consider covariances of energy dependent nuclear data, and present conditions for them to be positive and consistent with the sum rules of nuclear data. We show that for most of the covariances encoded in the ENDF-6 format (Trkov et al., 2012), the properties can be checked using the corresponding methods for multigroup covariance matrices. These methods can be used as a part of a quality assurance program.

In this paper we also propose that weighting should be used if nearby covariances or the nearest covariance matrices are sought. For this, we present how our earlier methods to find the nearest positive semidefinite and consistent covariance matrices in the Frobenius norm (Vanhanen, 2015a,b) can be modified to use weighted Frobenius norms. We will demonstrate a few practical weighted norms, some of which have a physical interpretation. The users of evaluated nuclear data files can use these methods to remove unphysical parts of covariances, while preserving most of the useful information.

The rest of the paper is organized as follows: theory is presented and implementation details are described in Section 2. Two test cases are described in Section 3 and their results analyzed in Section 4. The methods are discussed in Section 5 and the paper is concluded in Section 6.

2. Theory and implementation

2.1. Energy dependent nuclear data

2.1.1. Uncertainties of parameters of nuclear data

Nuclear data are uncertain, since the true nuclear data are not known. We consider energy dependent nuclear data to depend, in principle and many times in practice, on a finite number of underlying nuclear data, $\beta \in \mathbb{R}^k$. The underlying nuclear data might be resonance parameters, 2200 m/s cross sections or some other parameters which define the energy dependent nuclear data. The uncertainty in nuclear data should be understood in terms of the Bayesian probability interpretation. The subjective knowledge of the underlying nuclear data can then be represented as a joint probability

$$p(\beta_1, \ldots, \beta_k)d\beta_1 \cdots d\beta_k \tag{1}$$

that the true value of each piece of the underlying nuclear data is between β_i and $\beta_i + d\beta_i$ for each $i = 1, \ldots, k$ simultaneously (Trkov et al., 2012). The expectation operator $\mathrm{E}[\,\cdot\,]$ over the knowledge of the underlying nuclear data is defined as $\int \cdot\, p(\beta)d\beta$.

We require a finite number of parameters since the notion of probability density for uncountable sets is not as straightforward as for finite dimensional sets (Delaigle and Hall, 2010 and references therein). Alternatively, one could consider the energy dependent nuclear data as random functions of energy[1] (Blanc-Lapierre and Fortet, 1967). Both approaches lead to the same conclusions for the ENDF-6 format nuclear data.

2.1.2. Uncertainties of energy dependent nuclear data

A piece of energy dependent nuclear data, $x_i : \mathbb{R}^+ \times \mathbb{R}^k \to \mathbb{R}$, is a function of energy and the underlying nuclear data. For example, these can be average cosine of the scattering angle in the laboratory frame for elastic scattering, or average numbers of neutrons emitted from fission. We assume that in total, from all materials, there are n pieces of energy dependent nuclear data, and concatenate them into a vector $x = (x_1, \ldots, x_n)^\top$.

Under favorable conditions the first two moments of energy dependent nuclear data over the underlying nuclear data exist. The first moments,

$$\hat{x}_i(E) = \mathrm{E}[x_i(E;\beta)], \tag{2}$$

can also be concatented into a vector

$$\hat{x}(E) = \mathrm{E}[x(E;\beta)] = (\hat{x}_1(E), \ldots, \hat{x}_n(E))^\top. \tag{3}$$

They are also referred to as the best-estimates.

The second central moments, i.e., covariances,

$$k_{ij}(E, E') = \mathrm{E}[x_i(E;\beta)x_j(E';\beta)] - \hat{x}_i(E)\hat{x}_j(E'), \tag{4}$$

describe the uncertainties in the energy dependent nuclear data. The covariance $k_{ij}(E, E')$ is sometimes written as $\mathrm{cov}(x_i(E), x_j(E'))$. We require that the covariances belong to the normed linear spaces with the norms $\|k_{ij}\|_{ij}^2 = \int\int |k_{ij}(E, E')|^2 dE'dE$. The direct sum of the normed linear spaces of the covariances is a normed linear space. Its elements can be conveniently represented as the matrices

$$\begin{aligned} k(E, E') &= \mathrm{E}[x(E;\beta)x(E';\beta)^\top] - \hat{x}(E)\hat{x}(E')^\top \\ &= \begin{bmatrix} k_{11}(E, E') & \cdots & k_{1n}(E, E') \\ \vdots & \ddots & \vdots \\ k_{n1}(E, E') & \cdots & k_{nn}(E, E') \end{bmatrix} \end{aligned} \tag{5}$$

that can be added together and multiplied by scalars. We set the norm to be $\|k\|^2 = \sum_{i,j} \|k_{ij}(E, E')\|_{ij}^2$. Also the higher order moments contain information about the uncertainty, but they are beyond the scope of this article.

2.1.3. Covariance operator of nuclear data

We consider the covariance operator of nuclear data to act on energy dependent sensitivities s that are elements of a complete inner product space $\mathcal{H}_s$. The sensitivities can be partitioned for each piece of nuclear data so that $s = (s_1, \ldots, s_n)^\top$. We denote the inner product $\int s(E)^\top t(E)dE$ for $s, t \in \mathcal{H}_s$ by the brackets $\langle s, t\rangle$.

The covariance operator of nuclear data maps an element from $\mathcal{H}_s$ to the same space by $(Cs)(E) = \int k(E, E')s(E')dE'$. The kernel is symmetric, which makes the operator self-adjoint.

The covariance operator should have at least two properties: positivity[2] and consistency with respect to the sum rules. The former property can be stated as

$$\langle Cs, s\rangle \geq 0 \tag{6a}$$

for all sensitivities $s \in \mathcal{H}_s$. This is a generalization of the requirement that the variances should be non-negative. The requirement also guarantees that first order uncertainty propagation will not yield negative variances as results. The latter property can be stated as

$$\sum_{i=1}^{n} c_i k_{ij} = 0 \tag{6b}$$

[1] Random functions of time are usually referred to as stochastic processes.

[2] The property is sometimes referred to as non-negativity.

for all linearly dependent nuclear data, $\sum_{i=1}^{n} c_i x_i = 0$, where the coefficients c_i are defined to match the sum rules of nuclear data. The requirement is analogous to the requirement that best-estimate nuclear data must be consistent with the sum rules. If this requirement is not satisfied, the results of even simple calculations depend on which constituents of redundant data are used in the formulation of the problem.

2.2. A specific representation for the covariance operator

In many cases the kernel of the covariance operator is represented as a sum of functions that are absolutely or relatively piecewise constant in energy boxes. The energy boxes are defined for an energy grid $\{E_k\}_{k=1}^{g+1}$: a pair of energies, (E, E') belongs to (k, l)-th energy box if $E \in [E_k, E_{k+1})$ and $E' \in [E_l, E_{l+1})$ simultaneously. For example, the most of the energy dependent covariances of the ENDF-6 format (MFs 31, 33, and 35; LBs 0 through 7) can be described in this way. The kernel of the covariance operator is then represented as

$$k_{ij}(E, E') = \sum_{k,l} a_{ijkl} I_k(E) I_l(E') + \sum_{k,l} b_{ijkl} \hat{x}_i(E) \hat{x}_j(E') I_k(E) I_l(E') \tag{7}$$

where $I_k(E)$ is one if E is in $[E_k, E_{k+1})$ and zero otherwise.

Note that one cannot represent an arbitrary covariance operator in the form of Eq. (7), but only a subset of finite rank operators.

2.2.1. Positivity

The requirement of positivity, Eq. (6a), for the specific representation can be expressed in the form

$$\sum_{i,j,k,l} \left[a_{ijkl} s_{i,k} s_{j,l} \Delta E_k \Delta E_l + b_{ijkl} \hat{x}_{i,k} \hat{x}_{j,l} \tilde{s}_{i,k} \tilde{s}_{j,l} \Delta E_k \Delta E_l \right] \geq 0, \tag{8}$$

where, in energy region k, $s_{i,k}$ is the unweighted average sensitivity, $\int_k s_i(E)dE / \int_k dE$, $\tilde{s}_{i,k}$ is the best-estimate weighted average sensitivity, $\int_k s_i(E)\hat{x}_i(E)dE / \int_k \hat{x}_i(E)dE$, $\hat{x}_{i,k}$ is the unweighted average best-estimate, $\int_k \hat{x}_i(E)dE / \int_k dE$, and $\Delta E_k = E_{k+1} - E_k$ is the energy-interval. This condition must hold for all sensitivities. Collecting some of the variables into the vectors, $s_i = (s_{i,1}, \ldots, s_{i,g})^\top$, $\tilde{s}_i = (\tilde{s}_{i,1}, \ldots, \tilde{s}_{i,g})^\top$, $\hat{x}_i = (\hat{x}_{i,1}, \ldots, \hat{x}_{i,g})^\top$ and $\Delta E = (\Delta E_1, \ldots, \Delta E_g)^\top$, this can be expressed more compactly as the inequality

$$s^\top D A D s + \tilde{s}^\top D \hat{X} B \hat{X} D \tilde{s} \geq 0, \tag{9}$$

where the matrices $A_{(i-1)g+k,(j-1)g+l} = a_{ijkl}$ and $B_{(i-1)g+k,(j-1)g+l} = b_{ijkl}$ contain the information from the operator, the diagonal matrices $\mathrm{diag}(D) = (\Delta E, \ldots, \Delta E)$ and $\mathrm{diag}(\hat{X}) = (\hat{x}_1, \ldots, \hat{x}_n)$ act as scales, and the vectors $s = (s_1, \ldots, s_n)^\top$ and $\tilde{s} = (\tilde{s}_1, \ldots, \tilde{s}_n)^\top$ contain the information from the sensitivities.

A sufficient condition for Eq. (9) to hold is that both terms in the sum are non-negative. That is, a sufficient condition for positivity of covariances is that both the matrices A and B are positive semidefinite. Positive semidefinity can be tested by the same method that can be used for multigroup covariance matrices (Vanhanen, 2015b). The condition can be used to prove that a covariance operator is positive.

A necessary condition for Eq. (9) to hold is that the matrix $A + \hat{X} B \hat{X}$ is positive. This condition emerges, since for a given sensitivity one can always choose another sensitivity that preserves the unweighted average and whose unweighted average is equal to the best-estimate weighted average. The condition can be used to prove that a covariance operator is not positive by showing that the covariance operator violates the condition.

The necessary and sufficient conditions coincide if either the absolute or the relative component in the covariances is zero. This is not an uncommon situation. Also, there are covariance operators that cannot be classified by either of the above conditions. For these one must use an other approach.

2.2.2. Consistency with the sum rules

The requirement of consistency with respect to the sum rules, Eq. (6b), for the specific representation can be expressed in the form

$$\sum_{i=1}^{n} c_i \left[a_{ijkl} + b_{ijkl} \hat{x}_i \hat{x}_j \right] = 0, \tag{10}$$

for all k and l.

A sufficient condition for Eq. (10) to hold is that

$$\sum_{i=1}^{n} c_i \left[a_{ijkl} + b_{ijkl} \hat{x}_i(E) \hat{x}_j(E') \right] = 0 \tag{11}$$

holds for all j, E and E'. However, this is impractical to verify numerically, since one should compute the sum for all energy pairs. Therefore, in practice, one needs to settle for a less strict condition.

A necessary condition for Eq. (10) to hold, is that

$$\sum_{i=1}^{n} c_i \left[a_{ijkl} \Delta E_k \Delta E_l + b_{ijkl} \hat{x}_{i,k} \hat{x}_{j,l} \Delta E_k \Delta E_l \right] = 0. \tag{12}$$

This weaker condition is obtained by integrating Eq. (10) over the (k, l)-th energy box. The criterion can be made tighter by introducing additional energies to the energy grid. Dividing by $\Delta E_k \Delta E_l$, the equation can be expressed more compactly as

$$[A + \hat{X} B \hat{X}] v = 0, \tag{13}$$

where $v = [c_1, \ldots, c_n]^\top \otimes e_l$, e_l is the l-th Cartesian basis vector of g dimensional real space and the Kronecker product is denoted by $\cdot \otimes \cdot$. This condition can be tested by essentially the same method that can be used test a similar condition for multigroup covariance matrices (Vanhanen, 2015a).

The necessary and sufficient conditions coincide if all best-estimates are piece-wise constant on the energy grid. However, this is not a typical situation.

2.3. Finding a nearby more proper covariance operator

The preceding methods can be used to identify whether a covariance operator in the specific representation is not proper, that is, whether the covariance operator is not positive or is inconsistent with the sum rules. If a covariance operator is not proper and a re-evaluation is not possible or feasible, it might be acceptable to find a nearest covariance operator from which the improper parts have been removed.

While the improper covariance operator can be expressed using the specific representation, it might be that a nearest covariance operator cannot be expressed using the specific representation. Therefore, we propose that only a nearby more proper covariance operator in a fixed energy grid should be sought.

This can be done, for example, by finding a nearest positive semidefinite or consistent covariance matrix to the matrix $A + \hat{X} B \hat{X}$, so that the results will fulfill the necessary conditions. However, the results might not be proper covariances, but only more proper covariances. Also, the approach preserves information about absolute and relative components only if either A or B are zero.

It is also possible to find the nearest positive semidefinite matrices A and $\hat{X} B \hat{X}$ separately, thereby ensuring that the sufficient conditions for positivity are fulfilled. However, the approach might cause larger than necessary changes.

In the specific representation, it is not always possible to find satisfactory nearby covariances that would fulfill the sufficient criterion for consistency. Consider a material like natural carbon, whose

essential low energy cross sections are constant elastic scattering, $1/v$ capture and total as their sum, and consider the condition for elastic scattering as quantity j in a low energy box (k, l). Since elastic scattering has a constant cross section we can assume, without loss of generality, that $a_{ijkl} \equiv 0$. Now, in a low energy box (k, l), either $b_{s,t,k,l} = b_{s,s,k,l} = b_{s,\gamma,k,l}$ or Eq. (10) holds for at most a single energy. Therefore, while it is technically possible to find nearby consistent covariances, the specific representation might be too restricting to allow setting the covariances rather freely and still respecting the sum rules.

This technical obstacle can be ignored by allowing more freedom in specifying the covariances. In the ENDF-6 format, for example, one can specify that covariances for a piece of nuclear data should be derived from other pieces by a given derivation rule. This makes the energy dependent covariances, by definition, consistent.

We will proceed with these approaches for a class of weighted norms.

2.3.1. Weighted Frobenius norms

Let $C \in \mathbb{R}^{m\times m}$. The weighted Frobenius norms are defined by

$$\|C\|_W = \|W^{1/2} C W^{1/2}\|_F, \tag{14}$$

where W is required to be positive definite, and $\|C\|_F = \sum_{i,j} c_{ij}^2$ is the Frobenius norm.

2.3.2. A nearest positive semidefinite matrix

Higham (2002) proves the following result:

Let $C \in \mathbb{R}^{m\times m}$ be symmetric. The unique nearest positive semidefinite matrix $C_{\mathrm{psd},W}$ in the weighted Frobenius norm is

$$C_{\mathrm{psd},W} = W^{-1/2} \tilde{X} \max(\tilde{\Lambda}, 0) \tilde{X}^\top W^{-1/2} \tag{15}$$

where $\tilde{X}\tilde{\Lambda}\tilde{X}^\top$ is the eigendecomposition of the weighted matrix $\tilde{C} = W^{1/2} C W^{1/2}$ and $\max(\tilde{\Lambda}, 0)$ contains the eigenvalues of the weighted matrix with negative eigenvalues replaced by zeros.

In practice, one can form the weighted matrix, $\tilde{C}$, compute the nearest positive semidefinite matrix in the unweighted Frobenius norm and scale the results back by pre- and post-multiplying $\tilde{X} \max(\tilde{\Lambda}, 0) \tilde{X}^\top$ by $W^{-1/2}$. Vanhanen (2015b) presented a practical implementation without scaling.

2.3.3. A nearest symmetric matrix with specified null vectors

Vanhanen (2015a) proves the following:

Let $C \in \mathbb{R}^{m\times m}$ be symmetric, and $U \in \mathbb{R}^{m\times n}$ contain the specified null vectors as its columns. The unique nearest symmetric matrix with the specified null vectors in the Frobenius norm is

$$C_{\mathrm{s,snv}} = PCP, \tag{16}$$

where $P = (I - UU^+)$ and U^+ is the (Moore–Penrose) generalized inverse of U.

The results can be generalized for the weighted Frobenius norm, giving the following result: the unique nearest symmetric matrix with the specified null vectors in the weighted Frobenius norm is

$$C_{\mathrm{s,snv},W} = W^{-1/2} \tilde{P} \tilde{C} \tilde{P} W^{-1/2}, \tag{17}$$

where $\tilde{P} = (I - \tilde{U}\tilde{U}^+)$, $\tilde{C} = W^{1/2} C W^{1/2}$ and $\tilde{U} = W^{-1/2} U$.

Proof. The original problem is to find the symmetric $X \in \mathbb{R}^{m\times m}$ that is the smallest in the Frobenius norm and for which $(C+X)U = 0$. The equality requirement is identical to $(W^{1/2} C W^{1/2} + W^{1/2} X W^{1/2}) W^{-1/2} U = 0$, i.e., $(\tilde{C} + \tilde{X})\tilde{U} = 0$, where the tilded quantities are weighted matrices. Now, finding the nearest symmetric matrix to $\tilde{C}$ with the specified null vectors $\tilde{U}$ gives the difference $\tilde{X}$ whose Frobenius norm is the smallest. Now $\|\tilde{X}\|_F = \|W^{1/2} X W^{1/2}\|_F = \|X\|_W$, so the changes in the original problem are the smallest in the weighted Frobenius norm.□

In practice, one can form the weighted matrices $W^{1/2} C W^{1/2}$ and $W^{-1/2} U$, compute the nearest symmetric matrix with the specified null vectors in the unweighted Frobenius norm and scale the results back by pre- and post-multiplying $\tilde{P}\tilde{C}\tilde{P}$ by $W^{-1/2}$. Vanhanen (2015a) presented a practical implementation without scaling.

2.3.4. Practical weighted Frobenius norms

The previous considerations make it possible to choose in which sense the changes to covariances are minimized. The choice is not completely free, since we can only choose from the weighted Frobenius norms.

We consider eight diagonal norms, whose weights are:

$$W^{1/2} = I, \tag{18a}$$

$$W^{1/2} = |\hat{X}|^{-1}, \tag{18b}$$

$$W^{1/2} = |T|^{-1}, \tag{18c}$$

$$W^{1/2} = D, \tag{18d}$$

$$W^{1/2} = |\hat{X}|^{-1} D, \tag{18e}$$

$$W^{1/2} = |T|^{-1} D, \tag{18f}$$

$$W^{1/2} = \phi, \quad \text{and} \tag{18g}$$

$$W^{1/2} = |S|. \tag{18h}$$

Here, on their diagonals, $\hat{X}$ contains the unweighted average best-estimate nuclear data, T contains the unmodified standard deviations of nuclear data, D contains the energy-intervals, ϕ contains the neutron flux spectrum in a system, and S contains the averaged sensitivity profile for a response. We refer to these as (A) to (H) -weights and -norms. It is possible to construct other norms.

The weights (A) and (B) correspond to absolute and relative cases considered in earlier articles (Vanhanen, 2015a,b), when the best-estimates are positive. The weight (C) minimizes the differences in correlation coefficients, but does not force the variances to be preserved. This allows deflation of negative variances (Vanhanen, 2015b).

The weights (D) through (F) are the first three weights with additional energy-interval weighting. The weighting by energy-intervals is quite natural by the original inner product, and can also be interpreted as a flat-flux weight. The energy-interval weights have the additional advantage that augmenting the energy grid by an energy does not double the effective weight of the split energy-interval. However, since the energy-intervals vary by orders of magnitude the scaling might cause numerical problems.

The weights (A) through (F) can be used with the data on nuclear data files, but the weights (G) and (H) require additional data. This makes them system- and response-specific, thereby producing more proper covariances only for specific applications. The weight (G) is a generalization of the weight (D), since it allows an arbitrary flux weight instead of the flat-flux weight. Naturally the energy-interval weighting can be replaced by flux weighting also in the weights (E) and (F). Conceptually the weight (H) tries to minimize changes for a certain response, whose sensitivity profile is contained in S. For certain responses the weight (G) is an approximation of the weight (H). If it were possible to use S in place of $|S|$, the weight would minimize the change in variance of the response. However, if the sensitivity profile or flux is zero at some energy-interval, the weight cannot be used directly.

There is a practical situation where the inverse-best-estimate weights, (B) and (E), and inverse-standard-deviation weights, (C) and (F), cannot be used directly: if the best-estimate or standard-deviation is evaluated as zero, its inverse cannot be used in the weights.

If the best-estimate is zero, but the standard-deviation is non-zero, the most likely explanation is that the evaluator suspects, but

is not certain, that the best-estimate is zero. In such a case we use the standard deviation in lieu of the best-estimate in the weight, giving a proper order-of-magnitude. An example case is a threshold cross section right below the threshold.

If the standard-deviation is zero, but the best-estimate is non-zero, the most likely explanation is that the evaluator has not been able to estimate how well the piece of nuclear data is known. In such a case we use a large number times the best-estimate in lieu of the standard-deviation in the weight. The inverse of the large number in the weight makes it relatively inexpensive to change the data, so that the methods do not try to preserve the unevaluated variance and its covariances. The scaling by best-estimate gives the weight a proper order-of-magnitude. In practice we use inverse of square root of machine epsilon as the large number.

If both of these are zero, the most likely explanation is that the evaluator knows with certainty that the best-estimate is zero. A usual case is a threshold cross section far below the threshold. In such a case we set the weight and its inverse to zero. While this technically makes the norm a seminorm, practically it reduces the dimensions of the covariances to which the correction is applied to.

3. Calculations

We use a slightly modified `NJOY` 2012.50 (Kahler et al., 2012) to extract data for the averaged best-estimates and the specific representation, Eq. (7), of the covariances. We apply the methods to two examples where `NJOY` extracts either non-positive or inconsistent covariances, given the precision of the data. That is, the non-positivity and inconsistency cannot be explained by roundoff error. The examples were selected to demonstrate a few properties of the weights and methods. We do not imply that applying the proposed method is necessarily the best way to handle the non-positivity and inconsistency in the examples.

All `NJOY` computations use relative reconstruction tolerance of 10^{-5}, temperature of 0 K and flat-flux weight. We extract the covariances from `ERRORR` in their processing (double) precision, but note that the original data is roughly in single precision only.

The first example is covariances of cross sections of $^4_2$He from the low-fidelity covariance project (Little et al., 2008). The covariances are used with best-estimates from the `ENDF/B-VII.0` (Chadwick et al., 2006) evaluation. The material can only interact by elastic scattering in the evaluated energy region, and therefore the total and elastic scattering cross sections are identical. The absolute component of the covariances is zero. The low-fidelity covariances require the covariances of elastic scattering to be derived from covariances of total cross section, which makes them identical. Therefore the sum rules hold for the covariances. However, the covariances contain two negative eigenvalues. We will find the nearest positive covariances using the norms (A) through (F) in the evaluator's energy grid. We will also comment on how the methods would behave on a finer energy grid, which we construct by augmenting the evaluator's energy grid by ten equal lethargy energy-intervals between 10^{-5} eV and 20 MeV.

The second example is covariances of cross sections of $^{238}_{92}$U from the `JEFF-3.2` (OECD/NEA Data Bank, 2015) evaluation. The material has covariances for cross sections of total, elastic scattering, fission and radiative capture. The covariances have only been evaluated below 40.9 keV, but the covariances include all cross-reaction covariances between the listed cross sections. The absolute component of the covariances is zero. We assume that other covariances are zero, and therefore the only sum rule for the covariances is

$$\sigma_{\mathrm{n,t}} = \sigma_{\mathrm{n,e}} + \sigma_{\mathrm{n,f}} + \sigma_{\mathrm{n},\gamma}. \tag{19}$$

On the evaluator's energy grid the covariances are inconsistent with respect to this sum rule, and they contain a negative eigenvalue. We will find the nearest more consistent covariances using the norms (A) through (C) that will fulfill the necessary condition of Eq. (12). We will not deflate the negative eigenvalue. We will increase the energy resolution of the method by splitting each evaluator's energy-interval into two equal lethargy energy-intervals. Theoretically the energy-interval weighting does not have an effect here, so the norms (D) through (F) should give identical results to the norms (A) through (C), respectively.

4. Results

4.1. Covariances of cross sections of $^4_2$He

The weights for $^4_2$He are illustrated in Fig. 1. The weight (A) is unity for all energy-intervals. The weights (B) and (C) have the largest value on the energy-interval with the lowest energies, and their graphs coincide up to 500 keV. This occurs because the relative standard deviation is constant in the region. The weights (D) through (F) are scaled from the weights (A) through (C), respectively, by the weight (D). For this particular case the energy-interval scaling causes only small differences, since the widest energy-interval is only about 100 times the narrowest energy-interval: 0.1 vs. 10 MeV. In the augmented energy grid the narrowest energy-interval is only 1.6×10^{-4} eV – ten orders of magnitude less than the widest energy-interval. Therefore we expect numerical problems with the augmented energy grid and flat-flux weights.

The low-fidelity covariances of total cross section, elastic scattering cross section and their cross-reaction covariances are identical. After applying the method, maximum relative differences are at most 4×10^{-11}% for the weights (A) through (C), and at most 3×10^{-9}% for the weights (D) through (F). The factor of 100 is apparent here. Therefore, the method retains the equality, and thereby the consistency with respect to the sum rules, only approximatively but quite well. In the augmented energy grid the maximum relative difference of 1×10^{-4}% occurs for the weight (D). The origin of this quite poor numerical behavior is the flat-flux weight with differences of several orders of magnitude in its components.

Fig. 2 shows the original and modified eigenvalues of $\hat{X}B\hat{X}$ on a large scale. The weights (B) through (F) distort even a few of the largest eigenvalues: this is most evident for the largest eigenvalue for the weight (C). The distortions are not large, but demonstrate that scaling might, and in this case does, damage the eigenvalues. The weight (A) does not distort the large eigenvalues. Had the

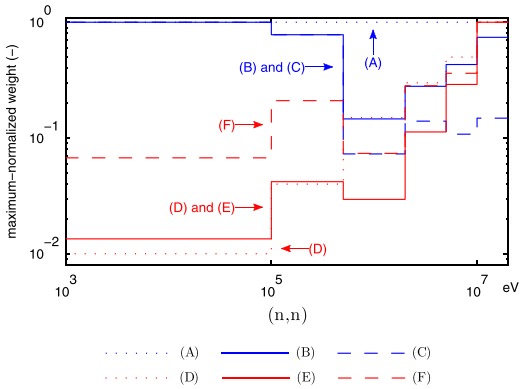

Fig. 1. The weights (A) through (F) for $^4_2$He. The weights have been normalized so that the largest element is unity. The weights for total cross section are identical.

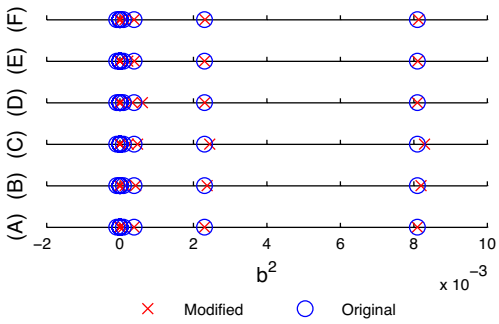

Fig. 2. Eigenvalues of original and modified covariances of $^{4}_{2}He$.

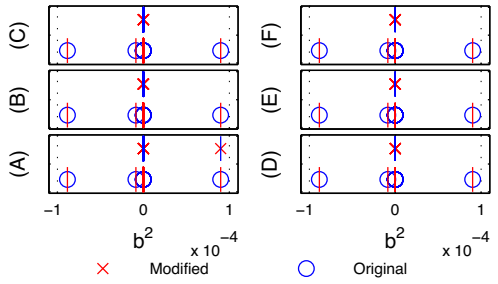

Fig. 3. Eigenvalues of original and modified covariances of $^{4}_{2}He$: magnification for negative eigenvalues. The box around each eigenvalue presents the estimated bounds due to finite precision computation (box colors inverted). The boxes appear as lines. (For interpretation of the references to color in this figure legend, the reader is referred to the web version of this article.)

correction been applied to the relative covariances, B, the unit weight would correspond to weight (B) of $\hat{X}B\hat{X}$ and would not distort eigenvalues.

Fig. 3 shows a magnification for negative eigenvalues. On this scale, it appears that all weights deflate the two negative eigenvalues. However, the weights (B) through (F) distort the eigenvalue near $10^{-4}b^2$ in contrast to the weight (A).

Fig. 4 shows a magnification of a region near the origin. There are 6 eigenvalues with zero eigenvalue that describe the sum rule, which states equality of total and elastic cross sections. Strictly speaking, the weights (D) and (E) do not manage to deflate the

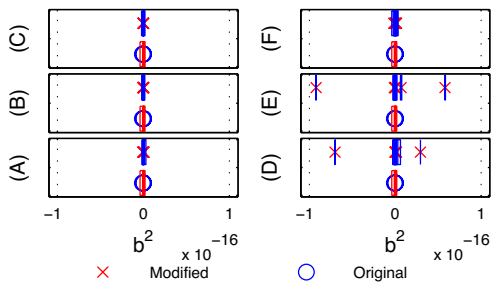

Fig. 4. Eigenvalues of original and modified covariances of $^{4}_{2}He$: magnification of a region near the origin. The box around each eigenvalue presents the estimated bounds due to finite precision computation (box colors inverted). Most of the boxes appear as lines. (For interpretation of the references to color in this figure legend, the reader is referred to the web version of this article.)

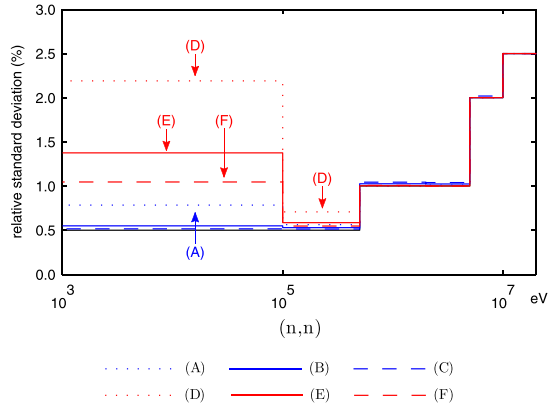

Fig. 5. Original and modified relative standard deviations of $^{4}_{2}He$. The original standard deviations are the smallest in all energy-intervals.

negative eigenvalues. The weight (E) even distorts one of the eigenvalues that describe the sum rule. The reason for this appears to be a small round-off error that is multiplied by a factor of up to 100 when the covariances are weighted back after deflation. In the augmented energy grid the remaining negative eigenvalues are on the order of $10^{-11}b^2$ for all three energy-interval weights. If one chooses to use energy-interval weights, an obvious remedy is to first use the energy-interval weights, and then remove any remaining negative eigenvalues by using the unweighted Frobenius norm.

The deflation modifies all elements of the covariances. The original and modified relative standard deviations are shown in Fig. 5. The largest changes occur in the energy-interval with the smallest energies. Here the energy-interval weighted norms cause the largest increases in the standard deviation. The weights (A) through (C) are larger here than the energy-interval-weights, which causes them to prefer modifying elements in other energy regions. The situation is reversed above 500 keV. Use of the weights (B) and (C) results in the most uniform changes, while the other weights concentrate their changes to the energy-interval with the smallest energies.

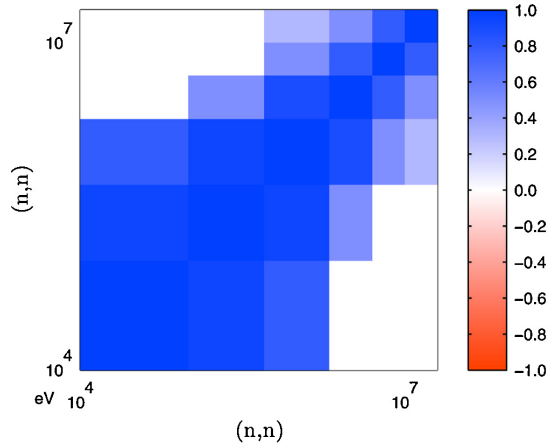

Fig. 6. Original correlations of $^{4}_{2}He$ for elastic scattering cross section. The correlations for total cross section and cross-reaction correlations are identical. The six separate energy-intervals are clearly visible.

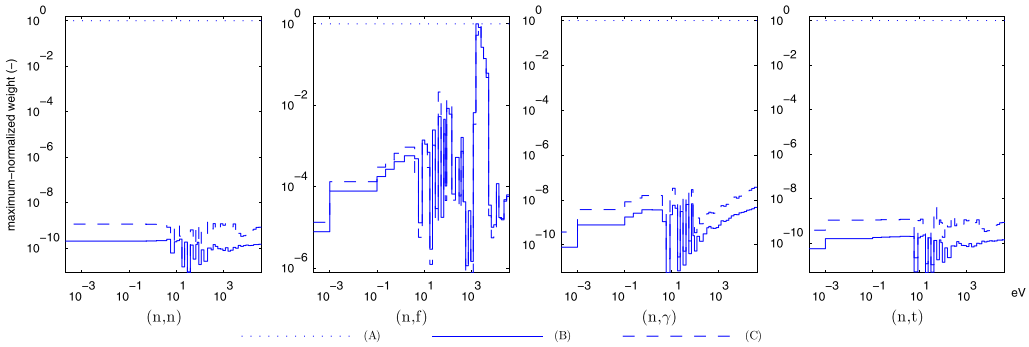

Fig. 7. The weights (A) through (C) for $^{238}_{92}$U. The weights have been normalized so that the largest element is unity.

The original correlations are shown in Fig. 6. The six separate energy-intervals are clearly visible. The deflations mostly reduce the positive correlations. For the weights (D) through (F) the largest decreases in the correlation coefficients are up to 0.63 between the lowest and third lowest energy-intervals. This results in less correlation between low and high energies. For the weights (A) and (B) the largest decreases occur for the same energy box, by 0.32 and 0.20, respectively. For the weight (C) the largest decreases occur in the energy box with third largest and third smallest energies, by 0.15. Again, this reduces the correlation between low and high energies. The weights (A) through (C) also replace zero correlations between the lowest and third highest energies with slightly positive correlations, up to 0.11, but reduce correlations of its nearest neighbors.

All modifications in the augmented energy grid are qualitatively similar to the non-augmented case. However, as expected the distortions in the non-negative eigenvalues are larger.

4.2. Covariances of cross sections of $^{238}_{92}U$

The weights for $^{238}_{92}$U are illustrated in Fig. 7. The resolution on which uncertainties are estimated is less than the energy resolution of the cross sections. Therefore, the resonance structure is not fully captured and appears as rapid increases and decreases of the unweighted averages of the best-estimates. The weight (A) is unity for all energy-intervals. It is worth noting that both the weights (B) and (C) have large weights for the fission cross section, and hence modifying covariances with the fission cross section is more expensive than changing covariances of other cross sections. For the weight (A) all changes are equally expensive. Otherwise the weights (B) and (C) are quite similar to each other, since their ratio is the relative standard deviation that varies only a little.

The energy-interval weighting does not have an effect here, so under exact arithmetic, the norms (D) through (F) give identical results to the weights (A) through (C), respectively. In this case the maximum relative differences between the weights were at most 2×10^{-7}%, which occurred for the weights (A) and (D). In the end, the modified covariances are consistent to about 12 decimals for the weights (A) and (D), 13 decimals for the weights (B) and (E) and 14 decimals for the weights (C) and (F) in the average sense of Eq. (13). Hence the finite precision computing did not cause large differences in the results.

Except for the weight (A) the modifications to standard deviations were small, as can be seen from Fig. 8. The weights (B) and (C) are very close to the original evaluation, with largest changes in the lowest energy-interval. Here the standard deviations are increased for radiative capture and decreased for total and elastic scattering. There are also other small differences. The weight (A) concentrates modifications to the standard deviations of the smaller cross sections. The relative standard deviation of radiative capture cross section is increased in the region above 1 eV to almost 32%. However, the relative standard deviation of the fission cross section is increased to well over 1000%. The weight is clearly not suitable for this case.

Fig. 9 shows the original correlations. The intra-reaction correlations are mostly positive, and there is a mostly positive correlation

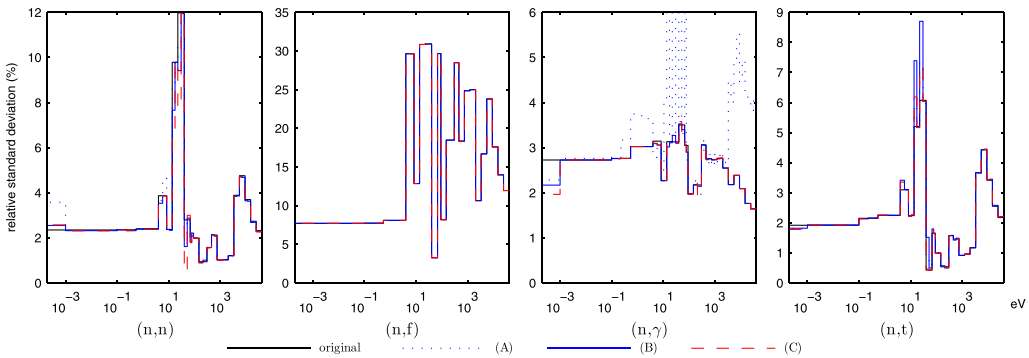

Fig. 8. Original and modified standard deviations of $^{238}_{92}$U. The differences between the original and weights (B) and (C) are less than line width in many places. For the fission cross section modified standard deviations using the weight (A) vary between 1000% and 7.5×10^8%, which are therefore out of figure. For radiative capture the maximum for the same weight is 32%.

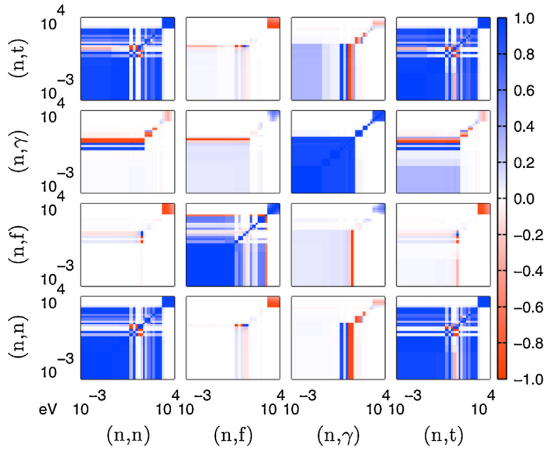

Fig. 9. Original correlations of $^{238}_{92}$U.

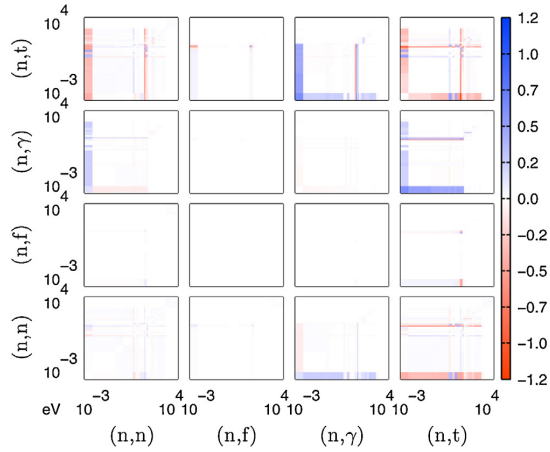

Fig. 11. Differences in correlations of $^{238}_{92}$U when the nearest consistent covariance are sought by weight (B).

between total cross section and elastic scattering. The cross-reaction correlations with the fission cross section are mostly small.

Fig. 10 shows the differences in the original and modified correlations for the weight (A). There are many changes where the correlations are flipped over from almost negative unity to almost positive unity, and vice-versa. Most clearly this is seen in the correlations of fission cross section, except for the diagonal that naturally remains to be unity. The large change agrees with the huge increase of the standard deviations. There are also large changes in a few energy boxes of correlations with radiative capture, but fairly small changes to correlations with total and elastic cross sections. This can be understood as follows: the magnitudes of the covariances are much smaller for the fission cross section than for other cross sections, since all original relative standard deviations were on the same order of magnitude and the fission cross section is several orders of magnitude smaller than other cross sections. Since the weight is unity for all components of the covariances, the smallest possible adjustments cause large relative changes to covariances with the fission cross section.

Fig. 11 shows the differences in the original and modified correlations for the weight (B). The weight removes the scale of cross sections from the covariances before finding the nearest consistent covariances. Therefore covariances with fission cross sections are modified less dramatically than with the weight (A). The magnitude of changes is also smaller than with the weight (A). The low energy portions of correlations with total cross section are modified the most, but some positive correlation is also introduced between low-energy elastic scattering and radiative capture.

Fig. 12 shows the differences in the original and modified correlations for the weight (C), which removes the scales of cross sections and uncertainties from the covariances before finding the nearest consistent covariances. The outcome is qualitatively similar to the outcome of the weight (B). Note that the magnitude of changes in correlations is smaller than for the weight (B). However, if relative standard deviations varied a lot, then the weight (B) would have a larger spread while the weight (C) would be scale-free in this sense. In such a case the elements with high uncertainty would change less with the weight (B) than with the weight (C), which might lead to smaller overall uncertainties for the weight (C).

Had the energy grid not been augmented, the changes would have been smaller: the changes in the correlation coefficients varied

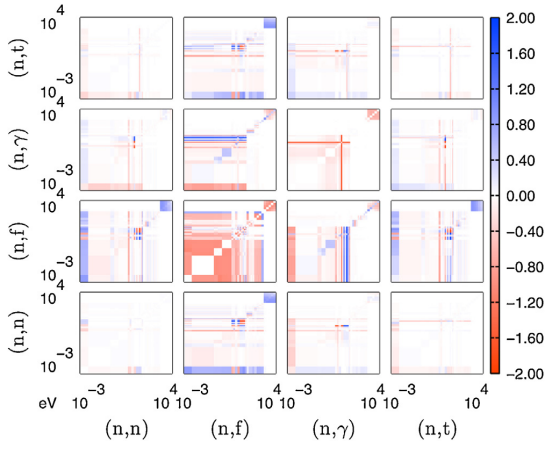

Fig. 10. Differences in correlations of $^{238}_{92}$U when the nearest consistent covariance are sought by weight (A).

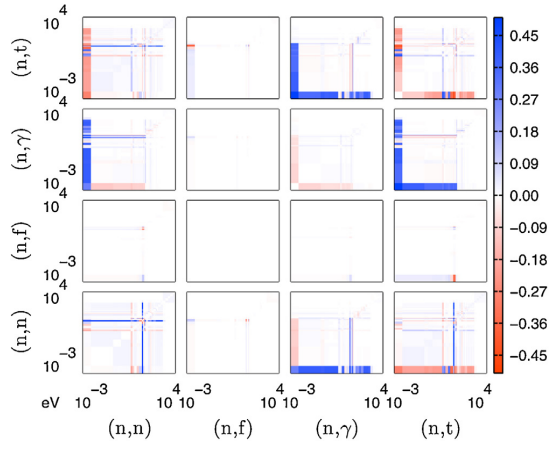

Fig. 12. Differences in correlations of $^{238}_{92}$U when the nearest consistent covariance are sought by weight (C).

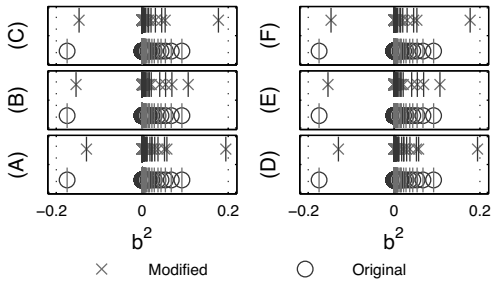

Fig. 13. Eigenvalues of original and modified covariances of $^{238}_{92}$U: magnification for negative eigenvalues. The box around each eigenvalue presents the estimated bounds due to finite precision computation (box colors inverted). The boxes appear as lines. (For interpretation of the references to color in this figure legend, the reader is referred to the web version of this article.)

between -1.01 and 1.00, -0.18 and 0.23, and -0.06 and 0.05 for the weights (A), (B) and (C), respectively. For the weight (A) the largest changes are still large. This demonstrates that the criterion in the augmented energy grid requires larger changes, since the criterion is tighter.

Fig. 13 illustrates the original and modified eigenvalues of $\hat{X}B\hat{X}$ near the origin. The negative eigenvalue is preserved. For this particular case, the weights (A) and (C) introduce 3 and 2 new zero eigenvalues, respectively. The weight (B) does not introduce any new zero eigenvalues, but only modifies eigenvectors of the existing ones. The eigenvalues are also shown for the weights (D) through (F): the small differences to the weights (A) through (C), respectively, cannot be seen in scale of the graph.

5. Discussion

Improper covariances are a result of either unphysical data, processing errors or rounding errors. Generally all these error types should be corrected, but it is also possible to find nearby covariances whose improper parts have been removed. What the practical implications of the changes made by removing improper parts are, and whether the use of the nearby proper covariances is safe, must still be judged case-by-case.

The implementations are straightforward if the corresponding methods are available for multigroup covariance matrices. For the methods to verify whether energy dependent covariances are proper, it suffices to use the flat-flux weight when averaging best-estimates. For methods to find a nearby more proper covariances, the multigroup methods can be used as-is for norms (A) and (B). For other norms it suffices to implement assembling of the weights and scaling of the covariances.

The effects of the weights differ for different cases. For the single-quantity case of ^4_2He the different weights played only a small role. For the larger, four-quantity case of $^{238}_{92}$U the different weights produced large differences.

The norms (B), (C), (E) and (F) are scale free in at least one sense, and hence they are likely to give better results than the weights (A) and (D) for medium to large changes. However, their numerical precision is worse than that of the weight (A). An obvious remedy is to make larger changes with the weights (B), (C), (E) and (F) and handle any remaining smaller corrections with the weight (A).

It is also possible to use other weights, such as the weights (G) and (H). Since the weights can be set rather freely, one can encode the belief that covariances of a piece of nuclear data are correctly evaluated in a specified energy-interval: setting the weight to a large value in the energy-interval will keep the corresponding variance and covariances nearly intact when finding nearby covariances. One can combine such trust based weight with other weights by multiplying them.

The norms (D), (G) and (H) have a physical interpretation. However, the results of the norm (D) were no better than those of the norm (A) for $^{238}_{92}$U, and the norms (G) and (H) are system specific.

The energy-interval weighting does not have an effect for consistency, but the necessary condition for sum rules can be made tighter by increasing energy resolution by augmenting energies to the energy grid.

The method to find nearby positive covariances was conservative in the case of ^4_2He, in the sense that it did not decrease variances. The method to find nearby consistent covariances is not conservative in the same sense.

The example of carbon (see Section 2.3) illustrates how inconvenient the relative representation is when there is some linearly redundant data present. In the ENDF-6 format it is perhaps the most practical to not encode all redundant data directly, but to use derivation rules to mark one component as being derived from others according to its sum rule. For inconsistent covariances, one can find nearby more consistent covariances, drop one component and mark it as being derived. However, this is not always necessary since, for example, the case of ^4_2He could be encoded directly without causing the covariances to be inconsistent.

The norms can also be used with the similar methods for multigroup covariance matrices.

The method to find nearest positive covariance matrices can be applied to covariances of resonance parameters, i.e., MF 32 of the ENDF-6 format. The covariances of resonance parameters seem to contain no redundant data in the ENDF-6 format. The different weights can be used to reduce the scaling effects. Žerovnik et al. (2014) have proposed finding nearest correlation matrices of resonance parameters. This is close to using the weight (C) but differs in that variances are required to be preserved when finding the nearest correlation matrix.

The method to find nearby consistent covariances can also be applied to find nearby consistent covariances for a probability distribution, e.g., covariances for energy distributions of secondary particles. The null vectors are $\nu = [1, \ldots, 1]^\top$ for (absolute) covariances. The weight $W^{-1} = |\hat{X}|D$ yields the formula that is listed in ENDF-6 Formats Manual (Trkov et al., 2012, Chapter 35.3) for covariances for energy distributions of secondary particles.

6. Conclusions

We have presented conditions for covariances of energy dependent nuclear data to be positive and consistent with the sum rules of nuclear data. We have given these conditions in a general form as well as for a specific representation of covariances. For the latter we have presented sufficient and necessary conditions for covariances of energy dependent nuclear data to be positive and consistent with sum rules. Most of the ENDF-6 format covariances (MFs 31, 33, and 35, LBs 0 through 7), for example, are covered by the representation. With the exception of the sufficient condition of consistency with respect to the sum rules, the conditions can be verified using methods that verify similar conditions for multigroup covariance matrices.

The evaluators can use these methods to verify that their covariances are proper. In the ENDF-6 format most covariances of redundant pieces of nuclear data should be marked to be derived from the covariances of the nuclear data that the redundant piece depends on.

We have also presented methods to find nearby more proper energy dependent covariances. In a case where a re-evaluation of improper covariances is not feasible, it is possible to find nearby more proper covariances using, for example, one of the methods,

with one of the norms, presented in this work. Making nearly minimal changes ensures that the evaluator's insight is respected nearly as much as possible, while still making the covariances more proper. What the practical implications of the changes are, and whether the use of the more proper covariances is acceptable, must still be judged case-by-case.

The methods to detect improper covariances would be valuable tools for evaluators, and the methods to find nearby more proper covariances might be useful for users of evaluated nuclear data files.

Acknowledgments

The author thanks J. Ala-Heikkilä and M. Lempinen for their valuable comments and interest in the work, and acknowledges the financial support of the YTERA Doctoral Programme for Nuclear Engineering and Radiochemistry.

References

Blanc-Lapierre, A., Fortet, R., 1967. Theory of Random Functions, vol. 1., 2nd ed. Gordon and Breach Science Publishers Ltd., New York (translated by J. Gani).

Cacuci, D., Ionescu-Bujor, M., 2010. Sensitivity and uncertainty analysis, data assimilation, and predictive best-estimate model calibration. In: Cacuci, D. (Ed.), Handbook of Nuclear Engineering. Springer, US, pp. 1913–2051.

Chadwick, M., Obložinský, P., Herman, M., Greene, N., McKnight, R., Smith, D., Young, P., MacFarlane, R., Hale, G., Frankle, S., Kahler, A., Kawano, T., Little, R., Madland, D., Moller, P., Mosteller, R., Page, P., Talou, P., Trellue, H., White, M., Wilson, W., Arcilla, R., Dunford, C., Mughabghab, S., Pritychenko, B., Rochman, D., Sonzogni, A., Lubitz, C., Trumbull, T., Weinman, J., Brown, D., Cullen, D., Heinrichs, D., McNabb, D., Derrien, H., Dunn, M., Larson, N., Leal, L., Carlson, A., Block, R., Briggs, J., Cheng, E., Huria, H., Zerkle, M., Kozier, K., Courcelle, A., Pronyaev, V., van der Marck, S., 2006, December. ENDF/B-VII.0: next generation evaluated nuclear data library for nuclear science and technology. Nuclear Data Sheets 107 (12), 2931–3118.

Delaigle, A., Hall, P., 2010. Defining probability density for a distribution of random functions. Ann. Stat. 38 (2), 1171–1193, 04.

Higham, N.J., 1988. Computing a nearest symmetric positive semidefinite matrix. Linear Algebr. Appl. 103 (C), 103–118.

Higham, N.J., 2002. Computing the nearest correlation matrix – a problem from finance. IMA J. Numer. Anal. 22 (3), 329–343.

Kahler, A.C., MacFarlane, R.E., Muir, D.W., Boicourt, R.M., 2012, December. The NJOY Nuclear Data Processing System, Version 2012. Los Alamos National Laboratory.

Kodeli, I.A., 2005. VITAMIN-J/COVA/EFF-3 cross-section covariance matrix library and its use to analyse benchmark experiments in SINBAD database. Fusion Eng. Des. 75–79, 1021–1025.

Little, R.C., Kawano, T., Hale, G.D., Pigni, M.T., Herman, M., Obložinský, P., Williams, M.L., Dunn, M.E., Arbanas, G., Wiarda, D., McKnight, R.D., McKamy, J.N., Felty, J.R., 2008. Low-fidelity covariance project. Nuclear Data Sheets 109 (12), 2828–2833.

Mattoon, C.M., Obložinský, P., 2011. Issues in neutron cross section covariances. J. Korean Phys. Soc. 59 (23), 1242–1247.

OECD/NEA Data Bank, 7 2015. JEFF-3.2. https://www.oecd-nea.org/dbdata/jeff/.

Smith, D.L., 2011. Evaluated nuclear data covariances: the journey from ENDF/B-VII.0 to ENDF/B-VII.1. Nuclear Data Sheets 112 (12), 3037–3053 (special Issue on ENDF/B-VII.1 Library).

Smith, D.L., Otuka, N., 2012. Experimental nuclear reaction data uncertainties: basic concepts and documentation. Nuclear Data Sheets 113 (12), 3006–3053 (special Issue on Nuclear Reaction Data).

Trkov, A., Herman, M., Brown, D.A., 2012. ENDF-6 Formats Manual. Brookhaven National Laboratory.

Vanhanen, R., 2015a. Computing more consistent multigroup nuclear data covariances. Nuclear Sci. Eng. 181 (1), 60–71.

Vanhanen, R., 2015b. Computing positive semidefinite multigroup nuclear data covariances. Nuclear Sci. Eng. 179 (4), 411–422.

Žerovnik, G., Trkov, A., Leal, L.C., 2014. Challenges and solutions for random sampling of parameters with extremely large uncertainties and analysis of the ^{232}Th resonance covariances. Nuclear Instrum. Methods Phys. Res. Sect. A: Accel. Spectrom. Detect. Assoc. Equip. 743, 39–43.

Publication IV

R. Vanhanen and M. Pusa. Survey of prediction capabilities of three nuclear data libraries for a PWR application. ***Annals of Nuclear Energy*****, 83, 408–421, September 2015;** `http://dx.doi.org/10.1016/j.anucene.2015.03.044`**.**

Annals of Nuclear Energy 83 (2015) 408–421

Contents lists available at ScienceDirect

Annals of Nuclear Energy

journal homepage: www.elsevier.com/locate/anucene

Survey of prediction capabilities of three nuclear data libraries for a PWR application

R. Vanhanen [a,*], M. Pusa [b]

[a] Aalto University School of Science, P.O. Box 14100, FI-00076 AALTO, Finland
[b] VTT Technical Research Center of Finland, P.O. Box 1000, FI-02044 VTT, Finland

ARTICLE INFO

Article history:
Received 26 January 2015
Received in revised form 26 March 2015
Accepted 28 March 2015
Available online 13 April 2015

Keywords:
Prediction capability
Uncertainty analysis
ENDF/B-VII.1
JEFF-3.2
JENDL-4.0u
Cross-material covariances

ABSTRACT

We survey prediction capabilities of ENDF/B-VII.1, JEFF-3.2 and JENDL-4.0u nuclear data libraries (NDLs) for the application of generating two-group homogenized assembly constants for a steady state diffusion model in the context of UAM-LWR (Uncertainty Analysis in Best-Estimate Modeling for Design, Operation and Safety Analysis of LWRs) Benchmark. We consider two different fuel assembly test cases representing a PWR. State of uncertainty quantification in each NDLs is presented for the application. We expect small differences between the NDLs due to the use of expert judgment in the evaluation processes, and identify several order-of-magnitude differences between the NDLs for significant contributors to uncertainty. We also quantify the contribution from cross-material correlations to the uncertainties.

1. Introduction

Evaluated nuclear data files contain estimates of physical quantities referred to as nuclear data. The estimates are a result of evaluation of theoretical models and empirical measurements, both of which are imperfect and therefore do not provide the true values of the nuclear data. Some evaluators have quantified the uncertainties resulting from these imperfections, and thereby quantitatively expressed their subjective degrees of belief on what the true values of nuclear data are.

In applications the nuclear data can be used to predict quantities of interest. Since the true nuclear data is not known, the quantities of interest are predicted using evaluated nuclear data. In uncertainty analysis, degrees of belief on the true values of the quantities of interest can be acquired by propagating the uncertainties of evaluated nuclear data to uncertainties of the quantities of interest. The propagated uncertainties can be interpreted as a measure of the prediction capability of the evaluated nuclear data for the considered application. In principle, the smaller the propagated uncertainties, the better the prediction capability of the evaluated data.

A nuclear data library (NDL) contains a set of evaluated nuclear data files, which have been evaluated to perform well both individually and together. In this article we consider three NDLs: ENDF/B-VII.1 (Chadwick et al., 2011), JEFF-3.2 (OECD/NEA Data Bank, 2014), and JENDL-4.0u (Shibata et al., 2011; Japan Atomic Energy Agency, 2013). The development of uncertainty estimates for the nuclear data is in progress in the NDLs (Ivanov et al., 2013). Therefore, the NDLs contain evaluations with fully quantified, partially quantified and unquantified uncertainties. The propagated uncertainties do not and can not include contribution from unquantified uncertainties, and this component of uncertainty must be taken into account by other means. Since the uncertainties are not sufficiently completely quantified in the NDLs, it is meaningless to compare their overall prediction capabilities directly.

In recent years there has been an increasing demand to be able to provide all calculation results depending on nuclear data with some uncertainty estimates. To promote this goal, a benchmark titled "Uncertainty Analysis in Best-Estimate Modeling for Design, Operation and Safety Analysis of LWRs" (UAM) was prepared in 2006 by the OECD/NEA Expert group on Uncertainty Analysis in Modeling (Ivanov et al., 2013). In the UAM benchmark, the goal is to be able to propagate nuclear data uncertainty through all stages of coupled neutronics/thermal-hydraulics calculations. As a first step, this requires developing uncertainty analysis methodologies for reactor physics codes that are used to produce homogenized constants for the following full core calculations.

* Corresponding author.
E-mail addresses: risto.vanhanen@aalto.fi (R. Vanhanen), maria.pusa@vtt.fi (M. Pusa).

http://dx.doi.org/10.1016/j.anucene.2015.03.044
0306-4549/

In this article we survey the prediction capabilities of the three NDLs in the context of the reactor physics phase of the UAM benchmark. We compute the two-group homogenized constants for a steady state diffusion model for a uranium dioxide and a mixed oxide assembly from the UAM-LWR benchmark. These act as representatives of PWR assemblies. Uncertainty analysis capability based on first order sensitivity analysis has been previously implemented to the fuel assembly burnup program CASMO-4 (Rhodes and Edenius, 2001; Pusa, 2012a,b, 2014), which is also used in this study. The multigroup adjoint-based approach, although approximative and indirect, allows to identify the contribution from each piece of nuclear data to the propagated uncertainties. For this purpose a piece of nuclear data is specified by a pair of material and quantity. Therefore the prediction capabilities of the NDLs can be compared quantity-wise for each material.

It should be emphasized that we expect small differences in the prediction capabilities of the NDLs, since available experimental data and theoretical information change in time, and the evaluation procedures include expert judgment which the evaluators use slightly differently. Therefore, the evaluators knowledge of the nuclear data differs slightly (Cacuci, 2003; Talou et al., 2011). However, an order-of-magnitude differences in prediction capabilities signal that an evaluator has not included all significant information in the evaluation or has made an error. In the former case the significant information might be missing from the evaluation with the larger or smaller uncertainties, since new information might increase or decrease the uncertainties.

We identify materials whose contributions to uncertainty might be important but which do not have uncertainty estimates in any of the three NDLs by using the ZZ-SCALE6/COVA-44G library (OECD/NEA Data Bank, 2011), which is complete for our purposes. The library is largely based on the uncertainty estimates from the low-fidelity covariance project (Little et al., 2008) whose aim was to provide crude uncertainty estimates for almost all materials. Due to low fidelity the identification is not very accurate but it is clearly beneficial to have some uncertainty estimates for the data whose uncertainty is otherwise considered as zero.

In this article we also quantify the sometimes neglected contribution from cross-material correlations.

The rest of the article is organized as follows: relevant parts of the theory are briefly reviewed in Section 2. The calculational procedure and the status of the uncertainty quantification in the considered NDLs is presented in Section 3 and the results are analyzed in Section 4. Finally, the conclusions are presented in Section 5.

2. Theory

2.1. Nuclear data and its uncertainties

Nuclear data is uncertain, since the true values of pieces of the nuclear data are not known. We cover only the finite-dimensional case for convenience, so the nuclear data α belongs to $\mathbb{R}^k$. The uncertainty should be understood in terms of the Bayesian probability interpretation. The subjective knowledge of the nuclear data can then be represented as a joint probability

$$p(\alpha_1, \ldots, \alpha_k) d\alpha_1 \cdots d\alpha_k, \tag{1}$$

that the true value of each piece of the nuclear data α_i is in $(\alpha_i, \alpha_i + d\alpha_i)$ for each $i = 1, \ldots, k$ simultaneously (Trkov et al., 2012). The first moments of the distribution are called the best-estimates of pieces of the nuclear data and denoted by $\hat{\alpha} \in \mathbb{R}^k$, and the second central moments form the covariance matrix which is denoted by $\mathrm{cov}(\alpha, \alpha) \in \mathbb{R}^{k \times k}$. The covariance matrix describes approximately the uncertainties of the nuclear data.

2.2. Uncertainty analysis

In applications quantities of interest, usually referred to as responses, $R \in \mathbb{R}^n$ are calculated from parameters $\alpha \in \mathbb{R}^k$, which in this case include the nuclear data, through a mapping $f : \mathbb{R}^k \to \mathbb{R}^n$.

In the first order uncertainty analysis the mapping is linearized so that

$$R = f(\alpha) = f(\hat{\alpha}) + S(\hat{\alpha})(\alpha - \hat{\alpha}) + \mathcal{O}(\|\alpha - \hat{\alpha}\|^2), \tag{2}$$

where $S \in \mathbb{R}^{n \times k}$ are the sensitivities of the mapping and are evaluated at the best-estimate values. The first order uncertainty propagation formula (see, e.g., Cacuci, 2003; Vanhanen, 2015a for derivation) is

$$\mathrm{cov}(R, R) = S(\hat{\alpha}) \mathrm{cov}(\alpha, \alpha) S(\hat{\alpha})^{\top} + \mathcal{O}(\|\alpha - \hat{\alpha}\|^3), \tag{3}$$

where $\mathrm{cov}(R, R) \in \mathbb{R}^{n \times n}$ is the covariance matrix of the responses. The equation is also known as the "sandwich rule" (Pusa, 2012b), the "second moment propagation" equation (Cacuci, 2003), and the "propagation of errors" formula (Trkov et al., 2012).

For certain mathematical models, the sensitivity matrix in Eq. (3) can be computed efficiently by utilizing the adjoint system of the original forward problem (Cacuci, 2003). In reactor physics the forward problem is the criticality equation and this approach is called (generalized) perturbation theory (Wigner, 1945; Usachev, 1964). This is the framework for the sensitivity analysis implementation in the modified CASMO-4 code used in this study (Pusa, 2012a,b).

2.3. Reaction models

CASMO-4 (Rhodes and Edenius, 2001) solves the transport corrected isotropic scattering approximation of the multigroup transport equation. The reaction model [1] is simplified by lumping all scattering reactions into a total scattering reaction, and the generated two-group homogenized constants are simplified by using an effective capture reaction. Therefore the reaction model in CASMO-4 consists of transport, total scattering, effective capture and fission reactions.

The reaction model in the ENDF-6 format is more fine grained. In the following, tilded quantities refer to multigroup constants generated from ENDF-6 quantities and other quantities refer to the CASMO-4 quantities.

The transport cross section is defined as

$$\sigma_{\mathrm{tr}} = \tilde{\sigma}_{\mathrm{tot}} - \tilde{\mu} \tilde{\sigma}_{\mathrm{s}}, \tag{4}$$

where σ_{tot} is the total cross section, μ is the scattering cross section weighted average cosine of the scattering angle in the laboratory frame and σ_{s} the scattering cross section.

The (isotropic) total scattering cross section (weighted by number of emitted neutrons) is defined as

$$\sigma_{\mathrm{s}} = \sum_i m_{\mathrm{s}_i} \tilde{\sigma}_{\mathrm{s}_i}, \tag{5}$$

where m_{s_i} is the multiplicity of each partial reaction. The index i runs over elastic and inelastic scattering reactions, which include thermal scattering in the appropriate energy region, and neutron duplication reaction in certain energy groups in the high energy region. Other reactions are ignored. The multigroup form of the scattered neutron spectrum from group h is defined as

[1] We consider only the reactions used in solving the approximation of the transport equation and generating the two-group homogenized constants for a steady state diffusion model.

$$p_{s,h\to g} = \sum_i m_{s_i} \tilde{\sigma}_{s_i} \tilde{p}_{s_i,h\to g} / \sigma_s, \tag{6}$$

so that the scattering cross section from group h to group g, $\sigma_{s,h\to g}$, is $\sigma_s p_{s,h\to g}$. The summation is the same as in Eq. (5).

The effective capture cross section is defined as

$$\sigma_c = \sum_i \tilde{\sigma}_i - \tilde{\sigma}_{2n}, \tag{7}$$

where the index i covers radiative capture and emissions of proton, deuterium, triton, hellion and alpha particles. The correction for neutron duplication eliminates the need of a separate two-group constant for neutron duplication. Other reactions are again ignored.

The fission reaction is described by the total average number of emitted neutrons per fission $\nu = \tilde{\nu}$, fission cross section $\sigma_f = \tilde{\sigma}_f$ and energy distribution of the emitted neutrons χ_f. The energy distribution is assumed to be independent of the incident neutron energy and is, in principle, a weighted average of distributions with different incident neutron energies. That is, in multigroup form

$$\chi_f = \sum_h w_h \tilde{\chi}_{f,h} \tag{8}$$

with suitable coefficients w_h.

We use the "sandwich rule", Eq. (3), to derive covariances for the CASMO-4 reaction model from the covariances in the ENDF-6 reaction model. This approach was first considered in Pusa (2012a). The sensitivities are mostly evident in Eqs. (4)–(8). However:

(a) We approximate the transport cross section in Eq. (4) by total cross section.
(b) The considered evaluations do not include covariances for the energy distributions of emitted neutrons except from fission reactions. Therefore the distributions in Eq. (6) are assumed to be exact.
(c) The covariances for thermal scattering cross sections are replaced by the covariances for the elastic and inelastic scattering cross sections in Eq. (5). The replacement would not be excusable in the corresponding energy distributions of emitted neutrons, i.e., Eq. (6).
(d) The coefficients w_h in Eq. (8) are approximated as one for the energy group which includes 0.625 eV and zero for others. For the considered evaluations this gives covariances for distributions whose incident neutron energy range is from at most 10^{-5} eV to at least 500 keV and therefore covers thermal and epithermal fissions but only approximates fissions caused by fast neutrons.

The assumption that $p_{s,h\to g}$ are exact and σ_s is the only quantity containing uncertainty is likely to underestimate the uncertainty due to the scattering reactions. Unfortunately some approximations need to be enforced as there is no covariance data available for the group-to-group scattering cross-sections currently. This issue is discussed in more detail in Pusa (2012a). Predicting this kind of model uncertainty, i.e., uncertainty caused by physical approximations in the model, is beyond the scope of this article and is omitted.

2.4. Importance ranking

In the first order sensitivity and uncertainty analysis the relative form of Eq. (3) gives the relative variance of a response R by

$$\mathrm{rvar}(R) = \sum_{i,j} \check{S}_i \mathrm{rcov}(\alpha_i, \alpha_j) \check{S}_j^\top = \sum_{i,j} c_{ij}, \tag{9}$$

where $\mathrm{rcov}(\alpha_i, \alpha_j)$ denotes the relative covariance matrix between ith and jth pieces of nuclear data and $\check{S}_k$ is the response and system dependent relative sensitivity coefficient vector of kth piece of nuclear data. For this purpose a piece of nuclear data is specified by a pair of material and quantity. It holds that $c_{ij} = c_{ji}$.

We consider the quantity

$$I_{ij} = \begin{cases} |c_{ij}| & \text{when } i = j, \\ |c_{ij} + c_{ji}| & \text{when } i > j, \\ 0 & \text{otherwise} \end{cases} \tag{10}$$

as the absolute importance of i,jth pair of material-and-quantity-pairs. Relative importance, sometimes called normalized importance, R_{ij} is defined as $I_{ij}/\sum_{i,j} I_{ij}$. Sometimes we list the sign of c_{ij} in front of absolute importances. Both importance and relative importance are sometimes referred to as contribution to variance or briefly as contribution. We rank the pairs by sorting them by their importance (Cacuci et al., 2005; Cacuci and Ionescu-Bujor, 2010).

This definition of importance corresponds to the absolute value of the change in the relative variance when the components c_{ij} change.

3. Calculations

We generate multigroup nuclear data covariances from the considered NDLs and perform first order uncertainty analysis using sensitivities computed for two assemblies.

3.1. The fuel assemblies

Our first assembly is the fresh TMI-1 15×15 PWR uranium dioxide (UO_2) assembly in hot zero power (HZP) conditions with inserted control rods from the UAM-LWR benchmark (Ivanov et al., 2013). The fuel pins are helium filled and Zircaloy-4 cladded. The assembly contains 4 pins with gadolinium as burnable absorber. The control rods have silver-indium-cadmium absorber cladded with Inconel 625, and are inserted in 16 Zircaloy-4 guide tubes. The moderator-coolant is free of absorbers.

Our second assembly is the GEN-III 17×17 PWR mixed oxide (MOX) assembly in hot full power (HFP) conditions with withdrawn control rods from the UAM-LWR benchmark (Ivanov et al., 2013). The fuel pins are helium filled and Zircaloy-4 cladded. The assembly contains no pins with burnable absorber. The moderator-coolant contains 1300 ppm of natural boron.

3.2. Responses and generation of their sensitivity profiles

We take the two-group homogenized constants for a steady state diffusion model as responses. The steady state diffusion model consists of the infinite multiplication factor k_{inf}, the group transfer constant $\Sigma_{s,1\to 2}$, and fast and thermal diffusion coefficients D_1 and D_2, (effective) absorption constants $\Sigma_{a,1}$ and $\Sigma_{a,2}$, neutron production constants $\nu\Sigma_{f,1}$ and $\nu\Sigma_{f,2}$, and assembly discontinuity factors f_1 and f_2. The responses are a subset of quantities that can be computed with CASMO-4.

We compute the sensitivity profiles for the responses in CASMO-4 40-group structure (Rhodes and Edenius, 2001) with CASMO-4 (Rhodes and Edenius, 2001; Pusa, 2012a,b, 2014) using its built-in nuclear data library. The built-in NDL is based on JEF2.2 and ENDF/B-IV data (Rhodes, 2005). Therefore the responses and the sensitivity profiles will be the same for all NDLs and any differences in the uncertainties arise only from differences in the uncertainties in the NDLs or their processing.

3.3. Materials and their uncertainty estimates

We model all nuclides in the absorbers, fuel and moderator-coolant. For structural materials we include oxygen, chromium,

iron, nickel, zirconium and niobium as elemental materials, and tin as isotopes. Covariances for the elemental materials are formed by using the "sandwich rule". Natural oxygen is assumed to consist of ^{16}O only.

The choice to use elemental materials is due to the built-in library having only elemental data for these elements, and hence only elemental sensitivity profiles can be generated. We also ignore the helium filling, since the built-in nuclear data library effectively assumes zero cross sections for it.

3.3.1. Intra-material covariances

The status of uncertainty quantification of nuclear data in the considered NDLs is presented in Table 1 for our application. In general, almost all of the individual evaluations cover necessary reactions, if the evaluation contains any uncertainty estimates in the first place. In a few cases the relevant energy region is only partially covered, e.g., because only the uncertainties of resonance parameters are quantified.

For the absorbers the quantified uncertainties vary by NDLs. Isotopes of boron are well covered in all the considered NDLs. However, JENDL-4.0u has no other estimates for uncertainty and JEFF-3.2 only for two isotopes of gadolinium. ENDF/B-VII.1 contains quantified uncertainties for most isotopes of gadolinium. For the control rods in the UO_2 assembly the only uncertainty estimates are for ^{109}Ag of ENDF/B-VII.1. Notably, there is no uncertainty estimates for the main absorber in the control rods, ^{113}Cd, in any NDL.

For the fuel materials the quantified uncertainties vary by NDLs. JENDL-4.0u contains all relevant uncertainty estimates for our application, and ENDF/B-VII.1 almost all relevant uncertainty estimates, lacking mostly few covariances of the total number of neutrons emitted from fission and few covariances of the energy distributions of neutrons emitted from fission. However, JEFF-3.2 lacks uncertainty estimates for many important fuel nuclides, including ^{235}U.

For the gas gap material the uncertainties are quantified for ENDF/B-VII.1, but not for the other two NDLs.

For the moderator-coolant and multipurpose materials the uncertainties are quantified for ENDF/B-VII.1, but JENDL-4.0u does not have uncertainty estimates for ^{1}H and JEFF-3.2 does not have uncertainty estimates for ^{16}O.

For the structural materials the quantified uncertainties vary by NDLs. JEFF-3.2 contains many uncertainty estimates but, compared to ENDF/B-VII.1, lacks uncertainty estimates for many isotopes of zirconium. In contrast to quite complete uncertainty estimates for the fuel nuclides, JENDL-4.0u lacks uncertainty estimates for many structural materials. General lack of covariances for tin is apparent, although JEFF-3.2 has covariances for ^{122,124}Sn.

Table 1
Status of uncertainty quantification in the considered NDLs for selected materials.

	ENDF/B-VII.1	JEFF-3.2	JENDL-4.0u
Absorber materials			
^{10}B	c, m+	c, m+	m-
^{11}B	m+	m+	m-
^{107}Ag	n	n	n
^{109}Ag	m+	n	n
$^{106,108,110-114,116}$Cd	n	n	n
^{113,115}In	n	n	n
$^{152-154}$Gd	m+	m+	n
$^{155-158,160}$Gd	m+	n	n
Fuel materials			
^{235}U	c, m+, f, ν, χ	n	c, m+, f, ν+, χ
^{238}U	c, m+, f, ν, χ	m-, f	c, m+, f, ν+, χ
^{238}Pu	m+, f, ν, χ	n	m+, f, ν+, χ
^{239}Pu	c, m+, f, ν, χ	m-, f	c, m+, f, ν+, χ
^{240}Pu	m+, f, ν	n	c, m+, f, ν+, χ
^{241}Pu	m+, f, ν	n	c, m+, f, ν+, χ
^{242}Pu	m+, f, ν+, χ	n	m+, f, ν+, χ
^{241}Am	m+, f, ν+	m-, f	m+, f, ν+, χ
Gas gap materials			
^{4}He	m−	n	n
Moderator-coolant materials			
^{1}H	m−	m−	n
Multipurpose materials			
^{16}O	m+	n	m+
Structural materials			
^{50}Cr	m+	m+	n
^{52,53}Cr	m+	m+	m+
^{54}Cr	m−	m+	n
^{54,57}Fe	m+	m+	n
^{56}Fe	m+	m+	m+
^{58}Fe	n	m+	n
^{58,60}Ni	m+	m+	m+
^{59}Ni	n	n	n
$^{61-62,64}$Ni	n	m+	n
^{90}Zr	m+	m+	m, e
$^{91,93,95-96}$Zr	m+	n	n
^{92,94}Zr	m+	m+	n
^{93}Nb	n	n	n
$^{112,114-120}$Sn	n	n	n
^{122}Sn	n	m+	n
^{124}Sn	n	m+	n
^{126}Sn	n	n	n

n No relevant covariances present.
m Covariances of cross-sections of major reaction channels present (elastic, inelastic or its levels and radiative capture).
m+ Above and more present.
m− Above and possibly more but no inelastic present.
f Covariances of fission cross section present.
ν Covariances of total, prompt or delayed ν present.
ν+ All above present.
χ Covariances of fission χ present.
c Cross material covariances present.
e No covariances of elastic reaction present.

3.3.2. Cross-material covariances

The cross-material covariances in the NDLs are listed in Table 2.

ENDF/B-VII.1 has cross-material correlations between some of the cross sections that are standards (Chadwick et al., 2006; Carlson et al., 2009). JEFF-3.2 has adopted evaluations from ENDF/B-VII.1 for ^{6}Li, ^{10}B and ^{197}Au, but not removed references to ^{235}U, ^{238}U and ^{239}Pu. Therefore the cross-material correlations remain, although ^{235}U has no covariances in JEFF-3.2.

ENDF/B-VII.1 has also cross-material correlations between average numbers of emitted neutrons per fission. These remain from the original ENDF/B-V evaluation. The covariances are from Peelle (Tomlinson et al., 1977), except the references to covariances of ν_t of ^{240,241}Pu were added from personal communication between Weston and Magurno (ENDF/B-V, 2014). In modern evaluations the referenced covariances of ν_t of ^{240,241}Pu are missing and we assumed them to be zero, thereby respecting Peelle's evaluation.

JENDL-4.0u has cross-material correlations because the six listed actinides were evaluated using empirical data from ratio measurements between the nuclides (Iwamoto et al., 2009).

The upcoming ENDF/B-VII.2 might contain cross-material correlations between isotopes of zirconium due to measurements using natural zirconium samples (Brown et al., 2014).

3.4. Multigroup nuclear data covariances

The multigroup nuclear data covariances in CASMO-4 40 group structure (Rhodes and Edenius, 2001) were generated using slightly modified NJOY 2012.22 (Kahler et al., 2012; Kahler, 2014). All NJOY computations used relative reconstruction tolerance of 5×10^{-5} and 551 K temperature. Maxwell + $1/E$ + fission spectrum weight was used with 0.1 eV thermal break, 820.3 keV

Table 2
Status of cross-material uncertainty data in the considered NDLs.[a]

ENDF/B-VII.1 and JEFF-3.2		^{6}Li σ_t	^{10}B σ_{α_1}	^{197}Au σ_γ	^{235}U σ_f	^{238}U σ_γ	^{239}Pu σ_f
^{6}Li	σ_t[b]		X		X		X
^{10}B	σ_{α_1}	X					
^{197}Au	σ_γ				X	X	X
^{235}U	σ_f	X		X			
^{238}U	σ_γ			X			
^{239}Pu	σ_f	X		X			
ENDF/B-VII.1		^{235}U ν_t	^{238}U ν_p	^{239}Pu ν_t	^{240}Pu ν_t	^{241}Pu ν_t	^{232}Th ν_t
^{235}U	ν_t		X	X	X	X	X
^{238}U	ν_p	X					
^{239}Pu	ν_t	X					
^{240}Pu	ν_t	X					
^{241}Pu	ν_t	X					
^{232}Th	ν_t	X					
JENDL-4.0u		^{233}U σ_f	^{235}U σ_f	^{238}U σ_f	^{239}Pu σ_f	^{240}Pu σ_f	^{241}Pu σ_f
^{233}U	σ_f		X	X	X	X	X
^{235}U	σ_f	X		X	X	X	X
^{238}U	σ_f	X	X		X	X	X
^{239}Pu	σ_f	X	X	X		X	X
^{240}Pu	σ_f	X	X	X	X		X
^{241}Pu	σ_f	X	X	X	X	X	

X Present.
[a] Some derivation rules imply further cross-material covariances.
[b] Tritium production.

fission break and 1.4 MeV fission temperature. The module PURR was run with 40 bins and 80 ladders and the covariances of resonance parameters are processed in ERRORR using NJOY's 1% sensitivity method, when applicable.

Many formatting issues were reported and fixed in the NDLs. Notably many cross-reaction covariances of JEFF-3.2 referenced themselves by their ZA-number instead of material number or self-reference. In these cases the cross-reaction covariances might be interpreted as cross-material covariances between the material and a non-existing material.

The multigroup nuclear data covariances were postprocessed by summing all redundant reactions from their partials, thereby ensuring consistency with respect to the sum rules (Vanhanen, in press). Negative eigenvalues were removed from all sets by finding the nearest positive semidefinite relative covariance matrix in the Frobenius norm (Vanhanen, 2015b).

We used the same temperature for all computations to avoid problems with temperatures of oxygen and materials with cross-material covariances. The temperature of 551 K is correct for the UO_2 HZP assembly, and close to correct for the MOX HFP assembly. Preliminary computations without cross-material covariances showed that a change from temperature of 551 K to 900 K resulted in at most 0.9% change in the uncertainties of the considered responses. Therefore we see conclusions based on differences larger than about 1% reasonable for the MOX assembly.

4. Results

4.1. Responses and their uncertainties

The correlation matrices between the responses are illustrated in Figs. 1–6. A positive correlation between two responses, R_1 and R_2, indicates that if a random realization of the NDL is such that the value of R_1 increases, this will also increase the value of R_2 on the average. A strong correlation between the two responses indicates that if the uncertainties of the NDL are reduced, by some means, so that the uncertainty of R_1 decreases, this is likely to decrease the uncertainty of R_2. However, the linear correlation

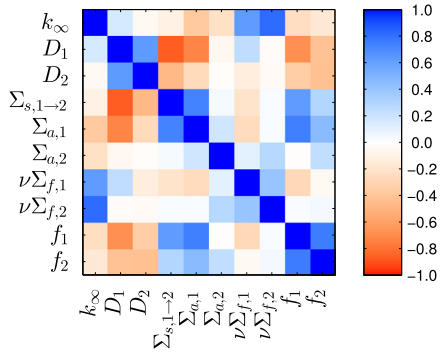

Fig. 1. Correlation matrix of the UO_2 HZP responses for ENDF/B-VII.1.

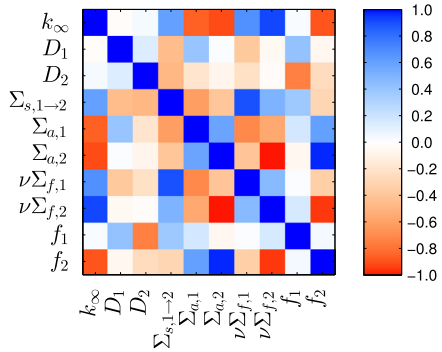

Fig. 2. Correlation matrix of the UO_2 HZP responses for JEFF-3.2.

accounts for effects only up to first order. It is worth noticing that the contributors to the correlations can be identified and ranked in

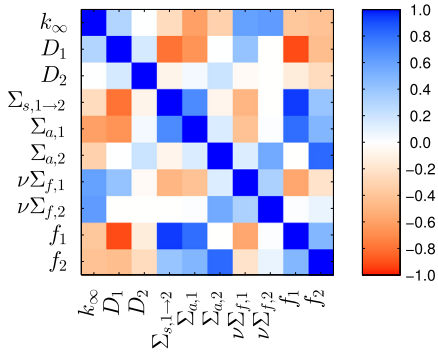

Fig. 3. Correlation matrix of the UO_2 HZP responses for JENDL-4.0u.

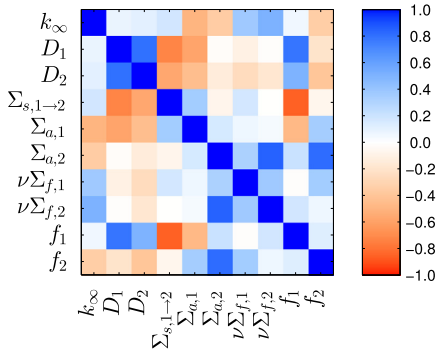

Fig. 4. Correlation matrix of the MOX HFP responses for ENDF/B-VII.1.

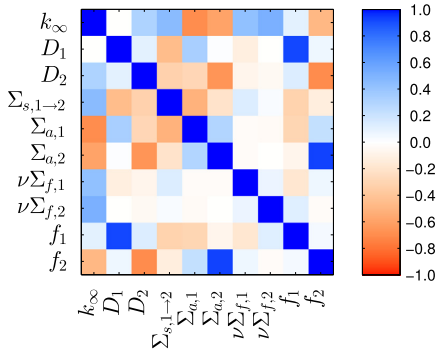

Fig. 5. Correlation matrix of the MOX HFP responses for JEFF-3.2.

the same manner as for the total uncertainties of the responses, although this is beyond the scope of the article.

It is interesting to see that for both assemblies, all responses and the three NDLs the fast and thermal responses are positively correlated. The spread is, however, large. For example, in the UO_2 assembly between diffusion coefficients the correlation coefficient varies between 0.11 (JEFF-3.2 and JENDL-4.0u) and 0.80 (ENDF/B-VII.1). Also infinite multiplication factor is positively correlated with fast and thermal neutron production constants, and negatively with fast and thermal absorption constants and thermal discontinuity factor for all assemblies and NDLs.

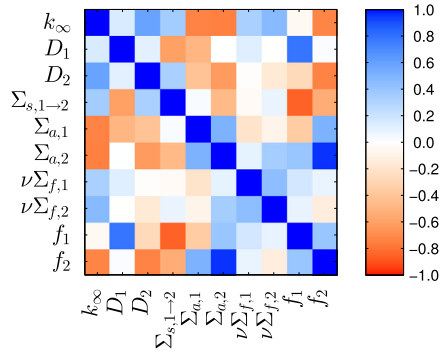

Fig. 6. Correlation matrix of the MOX HFP responses for JENDL-4.0u.

The responses and their uncertainties for the considered NDLs are listed in Table 3 for the UO_2 assembly and in Table 4 for the MOX assembly. In principle, the inverses of the uncertainties correspond to the prediction capabilities (Cacuci, 2003). All NDLs predict uncertainties in the same order-of-magnitude. However, uncertainty quantification is not complete for any considered NDL and essentially zero uncertainty has been assumed for the unquantified uncertainties. In a few cases the unquantified uncertainties are important. For example for ENDF/B-VII.1 the uncertainty of the UO_2 fast discontinuity factor has a contribution of 45% from ^{109}Ag. The lack of uncertainty estimate for ^{109}Ag in JEFF-3.2 and JENDL-4.0u is seen on the considerably smaller uncertainty for the response. The uncertainty is missing one of its main components, if the evaluators of JEFF-3.2 and JENDL-4.0u have roughly the same knowledge on the true values of nuclear data of ^{109}Ag as the evaluators of ENDF/B-VII.1. Therefore the prediction capabilities of the NDLs can not be directly inferred from the tables.

However, the contributions of pieces of nuclear data which have quantified uncertainties can be compared directly between the NDLs.

4.2. Most important materials

We identify the most important pairs of material-and-quantity-pairs by ranking them by their relative importance to variances of the responses for both assemblies. We consider, rather arbitrarily, pairs which have relative importances 5% or more for any response in either assembly as important, and consider any material in these pairs as important.

The shortlist of important materials is compiled in Table 5. Notably ^{235}U is not among the main contributors for any NDL for the MOX assembly: it is known so accurately that it contributes less than 5% to the variances in its MOX concentration.

The ZZ-SCALE6/COVA-44G library suggest that three additional materials might be important: ^{115}In has 5.5% and 12.1% relative importances to the uncertainty of fast and thermal discontinuity factor, respectively, ^{113}Cd has relative importance of 4.9% to the uncertainty of thermal discontinuity factor, and ^{107}Ag has relative importance of 3.1% to fast absorption constant.

4.3. Differences between the NDLs

We compare the most important materials listed in Table 5 by their (signed) absolute importances. The differences arise due to NDLs and their processing only, since the absolute importances are computed using assembly but not NDL specific sensitivities.

Table 3
Relative uncertainties of the rodded UO_2 HZP assembly.

Response	Value	ENDF/B-VII.1	JEFF-3.2	JENDL-4.0u
		Uncertainty (%)		
k_{inf}	1.0730	0.728	1.788	0.460
D_1	1.3620 cm	1.162	2.961	1.158
D_2	0.3618 cm	0.351	0.298	0.149
$\Sigma_{s,1\to2}$	0.0145 cm^{-1}	1.152	1.041	0.833
$\Sigma_{a,1}$	0.0129 cm^{-1}	0.716	1.402	0.615
$\Sigma_{a,2}$	0.1352 cm^{-1}	0.208	1.265	0.184
$\nu\Sigma_{f,1}$	0.0087 cm^{-1}	0.783	0.357	0.504
$\nu\Sigma_{f,2}$	0.1939 cm^{-1}	0.782	0.348	0.445
f_1	1.0180	0.0368	0.0130	0.0225
f_2	1.3700	0.0540	0.111	0.0230

Table 4
Relative uncertainties of the unrodded MOX HFP assembly.

Response	Value	ENDF/B-VII.1	JEFF-3.2	JENDL-4.0u
		Uncertainty (%)		
k_{inf}	1.1080	0.570	1.398	0.814
D_1	1.4580 cm	0.918	2.998	1.102
D_2	0.3188 cm	0.308	0.332	0.171
$\Sigma_{s,1\to2}$	0.0116 cm^{-1}	0.975	1.127	0.842
$\Sigma_{a,1}$	0.0155 cm^{-1}	0.590	1.080	0.665
$\Sigma_{a,2}$	0.2900 cm^{-1}	0.244	0.930	0.394
$\nu\Sigma_{f,1}$	0.0119 cm^{-1}	0.536	1.201	0.526
$\nu\Sigma_{f,2}$	0.4547 cm^{-1}	0.666	1.103	0.688
f_1	0.9881	0.0176	0.0497	0.0199
f_2	1.3830	0.0598	0.146	0.0997

Table 5
Maximum relative importances for the shortlisted materials.

Material	ENDF/B-VII.1	JEFF-3.2	JENDL-4.0u
	Relative importance (%) / response		
UO_2			
^{1}H	40.4 / D_2	65.6 / f_1	
^{nat}O	54.4 / D_2		73.3 / D_2
^{nat}Zr		98.5 / $\Sigma_{a,2}$	
^{109}Ag	44.9 / f_2		
^{157}Gd	7.2 / f_2		
^{235}U	83.0 / $\nu\Sigma_{f,2}$		84.9 / $\Sigma_{s,1\to2}$
^{238}U	16.9 / $\Sigma_{a,1}$	30.5 / D_2	40.9 / D_1
MOX			
^{1}H	62.4 / $\Sigma_{s,1\to2}$	46.6 / $\Sigma_{s,1\to2}$	
^{nat}O	43.5 / D_1		28.6 / D_2
^{nat}Zr		95.9 / D_1	
^{238}U	17.2 / $\nu\Sigma_{f,1}$	9.8 / D_2	49.1 / D_1
^{239}Pu	63.4 / $\nu\Sigma_{f,2}$	88.8 / $\nu\Sigma_{f,1}$	59.7 / $\nu\Sigma_{f,2}$
^{240}Pu	10.8 / f_2		52.3 / k_{inf}
^{241}Pu	17.2 / $\nu\Sigma_{f,1}$		32.0 / $\nu\Sigma_{f,1}$
^{242}Pu	25.9 / $\Sigma_{a,1}$		
^{241}Am	6.1 / D_2		6.3 / D_2

[a]Maximum relative importances of less than 5% are omitted.

Strictly speaking, the conclusions are restricted to the considered test cases only, but we believe that our test cases represent a reasonable share of PWRs.

The contributions of ^{1}H are identical for ENDF/B-VII.1 and JEFF-3.2, since the latter has adopted the evaluation from the former.

The only difference between the NDLs for ^{109}Ag and ^{157}Gd is that they have uncertainty estimates only in ENDF/B-VII.1, which estimates their contribution to be up to 45% and 7.2% for a response, respectively. The absolute importances of ^{157}Gd are typically an order-of-magnitude larger for ENDF/B-VII.1 than for ZZ-SCALE6/COVA-44G, which is based on the low-fidelity covariances (Little et al., 2008). This is an example of cases where the low-fidelity estimates do not identify important nuclides.

Table 6
Selected absolute importances of ^{16}O.[a]

Response	*i*th pair *j*th pair	ENDF/B-VII.1 I_{ij} ($\%^2$)	JENDL-4.0u I_{ij} ($\%^2$)
UO_2			
D_1	^{16}O, σ_s	3.48×10^{-1}	2.60×10^{-1}
D_2	^{16}O, σ_s	6.76×10^{-2}	1.69×10^{-2}
f_1	^{16}O, σ_s	6.72×10^{-5}	3.35×10^{-5}
f_2	^{16}O, σ_s	3.32×10^{-4}	8.09×10^{-5}
MOX			
D_1	^{16}O, σ_s	3.67×10^{-1}	3.06×10^{-1}
D_2	^{16}O, σ_s	4.42×10^{-2}	1.10×10^{-2}
f_1	^{16}O, σ_s	2.30×10^{-5}	2.69×10^{-5}

[a] Data with relative importances of less than 5% are omitted.

4.3.1. Natural oxygen (^{16}O)

The ENDF/B-VII.1 covariances for ^{16}O are based on the low-fidelity covariance library (Little et al., 2008) with data from varying sources. The JENDL-4.0u covariances are based on both experimental data and nuclear model calculations (Shibata et al., 1997), however, partials of the effective capture cross section are fitted to experimental data without using information from nuclear models.

The selected absolute importances for ^{16}O are listed in Table 6.

The important contributions from the scattering cross section are within an order-of-magnitude between the NDLs, although usually with JENDL-4.0u the contributions are smaller than with ENDF/B-VII.1.

The contributions from the effective capture cross-section have an order-of-magnitude difference between the NDLs for the fast absorption constant. With JENDL-4.0u data, the relative importance is 3.8%. The absolute importances are $5.49\times10^{-4}\%^2$ and $1.47\times10^{-2}\%^2$ for ENDF/B-VII.1 and JENDL-4.0u, respectively: the importances differ by a factor of 26.7. Large differences in contributions from the effective capture cross section are also observed for some, but not all, responses in the fast energy region. The differences seem to arise mostly from uncertainty of cross section of α emission, since the uncertainties in other partials are quite similar between the NDLs and the cross section for α emission dominates above its reaction threshold. There is an order-of-magnitude difference between the threshold and 10 MeV in the uncertainties: the low-fidelity estimate of ENDF/B-VII.1 is 2% while the JENDL-4.0u estimate is 18% due to discrepancies in the experimental data. The uncertainty estimates are less different above 10 MeV.

4.3.2. Natural zirconium

The covariances in ENDF/B-VII.1 are from COMMARA-2.0 (Herman et al., 2011) library for all constituents, and they are based on selected experimental data and nuclear model calculations. The JEFF-3.2 zirconium evaluations with covariances are adopted from TENDL-2012 (Koning and Rochman, 2012). We corrected the cross-reaction references before generating the multigroup covariances. The covariances in JENDL-4.0u are based on experimental data (Shibata et al., 1996).

The selected absolute importances for ^{nat}Zr are listed in Table 7. The large differences result partly from the use of elemental evaluation, whose constituents differ for the NDLs.

- For ENDF/B-VII.1 all constituents of natural zirconium have uncertainty estimates.

Table 7
Selected absolute importances of ^{nat}Zr.[a]

Response	*i*th pair *j*th pair	ENDF/B-VII.1 I_{ij} (%^{2})	JEFF-3.2 I_{ij} (%^{2})	JENDL-4.0u I_{ij} (%^{2})
UO_2				
k_{inf}	^{nat}Zr, σ_c	1.56×10^{-5}	$2.99 \times 10^{+0}$	2.95×10^{-3}
D_1	^{nat}Zr, σ_s	2.22×10^{-3}	$8.45 \times 10^{+0}$	1.16×10^{-2}
$\Sigma_{a,2}$	^{nat}Zr, σ_c	8.72×10^{-6}	$1.57 \times 10^{+0}$	4.20×10^{-5}
$\nu\Sigma_{f,2}$	^{nat}Zr, σ_c	6.47×10^{-7}	1.17×10^{-1}	3.12×10^{-6}
f_2	^{nat}Zr, σ_c	6.38×10^{-8}	1.16×10^{-2}	3.16×10^{-7}
MOX				
D_1	^{nat}Zr, σ_s	2.49×10^{-3}	$8.62 \times 10^{+0}$	1.36×10^{-2}
f_1	^{nat}Zr, σ_s	6.14×10^{-7}	2.22×10^{-3}	3.59×10^{-6}

[a] Data with relative importances of less than 80% for JEFF-3.2 are omitted.

- For JEFF-3.2 the isotopes ^{90,92,94}Zr have uncertainty estimates. These cover, roughly, 86% of natural abundance, 27% of thermal capture cross section and 78% of thermal elastic scattering cross section.
- For JENDL-4.0u only ^{90}Zr has uncertainty estimates. These cover half of natural abundance, only 2.8% of thermal capture cross section and no elastic scattering since there are no estimates for its uncertainty. The covariances of the scattering reaction include estimates for the inelastic reaction only.

The differences are not explained by the presence of constituents in the elemental evaluations, since the NDL with the most constituents with uncertainty estimates has the smallest contributions to the uncertainties.

The apparent several-orders-of-magnitude differences in contributions from both scattering and effective capture of JEFF-3.2 to the other two NDLs are not expected, and seem unrealistically large. The large differences are also observed for responses not included in the table. The difference between JEFF-3.2 and ENDF/B-VII.1 would be even larger if JEFF-3.2 had uncertainty estimates for all the isotopes of natural zirconium.

The origin of large uncertainties in JEFF-3.2 seems to be ^{90}Zr, which has uncertainties of dozens of per cent for the main reaction channels. The isotopes ^{92}Zr and ^{94}Zr have uncertainties of less than a dozen per cent, being in the same order-of-magnitude as the uncertainties in ENDF/B-VII.1.

The uncertainties from one isotope in JENDL-4.0u are larger than the combined uncertainties of all zirconium isotopes in ENDF/B-VII.1, and differ by a factor of 5–200. Including information from other experimental data and nuclear models might bring the uncertainties closer to current ENDF/B-VII.1 values, and including omitted experimental data might bring ENDF/B-VII.1 uncertainties closer to current JENDL-4.0u values.

Kodeli and Snoj (2012) found that SCALE 6.0 and JENDL-4.0 predict uncertainties within an order-of-magnitude for the effective multiplication factor of KRITZ-2 critical experiment due to ^{90}Zr. The uncertainty estimates in SCALE 6.0 are based on the low-fidelity covariances (Little et al., 2008).

4.3.3. Uranium-235

The cross section covariances in ENDF/B-VII.1 are based on experimental data and nuclear model calculations, the covariances of ν are based on experimental data, and the covariances of χ are based on experimental data and nuclear model calculations. Notably the covariances of ν_t carry over from ENDF/B-V. The cross section covariances in JENDL-4.0u are based on experimental data, nuclear model calculations and assumed uncertainties, depending on the piece of nuclear data and energy region. In some cases the evaluators have increased the uncertainties after formal uncertainty quantification. The covariances of ν are based on experimental data, but the uncertainty has been doubled after the analysis. The covariances of χ are based on experimental data and nuclear model calculations. The JENDL-4.0u covariances are revised from JENDL-4.0 due to unrealistically large uncertainties

Table 8
Selected absolute importances of ^{235}U.[a]

Response	*i*th pair *j*th pair	ENDF/B-VII.1 I_{ij} (%^{2})	JENDL-4.0u I_{ij} (%^{2})
UO_2			
k_{inf}	^{235}U, ν	3.40×10^{-1}	6.46×10^{-2}
k_{inf}	^{235}U, χ	3.75×10^{-2}	2.74×10^{-2}
k_{inf}	^{235}U, σ_c	2.62×10^{-2}	1.91×10^{-2}
k_{inf}	^{235}U, σ_c	1.22×10^{-2}	1.18×10^{-2}
	^{235}U, σ_f		
k_{inf}	^{235}U, σ_f	1.15×10^{-2}	1.29×10^{-2}
D_1	^{235}U, χ	6.92×10^{-1}	5.14×10^{-1}
$\Sigma_{s,1\to2}$	^{235}U, χ	7.46×10^{-1}	5.91×10^{-1}
$\Sigma_{a,1}$	^{235}U, χ	2.80×10^{-1}	2.26×10^{-1}
$\Sigma_{a,2}$	^{235}U, σ_f	2.68×10^{-2}	2.68×10^{-2}
$\Sigma_{a,2}$	^{235}U, σ_c	-1.67×10^{-2}	-1.67×10^{-2}
	^{235}U, σ_f		
$\Sigma_{a,2}$	^{235}U, σ_c	1.61×10^{-2}	1.61×10^{-2}
$\nu\Sigma_{f,1}$	^{235}U, ν	2.44×10^{-1}	2.17×10^{-2}
$\nu\Sigma_{f,1}$	^{235}U, χ	1.46×10^{-1}	8.17×10^{-2}
$\nu\Sigma_{f,1}$	^{235}U, ν	4.20×10^{-2}	
	^{238}U, ν		
$\nu\Sigma_{f,1}$	^{235}U, σ_f	3.36×10^{-2}	8.52×10^{-2}
$\nu\Sigma_{f,2}$	^{235}U, ν	5.07×10^{-1}	9.66×10^{-2}
$\nu\Sigma_{f,2}$	^{235}U, σ_f	8.50×10^{-2}	8.50×10^{-2}
$\nu\Sigma_{f,2}$	^{235}U, σ_c	1.25×10^{-2}	1.25×10^{-2}
	^{235}U, σ_f		
f_1	^{235}U, χ	4.97×10^{-4}	3.87×10^{-4}
f_2	^{235}U, σ_f	2.87×10^{-4}	2.87×10^{-4}
f_2	^{235}U, σ_c	-1.79×10^{-4}	-1.79×10^{-4}
	^{235}U, σ_f		
f_2	^{235}U, σ_c	1.74×10^{-4}	1.74×10^{-4}
f_2	^{235}U, χ	1.11×10^{-4}	9.06×10^{-5}

[a] Data with relative importances of less than 5% are omitted.

Table 9
Selected absolute importances of ^{238}U.[a]

Response	*i*th pair *j*th pair	ENDF/B-VII.1 I_{ij} (%^{2})	JEFF-3.2 I_{ij} (%^{2})	JENDL-4.0u I_{ij} (%^{2})
UO_2				
k_{inf}	^{238}U, σ_c	6.28×10^{-2}	2.01×10^{-1}	6.40×10^{-2}
D_1	^{238}U, σ_s	3.33×10^{-2}	3.87×10^{-3}	5.51×10^{-1}
D_2	^{238}U, σ_s	5.14×10^{-3}	2.70×10^{-2}	5.14×10^{-3}
$\Sigma_{s,1\to2}$	^{238}U, σ_c	2.86×10^{-2}	1.13×10^{-1}	2.84×10^{-2}
$\Sigma_{s,1\to2}$	^{238}U, σ_s	2.52×10^{-3}	2.77×10^{-5}	6.26×10^{-2}
$\Sigma_{a,1}$	^{238}U, σ_c	8.70×10^{-2}	2.31×10^{-1}	9.48×10^{-2}
$\Sigma_{a,1}$	^{238}U, σ_s	1.18×10^{-3}	3.03×10^{-6}	2.65×10^{-2}
$\Sigma_{a,2}$	^{238}U, σ_c	7.44×10^{-3}	1.61×10^{-2}	7.47×10^{-3}
$\nu\Sigma_{f,1}$	^{235}U, ν	4.20×10^{-2}		
	^{238}U, ν			
$\nu\Sigma_{f,1}$	^{238}U, ν	9.07×10^{-2}		2.31×10^{-2}
$\nu\Sigma_{f,1}$	^{238}U, σ_f	1.74×10^{-2}	1.36×10^{-7}	2.17×10^{-2}
$\nu\Sigma_{f,1}$	^{238}U, σ_c	7.04×10^{-3}	2.10×10^{-2}	7.05×10^{-3}
f_1	^{238}U, σ_s	4.65×10^{-6}	4.51×10^{-6}	7.92×10^{-5}
f_2	^{238}U, σ_c	7.51×10^{-5}	1.28×10^{-4}	7.56×10^{-5}
MOX				
k_{inf}	^{238}U, σ_c	4.15×10^{-2}	1.21×10^{-1}	4.32×10^{-2}
D_1	^{238}U, σ_s	3.50×10^{-2}	3.75×10^{-3}	6.01×10^{-1}
D_2	^{238}U, σ_s	2.10×10^{-3}	1.11×10^{-2}	2.09×10^{-3}
$\Sigma_{s,1\to2}$	^{238}U, σ_c	3.13×10^{-2}	1.22×10^{-1}	3.11×10^{-2}
$\Sigma_{s,1\to2}$	^{238}U, σ_s	2.82×10^{-3}	1.32×10^{-5}	7.07×10^{-2}
$\Sigma_{a,1}$	^{238}U, σ_c	4.80×10^{-2}	1.17×10^{-1}	5.40×10^{-2}
$\Sigma_{a,1}$	^{238}U, σ_s	1.40×10^{-3}	1.73×10^{-6}	3.31×10^{-2}
$\nu\Sigma_{f,1}$	^{238}U, ν	5.05×10^{-2}		1.27×10^{-2}
f_1	^{238}U, σ_s	3.78×10^{-6}	3.23×10^{-7}	7.09×10^{-5}

[a] Data with relative importances of less than 5% are omitted.

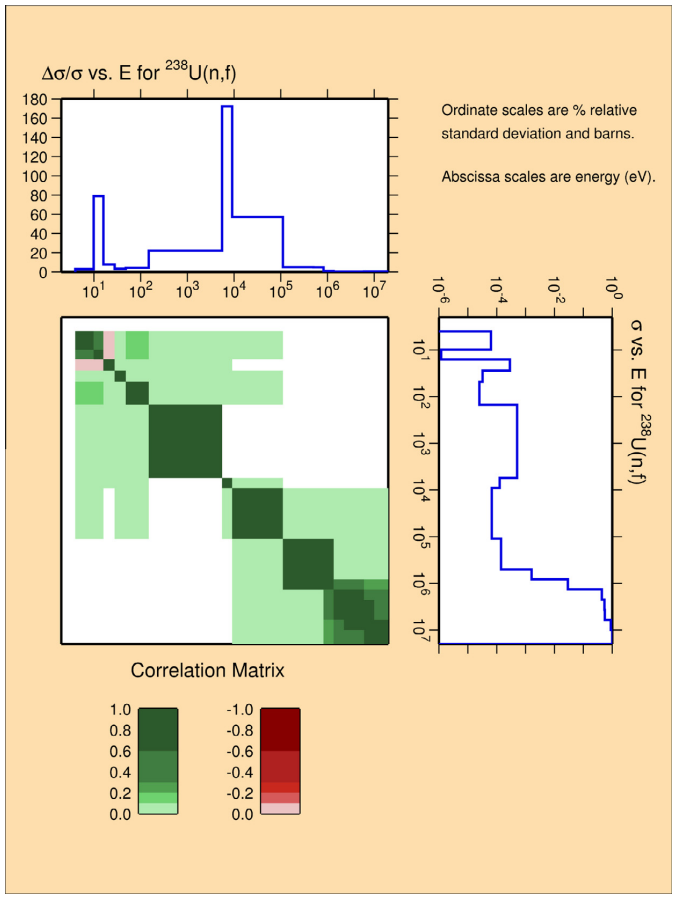

Fig. 7. Relative covariance matrix of ^{238}U(n,f) cross section for ENDF/B-VII.1.

(Hernández-Solís et al., 2013a,b). The uncertainties propagated from the resonance parameters uncertainties seem to coincide below 500 eV for the evaluations.

The selected absolute importances for ^{235}U are listed in Table 8.

The important contributions from the number of emitted neutrons per fission are quite different between the NDLs: the contributions to the uncertainty of the fast neutron production constant have an order-of-magnitude difference, and the contributions to the uncertainties of the thermal neutron production constant and the infinite multiplication factor differ by a factor of 5. In both cases JENDL-4.0u claims a better knowledge of the number of emitted neutrons per fission over the whole energy region. The ENDF/B-VII.1 covariances seem to be inconsistent: the relative standard deviations of ν_t and ν_p are on the orders of 0.7% and 0.2%, respectively. Assuming that these are correct, the uncertainty of ν_d needs to be on the order of 77–138% depending on the correlation coefficient between delayed and prompt neutrons.

The important contributions from the fission spectrum are within an order-of-magnitude for all responses.

All thermal responses have the same contributions within almost three digits from the cross sections. For the thermal discontinuity factor and the thermal absorption constant the cross-reaction covariance between the capture and fission cross sections diminishes the uncertainty of the responses. Physically the diminishing occurs because the responses depend more on the sum of the cross sections than on the absolute values of the cross sections and the sum of the cross sections is better known than its partials. The latter fact is visible in mostly negative correlation between the cross sections. The other side of the effect is seen for the infinite multiplication factor and thermal neutron production constants.

The contribution from the effective capture cross section to the fast absorption constant has an order-of-magnitude difference between the NDLs. With ENDF/B-VII.1 data, the relative importance is 4.6%. The absolute importances of ENDF/B-VII.1 and JENDL-4.0u are $2.39 \times 10^{-2}\%^2$ and $2.76 \times 10^{-3}\%^2$, respectively. The difference seems to origin from large differences of the uncertainties of radiative capture cross section: in ENDF/B-VII.1 the uncertainty is 30–40% between 7 keV and 500 keV, while in JENDL-4.0u the uncertainty is only 2–4% in the same energy range.

The contribution from the fission cross section to the fast neutron production constant is within an order-of-magnitude for the NDLs.

4.3.4. Uranium-238

The cross section covariances in ENDF/B-VII.1 are based on experimental data and nuclear model calculations, and the

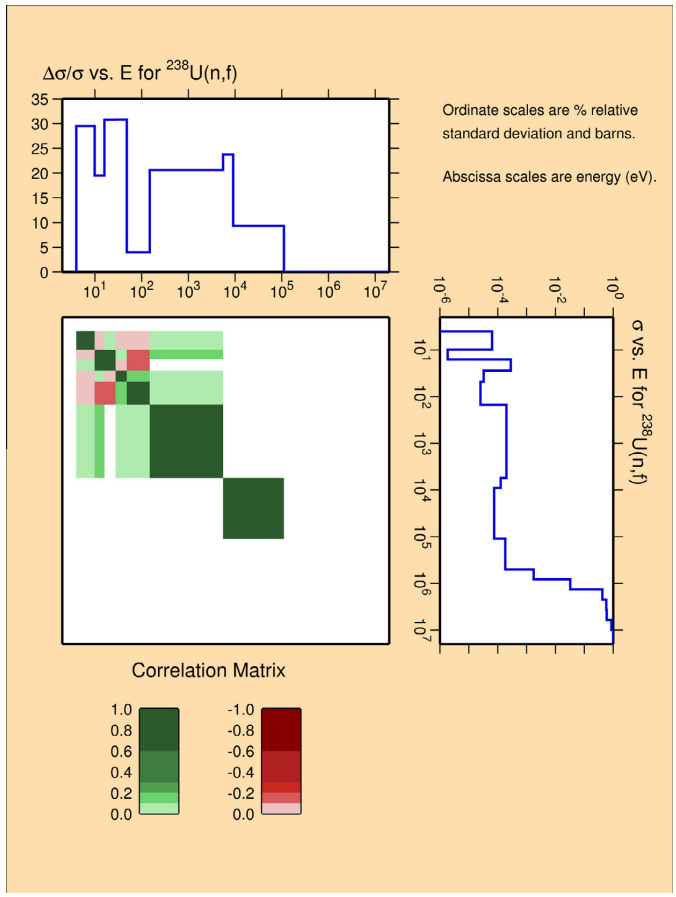

Fig. 8. Relative covariance matrix of ^{238}U(n,f) cross section for JEFF-3.2.

covariances of ν are based on experimental data. The cross section covariances in JEFF-3.2 are based on experimental data and cover only the energy region below 100 keV. The cross section covariances in JENDL-4.0u are based on experimental data, nuclear model calculations and assumed uncertainties, depending on the piece of nuclear data and energy region. In some cases the evaluators have increased the uncertainties after formal uncertainty quantification. The covariances of ν are based on experimental data. JENDL-4.0u covariances are from the revised NDL. The uncertainties propagated from the resonance parameters uncertainties seem to coincide below 20 keV for ENDF/B-VII.1 and JENDL-4.0u.

The selected absolute importances for ^{238}U are listed in Table 9.

The important contributions from the number of emitted neutrons per fission are within an order-of-magnitude for ENDF/B-VII.1 and JENDL-4.0u for all responses in both UO_2 and MOX assemblies. The importances of ENDF/B-VII.1 are larger than the importances of JENDL-4.0u by a factor of 5.

The important contributions from the effective capture cross section are within an order-of-magnitude for all NDLs for all responses in both UO_2 and MOX assemblies. However, the importances of JEFF-3.2 differ by a factor of 2–4 to the other NDLs and for the fast responses the differences would be even larger if JEFF-3.2 had quantified uncertainties above 100 keV.

The important contribution from the fission cross section is within an order-of-magnitude for ENDF/B-VII.1 and JENDL-4.0u, but different by several orders-of-magnitude for JEFF-3.2. The uncertainty is smaller in JEFF-3.2, but the effect would be diminished if the uncertainties were fully quantified. The covariances in the used group structure are illustrated in Figs. 7–9. The partial quantification is apparent in JEFF-3.2 and the larger uncertainties in the other NDLs. The differences between the NDLs in the best-estimates seem to be smaller than in the uncertainties.

The important contributions from the scattering cross section to thermal responses are within an order-of-magnitude for ENDF/B-VII.1 and JENDL-4.0u. The importances of JEFF-3.2 differ by a factor of 5 to the other NDLs. However, for the fast responses the order-of-magnitude differences between the NDLs are not exceptions. The importances of JENDL-4.0u are larger than the importances of ENDF/B-VII.1 by a factor of 17–25. The difference is at least partly explained by the larger uncertainty of JENDL-4.0u in neutron duplication and the negative correlation between the elastic and inelastic cross sections in ENDF/B-VII.1, which is missing in JENDL-4.0u. In this case the differences between JEFF-3.2 and the other NDLs would be diminished if JEFF-3.2 had uncertainty estimates for the whole energy region. There are no qualitative differences between the UO_2 and MOX assemblies.

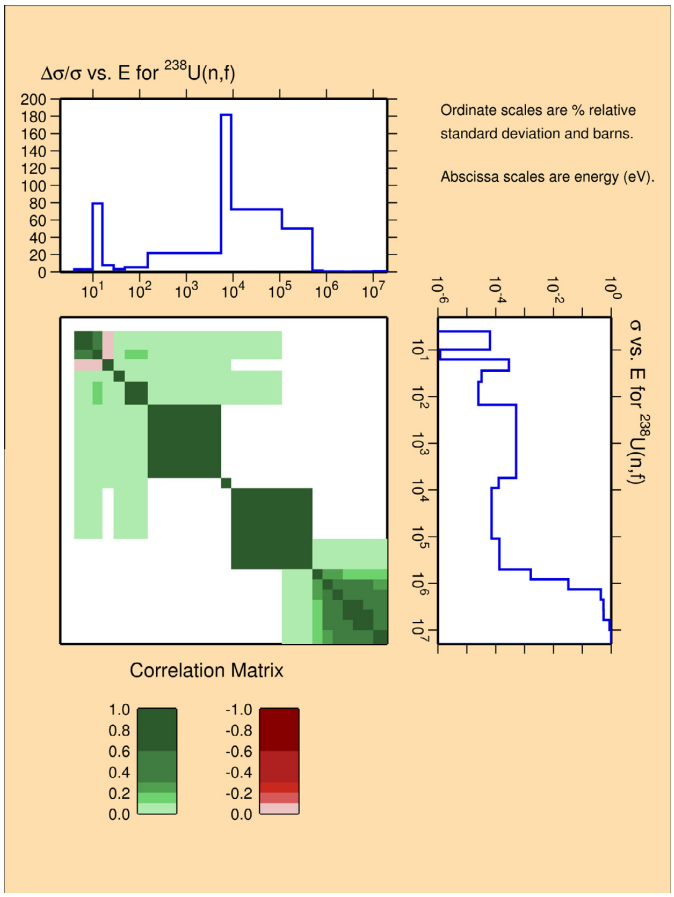

Fig. 9. Relative covariance matrix of ^{238}U(n,f) cross section for JENDL-4.0u.

The difference between JEFF-3.2 and the other NDLs is partly explained by the energy regions with unquantified uncertainties.

4.3.5. Plutonium-239

The cross section covariances in ENDF/B-VII.1 are based on experimental data and nuclear model calculations, and the covariances of ν are based on experimental data. The origin of covariances of χ is not documented. The cross section covariances in JEFF-3.2 are based on experimental data and cover only the energy region below 2.5 keV. The cross section covariances in JENDL-4.0u are based on experimental data, nuclear model calculations and assumed uncertainties, depending on the piece of nuclear data and energy region. In some cases the evaluators have increased the uncertainties after formal uncertainty quantification. The covariances of ν are based on experimental data, and the covariances of χ are based on experimental data and nuclear model calculations. The JENDL-4.0u covariances are from the revised NDL. The uncertainties propagated from the resonance parameters uncertainties seem to coincide below 2.5 keV for ENDF/B-VII.1 and JENDL-4.0u.

The selected absolute importances for ^{239}Pu are listed in Table 10.

The important contributions from the number of emitted neutrons per fission are within an order-of-magnitude for ENDF/B-VII.1 and JENDL-4.0u for all responses in both UO_2 and MOX assemblies. The importances of ENDF/B-VII.1 are larger than the importances of JENDL-4.0u by a factor of 5.

The important contributions from the fission spectrum are within an order-of-magnitude for all responses.

The important contributions from cross sections of ENDF/B-VII.1 and JENDL-4.0u are within an order-of-magnitude for all responses, and in many cases the same within almost 3 digits.

In the thermal region the contributions from the total scattering cross section are larger by a factor of 10–12 for JEFF-3.2 than for the other NDLs. The uncertainty of the elastic scattering cross section is between 3% and 5% for JEFF-3.2 in the thermal region, while it is less than 1% for the other NDLs. In the thermal region the contributions from the fission cross section are within an order-of-magnitude.

The cross-reaction contributions are mostly within an order-of-magnitude between JEFF-3.2 and the other NDLs, except the contribution to the thermal absorption constant. In the fast region the differences are larger and would be even larger if the uncertainties in JEFF-3.2 were quantified in the whole energy region.

The different signs between JEFF-3.2 and the other NDLs for the contribution to the uncertainty of the thermal discontinuity factor is interesting: the correlation between the effective capture and fission cross sections is mostly positive for JEFF-3.2 while it is negative in the other NDLs.

Table 10
Selected absolute importances of ^{239}Pu.[a]

Response	*i*th pair *j*th pair	ENDF/B-VII.1 I_{ij} (%^{2})	JEFF-3.2 I_{ij} (%^{2})	JENDL-4.0u I_{ij} (%^{2})
MOX				
k_{inf}	^{239}Pu, σ_f	5.38×10^{-2}	2.19×10^{-1}	5.42×10^{-2}
k_{inf}	^{239}Pu, σ_c	4.53×10^{-2}	5.81×10^{-1}	4.51×10^{-2}
k_{inf}	^{239}Pu, σ_c ^{239}Pu, σ_f	3.64×10^{-2}	2.91×10^{-2}	3.66×10^{-2}
D_1	^{239}Pu, χ	1.26×10^{-1}		2.89×10^{-1}
D_2	^{239}Pu, σ_c ^{239}Pu, σ_f	-4.49×10^{-3}	-1.60×10^{-3}	-4.51×10^{-3}
D_2	^{239}Pu, σ_f	4.19×10^{-3}	1.50×10^{-2}	4.21×10^{-3}
D_2	^{239}Pu, σ_c	3.29×10^{-3}	3.53×10^{-2}	3.30×10^{-3}
$\Sigma_{s,1\to2}$	^{239}Pu, χ	1.38×10^{-1}		3.35×10^{-1}
$\Sigma_{s,1\to2}$	^{239}Pu, σ_c	1.43×10^{-3}	7.02×10^{-2}	1.25×10^{-3}
$\Sigma_{a,1}$	^{239}Pu, χ	5.88×10^{-2}		1.43×10^{-1}
$\Sigma_{a,1}$	^{239}Pu, σ_c	2.26×10^{-3}	8.04×10^{-2}	1.76×10^{-3}
$\Sigma_{a,2}$	^{239}Pu, σ_f	5.43×10^{-2}	1.62×10^{-1}	5.45×10^{-2}
$\Sigma_{a,2}$	^{239}Pu, σ_c ^{239}Pu, σ_f	-4.39×10^{-2}	-4.46×10^{-3}	-4.40×10^{-2}
$\Sigma_{a,2}$	^{239}Pu, σ_c	3.31×10^{-2}	4.26×10^{-1}	3.32×10^{-2}
$\nu\Sigma_{f,1}$	^{239}Pu, σ_f	1.06×10^{-1}	$1.28 \times 10^{+0}$	1.08×10^{-1}
$\nu\Sigma_{f,1}$	^{239}Pu, χ	1.06×10^{-2}		1.45×10^{-2}
$\nu\Sigma_{f,2}$	^{239}Pu, σ_f	2.82×10^{-1}	9.21×10^{-1}	2.83×10^{-1}
$\nu\Sigma_{f,2}$	^{239}Pu, σ_c ^{239}Pu, σ_f	8.67×10^{-2}	2.02×10^{-2}	8.68×10^{-2}
$\nu\Sigma_{f,2}$	^{239}Pu, ν	2.47×10^{-2}		4.38×10^{-3}
$\nu\Sigma_{f,2}$	^{239}Pu, σ_c	2.34×10^{-2}	2.67×10^{-1}	2.34×10^{-2}
f_1	^{239}Pu, χ	8.08×10^{-5}		1.98×10^{-4}
f_2	^{239}Pu, σ_f	1.81×10^{-3}	4.79×10^{-3}	1.82×10^{-3}
f_2	^{239}Pu, σ_c ^{239}Pu, σ_f	-1.10×10^{-3}	1.84×10^{-4}	-1.10×10^{-3}
f_2	^{239}Pu, σ_c	9.05×10^{-4}	1.17×10^{-2}	9.06×10^{-4}

[a] Data with relative importances of less than 5% are omitted.

4.3.6. Plutonium-240

The cross section covariances in ENDF/B-VII.1 and JENDL-4.0u are based on experimental data and nuclear model calculations, although the JENDL-4.0u evaluators have increased uncertainties by a few per cent after formal uncertainty quantification.

The selected absolute importances for ^{240}Pu are listed in Table 11.

All the important contributions are from the effective capture cross section. The absolute importances differ by factors of 7–18. There is no large difference between thermal and fast regions. The order-of-magnitude difference is evident in the uncertainties of radiative capture cross section, although the cross sections are quite close to each other.

4.3.7. Plutonium-241

The cross section covariances in ENDF/B-VII.1 are based on the low-fidelity covariances (Little et al., 2008), except the covariances of the fission cross section above 1 keV are based on experimental data. The cross section covariances of JENDL-4.0u are based on experimental data, nuclear model calculations and assumed uncertainties, and in some cases the evaluators have increased the uncertainties after formal uncertainty quantification.

Table 11
Selected absolute importances of ^{240}Pu.[a]

Response	*i*th pair *j*th pair	ENDF/B-VII.1 I_{ij} (%^{2})	JENDL-4.0u I_{ij} (%^{2})
MOX			
k_{inf}	^{240}Pu, σ_c	1.97×10^{-2}	3.47×10^{-1}
D_2	^{240}Pu, σ_c	1.07×10^{-3}	1.02×10^{-2}
$\Sigma_{s,1\to2}$	^{240}Pu, σ_c	1.24×10^{-2}	2.31×10^{-1}
$\Sigma_{a,1}$	^{240}Pu, σ_c	9.29×10^{-3}	1.64×10^{-1}
$\Sigma_{a,2}$	^{240}Pu, σ_c	4.52×10^{-3}	6.83×10^{-2}
f_1	^{240}Pu, σ_c	6.39×10^{-6}	4.71×10^{-5}
f_2	^{240}Pu, σ_c	6.29×10^{-4}	5.92×10^{-3}

[a] Data with relative importances of less than 5% are omitted.

Table 12
Selected absolute importances of ^{241}Pu.[a]

Response	*i*th pair *j*th pair	ENDF/B-VII.1 I_{ij} (%^{2})	JENDL-4.0u I_{ij} (%^{2})
MOX			
k_{inf}	^{241}Pu, σ_c	7.05×10^{-3}	5.02×10^{-2}
$\Sigma_{a,2}$	^{241}Pu, σ_c	8.32×10^{-4}	2.09×10^{-2}
$\nu\Sigma_{f,1}$	^{241}Pu, σ_f	5.05×10^{-2}	8.54×10^{-2}
$\nu\Sigma_{f,2}$	^{241}Pu, σ_f	2.22×10^{-2}	3.95×10^{-2}
f_2	^{241}Pu, σ_c	9.87×10^{-5}	9.73×10^{-4}

[a] Data with relative importances of less than 5% are omitted.

The selected absolute importances for ^{241}Pu are listed in Table 12.

The important contributions from the fission cross section are within an order-of-magnitude for both NDLs.

The important contributions from the effective capture cross section have an order-of-magnitude difference: the importances of JENDL-4.0u are larger by a factor of 7–25. The uncertainty of radiative capture in the thermal region seems to be underestimated in the low-fidelity covariances, as observed by the evaluators in the low-fidelity covariance project (Little et al., 2008).

4.3.8. Plutonium-242

The cross section covariances in ENDF/B-VII.1 are based on the uncertainty estimates from COMMARA-2.0 (Herman et al., 2011) up to 1 keV. Other covariances seem to be from JENDL-4.0. The cross section covariances of JENDL-4.0u are based on

Table 13
Selected absolute importances of ^{242}Pu.[a]

Response	*i*th pair *j*th pair	ENDF/B-VII.1 I_{ij} (%^{2})	JENDL-4.0u I_{ij} (%^{2})
MOX			
k_{inf}	^{242}Pu, σ_c	6.30×10^{-2}	7.02×10^{-3}
$\Sigma_{s,1\to2}$	^{242}Pu, σ_c	1.17×10^{-1}	1.26×10^{-2}
$\Sigma_{a,1}$	^{242}Pu, σ_c	9.05×10^{-2}	9.44×10^{-3}
f_1	^{242}Pu, σ_c	2.44×10^{-5}	3.32×10^{-6}
f_2	^{242}Pu, σ_c	3.58×10^{-4}	6.89×10^{-5}

[a] Data with relative importances of less than 5% are omitted.

Table 15
Large relative importances of cross-material covariances for each case.[a]

Relative importance (%) / response	ENDF/B-VII.1	JENDL-4.0u
UO_2	1.86 / k_{inf} 7.37 / $\nu\Sigma_{f,1}$	2.06 / $\nu\Sigma_{f,1}$
MOX	0.99 / k_{inf} 7.33 / $\nu\Sigma_{f,1}$ 0.578 / $\nu\Sigma_{f,2}$ 0.241 / f_1	1.94 / $\nu\Sigma_{f,1}$

[a] Relative importances less than 0.1% are omitted.

nuclear model calculations and assumed uncertainties, and in some cases the evaluators have increased the uncertainties after formal uncertainty quantification. The JENDL-4.0u covariances are from the revised NDL.

The selected absolute importances for ^{242}Pu are listed in Table 13.

The important contributions from the effective capture cross section have almost an order-of-magnitude difference: the importances of ENDF/B-VII.1 are larger by a factor of 5–10. The difference in importances is visible in the uncertainties and is one of the reasons for the JENDL-4.0 revision.

4.3.9. Americium-241

The covariances of the resonance parameters in ENDF/B-VII.1 are adopted from JENDL-4.0, and other covariances are based on experimental data and nuclear model calculations. The covariances of JEFF-3.2 are partial, quantified up to 150 eV. The covariances of JENDL-4.0u are based on experimental data, nuclear model calculations and assumed uncertainties, and in some cases the evaluators have increased the uncertainties after formal uncertainty quantification. The JENDL-4.0u covariances are from the revised NDL.

The selected absolute importances for ^{241}Am are listed in Table 14.

The important contribution from the scattering cross section has an order-of-magnitude difference between ENDF/B-VII.1 and the other NDLs. The uncertainties of the elastic scattering are about 4.4% for JEFF-3.2, 16% for JENDL-4.0u and over 100% for ENDF/B-VII.1 in the thermal region. The large resonance parameter uncertainties are one of reasons for JENDL-4.0 revision, and this can be still seen in the uncertainties of ENDF/B-VII.1.

The important contribution from the effective capture cross section has an order-of-magnitude difference between JENDL-4.0u and JEFF-3.2. The contribution from ENDF/B-VII.1 falls between the other NDLs. The difference seems to emerge, at least partly, from a sudden increase in the uncertainty from 4% to 10–16% above 0.1 eV in JENDL-4.0u, while the uncertainties in JEFF-3.2 remain at a level of 3–6%.

4.4. Contributions from cross-material covariances

Generally the contributions to uncertainties from cross-material covariances are small: the summed relative importances of cross-material covariances are typically less than 0.1%. However, in a few cases the cross-material covariances have a larger contribution to the variance.

Table 14
Selected absolute importances of ^{241}Am.[a]

Response	*i*th pair *j*th pair	ENDF/B-VII.1 I_{ij} (%^{2})	JEFF-3.2 I_{ij} (%^{2})	JENDL-4.0u I_{ij} (%^{2})
MOX				
D_2	^{241}Am, σ_s	6.48×10^{-3}	1.94×10^{-8}	9.00×10^{-7}
D_2	^{241}Am, σ_c	5.98×10^{-4}	2.25×10^{-4}	2.44×10^{-3}

[a] Data with relative importances of less than 5% are omitted.

The relative importances of cross-material covariances in JEFF-3.2 are small, at most 4.24×10^{-5}% for the fast discontinuity factor of the UO_2 assembly and at most 2.45×10^{-4}% for the fast neutron production constant of the MOX assembly.

The larger, over 0.1%, relative importances of the cross-material covariances are listed in Table 15. For both ENDF/B-VII.1 and JENDL-4.0u the largest contributions are to the fast neutron production constant for both UO_2 and MOX assemblies.

For JENDL-4.0u the largest contribution for the UO_2 assembly is solely from the covariance between ^{235}U σ_f and ^{238}U σ_f, but has multiple cross-material contributors for the MOX assembly.

For ENDF/B-VII.1 the largest contribution for the UO_2 assembly is mostly from the covariance between ^{235}U ν and ^{238}U ν, although the covariance between ^{235}U σ_f and ^{238}U σ_f has a small contribution. For the MOX assembly cross-material covariances with ^{239}Pu ν have the largest contributions.

5. Conclusions

We have surveyed prediction capabilities of three NDLs by performing uncertainty analysis on two PWR assemblies from the UAM benchmark (Ivanov et al., 2013). The considered responses were two-group homogenized assembly constants for a steady state diffusion model.

We have considered intra-material and cross-material covariances, and in general the contributions from cross-material covariances are small. However, for ENDF/B-VII.1 and JENDL-4.0u these have a moderate contribution to the (fast) neutron production constants and for ENDF/B-VII.1 also for other responses.

In many cases the NDLs claim about the same level of knowledge of the nuclear data. However, for several important pieces of nuclear data the uncertainties have an order-of-magnitude differences between the NDLs. These are observed between ENDF/B-VII.1 and JENDL-4.0u for ^{238}U σ_s, ^{240}Pu σ_c and ^{241}Pu σ_c. In addition JEFF-3.2 has large uncertainties for ^{90}Zr and JENDL-4.0u is missing uncertainty estimate for the elastic scattering of ^{90}Zr. The ENDF/B-VII.1 covariances of ^{235}U ν seem to be inconsistent, and ^{242}Pu and ^{241}Am of ENDF/B-VII.1 use covariances from JENDL-4.0, which have been updated in JENDL-4.0u because of significant errors.

If the evaluations are not erroneous, the differences are a result of different evaluation methods or different use of expert judgment. In the latter cases the evaluators should verify that they have included all relevant, both empirical and theoretical, information in the quantified uncertainties. Uncertainty estimates should reflect the fact that each estimation method includes systematic, random and methodological components (Cacuci, 2003).

The uncertainty quantification is not complete in the NDLs. (I) There are no uncertainty estimates for secondary neutron energy distributions for reactions other than fission. For non-thermal energies the information can be, at the expense of volume of the

data, encoded in ENDF-6 format, but handling thermal upscattering might be problematic without a format for File 37. (II) There are many nuclides whose uncertainties are only partially quantified. From the viewpoint of our application, the state of uncertainty quantification is compiled in Table 1. (III) In some cases the uncertainties are quantified only for a partial energy range. Usually this is because only the uncertainties of resonance parameters have been quantified. ENDF/B-VII.1 ^{54}Cr, and JEFF-3.2 ^{239}Pu and ^{241}Am fall into this category. (IV) In some cases there are no uncertainty estimates for a material. Concerning the two test assemblies there are no uncertainty estimates for ^{115}In, ^{113}Cd and ^{107}Ag in the three NDLs, although uncertainty estimates in the ZZ-SCALE6/COVA-44G library suggest that their contribution is important. For at least one NDL there are no uncertainty estimates for ^{1}H, ^{16}O, all isotopes of ^{nat}Zr, ^{109}Ag, ^{157}Gd and most nuclides in the fuel. It should be mentioned that the test cases do not contain fission product poisons. In general, uncertainties of strong absorbers need to be quantified.

Comparing the overall prediction capabilities of the NDLs is meaningless, since the uncertainty quantification is not sufficiently complete in the NDLs. Practical uncertainty propagation can be performed if simple estimates, for example from the ZZ-SCALE6/COVA-44G-library (OECD/NEA Data Bank, 2011) or from the low-fidelity covariance project (Little et al., 2008), are used when no high-fidelity uncertainty estimates are available. However, the contribution from simple estimates should remain low when quantitative results are needed, and even then important sources of uncertainty might not be identified, as ^{16}O, ^{157}Gd and ^{241}Pu demonstrate for our case. Fortunately the number of high-fidelity uncertainty estimates is larger than in previous releases of the NDLs and continues to grow as new evaluations are made with quantified uncertainties and new releases of NDLs are published.

Acknowledgments

The first author thanks P. Aarnio, J. Ala-Heikkil and E. Dorval for their valuable comments and interest in the work, and acknowledges the financial support of the YTERA Doctoral Programme for Nuclear Engineering and Radiochemistry.

References

Brown, D., Arcilla, R., Capote, R., Mughabghab, S., Herman, M., Trkov, A., Kim, H., 2014. Zirconium evaluations for ENDF/B-VII.2 for the fast region. Nucl. Data Sheets 118 (0), 144–146.

Cacuci, D., 2003. Sensitivity and Uncertainty Analysis: Theory. Chapman & Hall/CRC.

Cacuci, D., Ionescu-Bujor, M., 2010. Sensitivity and uncertainty analysis, data assimilation, and predictive best-estimate model calibration. In: Cacuci, D. (Ed.), Handbook of Nuclear Engineering. Springer, US, pp. 1913–2051.

Cacuci, D., Ionescu-Bujor, M., Navon, I., 2005. Sensitivity and Uncertainty Analysis: Applications to Large-Scale Systems. Taylor & Francis.

Carlson, A., Pronyaev, V., Smith, D., Larson, N., Chen, Z., Hale, G., Hambsch, F.-J., Gai, E., Oh, S.-Y., Badikov, S., Kawano, T., Hofmann, H., Vonach, H., Tagesen, S., 2009. International evaluation of neutron cross section standards. Nucl. Data Sheets 110 (12), 3215–3324 (Special Issue on Nuclear Reaction Data).

Chadwick, M., Obložinský, P., Herman, M., Greene, N., McKnight, R., Smith, D., Young, P., MacFarlane, R., Hale, G., Frankle, S., Kahler, A., Kawano, T., Little, R., Madland, D., Moller, P., Mosteller, R., Page, P., Talou, P., Trellue, H., White, M., Wilson, W., Arcilla, R., Dunford, C., Mughabghab, S., Pritychenko, B., Rochman, D., Sonzogni, A., Lubitz, C., Trumbull, T., Weinman, J., Brown, D., Cullen, D., Heinrichs, D., McNabb, D., Derrien, H., Dunn, M., Larson, N., Leal, L., Carlson, A., Block, R., Briggs, J., Cheng, E., Huria, H., Zerkle, M., Kozier, K., Courcelle, A., Pronyaev, V., van der Marck, S., 2006. ENDF/B-VII.0: next generation evaluated nuclear data library for nuclear science and technology. Nucl. Data Sheets 107, 2931–3118.

Chadwick, M., Herman, M., Obložinský, P., Dunn, M., Danon, Y., Kahler, A., Smith, D., Pritychenko, B., Arbanas, G., Arcilla, R., Brewer, R., Brown, D., Capote, R., Carlson, A., Cho, Y., Derrien, H., Guber, K., Hale, G., Hoblit, S., Holloway, S., Johnson, T., Kawano, T., Kiedrowski, B., Kim, H., Kunieda, S., Larson, N., Leal, L., Lestone, J., Little, R., McCutchan, E., MacFarlane, R., MacInnes, M., Mattoon, C., McKnight, R., Mughabghab, S., Nobre, G., Palmiotti, G., Palumbo, A., Pigni, M., Pronyaev, V., Sayer, R., Sonzogni, A., Summers, N., Talou, P., Thompson, I., Trkov, A., Vogt, R., van der Marck, S., Wallner, A., White, M., Wiarda, D., Young, P., 2011. ENDF/B-VII.1 nuclear data for science and technology: cross sections, covariances, fission product yields and decay data. Nucl. Data Sheets 112 (12), 2887–2996 (Special Issue on ENDF/B-VII.1 Library).

ENDF/B-V evaluated nuclear data library. http://www.nndc.bnl.gov/endf/b5/index.html, cited 31.12.2014.

Herman, M., Oblozinsky, P., Mattoon, C., Pigni, M., Hoblit, S., Mughabghab, S., Sonzogni, A., Talou, P., Chadwick, M., Hale, G., Kahler, A., Kawano, T., Little, R., Young, P., 2011. COMMARA-2.0 Neutron Cross Section Covariance Library. Brookhaven National Laboratory, 2011. 94830-2011.

Hernández-Solís, A., Demazière, C., Ekberg, C., 2013a. Uncertainty and sensitivity analyses applied to the DRAGONv4.05 code lattice calculations and based on JENDL-4 data. Ann. Nucl. Energy 57 (0), 230–245.

Hernández-Solís, A., Demazière, C., Ekberg, C., 2013b. Uncertainty analyses applied to the UAM/TMI-1 lattice calculations using the DRAGON (version 4.05) code and based on JENDL-4 and ENDF/B-VII.1 covariance data. Sci. Technol. Nucl. Installations 2013.

Ivanov, K., Avramova, M., Kamerow, S., Kodeli, I., Sartori, E., Ivanov, E., Cabellos, O., 2013. "Benchmarks for uncertainty analysis in modelling (UAM) for the design, operation and safety analysis of LWRs," Tech. Rep. 7, OECD Nuclear Energy Agency. Version 2.1.

Iwamoto, O., Nakagawa, T., Otuka, N., Chiba, S., Okumura, K., Chiba, G., Ohsawa, T., Furutaka, K., 2009. JENDL actinoid file 2008. J. Nucl. Sci. Technol. 46 (5), 510–528.

N.D.C. Japan Atomic Energy Agency, 2013. "JENDL 4.0u." <http://wwwndc.jaea.go.jp/jendl/j40/update/>.

Kahler, A.C., 2014. Personal communication. NJOY 2012 update 22.

Kahler, A.C., MacFarlane, R.E., Muir, D.W., Boicourt, R.M., 2012. The NJOY Nuclear Data Processing System, Version 2012. Los Alamos National Laboratory.

Kodeli, I., Snoj, L., 2012. Evaluation and uncertainty analysis of the KRITZ-2 critical benchmark experiments. Nucl. Sci. Eng. 171 (3), 231–238.

Koning, A., Rochman, D., 2012. Modern nuclear data evaluation with the TALYS code system. Nucl. Data Sheets 113, 2841.

Little, R.C., Kawano, T., Hale, G.D., Pigni, M.T., Herman, M., Obložinský, P., Williams, M.L., Dunn, M.E., Arbanas, G., Wiarda, D., McKnight, R.D., McKamy, J.N., Felty, J.R., 2008. Low-fidelity covariance project. Nucl. Data Sheets 109 (12), 2828–2833.

OECD/NEA Data Bank, 2011. ZZ-SCALE6/COVA-44G, a 44-group cross section covariance matrix library retrieved from the SCALE-6 package (USCD1236/03).

OECD/NEA Data Bank, 2014. "JEFF-3.2." <https://www.oecd-nea.org/dbdata/jeff/>.

Pusa, M., 2012a. Incorporating sensitivity and uncertainty analysis to a lattice physics code with application to CASMO-4. Ann. Nucl. Energy 40 (1), 153–162.

Pusa, M., 2012b. Perturbation-theory-based sensitivity and uncertainty analysis with CASMO-4. Sci. Technol. Nucl. Installations 2012.

Pusa, M., 2014. Adjoint-based sensitivity and uncertainty analysis of lattice physics calculations with CASMO-4. In: Proceedings of the PHYSOR 2014 Conference.

Rhodes, J., 2005. JEF 2.2 and ENDF/B-IV 70 group neutron data libraries.

Rhodes, J., Edenius, M., 2001. CASMO-4, A Fuel Assembly Burnup Program. User's Manual.

Shibata, K., Nakajima, Y., Fukahori, T., C.S., Nakagawa, T., Kawano, T., 1996. Estimation of uncertainties in ^{1}H, Zr and ^{238}U nuclear data contained in JENDL-3.2 [in japanese], Tech. Rep. 96-041, JAERI.

Shibata, K., Akajima, Y., Kawano, T., Oh, S.Y., Hiroyuki, M., Murata, T., 1997. Estimation of covariances of ^{16}O, ^{23}Na, Fe, ^{235}U, ^{238}U and ^{239}Pu neutron nuclear data in JENDL-3.2, Tech. Rep. 97-074, JAERI.

Shibata, K., Iwamoto, O., Nakagawa, T., Iwamoto, N., Ichihara, A., Kunieda, S., Chiba, S., Furutaka, K., Otuka, N., Ohsawa, T., Murata, T., Matsunobu, H., Zukeran, A., Kamada, S., Katakura, J.-I., 2011. JENDL-4.0: a new library for nuclear science and engineering. J. Nucl. Sci. Technol. 48 (1), 1–30.

Talou, P., Young, P., Kawano, T., Rising, M., Chadwick, M., 2011. Quantification of uncertainties for evaluated neutron-induced reactions on actinides in the fast energy range. Nucl. Data Sheets 112 (12), 3054–3074 (Special Issue on ENDF/B-VII.1 Library).

Tomlinson, E., deSaussure, D., Weisbin, C., 1977. Sensitivity analysis of TRX-2 lattice parameters with emphasis on epithermal 238-U capture, Tech. Rep. 252.

Trkov, A., Herman, M., Brown, D.A., 2012. ENDF-6 Formats Manual. Brookhaven National Laboratory.

Usachev, L., 1964. Perturbation theory for the breeding ratio and for other number ratios pertaining to various reactor processes. J. Nucl. Energy A/B 18, 571.

Vanhanen, R., 2015a. Uncertainty analysis of infinite homogeneous lead and sodium cooled fast reactors at beginning of life. Nucl. Eng. Des. 283 (0), 168–174, SI:NENE 2013.

Vanhanen, R., 2015b. Computing positive semidefinite multigroup nuclear data covariances. Nucl. Sci. Eng. http://dx.doi.org/10.13182/NSE14-75.

Vanhanen, R., in press. Computing more consistent multigroup nuclear data covariances. Nucl. Sci. Eng.

Wigner, E.P., 1945. Effect of small perturbations on pile period, Tech. Rep. CP-3048.

Publication V

R. Vanhanen. Uncertainty analysis of infinite homogeneous lead and sodium cooled fast reactors at beginning of life. ***Nuclear Engineering and Design,*** **SI: NENE, 283, 168–174, March 2015;** `http://dx.doi.org/10.1016/j.nucengdes.2014.06.023`**.**

Nuclear Engineering and Design 283 (2015) 168–174

Contents lists available at ScienceDirect

Nuclear Engineering and Design

journal homepage: www.elsevier.com/locate/nucengdes

Uncertainty analysis of infinite homogeneous lead and sodium cooled fast reactors at beginning of life

R. Vanhanen*

Aalto University School of Science, P.O. Box 14100, FI-00076 Aalto, Finland

ARTICLE INFO

Article history:
Received 6 March 2014
Received in revised form 5 June 2014
Accepted 6 June 2014

ABSTRACT

The objective of the present work is to estimate breeding ratio, radiation damage rate and minor actinide transmutation rate of infinite homogeneous lead and sodium cooled fast reactors. Uncertainty analysis is performed taking into account uncertainty in nuclear data and composition of the reactors. We use the recently released ENDF/B-VII.1 nuclear data library and restrict the work to the beginning of reactor life.

We work under multigroup approximation. The Bondarenko method is used to acquire effective cross sections for the homogeneous reactor. Modeling error and numerical error are estimated.

The adjoint sensitivity analysis is performed to calculate generalized adjoint fluxes for the responses. The generalized adjoint fluxes are used to calculate first order sensitivities of the responses to model parameters. The acquired sensitivities are used to propagate uncertainties in the input data to find out uncertainties in the responses.

We show that the uncertainty in model parameters is the dominant source of uncertainty, followed by modeling error, input data precision and numerical error. The uncertainty due to composition of the reactor is low. We identify main sources of uncertainty and note that the low-fidelity evaluation of ^{16}O is problematic due to lack of correlation between total and elastic reactions.

1. Introduction

The proven uranium reserves and estimated resources are sufficient to fuel the current open fuel cycle for 250 years (Waltar et al., 2012). The thermal reactors produce minor actinides, which are more radiotoxic than natural uranium for hundreds of thousands of years. The same amount of uranium would last for 16,000–19,000 years with breeder reactors and closed fuel cycle (Waltar et al., 2012). Fast breeder reactors produce insignificant amounts of minor actinides and could also transmute the presently accumulated minor actinides. Compared to thermal reactors the materials in fast reactors suffer from high radiation damage.

Nuclear data is less well known in the neutron spectrum of fast reactors than in the thermal region. The distribution of our subjective knowledge of the nuclear data can be interpreted according to the Bayesian probability interpretation. Recent evaluated nuclear data files contain rather complete sets of uncertainty estimates, i.e., evaluations of the second moments of the distribution of our subjective knowledge of the nuclear data. This allows us to estimate the second moments of the posterior distribution of the responses, giving us meaningful estimates of uncertainty due to our limited knowledge of nuclear data.

In addition to nuclear data also the composition of the reactor is taken to be uncertain in this study. The idea is not new (Greenspan, 1976). Even though not applied in this work, it should be noted that calculation of the sensitivities to nuclide concentrations can be used in optimization of designs against rather arbitrary performance parameters.

Since we are interested in a small number of responses and the number of parameters needed to calculate them is large, it is advantageous to use adjoint sensitivity analysis, also known as generalized perturbation theory (Usachev, 1964). In this work its multigroup form is derived and used, i.e., the so called implicit sensitivites or spectral fine structure effects (Greenspan, 1982) are not taken into account. The point of view is then that the self-shielded multigroup cross sections correctly represent the underlying physics or that the analysis is carried in a nearby universe, where the multigroup presentation is correct. The method relies on the narrow resonance approximation (Dresner, 1956, and references therein), which is well valid within energy spectrum of

* Tel.: +358 504331135.
E-mail address: risto.vanhanen@aalto.fi

http://dx.doi.org/10.1016/j.nucengdes.2014.06.023
0029-5493/

fast reactors (Waltar et al., 2012). However, the resonance interference effect is lost.

2. Theory

The G group form of the steady state neutron criticality equation in an infinite reactor can be written as

$$\Sigma_{t,g}\Phi_g = \sum_{r\neq f}\sum_{g'=1}^{G}\Sigma_{r,g'\to g}\Phi_{g'} + \frac{1}{k}\sum_{g'=1}^{G}\Sigma_{f,g'\to g}\Phi_{g'} \quad \text{for} \quad g = 1,\ldots,G, \tag{1}$$

where k is the multiplication factor and $\boldsymbol{\Phi}\in\mathbb{R}^G$ is the scalar neutron flux. The summation over reactions r runs over all neutron emitting reactions, except fission. The macroscopic total cross section $\Sigma_{t,g}$ and the macroscopic group-to-group transfer matrices $\Sigma_{rg'\to g}$ are defined as

$$\Sigma_{t,g} = \sum_{i=1}^{I} n_i\sigma_{i,t,g} \quad \text{and} \tag{2a}$$

$$\Sigma_{r,g'\to g} = \sum_{i=1}^{I} n_i\sigma_{i,r,g'\to g}, \tag{2b}$$

where n_i is the number density for the ith nuclide and the microscopic transfer matrix can be written in the form

$$\sigma_{i,r,g'\to g} = m_{i,r,g'}\sigma_{i,r,g'}p_{i,r,g'\to g}, \tag{3}$$

where $\sigma_{i,r,g'}$ is the cross section of the reaction, $m_{i,r,g'}$ is the multiplicity and $p_{i,r,g'\to g}$ is the energy group distribution of the emitted neutrons. Specifically for fission $r=f$ and $m_{i,r,g'} = \overline{\nu}_{i,p,g'} + \overline{\nu}_{i,d,g'}$ is the sum of average number of prompt and delayed neutrons emitted per fission.

Reaction rate densities are acquired by taking the standard $\mathbb{R}^G$ inner product between a macroscopic cross section $\Sigma_r\in\mathbb{R}^G$ and the scalar flux:

$$\langle\boldsymbol{\Sigma}_r, \boldsymbol{\Phi}\rangle = \boldsymbol{\Sigma}_r^{\top}\boldsymbol{\Phi}, \tag{4}$$

where $^{\top}$ denotes the transpose of a vector. The macroscopic cross section in Eq. (4) is arbitrary. In fact there are many situations where it may be zero for some groups and it may also include consequences of a reaction and not just the reaction rate, e.g., heat deposition rate or radiation damage rate.

2.1. Model parameters

The parameters in the model are nuclide concentrations n_i, cross sections $\sigma_{i,r,g}$, multiplicities $m_{i,r,g}$ and energy distributions of emitted neutrons $p_{i,r,g'\to g}$. The parameters include any cross sections and nuclide concentrations that are needed to calculate the responses. Together these N parameters can be collected to a vector, denoted by $\boldsymbol{\alpha}\in\mathbb{R}^N$.

Our subjective knowledge of the nuclide concentrations and multigroup nuclear data can be represented as a joint probability

$$p(\alpha_1,\ldots,\alpha_N)d\alpha_1\cdots d\alpha_N \tag{5}$$

that the true value of each parameter α_n lies in range $(\alpha_n, \alpha_n + d\alpha_n)$ for each $n = 1,\ldots,N$ simultaneously (MacFarlane and Kahler, 2010). The probability distribution is denoted by $p(\boldsymbol{\alpha})$.

Current nuclear data files contain enough information to process the first moments and second (central) moments of the nuclear data to multigroup form. Assuming that we can estimate the first and second moments of the nuclide concentrations we have the first moments $E(\boldsymbol{\alpha})$ and the second moments $\mathrm{cov}(\boldsymbol{\alpha},\boldsymbol{\alpha})$ of the probability distribution:

$$E(\boldsymbol{\alpha}) = \langle\boldsymbol{\alpha}\rangle \quad \text{and} \tag{6a}$$

$$\mathrm{cov}(\boldsymbol{\alpha},\boldsymbol{\alpha}) = \langle(\boldsymbol{\alpha}-E(\boldsymbol{\alpha}))(\boldsymbol{\alpha}-E(\boldsymbol{\alpha}))\rangle, \tag{6b}$$

Here the brackets $\langle\cdot\rangle = \int\cdot\int p(\boldsymbol{\alpha})d\boldsymbol{\alpha}$ indicate integration over the probability distribution.

If it is acknowledged that some of the contents of the probability distribution are non-negative, e.g., nuclide concentrations or multigroup cross sections, it follows that the distribution cannot be a normal distribution. Normality is not required in the present analysis.

2.2. State variables

The state variables in the model are the components of the neutron flux $\boldsymbol{\Phi}$. The state variables depend on the parameters through Eq. (1). Concatenation of the state variables and parameters is denoted by $\boldsymbol{e} = (\boldsymbol{\Phi},\boldsymbol{\alpha})\in\mathbb{R}^{G+N}$.

2.3. Nominal values

The nominal values $\hat{\boldsymbol{\alpha}}$ of the parameters are chosen to be the first moments $E(\boldsymbol{\alpha})$. The nominal values of the state variables $\hat{\boldsymbol{\Phi}}$ can be calculated by solving Eq. (1) using the nominal values of the parameters. The concatenation of the nominal values of the state variables and parameters is denoted by $\hat{\boldsymbol{e}} = (\hat{\boldsymbol{\Phi}},\hat{\boldsymbol{\alpha}})\in\mathbb{R}^{G+N}$.

2.4. Responses

In this work we are interested in L ratios of reaction rates, giving us responses of the type

$$R_l(\boldsymbol{e}) = \frac{\langle\boldsymbol{\Sigma}_{r_l},\boldsymbol{\Phi}\rangle}{\langle\boldsymbol{\Sigma}_{p_l},\boldsymbol{\Phi}\rangle}. \tag{7}$$

In principle we are interested in the full posterior distribution $p(\boldsymbol{R}(\boldsymbol{e}))$ for the responses $\boldsymbol{R}\in\mathbb{R}^L$. Alas, since we have not fully characterized our knowledge of the parameters we cannot calculate the full posterior distribution.

We can, however, approximate its first moment by linearizing the response at the nominal values of the parameters. The linearized response is

$$R_l(\boldsymbol{e}) = R_l(\hat{\boldsymbol{e}}) + \boldsymbol{S}_l(\hat{\boldsymbol{e}})(\boldsymbol{\alpha}-\hat{\boldsymbol{\alpha}}) + \mathcal{O}(\|\boldsymbol{\alpha}-\hat{\boldsymbol{\alpha}}\|^2), \tag{8}$$

where the sensitivity $\boldsymbol{S}_l(\hat{\boldsymbol{e}})$ accounts for both direct effects, due to variations in the parameters, and indirect effects, due to variations in the state variables which arise because of the variations in the parameters. Applying $\langle\cdot\rangle$ to both sides of Eq. (8) gives

$$E(R_l(\boldsymbol{e})) = R_l(\hat{\boldsymbol{e}}) + \mathcal{O}(\|\boldsymbol{\alpha}-\hat{\boldsymbol{\alpha}}\|^2), \tag{9}$$

since the nominal values of the parameters were chosen to be the first moments. The result is that the first moments of the responses are approximately the nominal responses. The approximation is accurate up to second order in parameters. (Cacuci and Ionescu-Bujor, 2003)

2.5. Uncertainty analysis

The purpose of uncertainty analysis is to estimate the higher moments of the responses. Usually it suffices to calculate the second (central) moments. An approximation for the second moments can be acquired by integrating $(R_l(\boldsymbol{e}) - E(R_l(\boldsymbol{e})))(R_m(\boldsymbol{e}) - E(R_m(\boldsymbol{e})))$ over

the distribution of our subjective knowledge of the parameters. This gives

$$\operatorname{cov}(R_l(\boldsymbol{e}), R_m(\boldsymbol{e})) = \boldsymbol{S}_l(\hat{\boldsymbol{e}}) \operatorname{cov}(\boldsymbol{\alpha}, \boldsymbol{\alpha}) \boldsymbol{S}_m^{\top}(\hat{\boldsymbol{e}}) + \mathcal{O}(\|\boldsymbol{\alpha} - \hat{\boldsymbol{\alpha}}\|^3), \tag{10}$$

which is also known as the sandwich formula. The approximation is accurate up to third order in parameters. (Cacuci and Ionescu-Bujor, 2003)

Calculation of third and higher moments of the responses is infeasible with the current evaluations of nuclear data, because required third and higher moments of nuclear data are not characterized. However, the first two moments should suffice if our knowledge of the data is good enough.

2.6. Sensitivity analysis

A general tool for the local sensitivity analysis is the directional derivative called Gâteaux variation (Cacuci, 2003). The sensitivity of a response R to variations in the parameters and state variables $\boldsymbol{h} = (\boldsymbol{h}_{\boldsymbol{\Phi}}, \boldsymbol{h}_{\boldsymbol{\alpha}}) \in \mathbb{R}^{G+N}$, respectively, at the point $\hat{\boldsymbol{e}} \in \mathbb{R}^{G+N}$ can be defined to be

$$\delta R(\hat{\boldsymbol{e}}; \boldsymbol{h}) = \lim_{t \to 0} \frac{1}{t} \left(R(\hat{\boldsymbol{e}} + t\boldsymbol{h}) - R(\hat{\boldsymbol{e}}) \right). \tag{11}$$

For the reaction ratio responses considered in this work the sensitivities can be represented as

$$\delta R_l(\hat{\boldsymbol{e}}; \boldsymbol{h}) = R'_{l,\boldsymbol{\Phi}}(\hat{\boldsymbol{e}}) \boldsymbol{h}_{\boldsymbol{\Phi}} + R'_{l,\boldsymbol{\alpha}}(\hat{\boldsymbol{e}}) \boldsymbol{h}_{\boldsymbol{\alpha}} = \langle \nabla_{\boldsymbol{\Phi}} R_l(\hat{\boldsymbol{e}}), \boldsymbol{h}_{\boldsymbol{\Phi}} \rangle + R'_{l,\boldsymbol{\alpha}}(\hat{\boldsymbol{e}}) \boldsymbol{h}_{\boldsymbol{\alpha}} \tag{12}$$

where $R'_{l,\boldsymbol{\Phi}}$ and $R'_{l,\boldsymbol{\alpha}}$ are the gradients of the response with respect to variations in the state variables and parameters, respectively. From the viewpoint of uncertainty analysis it is the purpose of the sensitivity analysis to map $\boldsymbol{h}_{\boldsymbol{\Phi}}$ to $\boldsymbol{h}_{\boldsymbol{\alpha}}$, in first order, so Eq. (12) can be expressed linearly in $\boldsymbol{h}_{\boldsymbol{\alpha}}$. This allows construction of the sensitivity as used in Eq. (8).

In operator form Eq. (1) can be written as

$$\boldsymbol{A}(\boldsymbol{\alpha}) \boldsymbol{\Phi} = \frac{1}{k(\boldsymbol{e})} \boldsymbol{B}(\boldsymbol{\alpha}) \boldsymbol{\Phi}. \tag{13}$$

where $\boldsymbol{A} : \mathbb{R}^{G+N} \to \mathbb{R}^G$ and $\boldsymbol{B} : \mathbb{R}^{G+N} \to \mathbb{R}^G$ are linear in $\boldsymbol{\Phi}$ but nonlinear in $\boldsymbol{\alpha}$.

The adjoint system (Cacuci, 2003) of Eq. (13) is defined by the identity

$$\left\langle \boldsymbol{\Phi}^{\dagger}, \left(\boldsymbol{A}(\boldsymbol{\alpha}) - \frac{1}{k(\boldsymbol{e})} \boldsymbol{B}(\boldsymbol{\alpha}) \right) \boldsymbol{\Phi} \right\rangle = \left\langle \left(\boldsymbol{A}^{\dagger}(\boldsymbol{\alpha}) - \frac{1}{k(\boldsymbol{e})} \boldsymbol{B}^{\dagger}(\boldsymbol{\alpha}) \right) \boldsymbol{\Phi}^{\dagger}, \boldsymbol{\Phi} \right\rangle, \tag{14}$$

where $\boldsymbol{\Phi}^{\dagger} \in \mathbb{R}^G$ is an adjoint flux. The associated bilinear form vanishes because boundary of the phase space is an empty set.

The forward sensitivity system (Cacuci, 2003) of Eq. (13) is defined as

$$\boldsymbol{A}(\hat{\boldsymbol{e}}) \boldsymbol{h}_{\boldsymbol{\Phi}} + \boldsymbol{A}'_{\boldsymbol{\alpha}}(\hat{\boldsymbol{e}}) \boldsymbol{h}_{\boldsymbol{\alpha}} = \frac{1}{k(\hat{\boldsymbol{e}})} \boldsymbol{B}(\hat{\boldsymbol{e}}) \boldsymbol{h}_{\boldsymbol{\Phi}} + \frac{1}{k(\hat{\boldsymbol{e}})} \boldsymbol{B}'_{\boldsymbol{\alpha}}(\hat{\boldsymbol{e}}) \boldsymbol{h}_{\boldsymbol{\alpha}} - \frac{1}{k^2(\hat{\boldsymbol{e}})} \delta k(\hat{\boldsymbol{e}}; \boldsymbol{h}) \boldsymbol{B}(\hat{\boldsymbol{\alpha}}) \hat{\boldsymbol{\Phi}}, \tag{15}$$

which can be derived by taking Gâteaux variations at $\hat{\boldsymbol{e}}$ on both sides and noticing that in this case the derivatives reduce to Jacobians.

The generalized adjoints $\boldsymbol{\Gamma}_l^{\dagger}$ for the responses R_l are defined as

$$(\boldsymbol{A}^{\dagger}(\boldsymbol{\alpha}) - \frac{1}{k(\boldsymbol{e})} \boldsymbol{B}^{\dagger}(\boldsymbol{\alpha})) \boldsymbol{\Gamma}_l^{\dagger} = \nabla_{\boldsymbol{\Phi}} R_l(\boldsymbol{e}) = R_l(\boldsymbol{e}) \left(\frac{\boldsymbol{\Sigma}_{r_l}}{\langle \boldsymbol{\Sigma}_{r_l}, \boldsymbol{\Phi} \rangle} - \frac{\boldsymbol{\Sigma}_{p_l}}{\langle \boldsymbol{\Sigma}_{p_l}, \boldsymbol{\Phi} \rangle} \right), \tag{16}$$

where the operator $\boldsymbol{A}^{\dagger} - \frac{1}{k} \boldsymbol{B}^{\dagger}$ will be evaluated at the nominal values of the parameters and is therefore singular. The condition $\langle \nabla_{\boldsymbol{\Phi}} R_l(\hat{\boldsymbol{e}}), \hat{\boldsymbol{\Phi}} \rangle = 0$ is necessary for a solution to exist, but the reaction rate ratios do fulfill this condition (Greenspan, 1982). The general solution to Eq. (16) is $\boldsymbol{\Gamma}_l^{\dagger} = a \boldsymbol{\Phi}^{\dagger} + \boldsymbol{\Gamma}_{l,p}^{\dagger}$, where $a \in \mathbb{R}$, the fundamental adjoint $\boldsymbol{\Phi}^{\dagger}$ is the solution to corresponding homogeneous equation and $\boldsymbol{\Gamma}_{l,p}^{\dagger}$ is the particular solution to the inhomogeneous equation. It proves to be advantageous to pick the solution which is orthogonal to the fission source, i.e., $\langle \hat{\boldsymbol{\Gamma}}_l^{\dagger}, \boldsymbol{B}(\hat{\boldsymbol{\alpha}}) \hat{\boldsymbol{\Phi}} \rangle = 0$.

Finally applying Eq. (16) to Eq. (12) and using the adjoint property of the operators, the forward sensitivity system and the orthogonality of the generalized adjoint to the fission source gives

$$\delta R_l(\hat{\boldsymbol{e}}; \boldsymbol{h}) = -\left\langle \hat{\boldsymbol{\Gamma}}_l^{\dagger}, \left(\boldsymbol{A}'_{\boldsymbol{\alpha}}(\hat{\boldsymbol{e}}) - \frac{1}{k(\hat{\boldsymbol{e}})} \boldsymbol{B}'_{\boldsymbol{\alpha}}(\hat{\boldsymbol{e}}) \right) \boldsymbol{h}_{\boldsymbol{\alpha}} \right\rangle + R'_{l,\boldsymbol{\alpha}}(\hat{\boldsymbol{e}}) \boldsymbol{h}_{\boldsymbol{\alpha}}, \tag{17}$$

which is linear in $\boldsymbol{h}_{\boldsymbol{\alpha}}$ and can thus be used to construct $\boldsymbol{S}_l(\hat{\boldsymbol{e}})$ of Eq. (8).

3. Calculations

3.1. LFR and SFR specification

The theory is applied to infinite homogeneous lead and sodium cooled fast reactors at beginning of reactor life.

The LFR case corresponds to volume averaged hexagonal pin cell lattice with pellet radius of 0.330 cm, gap outer radius of 0.340 cm, cladding outer radius of 0.455 cm and pin pitch of 1.365 cm.

The fuel is typical mixed oxide fuel, but contains 3.8% americium. The fuel composition is listed in Table 1. Its smeared density is 9.435 g/cm^3 at 1500 K. The cladding is an approximation of T91 steel at 900 K with density of 7.87 g/cm^3. Isotopes of iron and chromium are included. The coolant is natural lead at 600 K. Its density is 10.66 g/cm^3.

The SFR case corresponds to volume averaged hexagonal pin cell lattice with pellet radius of 0.300 cm, gap outer radius of 0.310 cm, cladding outer radius of 0.345 cm and pin pitch of 0.828 cm.

The fuel is the same as with the LFR but the cladding is an approximation of 15-15Ti steel at 900 K with density of 7.87 g/cm^3. It contains iron, chromium and nickel. The coolant is ^{23}Na with 0.821 g/cm^3 at 600 K.

The relative number density uncertainties correspond to 0.1% uncertainties for fuel density, 1% uncertainties for coolant and cladding densities and 1% uncertainty for weight fractions without any correlation. Strictly speaking this is incorrect since the weight fractions are constrained by sum of unity, implying that the number densities are correlated.

3.2. Responses

The responses (quantities of interest) are breeding ratio, denoted by $R_{\mathrm{c,fer}}/R_{\mathrm{a,fis}}$; ratio of damage energy deposition rate in cladding to heat deposition rate, denoted by $R_{\mathrm{dame}}/R_{\mathrm{heat}}$ and ratio of ^{241}Am transmutation rate to heat deposition rate, denoted by $R_{241}/R_{\mathrm{heat}}$. The latter two will be referred as damage rate and transmutation rate, respectively. The transmutation rate is here defined to be sum of ^{241}Am capture and fission rates, although captures leave some ^{242}Am to be fissioned. The absorption rate of fissile materials in the breeding ratio is approximated as sum of their capture and fission rate.

3.3. Nuclear data

The relevant nuclear data was converted into multigroup (Bondarenko et al., 1964) form using NJOY (MacFarlane and Muir, 1994; NJOY, 2014) nuclear data processing system. The recently released nuclear data file ENDF/B-VII.1 (Chadwick et al., 2011) was used due its rather complete set of covariances. The processing was performed with 10^{-5} relative tolerance. The ECCO 1968 group

Table 1
Composition of the fuel of the infinite LFR and SFR.

Nuclide	Number density (1/cm-barn)	Uncertainty (1/cm-barn)	Nuclide	Number density (1/cm-barn)	Uncertainty (1/cm-barn)
^{238}Pu	1.0540×10^{-4}	1.0593×10^{-6}	^{235}U	4.7284×10^{-5}	4.7520×10^{-7}
^{239}Pu	2.7336×10^{-3}	2.7472×10^{-5}	^{238}U	1.5516×10^{-2}	1.5593×10^{-4}
^{240}Pu	1.1997×10^{-3}	1.2057×10^{-5}	^{241}Am	8.9569×10^{-4}	9.0016×10^{-6}
^{241}Pu	1.8103×10^{-4}	1.8193×10^{-6}	^{16}O	4.1917×10^{-2}	4.2126×10^{-4}
^{242}Pu	3.3351×10^{-4}	3.3517×10^{-6}			

structure was used. Energy distributions were assumed to be exact and their covariances were not processed. Cross-material covariances were not included. NJOY does not calculate covariances for radiation damage cross section or heat deposition cross section. Only indirect contributions are included for these reactions.

The processed correlation matrices for ^{207}Pb and ^{208}Pb were not positive semidefinite, which caused unphysical, negative, variances for the results. These were omitted from the calculations. The problem is most apparent with correlation matrix of total and elastic scattering cross sections.

The calculated first moments were compared to Monte Carlo code Serpent (Leppänen, 2007) to assess modeling error caused by multigroup discretization. NJOY was used to produce an ACE library for Serpent with 5×10^{-4} relative tolerance. NJOY had trouble processing ^{204,208}Pb into dosimetry ACE form and Serpent had trouble reading the dosimetry file of ^{206}Pb. These were left out of the total heat deposition for Serpent, but were used in the transport cycles.

3.4. Calculation details

Typically the neutron flux, the adjoint flux and the generalized adjoint fluxes are solved using problem specific algorithms. We use standard linear algebra packages (Lawson et al., 1979; Anderson et al., 1999; AMD Core Math Library, 2014). This separates the problem from its solution algorithm and with modern routines gives estimates for upper bounds of numerical error. We choose to use direct solution methods due to the modest size of the problem.

The matrices in Eq. (1) are assembled using Eqs. (2) and (3) with self-shielded nuclear data.

The neutron fluxes and adjoint fluxes are solved from Eq. (13), which describes a generalized non-symmetric eigenproblem. The fundamental mode is recognized by the smallest real and positive eigenvalue and its inverse is the multiplication factor. The fundamental neutron flux and fundamental adjoint flux are its right and left generalized eigenvectors, respectively.

The generalized adjoints are solved from a linear equation, which is constructed from Eq. (16) by adding scaled fission source to all rows of the matrix. The fission source is scaled suitably for each row. Note that the inhomogeneous terms are not modified. This enforces the orthogonality of the generalized adjoints to the fission source. In practice this adds one rank to the matrix making it invertible, and therefore allows the use of standard solution algorithms. The inhomogeneous terms are assembled from self-shielded cross sections and the fundamental neutron flux.

The sensitivities for all model parameters are constructed according to Eq. (17). A sensitivity profile is formed for each model parameter which is naturally a vector, while a single sensitivity coefficient suffices for each nuclide concentration.

Finally the uncertainties are propagated by the sandwich formula in Eq. (10). Standard matrix multiplication routines are used where possible.

4. Results

The values of the responses are listed in Table 2. Both reactors have breeding ratio close to unity, allowing them to run by consuming almost only ^{238}U. However, the infinite reactor does not account for any leakage. Due to the uncertainties we cannot predict whether either of the reactors would be a breeder or converter. However, with more input data, e.g. integral experiments, the prediction could be improved.

The softer spectrum of the SFR is seen on the radiation damage energy rate, which is about third of the LFR value. Since the difference between the two is about 3.5 standard deviations, it is quite safe to say that the LFR would suffer from more radiation damage.

On best estimate the LFR is marginally more effective in transmutation. However, the difference between the two reactors is only half standard deviation. Therefore we cannot predict which reactor would be more effective in transmutation. If transmutation is not the main objective, there is no real difference between the two reactors.

4.1. Modeling and numerical errors

The modeling error, as compared to essentially exact result from Serpent, is quite low compared to the uncertainties in the input data. The maximum relative error of the responses in the LFR case is 1.1% for damage energy rate, when heat deposition in ^{204,206,208}Pb is omitted in both multigroup and Serpent calculations. The maximum relative error for the SFR case is 1.2% for the damage energy rate. The other errors are less than 1%.

The numerical error caused by finite precision (about 15 significant decimals) arithmetic is lower than modeling errors for both the LFR and SFR. While the matrices were assembled to almost full precision, the fundamental mode was solved to 6 significant decimals. The large, but not catastrophic, loss of significant digits occurred regardless of the fundamental mode being well separated from the other eigenvalues. The angle between the computed and the exact fundamental neutron flux was less than 2×10^{-8} rad. The same bound applies for the fundamental adjoint flux. The generalized adjoints were solved to 7 significant decimals. The numerical errors from assembling sensitivities and uncertainty propagation were small considering accuracy of the intermediate values from which they were assembled.

While no running error analysis is performed, the results indicate that modeling error is larger than numerical error and therefore the solution is numerically accurate enough. The losses in significant digits are rather large and there is room for improvement. However, this does not imply that there is need for improvement.

4.2. Neutron spectra and generalized adjoints

The LFR and SFR neutron spectra and the generalized adjoints corresponding to the responses are shown in Figs. 1 and 2, respectively. Note that the division by lethargy emphasizes the high energy region. In both cases the neutron spectrum is typical with visible flux depression for energies in large resonances of ^{54}Fe at 7.79 keV, ^{56}Fe at 27.7 keV and ^{16}O at 434 keV and 1 MeV. For the LFR isotopes of lead have many resolved resonances up to 1 MeV, creating less smooth spectrum. For the SFR there is a large flux depression near the huge resonance of ^{23}Na at 2.81 keV.

Table 2
LFR and SFR responses.

Case	Response	Unit	Multigroup		Monte Carlo
			Best-estimate	Uncertainty	Best-estimate[a]
LFR	$R_{c,fer}/R_{a,fis}$	–	1.0575	0.0696	1.0618
LFR	R_{dame}/R_{heat}	–	1.1342×10^{-3}	0.1402×10^{-3}	1.1610×10^{-3}
LFR	R_{241}/R_{heat}	1/MeV	1.4939×10^{-3}	0.1398×10^{-3}	1.4970×10^{-3}
SFR	$R_{c,fer}/R_{a,fis}$	–	9.8226×10^{-1}	0.8795×10^{-1}	9.7326×10^{-1}
SFR	R_{dame}/R_{heat}	–	4.4633×10^{-4}	0.5457×10^{-4}	4.5186×10^{-4}
SFR	R_{241}/R_{heat}	1/MeV	1.3445×10^{-3}	0.1623×10^{-3}	1.3438×10^{-3}

[a] The relative statistical error in MC is less than 10^{-4}.

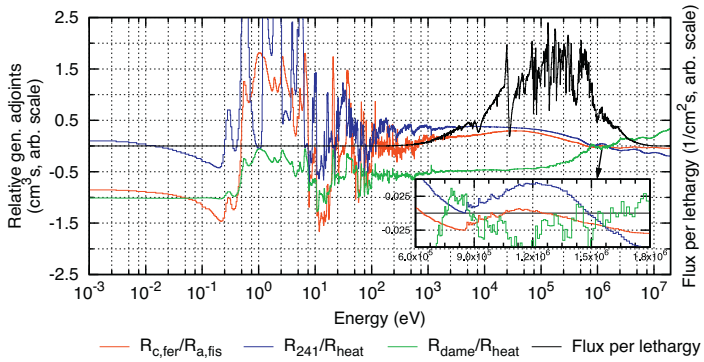

Fig. 1. The LFR flux and relative generalized adjoints for the considered responses. Small figure: high energy sign changes of the generalized adjoints.

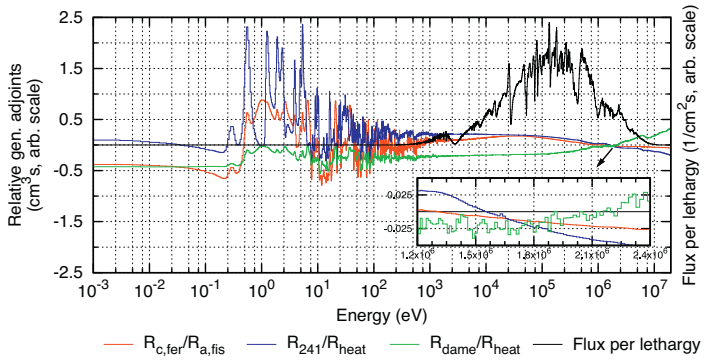

Fig. 2. The SFR flux and relative generalized adjoints for the considered responses. Small figure: high energy sign changes of the generalized adjoints.

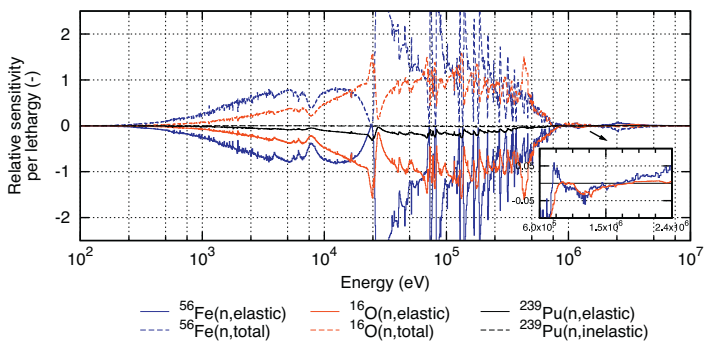

Fig. 3. Selected sensitivity profiles for the LFR damage rate. Small figure: high energy behavior of sensitivity profiles of elastic reactions.

Table 3
Selected contributions of LFR damage rate.

#	Parameter pair		Relative total sensitivities[a] (–)		Contribution (–)
1	^{56}Fe(n,elastic)	^{56}Fe(n,elastic)	−6.4872	−6.4872	1.8084×10^{1}
2	^{56}Fe(n,elastic)	^{56}Fe(n,total)	−6.4872	6.4023	1.7820×10^{1}
3	^{56}Fe(n,total)	^{56}Fe(n,elastic)	6.4023	−6.4872	1.7820×10^{1}
4	^{56}Fe(n,total)	^{56}Fe(n,total)	6.4023	6.4023	1.7610×10^{1}
9	^{16}O(n,elastic)	^{16}O(n,elastic)	−4.1881	−4.1881	6.5454×10^{3}
13	^{16}O(n,total)	^{16}O(n,total)	4.0663	4.0663	6.1781×10^{3}
19	^{52}Cr(n,elastic)	^{52}Cr(n,elastic)	-5.1923×10^{1}	-5.1923×10^{1}	8.4719×10^{4}
24	^{52}Cr(n,total)	^{52}Cr(n,total)	5.1318×10^{1}	5.1318×10^{1}	4.7426×10^{4}
44	^{56}Fe[b]	^{56}Fe[b]	6.6851×10^{1}	6.6851×10^{1}	8.3809×10^{5}
54	^{239}Pu[b]	^{239}Pu[b]	-5.2828×10^{1}	-5.2828×10^{1}	2.6430×10^{5}

[a] Integral of relative sensitivity profile over all energies.
[b] Number density of the nuclide.

The relative generalized adjoint is defined to be $\Gamma_l^{\dagger}/R_l(\hat{e})$. The generalized adjoints can be interpreted as importances of neutrons for the corresponding response. If the sign is positive, every neutron introduced in the energy will increase the numerator of the response more than the denominator. The magnitude carries information but units depend on the units of the corresponding response.

The generalized adjoint of breeding ratio is negative above 1.3 MeV for both the LFR and SFR. This corresponds to the ^{238}U fission threshold and decrease of its capture cross section. For the LFR the breeding ratio increases for every neutron introduced to the energy range 0.7–630 keV. The sign changes several times in the region between 630 keV and 1000 keV due to resonances in isotopes of lead. For the SFR the breeding ratio increases in the range 0.8–1300 keV due to the lack of resonant parasitic isotopes in this region. The generalized adjoints are also positive between 0.5 eV and 7.5 eV, except the SFR between 4.2 eV and 4.6 eV. The positivity is caused by large resonances of fertile nuclei and the SFR exception by ^{241}Pu resonances. For the LFR the ^{241}Pu resonance is not strong enough to stop breeding. However, the low energy region has little practical interest for a fast reactor.

Fast neutrons deposit the most radiation damage energy: for LFR above 1.7 MeV the generalized adjoint is positive and below 0.7 MeV it is negative. There are few sign changes in between. For the SFR the respective energies are noticeable higher: 2.3 MeV and 1.9 MeV. The change in sign occurs because lower energy neutrons cause more heat deposition than radiation damage. For the SFR this transition occurs in higher energies than for the LFR.

The generalized adjoint of transmutation is qualitatively similar to breeding ratio for both LFR and SFR. However, the low energy peaks correspond to absorption resonances of ^{241}Am.

4.3. Sensitivity profiles for the LFR damage rate

Fig. 3 shows selected sensitivity profiles for the LFR damage energy rate. The relative sensitivity is defined as sensitivity scaled with the ratio of the model parameter and the response. The lethargy scaling emphasizes high energy region.

The damage rate is highly sensitive to changes in ^{56}Fe elastic cross section between 1 keV and 1 MeV. An increase in it will cause damage rate to be reduced. Physically this results from softer spectrum, which would be if the elastic scattering would be increased. Note that an increase in elastic cross section effectively decreases absorption, because as a model parameter the total cross section is held constant. The absolute value of the sensitivity has a peak near the 27.7 keV resonance of ^{56}Fe and has a local minimum in the 24.4 keV window of ^{56}Fe. The sensitivity profile of total cross section qualitatively mirrors the one of elastic scattering cross section. This occurs mainly because elastic cross section is a large part of total cross section, because the elastic cross section is relatively smooth and because elastic downscatter from ^{56}Fe is only a few groups wide in this energy region.

The sensitivity to elastic scattering of ^{16}O is negative between 1 keV and 1 MeV with the same implications as for ^{56}Fe. However, the local minimum and maximum in 27.7 keV and 24.4 keV are reversed for ^{16}O even though the cross sections for oxygen are smooth in the region. This occurs because the flux is depressed in the resonance and peaked in the cross section window. Again, the sensitivities to total cross section mostly mirror the elastic cross section.

The damage rate is much less sensitive to elastic and inelastic cross sections of ^{239}Pu. Both of the sensitivities are slightly negative. The behavior is similar to ^{16}O in the local extrema in 27.7 keV and 24.4 keV.

In this case the generalized adjoint is so smooth that its effect is hard to see. The clearest effect comes from the reversal of sensitivities to total and elastic cross section above 1.7 MeV: an increase in elastic scattering in the region causes a reduction in radiation damage. See the small figure in Fig. 3.

4.4. Uncertainty analysis

The uncertainties of the responses are quite high. The LFR damage rate is known worst with 12.3% relative standard deviation and the LFR breeding ratio is known best with 6.6% relative standard deviation. The main contributions to the LFR damage rate are listed in Table 3. Here “contribution” means absolute value of covariance between the parameter pair divided by sum of absolute values of covariances of all parameter pairs. The value depends on what is considered to be a parameter pair, but the value can be used to for importance ranking between the selected parameter pairs. Here we consider individual reactions and nuclide concentrations.

The LFR is very sensitive to changes in ^{56}Fe total and elastic cross sections, but the effects are opposite. Therefore the high contribution to uncertainty of ^{56}Fe total and elastic reactions is diminished by high correlation between the two reactions. The effective share of combined ^{56}Fe total and elastic reactions to LFR damage rate variance is only 3.7%. Similar diminishing occurs for many nuclides, including ^{206}Pb, ^{238}U and ^{54}Fe.

The covariances of ^{16}O are from so called low-fidelity evaluation (Chadwick et al., 2011) and have zero correlation between total and elastic reactions, and actually the ^{16}O(n,total) gives the highest non-diminished contribution to uncertainties of all responses. Without uncertainties from oxygen the relative standard deviations for the LFR breeding ratio, damage rate and transmutation rate would be 3.1%, 4.1% and 4.0%, respectively. For the SFR these would be 4.1%, 5.0% and 4.8% in the same order.

The contributions of uncertainties in nuclide concentrations are mostly small. The highest contributions are ^{239}Pu with 0.14% contribution to SFR breeding ratio and ^{241}Am with 0.07% contribution

for the SFR transmutation rate. They have impact on a few of the last printed digits of the uncertainties. The uncertainty caused by nuclide density uncertainties is likely higher in high burnup fuels. However, correlations might diminish the effect as with cross sections.

Most contributions to uncertainties are indirect. This might be partly result of the infinite homogeneous model which has only nuclear data dependency but no geometrical contributions, e.g., leakage. In the case of damage rate it results from the fact that there were no covariances for damage and heat energy deposition cross sections.

5. Conclusions

Uncertainty analysis of infinite lead and sodium cooled fast reactors has been performed by treating multigroup constants as correct representation of the underlying physics. Only the first order uncertainty analysis was performed. This implies that the calculated uncertainties are not exact, but they are still usable as yardsticks.

The uncertainties in the responses are rather large due to uncertainties in the ENDF/B-VII.1 nuclear data. In the case of breeding ratio we cannot predict, with the considered data, whether the reactors would be breeders or converters. Overall there is no large difference in the level of uncertainty between the responses of the LFR and the SFR, but uncertainties in the SFR case seem to be larger. The impact of uncertainties in nuclide concentrations was small, but is potentially meaningful for high burnup fuels.

The uncertainty in model parameters is the dominant source of uncertainty, being 3–10%. The modeling error is in the order 1%, input data precision is 10^{-3} % and numerical error less than 10^{-4}%. The modeling error, input data precision and numerical error could be improved on, but there is no need to do so until uncertainties in the model parameters are reduced.

The main sources of uncertainty were analyzed and listed for the LFR damage rate, i.e., the LFR damage energy deposition rate divided by heat deposition rate. If the value of a response needs to be known with better precision, a similar ranking can be performed for the response to recognize which parameters cause the largest uncertainty. These parameters can then be measured more precisely, which improves our capability to estimate the response. The low-fidelity evaluation of ^{16}O is problematic because it contains no correlation for total and elastic reactions in covariances. This is unphysical because any increase in elastic cross section also increases the total cross section. This should be corrected in future evaluations since ^{16}O is commonly found in many reactors, including typical LFRs and SFRs.

The processed covariance matrices of ^{207}Pb and ^{208}Pb had negative eigenvalues, i.e., they are not proper covariance matrices. The negative eigenvalues might results from improper original data in the evaluation or a problem in the processing code.

Acknowledgments

The author thanks P.A. Aarnio and L. Rintala for their valuable comments on the manuscript. We acknowledge the financial support of the YTERA Doctoral Programme for Nuclear Engineering and Radiochemistry.

References

AMD Core Math Library, version 5.3.0. http://developer.amd.com/acml (cited 15.2.14).
Anderson, E., et al., 1999. LAPACK Users' Guide, 3rd ed. Society for Industrial and Applied Mathematics, Philadelphia, PA.
Bondarenko, I.I., et al., 1964. Group Constants for Nuclear Reactor Calculations. Consultants Bureau, New York.
Cacuci, D.G., Ionescu-Bujor, M., 2003. Sensitivity and uncertainty analysis data assimilation, and predictive best-estimate model calibration. In: Cacuci, D.G. (Ed.), Handbook of Nuclear Engineering. Springer, New York, pp. 1913–2051 (chapter 17).
Cacuci, D.G., 2003. Sensitivity and Uncertainty Analysis, vol. 1. Chapman & Hall/CRC, Boca Raton, FL.
Chadwick, M.B., Herman, M., Oblož inský, P., et al., 2011. ENDF/B-VII.1 nuclear data for science and technology: cross sections, covariances, fission product yields and decay data. Nucl. Data Sheets 112, 2887–2996.
Dresner, L., 1956. Resonance Absorption of Neutrons. ORNL, Oak Ridge, Tennessee.
Greenspan, E., 1976. Developments in perturbation theory. In: Henley, E., Lewins, J. (Eds.), In: Advances in Nuclear Science and Techonology, vol. 9. Plenum Press, New York/London, pp. 181–268.
Greenspan, E., 1982. Sensitivity functions for uncertainty analysis. In: Lewins, J., Becker, M. (Eds.), In: Advances in Nuclear Science and Techonology, vol. 14. Plenum Press, New York/London, pp. 193–246.
Lawson, C.L., et al., 1979. Basic linear algebra subprograms for FORTRAN usage. ACM Trans. Math. Soft. 5, 308–323.
Leppänen, J., 2007. Development of a New Monte Carlo Reactor Physics Code. Helsinki University of Technology (VTT Publications 640) (D.Sc. thesis).
MacFarlane, R.E., Kahler, A.C., 2010. Methods for processing ENDF/B-VII with NJOY. Nucl. Data Sheets 111, 2739–2890.
MacFarlane, R.E., Muir, D.W., 1994. The NJOY Nuclear Data Processing System, Version 91. Los Alamos National Laboratory, report LA-12740-M.
NJOY 99.393, http://t2.lanl.gov/nis/codes/njoy99/ (cited 15.2.2014).
Usachev, L.N., 1964. Perturbation theory for the breeding ratio and for other number ratios pertaining to various reactor processes. J. Nucl. Energy A/B 18, 571.
Waltar, A.E., Todd, D.R., Tsvetkov, P.V. (Eds.), 2012. Fast Spectrum Reactors. Springer, New York.

People encounter uncertainties in their everyday lives: the more serious uncertainties cause anxiety and the lighter ones bring excitement. Also computational results include uncertainty. Its sources are, among other things, idealizations in the computational model and inexact knowledge of its parameters. These uncertainties can be, taking into account different sources of uncertainty, managed by quantifying the uncertainties of the computed quantities. This is called uncertainty analysis. -

The results of uncertainty analyses are at most as good as the data used in them. Quality assurance methods aim to ensure that the data used in the analyses are adequate, e.g., have certain properties. This dissertation takes a look at uncertainty analysis applied to reactor physics from the viewpoint of quality assurance.

ISBN 978-952-60-6729-2 (printed)
ISBN 978-952-60-6730-8 (pdf)
ISSN-L 1799-4934
ISSN 1799-4934 (printed)
ISSN 1799-4942 (pdf)

Aalto University
School of Science
Department of Applied Physics
www.aalto.fi

BUSINESS + ECONOMY

ART + DESIGN + ARCHITECTURE

SCIENCE + TECHNOLOGY

CROSSOVER

DOCTORAL DISSERTATIONS

Aalto-DD 58/2016